Formation, transportation and transformation processes of organic matter from the surface ocean to the deep sea

Dissertation

zur Erlangung des akademischen Grades eines Doktors der Naturwissenschaften

-Dr. rer. nat.-

im Fachbereich Geowissenschaften der Universität Bremen

Vorgelegt von

Lili Sanna Hufnagel

Bremen, Dezember 2023

Erster Gutachter:	Prof. Dr. Morten H. Iversen
Zweiter Gutachter:	Dr. Matthieu Bressac
Tag der mündlichen Prüfung:	12.04.2024

Summary

The ocean plays an important role as carbon sink, especially under the rapid anthropogenic climate change. The biological carbon pump is one of the main mechanisms, which export organic carbon from the surface ocean to the deep sea, where it can be stored for hundreds of years. The formation of carbon-rich, organic aggregates, their transport to deep water layers, and the ongoing transformation while sinking are of importance for the magnitude of the carbon export. At the moment, however, it is not fully understood how those processes are impacted by environmental conditions.

Polar regions are subjected to rising temperatures and increasing ice melt, resulting in a large input of melt water (freshwater) in the surface ocean which impacts physical, biological, and chemical processes in the ecosystems. Therefore, the present thesis identifies how processes involved of formation, transportation, and transformation of exported particulate organic matter are impacted in polar regions.

In **Chapter I** the carbon export by sinking aggregates and the aggregates' interaction with microbes and zooplankton in the Arctic fjord Scoresby Sund in East Greenland was investigated using 16S and 18S rDNA sequencing, catalyzed reporter deposition fluorescence *in situ* hybridization (CARD-FISH), *in situ* camera particle profiles, and biogeochemical flux measurements. In the fjord, estuarine horizontal water movement impacted the carbon export leading to a translocation of sinking aggregates in the fjord. Aggregates were formed in the inner Nordvestfjord and laterally transported out of the fjord in the upper water column by the outflowing water while being retained at an increasing salinity gradient. The export through the fjord was driven by zooplankton and its production of fecal pellets. Close to the marine-terminating Daugaard-Jensen Glacier aggregates were ballasted by silt facilitating faster sinking. The formation of the aggregates and zooplankton-mediated export affected the composition of the aggregate-attached microbial community.

The **Chapter II** focused on the particle export in open waters of the Southern Ocean, near to the island South Georgia. The temporal development of particle export during an Antarctic phytoplankton bloom was investigated in a high temporal resolution using particulate organic carbon measurements, *in situ* camera profiles, and *in situ* sinking velocity measurements at two different depth through the mesopelagic zone. Attenuation of the particle flux was not only dependent on zooplankton feeding and microbial remineralization, but also dependent on particle retention in the surface ocean due to physical conditions. Especially large, porous aggregates were efficiently retained at increasing salinities in the water column. Salinity

gradient based particle retention at the surface resulted in a carbon export decoupling at depth from the particle concentration in the epipelagic zone.

In **Chapter III**, the carbon export in a polar front system at the marginal ice zone in the Fram Strait in the Arctic Ocean was explored. Biogeochemical flux and primary production were assessed and combined with data of different *in situ* camera systems, sinking velocities of aggregates, microbial respiration, and physical oceanographic processes. The characteristics and complex movement of water masses and varying ice condition had a direct impact on the carbon export. The subduction of chlorophyll-rich water resulted in enhanced aggregate formation, including deep aggregate formation down to 100 m depth. Aggregates formed at depth were less subjected to surface stratification and were likely exported more quickly from the epipelagic zone. The majority of exported aggregates were composed of a mix of the haptophyte *Phaeocystis* and diatoms and were ballasted by silica-rich diatom frustules. Occasionally, ballasting of aggregates by cryogenic minerals was observed which increased their size-specific settling velocities significantly in comparison to diatom-ballasted aggregates.

Overall, the present thesis identifies the dominating carbon export mechanisms in the investigated polar systems to improve the understanding how ongoing anthropogenic climate change will affect the biological carbon pump in the Arctic and Antarctic. Together, the results demonstrate that it is essential to investigate the impact of increasing meltwater input on the carbon export in polar systems and to include saline-based particle retention in regional and global oceanic carbon export models. Furthermore, horizontal and vertical translocation of aggregates, as were observed in the present thesis, shape the efficiency of the carbon export in meltwater-impacted polar marine regions. Thus, those processes should be reflected in future carbon export models to allow a more precise determination of the ocean's role as carbon sink.

Zusammenfassung

Der Ozean spielt eine wichtige Rolle als Kohlenstoffsenke, vor allem angesichts des rasanten, anthropogenen Klimawandels. Die biologische Kohlenstoffpumpe ist einer der wichtigsten Mechanismen für den Export von organischem Kohlenstoff aus dem Oberflächennahen Gewässern in die Tiefsee, in der Kohlenstoff für hunderte von Jahren gespeichert werden kann. Der Umfang des Kohlenstoffexportes ist abhängig von der Bildung organischer, kohlenstoffhaltiger Aggregate, deren Transport in tiefere Wasserschichten und deren kontinuierliche Transformation während des Absinkens. Derzeit ist jedoch noch nicht vollständig geklärt, wie diese Prozesse durch Umweltbedingungen beeinflusst werden.

Die Polarregionen sind steigenden Temperaturen und einer zunehmenden Eisschmelze ausgesetzt, was zu einem großen Eintrag von Schmelzwasser (Süßwasser) in den Oberflächenozean führt. Dies wirkt sich auf physikalische, biologische und chemische Prozesse in den Ökosystemen aus. In der vorliegenden Arbeit wird daher untersucht, wodurch und in welchem Maße die Prozesse der Bildung, des Transports und der Umwandlung von exportiertem partikulärem organischem Material in den Polarregionen beeinflusst werden.

In **Kapitel I** wurde der Kohlenstoffexport durch sinkende Aggregate und die Interaktion der Aggregate mit Mikroben und Zooplankton im arktischen Fjord Scoresby Sund in Ostgrönland untersucht. Dazu wurden die Methoden der 16S- und 18S-rDNA-Sequenzierung, katalysierter Reporterdepositions-Fluoreszenz-in-situ-Hybridisierung (CARD-FISH), In-situ-Kamerapartikelprofilen und biogeochemischen Partikelflussmessungen genutzt. Die gesammelten Daten konnten zeigen, dass sich die horizontale Wasserbewegung auf den Kohlenstoffexport im Fjord auswirkte, was zu einer Translokation von sinkenden Aggregaten im Fjord führte. Die Aggregate bildeten sich im inneren Nordvestfjord und wurden durch das herausfließende Wasser in der oberen Wassersäule Fjord-auswärts transportiert, während sie von einem zunehmenden Salzgehalt in der oberen Wassersäule zurückgehalten wurden. Der Export durch den Fjord wurde durch Zooplankton und deren Produktion von Kot-Pellets gesteuert. Darüber hinaus wurden in der Nähe des marinen Endes des Daugaard-Jensen-Gletschers Aggregate durch feinen Sand beschwert, was ein schnelleres Absinken der Partikel begünstigt. Die Bildung der Aggregate und der durch Zooplankton vermittelte Export wirkten sich auf die Zusammensetzung der an die Aggregate assoziierte mikrobielle Gemeinschaft aus.

Das **Kapitel II** befasste sich mit dem Partikelexport in offenen Gewässern des Südlichen Ozeans, nahe der Insel Südgeorgien. Die zeitliche Entwicklung des Partikelexports während einer antarktischen Phytoplanktonblüte wurde mit Hilfe von Messungen des

partikulären organischen Kohlenstoffs, In-situ-Kameraprofilen und In-situ-Sinkgeschwindigkeitsmessungen in zwei verschiedenen Tiefen der mesopelagischen Zone in hoher zeitlicher Auflösung untersucht. Dabei konnte gezeigt werden, dass die Abschwächung des Partikelflusses nicht nur von der Aufnahme durch das Zooplankton und der mikrobiellen Remineralisierung abhängig ist, sondern auch von der Retention der Partikel in Oberflächen-nahen Zonen durch physikalische Prozesse. Bei steigendem Salzgehalt in der Wassersäule, wurden vor allem große, poröse Aggregate effizient zurückgehalten und ein Absinken verzögert. Diese, durch den Salzgehalt gesteuerte Retention der Partikel an der Oberfläche, führte zu einer Entkopplung des Kohlenstoffexports in der Tiefe von der Partikelkonzentration in der epipelagischen Zone.

In **Kapitel III** wurde der Kohlenstoffexport in einem polaren Frontsystem am Rande der Eiszone in der Framstraße im Arktischen Ozean untersucht. Messungen biogeochemische Partikelflüsse und der Primärproduktion wurden mit Daten verschiedener In-situ-Kamerasysteme, Sinkgeschwindigkeiten von Aggregaten, mikrobieller Respiration und physikalischen ozeanografischen Prozessen kombiniert. Die Eigenschaften und die komplexen Bewegungen der Wassermassen, sowie die unterschiedlichen Eisbedingungen, hatten einen direkten Einfluss auf den Kohlenstoffexport. Die Subduktion von chlorophyllreichem Wasser führte zu einer verstärkten Bildung von Aggregaten, einschließlich in Tiefen von bis zu 100 m. In der Tiefe gebildete Aggregate waren weniger stark der Stratifikation des Oberflächenwassers ausgesetzt und wurden daher vermutlich schneller aus der epipelagischen Zone exportiert. Die Mehrzahl der exportierten Aggregate bestand aus einer Mischung aus den Haptophyten *Phaeocystis* und Diatomeen und wurden von Siliziumdioxid-haltigen Diatomeen-Schalen beschwert. Gelegentlich wurden Aggregate durch die Aufnahme von kryogenen Mineralien beschwert, was ihre größenspezifischen Sinkgeschwindigkeiten im Vergleich zu Aggregaten mit ausschließlich Diatomeen deutlich erhöhte.

In der vorliegenden Arbeit werden die dominierenden Mechanismen des Kohlenstoffexports in den untersuchten polaren Systemen identifiziert, um das Verständnis dafür zu verbessern, wie sich der fortschreitende anthropogene Klimawandel auf die biologische Kohlenstoffpumpe in arktischen und antarktischen Systemen auswirken wird. Zusammengefasst zeigen die Ergebnisse die Notwendigkeit die Auswirkungen des zunehmenden Schmelzwassereintrags in polaren Systemen auf den Kohlenstoffexport zu berücksichtigen. Wichtig ist es dabei die Salzgehalt-abhängige Retention von Partikeln in regionale und globale ozeanische Kohlenstoffexportmodelle mit einzubeziehen. Für die Effizienz des Kohlenstoffexports in polaren, Schmelzwasser-beeinflussten Gebieten spielen

ebenfalls die horizontale und vertikale Verlagerung von Aggregaten, wie sie in der vorliegenden Arbeit beobachtet wurden, eine große Rolle. Daher sollten auch diese Mechanismen in zukünftigen Modellen zum Kohlenstoffexport berücksichtigt werden, um eine präzisere Berechnung der Rolle des Ozeans als Kohlenstoffsenke zu ermöglichen.

Table of content

List of abbreviations

ADCP	Acoustic Doppler Current Profiler
ANOVA	Analysis of variance
ASVs	Amplicon sequence variants
AW	Atlantic Water
BCP	Biological carbon pump
bSi	Biogenic silica
C	Carbon
$CaCO_3$	Calcium carbonate
CARD-FISH	Catalyzed reporter deposition fluorescence *in situ* hybridization
Chla	Chlorophyll a
Chla max	Chlorophyll a maximum
CO_2	Carbon dioxide
CTD	Conductivity temperature depth
DAPI	4',6-diamidino-2-phenylindole
DCM	Deep chlorophyll a maximum
DIC	Dissolved inorganic carbon
DNA	Deoxyribonucleic acid
DOC	Dissolved organic carbon
DOM	Dissolved organic matter
DW	Dry weight
e.g.	exempli gratia, for example
EGC	East Greenland Current
ESD	Equivalent spherical diameter
et al.	et alii, and others
FL	Free-living
HCl	Hydrochloric acid
$HgCl_2$	Mercury(II) chloride
HNCL region	High nutrient and low chlorophyll region
i.e.	id est, that is
IPCC	Intergovernmental Panel on Climate Change
ISC	*In situ* camera system
MIZ	Marginal ice zone

MSC	Marine Snow Catcher
N	Nitrogen
NaCl	Sodium chloride
NMDS	Non-metric Multi-dimensional Scaling
nVd	Normalized volume spectrum
NVSTF	Nordvestfjord
OSS	Outer Scoresby Sund
PA	Particle-attached
PAR	Photosynthetically active radiation
PCA	Principal Component Analysis
PCR	Polymerase chain reaction
PELAGRA trap	**P**article **E**xport measurement using a **LAGRA**ngian trap
PIC	Particulate inorganic carbon
POC	Particulate organic carbon
POM	Particulate organic matter
PON	Particulate organic nitrogen
PP	Primary production
PVC	Polyvinyl chloride
PW	Polar Water
RCF	Red Camera Frame
UVP	Underwater Vision Profiler
RDA	Redundancy analysis
rDNA	Ribosomal DNA
ROSINA	Remotely Observing *In Situ* Camera for Aggregates
rRNA	Ribosomal ribonucleic acid
RT	Room temperature
TEP	Transparent exopolymer particle
TPM	Total particulate mass
WSC	West Spitsbergen Current

List of units

%	Percent
°C	Degree Celsius
µg	Microgram
µgC	Microgram carbon
µL	Microliter
µm	Micrometer
µM	Micromolar
cm	Centimeter
cm^3	Cubic centimeter
d	Day
gC	Gram carbon
Gt	Gigaton
h	Hour
kg	Kilogram
kHz	Kilohertz
km	Kilometer
km^2	Square kilometer
km^3	Cubic kilometer
L	Liter
m	Meter
m^2	Square meter
m^3	Cubic meter
mg	Milligram
mgC	Milligram carbon
min	Minute
mL	Milliliter
mm	Millimeter
mm^2	Square millimeter
mm^3	Cubic millimeter
Mt	Megaton
nm	Nanometers
pixel	Pixel

ppm	Parts per million
PSU	Practical salinity unit
s	Second
yr	Year
#	Number

General Introduction

Importance of the ocean for global carbon budget

In the modern times, the planet Earth is subjected to anthropogenic climate change resulting in rapid global warming, ice melt, and sea-level rise (IPCC 2021). These changes are the consequence of anthropogenic carbon emissions, i.e. the increase of carbon dioxide (CO_2) concentration in the atmosphere by emissions from human activities (IPCC 2021). The carbon dioxide concentration in the atmosphere was between 260 to 270 ppm in pre-industrial times (Wigley 1983) – with a narrow fluctuation margin (Siegenthaler et al. 2005, Fig. 1). At present times, the average atmospheric carbon dioxide concentration increased to levels around 410 ppm due to anthropogenic burning of fossil fuels and land-use changes (IPCC 2021, Fig. 1). The recent IPCC report on the physical science basis suggests that aside from the atmosphere, which takes up 46% of the anthropogenic carbon emissions per year, the terrestrial biosphere and the ocean store 31% and 23%, respectively (IPCC 2021). These numbers tend to change with the newest scientific findings, as only a fraction of the physical, chemical and biological processes in the ocean are understood. For example, in 2013/2014, the contribution of the ocean to the anthropogenic carbon uptake was estimated to be around 30% (IPCC 2013) and was adjusted downwards since then. To understand the ocean's carbon storage potential, further investigation is needed to close knowledge gaps on oceanic processes involved in carbon uptake and transformation.

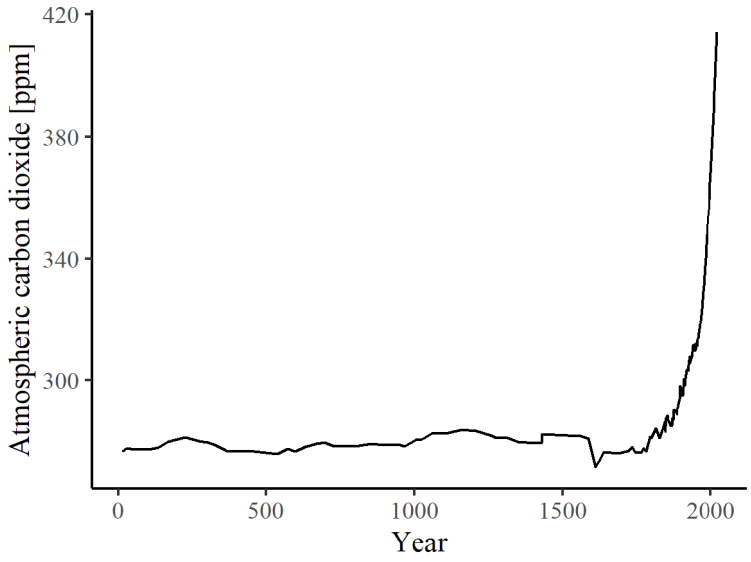

Fig. 1: Atmospheric CO_2 record [ppm] based on ice-core data before 1959 (MacFarling Meure et al. 2006) and yearly averages of direct observations from Mauna Loa and the South Pole in from 1959 to 2000 (Keeling et al. 2001).

Oceanic uptake of carbon dioxide is regulating and buffering the carbon dioxide concentrations in the atmosphere (Sabine et al. 2004; Sabine and Tanhua 2010), reducing the pre-industrial atmospheric carbon dioxide concentration by around 50%, i.e. by 200 - 300 ppm (Heinze et al. 2015). The understanding of the physical, chemical, and biological processes in the ocean is crucial, to predict the impact of the global climate change on the carbon storage capacity of the ocean. If effects from global climate change will reduce the storage capacity of carbon in the ocean, it will have major consequences on all earth systems. In the following, key processes of the carbon cycle involving the ocean are described.

Carbon uptake by the oceans

The primary process for carbon uptake is the dissolution of atmospheric carbon dioxide into the ocean (Sabine and Tanhua 2010). If the partial pressure of carbon dioxide is increasing in the atmosphere, there is a net influx of carbon dioxide into the surface ocean (Siegenthaler and Sarmiento 1993). The carbon dioxide is dissolved in seawater resulting in carbonic acid, which dissociates into bicarbonate and carbonate (Sabine and Tanhua 2010). This dissolved inorganic carbon (DIC) is the most abundant carbon pool in the ocean (Siegenthaler and Sarmiento 1993) with the main component being bicarbonate (Sabine and Tanhua 2010). If the carbon dioxide is transferred into particulate forms of organic and inorganic carbon in the surface ocean and transported into deeper layers of the ocean, which do not mix with the surface ocean, the carbon is removed from the surface ocean (carbon export) and can be stored long-term in the ocean (Ducklow et al. 2001; Falkowski et al. 2000; Jiao et al. 2010; Sabine and Tanhua 2010; Volk and Hoffert 1985). The downward transport and respiration of organic carbon result in increased concentrations of dissolved inorganic carbon in the deep ocean (Volk and Hoffert 1985).

Carbon pumps

Carbon export mechanisms are complex and include a mixture of physical, chemical, and biological processes. There are different carbon export concepts, so-called carbon pumps, in the ocean. The carbon is thereby transported through the different oceanic layers from the upper epipelagic (0 – 200 m), through the mesopelagic (200 – 1000 m) down to deeper layers such as the bathypelagic (1000 – 4000 m) or even deeper zones.

The **solubility pump** is based on the solubility of carbon dioxide, which is primarily depending on temperature, alkalinity, and concentration gradients (Sarmiento and Bender 1994; Volk and Hoffert 1985). Dissolved carbon dioxide is transported along with the moving water mass, e.g. in the thermohaline circulation, into the deep ocean and is stored until the water mass

resurfaces (Falkowski et al. 2000). Cold temperatures increase the solubility of carbon dioxide in water, thus, the greatest effect of the solubility pump can be observed in polar regions (Falkowski et al. 2000). This means that high latitudes are generally consider as carbon sink regions (Falkowski et al. 2000), while upwelling regions at low latitudes release carbon to the atmosphere (Keeling 1968).

Carbon export driven by the generation of particles in the surface ocean and their gravitational settling is classified as the **biological carbon pump** (Volk and Hoffert 1985). Carbon dioxide is converted into biomass via photosynthesis by phytoplankton (carbon fixation) which form aggregates and sink from the surface ocean down to deeper layers (Turner 2015). The different processes involved in the biological carbon pump will be discussed in more detail below in the section ”The biological carbon pump”.

While fast-sinking particles are exported via gravitational sinking, slow-sinking and non-sinking particles can be exported via **physical particle injection pumps** (Boyd et al. 2019). The physical particle injection pumps are comprised of a combination of the generation of particles and the export by physical processes, e.g. by subduction of the water mass (Boyd et al. 2019). There are three main physical particle injection pumps: the *mixed-layer pump* (subduction via shallowing of the mixed layer), *eddy-subduction pump* (subduction via mesoscale and submesoscale frontal and eddy circulation, scaled 1 - 100 km) and the *large-scale subduction pump* (subduction via large scale ocean-circulation, e.g. by Ekman pumping, scaled 100 - 1,000 km) (Boyd et al. 2019).

Additionally, organic carbon can also be exported by vertical migration of zooplankton in the mesopelagic zone, i.e. in **biologically mediated particle injection pumps** (Boyd et al. 2019). Many zooplankton species show a diel vertical migration to deeper layers and are acting as vectors for carbon transport (Schnetzer and Steinberg 2002). In the epipelagic zone the organic matter is fed on and can be either respired or released as dissolved organic carbon and fecal pellets at depth (Steinberg et al. 2000). The two main biological mediated particle injection pumps are the *meso-pelagic migrant pump* (carbon export via diurnal vertical migration for feeding) and the *seasonal lipid pump* (carbon export via the winter hibernation during winter) (Boyd et al. 2019).

Carbon storage

If the carbon is exported from the surface ocean by either of these carbon pumps, the ocean can sequester the carbon dioxide and store it for thousands or millions of years (Ducklow et al. 2001; Eppley and Peterson 1979; Jiao et al. 2010; Passow and Carlson 2012). Yet, only 1 - 3% of the organic matter in the surface ocean are exported to the deep sea (De La Rocha and Passow 2007) and account for the sequestration flux from the mesopelagic zone at 1000 m, which is stored in the ocean long-term for more than 100 years (Passow and Carlson 2012). In total, only 1% of the organic biomass, that sinks out of the upper ocean as particles, is transported to the marine sediments where it potentially can be stored for millions of years (Ducklow et al. 2001). The length of carbon storage is determined by the remineralization depth (Kwon et al. 2009), i.e. the depth where organic carbon is remineralized and converted to carbon dioxide, e.g. by microbes or zooplankton. The deeper the remineralization takes place in the water column, the greater is the time span of the carbon storage (Fig. 2) and the lower the likelihood that the CO_2 is released back into the atmosphere (Kwon et al. 2009).

Biological carbon pump

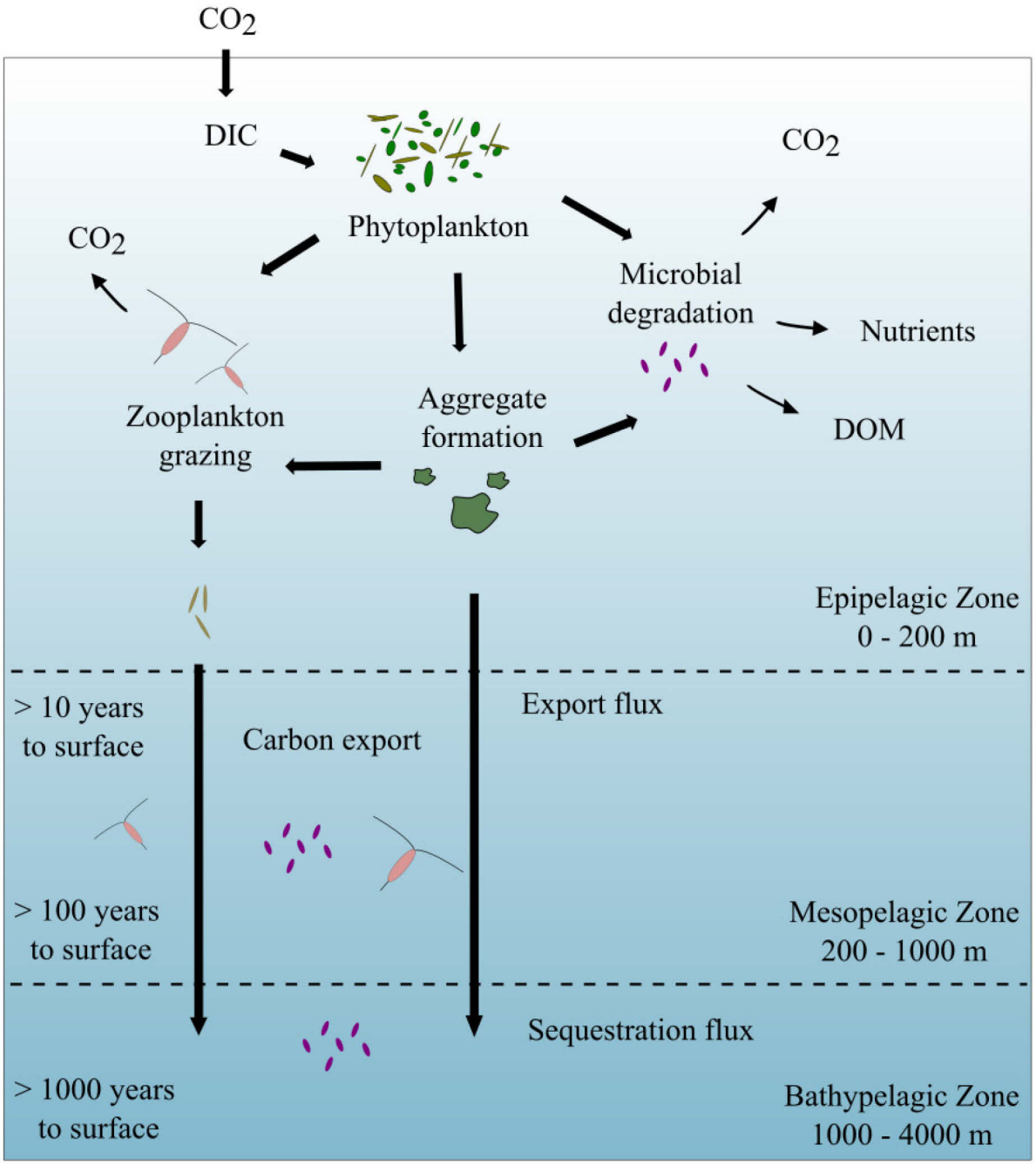

Fig. 2: Overview of biological carbon pump: Carbon dioxide dissolves in seawater, dissolved inorganic carbon (DIC) is taken up by phytoplankton during photosynthesis and converted to organic matter. Phytoplankton form aggregates. Phytoplankton and aggregates are degraded by microbes and nutrients and dissolved organic matter (DOM) are released. Zooplankton feed on phytoplankton and aggregates and egests fecal pellets. Aggregates and fecal pellets are exported into the mesopelagic zone (200 – 1000 m) as part of the export flux. In the mesopelagic zone the aggregates and fecal pellets are subjected to further zooplankton degradation and microbial remineralization. The carbon is stored between > 10 to 100 years in the mesopelagic zone. If the aggregates and fecal pellets sink into the bathypelagic zone (1000 - 4000 m) as part of the sequestration flux, they can be stored > 100 years.

Primary production

The magnitude of the carbon export via the biological carbon pump (Fig. 2) is highly dependent on the respective phytoplankton communities in the ecosystem and their primary production, i.e. the conversion of carbon dioxide via photosynthesis to organic matter (Passow and Carlson 2012). The export of fixed carbon can either be in form of particulate organic carbon (POC) or calcium carbonate, forming the soft-tissue pump and the hard-tissue pump (Volk and Hoffert 1985). Yet, the majority of the carbon dioxide is exported in form of organic carbon (Sarmiento et al. 2002). The uptake of dissolved inorganic carbon by phytoplankton causes a disequilibrium between the different carbon pools in the ocean and the atmospheric partial pressure of carbon dioxide and need to be compensated by the uptake of atmospheric carbon dioxide (Falkowski et al. 2000). This is causing a draw-down of the carbon dioxide from the atmosphere until the equilibrium is restored (Sarmiento and Bender 1994). Primary production differs in terms of magnitude and species composition according to the environmental conditions, e.g. light, temperature, nutrient availability, and the food-web structure (Falkowski et al. 1998; Sakshaug 2004). Low or only seasonal light availability together with the availability of nutrients are the main limiting factors for primary productivity in polar regions with ice coverage (Sakshaug 2004).

Aggregation

Marine aggregates (Fig. 3), coagulations of smaller particles, act vectors to transport particulate carbon from the upper ocean to the deeper layers (Fowler and Knauer 1986). The aggregate formation depends on the concentration of organic material in the water column, e.g. phytoplankton cells, and its properties (Kiørboe 2001). The aggregates form at the depth of high chlorophyll concentrations in the euphotic zone (high phytoplankton cell abundances), as the high concentration of particles increases the likelihood, that particles collide and remain coagulated by physical processes (Kiørboe 2001). The generation of transparent exopolymer particles (TEP), i.e. external polysaccharides of some phytoplankton species (Alldredge et al. 1993), can enhance the coagulation potential of aggregates and act as adhesive (Engel 2000; Passow 2002). The magnitude of the formation of TEP by phytoplankton depends on the specific microbes associated with the aggregates (Gärdes et al. 2011). Apart from physical coagulation, aggregates can also be formed by zooplankton egestion (fecal pellets, Fig. 3B) or the production of feeding structures or houses by zooplankton (Alldredge 2005; Bathmann et al. 1991; Bruland and Silver 1981; Turner 2002). If the aggregates reach a diameter greater than

500 µm during the aggregation process, they are called “Marine Snow” (Alldredge and Silver 1988).

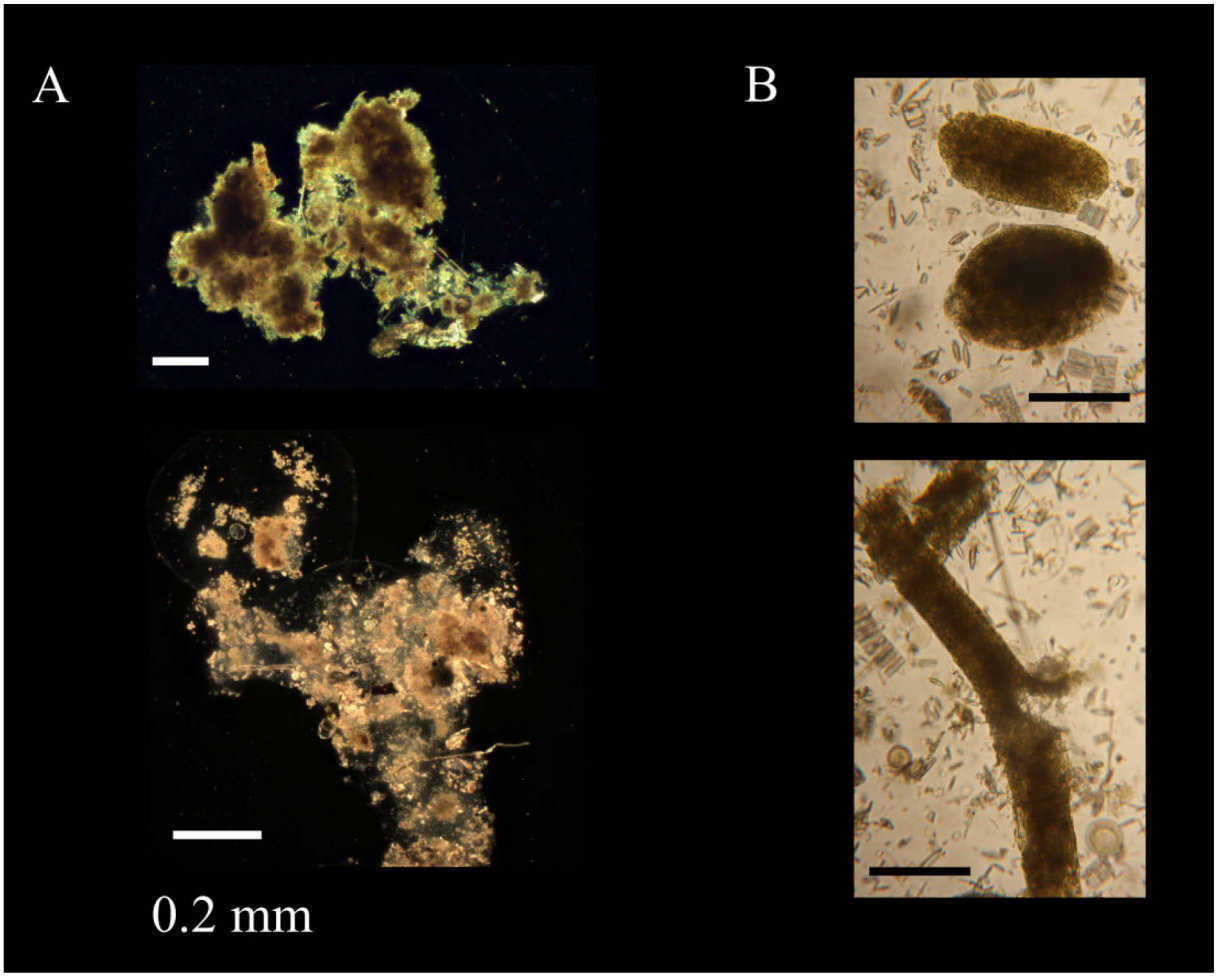

Fig. 3: (A) Phytoplankton aggregates and (B) fecal pellets. Scale bars represent a distance of 0.2 mm.

Retention time

When aggregates have formed, they sink from the surface ocean into deeper water layers. In regions with water layers with sharp density increases, aggregates are retained at these so-called pycnoclines (Alldredge et al. 2002; MacIntyre et al. 1995). Only when the aggregates have a higher excess density than the sea water below, due to diffusive equilibration of the water in the pore space with lower density by heat and salt exchange with the denser sea water in the surrounding water column, they can continue to sink (Kindler et al. 2010; MacIntyre et al. 1995; Prairie et al. 2013). The diffusion of salt is around 100 times slower in comparison to heat diffusion (Gargett et al. 2003), so salinity-based density changes result in a longer retention time for the aggregates in the pycnocline (Kindler et al. 2010; MacIntyre et al. 1995; Prairie et

al. 2013). Larger aggregates, with lower excess density and higher porosity, are retained for a longer time period as smaller aggregates in a density gradient and thus accumulate in the pycnocline (Kindler et al. 2010). The chemical composition of the aggregate also plays a role in the particle retention: If the aggregates contain positively buoyant TEP, the retention time of the aggregate is prolonged due to low densities (Azetsu-Scott and Passow 2004; Mari et al. 2017). During the diffusion of heat and salt into the pore space, the aggregate is retained in the surface ocean and is subjected to degradation by zooplankton feeding and remineralization by microbes (Giering et al. 2014; Iversen et al. 2010; Möller et al. 2012), resulting in a strong attenuation of the carbon flux.

Sinking velocities

The efficiency of the carbon export is widely determined by the sinking velocities of the organic material which are dependent on the properties of the aggregates, like size, excess density and aggregate type (Iversen and Ploug 2010; Ploug et al. 2008a). There is a general size to settling relationship for the aggregates according to Stoke's equation (Hamm 2002; Passow and De La Rocha 2006), which is applicable for aggregates of the same type (Iversen and Ploug 2010; Iversen and Ploug 2013). *In situ* aggregates tend to be heterogenous in their composition and their properties, e.g. by changing environmental conditions and altering phytoplankton communities (Nowald et al. 2015), thus, the size to settling relationship is less substantially when observing *in situ* aggregates (Iversen and Lampitt 2020). Instead, the aggregate composition and excess density seem to be the determining factor for sinking velocities when considering different types of aggregates (Iversen and Lampitt 2020; Iversen and Ploug 2010; Ploug et al. 2008a). The differences in settling velocities result in the formation of bigger aggregates from small aggregates while sinking, when fast-sinking particles incorporate slow-sinking particles by differential settling (Burd and Jackson 2009; McCave 1984).

Ballasting

Factors which increase the excess densities of the sinking aggregates and thus their sinking velocities, such as the availability of ballast material (De La Rocha and Passow 2007), directly impact the carbon flux. While the availability of ballast material has no influence on the rate of microbial degradation, it increases the density of the aggregates (Iversen et al. 2010; Iversen and Ploug 2010; Iversen and Robert 2015; Ploug et al. 2008a; Ploug et al. 2008b). Additionally, when ballast material is incorporated into aggregates, the porosity of the aggregate decreases (De La Rocha and Passow 2007). Together with the increasing density,

this results in enhanced sinking velocities of the ballasted aggregates (De La Rocha and Passow 2007; Iversen and Robert 2015).

The main ballast minerals are biogenic silica, calcium carbonate and lithogenic ballast minerals (Klaas and Archer 2002). Organism like diatoms, radiolarians and silicoflagellates produce biogenic silica as part of their skeletal structures (Tréguer et al. 1995). Diatoms can make up about 40% of the total POC export (Jin et al. 2006) due to their silica frustules (cell walls) and the resulting ballasting of aggregates and fecal pellets when they are incorporated into the aggregates (Tréguer et al. 2018).

Particulate inorganic carbon (PIC), i.e. calcium carbonate, does not only act as vector of the calcium-carbonate facilitated part of the biological carbon pump (Volk and Hoffert 1985) but also acts as ballasting material for aggregates (Schmidt et al. 2014). PIC is also produced as part of the skeletal structures of organism, such as coccolithophores, foraminifera, and pteropods (Buitenhuis et al. 2019; Schmidt et al. 2014) and can get incorporated into aggregates. Rising carbon dioxide concentration by anthropogenic emissions can limit the production of calcium-carbonate, which may ultimately lead to a reduction of deep carbon export, since less calcium-carbonate structures will be available for ballasting the aggregates (Biermann and Engel 2010).

Lithogenic ballast materials originate, for instance, from desert dust (van der Jagt et al. 2018), sediment input by rivers (Rixen et al. 2019), or melting glaciers (Seifert et al. 2019). When lithogenic minerals are integrated into the aggregates, they decrease the stickiness and thereby cohesion of the aggregated particles by TEP (Engel 2000), which then results into smaller but fast-sinking and denser aggregates being formed (Iversen and Robert 2015; Passow and De La Rocha 2006). In polar regions the generation of cryogenic ballast material, mainly gypsum particles, takes place in ice brine channels or pockets (Geilfus et al. 2013; Wollenburg et al. 2020). When the ice melts, these fast-sinking cryominerals are released and can act as ballast minerals if scavenged by aggregates in the pelagic zone (Wollenburg et al. 2020; Wollenburg et al. 2018).

Zooplankton feeding

Only a fraction of the carbon that is fixed via primary production (5 - 25%) leaves the euphotic zone, the surface water layer in which light intensities are sufficient for photosynthesis, and reaches the twilight zone (see De La Rocha and Passow 2007 and references therein). The majority of the carbon flux is attenuated already in the epipelagic zone (0 – 200 m). Aggregate turnover by zooplankton (via feeding, egestion, and respiration) is the

main carbon attenuation mechanism in the epipelagic and the upper mesopelagic zone (200 – 500 m) (Iversen et al. 2010; Stemmann et al. 2004), as zooplankton act as gate keeper for the carbon flux at these depths (Jackson and Checkley Jr 2011). The impact of zooplankton feeding on the carbon flux differs regionally and seasonally, e.g. with zooplankton being responsible for 8 to 30% of the carbon attenuation in the North Atlantic (Giering et al. 2014) and more than 60 to 67% in the Arctic Shelf Sea (van der Jagt et al. 2020). Aside from attenuating the carbon flux, zooplankton feeding leads to the transformation of the organic material, e.g. by the production of fecal pellets, zooplankton carcasses, and mucous feeding nets or houses, which can be important contributors to the carbon flux (Alldredge 2005; Bathmann et al. 1991; Sampei et al. 2012; Turner 2002). Fecal pellets can make up to 100% of the particulate carbon flux depending on region and season and are effective carbon transport vectors due to their fast sinking velocities, i.e. copepod fecal pellets can reach sinking velocities of 5 – 220 m d^{-1} (see Turner 2002 and references therein).

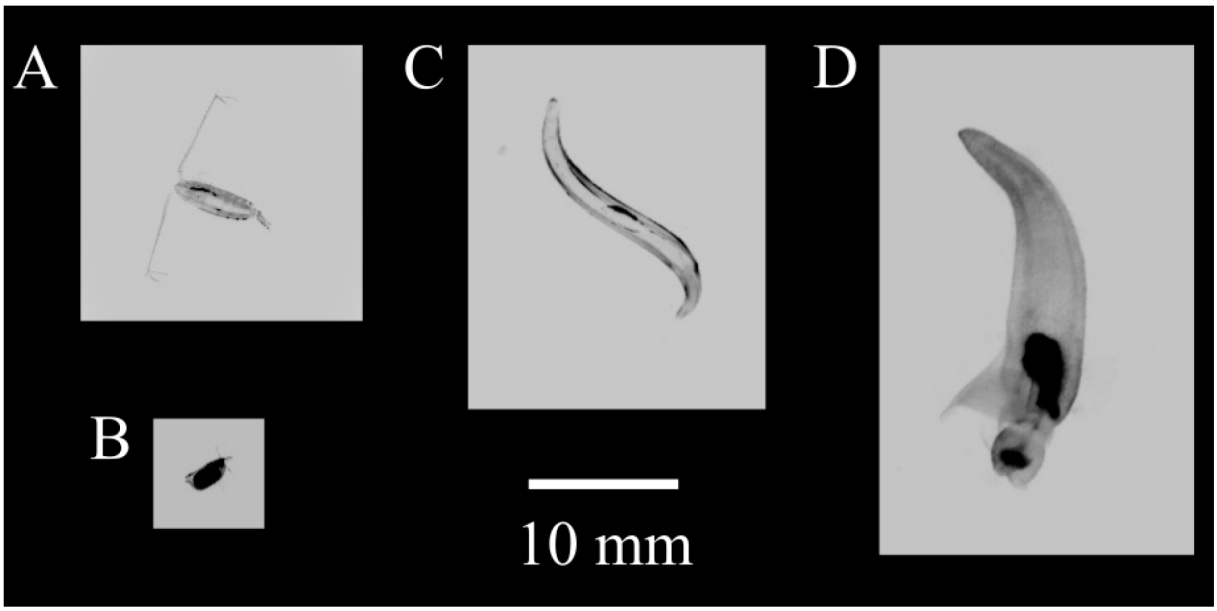

Fig. 4: Examples for zooplankton: (A) Copepod, (B) Ostracod, (C) Chaetognath and (D) Pteropod

When zooplankton (Fig. 4), such as copepods, feed on organic material, aggregates or fecal pellets, they fragment into smaller aggregates (Briggs et al. 2020; Dilling and Alldredge 2000; Iversen and Poulsen 2007), and thereby reduce the efficiency of the carbon export (Briggs et al. 2020). Fragmentation has been suggested to be advantageous to the zooplankton since in the process nutritious value is added to the aggregates by enhancing the growth of microbes on the aggregates (Mayor et al. 2014).

Microbial remineralization

While zooplankton interactions with the aggregates are the main driver that influences the carbon attenuation in the epipelagic zone, the microbial degradation is responsible for the majority of carbon attenuation below the surface ocean in the lower mesopelagic zone (500 - 1000 m) and in the deep ocean (Iversen et al. 2010; Stemmann et al. 2004). In some regions, the microbial remineralization even dominates the carbon degradation making up between 70 - 92% of the carbon attenuation (Giering et al. 2014). In general, the microbial remineralization is the regulating carbon attenuation mechanism if only low quantities of primary producers and thus also low zooplankton biomass is available in an ecosystem, e.g. during prebloom (Belcher et al. 2016). While only low average concentrations (10^4 to 10^6 cells ml^{-1}) of prokaryotes are found in the water column (Schattenhofer et al. 2009; Whitman et al. 1998), aggregates contain much higher concentrations of prokaryotes, with bacteria alone amounting to 10^6 to 10^{10} cells cm^{-3} (Thiele et al. 2015). Aggregates are thus a nutrient-rich hot-spot of microbial activity, growth, and carbon turnover (Azam and Long 2001; Azam et al. 1994; Smith et al. 1992). Small protist, e.g. ciliates and nanoflagellates, also take part in the microbial carbon degradation, as they feed on aggregates, fecal pellets, and their associated bacteria (Hansen et al. 1996; Iversen and Robert 2015; Ploug and Grossart 2000; Poulsen and Iversen 2008). Depending on the environmental conditions, the carbon-specific respirations rates by microbes are between 0.03-0.21 d^{-1} (Iversen et al. 2010; Iversen and Ploug 2010; Iversen and Ploug 2013; Iversen and Robert 2015; Ploug and Grossart 2000; Ploug et al. 2008b). The magnitude of the microbial degradation thereby depends on the temperature (Iversen and Ploug 2013) and hydrostatic pressure of the ambient water (see Tamburini et al. 2013 and references therein). Especially in sinking aggregates, the respiration of colonizing bacteria, which originate from the surface ocean, can be heavily impacted and reduced with increasing hydrostatic pressure during sinking (Stief et al. 2021).

How exactly the microbes colonize the aggregates is still not clear. Bacterial colonization of the aggregates seems to take place in the surface ocean in the layer of high chlorophyll in the euphotic zone (Bachmann et al. 2018; Fadeev et al. 2021; Mestre et al. 2018; Thiele et al. 2015). During sinking the aggregate-attached bacterial community is subjected to internal community succession (Fadeev et al. 2021; Thiele et al. 2015). Changes in the available carbon and nutrient sources with continuing degradation while sinking favor a shift from primary degraders to secondary consumers in the aggregates (Datta et al. 2016). Further colonization of the sinking aggregates at depth seems to take place only to a lesser extent (Mestre et al. 2018; Thiele et al. 2015). The aggregate-attached bacteria (Fig. 5) are exported

from the surface ocean to the depth and to the seafloor, where they are released and act as a seeding community (Fadeev et al. 2021; Mestre et al. 2018; Rapp et al. 2018; Ruiz-González et al. 2020).

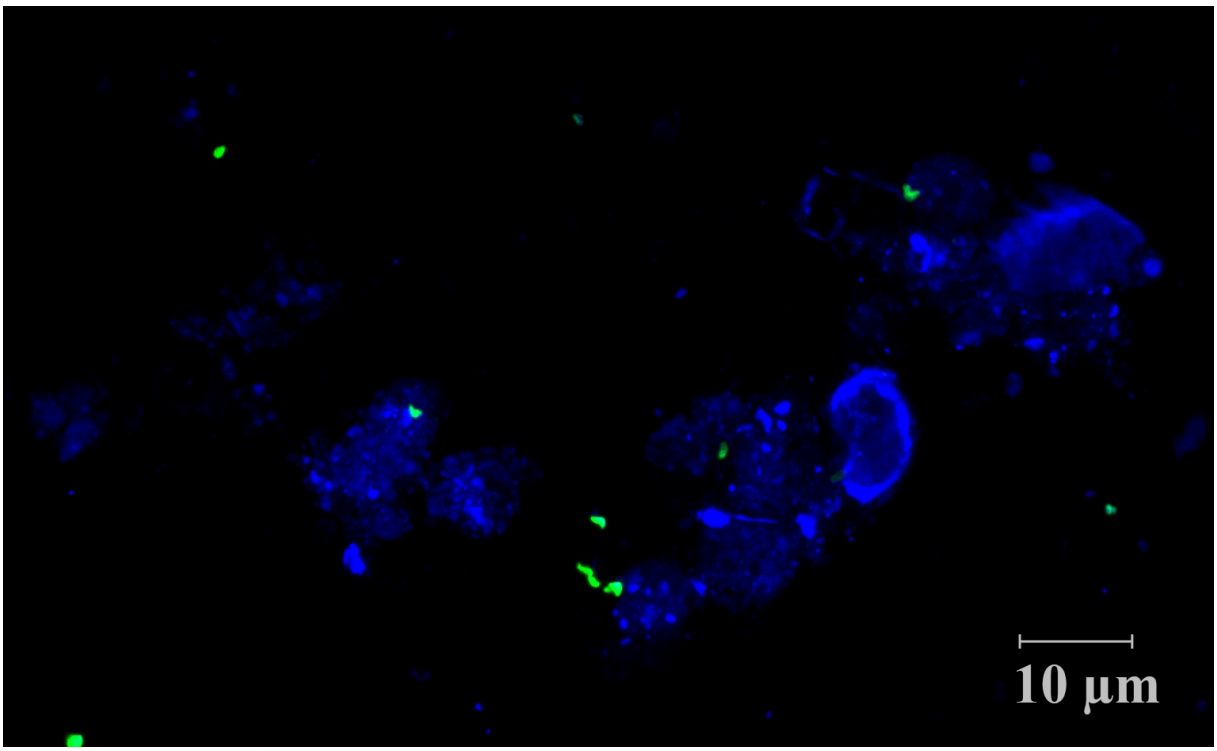

Fig. 5: Aggregate-attached bacteria (green) stained by catalyzed reporter deposition fluorescence *in situ* hybridization (CARD-FISH) with the probe PSA184 (Eilers et al. 2000). Images were acquired using a confocal laser scanning microscope.

The microbes remineralize parts of the aggregates they colonize and release dissolved organic matter (DOM) and nutrients into the surrounding water column (Karthäuser et al. 2021; Kiørboe et al. 2001). Iversen (2023) proposed that aggregates can be enriched in carbon through preferential nutrient recycling by bacteria and zooplankton resulting in higher carbon-to-nutrient ratios within the aggregates that are exported. The high rates of nutrients released from the sinking aggregates could thereby support further primary production in the surface ocean, which might lead to enhanced carbon export through remineralization (Iversen 2023). Furthermore, organic carbon can also be transformed into recalcitrant dissolved organic matter by microbes (termed the microbial carbon pump), which enhances the carbon storage time in the ocean (Jiao et al. 2010).

Carbon export in fjords

Carbon is not only stored in the open ocean and deep-sea sediments but also in fjords' basins world-wide (Smith et al. 2015). 18 Mt of organic carbon are sequestered in fjord sediments per year (Smith et al. 2015). This means that fjord sediments provide for 11% of the global annual marine carbon burial (Smith et al. 2015). In particular fjords with deep basins can be effective carbon storage locations if deep water is retained, e.g. by submarine sills, and is subjected to little mixing and little oxygen intrusion, resulting in deep-water anoxia (Sørensen et al. 2015; Zaikova et al. 2010). This lowers the carbon attenuation and enhance the carbon sequestration potential in the fjord basins, as low oxygen or anoxic conditions reduce the turnover of organic matter by microbes and zooplankton as seen in oxygen minimum zones (Cavan et al. 2017; Devol and Hartnett 2001; Weber and Bianchi 2020). Furthermore, estuarine water movement can transport organic matter from the adjacent shelf into the fjord, where it can be stored within the basins (Sørensen et al. 2015).

In polar ecosystems the ongoing global warming and intrusion of subtropical water reduces the glaciers and ice coverage in the fjords (Straneo et al. 2010). The ongoing ice melt has already caused considerable changes in high latitude ecosystems and it is expected to continue to impact future ecosystems. Longer ice-free periods result in an intensification of primary production due to longer light availabilities throughout the year, which might enhance the carbon export in fjord systems in the future (Rysgaard and Glud 2007; Sørensen et al. 2015). Land-terminating glaciers release lithogenic material in their run-offs that can limit the light availability in the water and thus the primary production (Meire et al. 2017; Murray et al. 2015; Seifert et al. 2019). On the other hand, increasing silt input from the glaciers can also enhance the carbon export in the fjord by silt-ballasting of aggregates (Seifert et al. 2019). Marine-terminating glacier often release meltwater below the surface, which then ascends and thereby brings up nutrients from deeper water layers enhancing the primary productivity (Kanna et al. 2018; Meire et al. 2017). However, marine-terminated glaciers will likely be less important in the future due to their retreat to the dry land (Howat and Eddy 2011; Meire et al. 2017). Increasing ice melt generally intensifies the stratification and lowers the salinities in polar fjords, forming surface meltwater layers (Meire et al. 2017; Seifert et al. 2019). Changes in circulation, nutrient supply, light, and lithogenic material availability will likely impact the community structure of primary producers, consumers, and biogeochemical processes. As the biogeochemistry and export processes in polar fjords are widely uninvestigated, this makes further detailed research necessary to understand the current and future potential for carbon export and sequestration in fjords and their role in the global carbon cycling.

Carbon export in the Arctic Ocean

Polar regions like the Arctic are highly impacted by climate change: Especially rising temperature and decreasing ice coverage will change the Arctic ecosystem (Wassmann 2011). The Arctic ecosystem is characterized by strong seasonality in the primary production due to ice coverage and limited light availability (Hill and Cota 2005; Sakshaug 2004). Ice algae form blooms under the sea-ice, which are efficiently exported during ice-melt (Arrigo et al. 2012; Boetius et al. 2013). When the ice breaks and high light and nutrient conditions are prevailing, rapid phytoplankton blooms develop (Hill and Cota 2005; Sakshaug 2004), which fuel zooplankton growth. Zooplankton seem to be responsible for a strong carbon attenuation in the upper ocean in the Arctic, with few zooplankton key species, i.e. *Calanus* and *Pseudocalanus*, accounting for 60 - 67 % of the degradation (van der Jagt et al. 2020).

In the past, the flux of organic matter was mainly dominated by spring bloom of diatoms and large phytoplankton cells (Buesseler 1998). At present, the increasing freshwater-input by melting ice in the Arctic increases stratification of the water masses, which leads to lower nutrient supply from depth, and thus impairs phytoplankton growth and primary production (Carmack and McLaughlin 2011). This will probably lead to a shift in the Arctic phytoplankton community towards small-celled organisms in the future (Li et al. 2009). The abundance of flagellate primary producers, such as *Phaeocystis spp.*, will likely increase in the future (Nöthig et al. 2015). This is predicted to decrease the carbon export efficiency in the Arctic, as aggregates made from *Phaeocystis spp.* under ice-free conditions have lower sinking velocities than diatom aggregates and are more likely to be recycled (Fadeev et al. 2021; Reigstad and Wassmann 2007). Consequently, it is necessary to investigate how the increasing extent of ice-free regions and time periods will affect the Arctic ecosystem, the biogeochemical processes, and the carbon export in the Arctic.

Carbon export in the Southern Ocean

The Antarctic ecosystem is – like the Arctic ecosystem – highly impacted by climate change with increasing sea surface temperature and decreasing sea ice cover (Constable et al. 2014). Though being one of the smaller principal oceans, the Southern Ocean alone is responsible for around 40% of the carbon dioxide uptake in the oceans worldwide (Frölicher et al. 2015; Khatiwala et al. 2009). It is mostly dominated by high nutrient and low chlorophyll (HNCL) regions, i.e. regions with a large concentration of macronutrients, such as nitrogen and phosphate, but with low phytoplankton productivity (Comiso et al. 1993; Martin et al. 1990). This is primarily due the limited availability of iron in the Southern Ocean (Boyd et al. 2007;

Martin et al. 1990). Intense spring and summer blooms can develop in case of iron input, e.g. by the sediments from the shelf or land around islands like South Georgia (Borrione and Schlitzer 2013; Korb and Whitehouse 2004; Korb et al. 2008; Manno et al. 2015), Kerguelen (Blain et al. 2008; Blain et al. 2001; Rembauville et al. 2015a; Rembauville et al. 2015b) and Crozet (Pollard et al. 2009; Salter et al. 2012). Characteristic for iron fertilization is the development of large blooms, mostly by diatoms, which can account for more than 85% of the phytoplankton primary production in the Southern Ocean (Quéguiner 2013; Rousseaux and Gregg 2013). Due to their large size and silica frustules, diatoms dominate the export of the biological carbon in that region (Assmy et al. 2013; Buesseler et al. 2001; Rigual-Hernández et al. 2016) either by sinking out of the surface ocean directly or by being fed on by zooplankton and leaving the upper ocean as silica-ballasted fecal pellets (Belcher et al. 2017; Manno et al. 2015).

Interestingly, an opposite relationship of the primary production and the export efficiency in the Southern Ocean has been observed, i.e. high phytoplankton biomass and concurrent low carbon export conditions (Lam and Bishop 2007). The export efficiencies decrease with increasing primary production, suggesting a decoupling of the primary production and carbon export in the Southern Ocean and pointing towards a relative constant POC export to depth independent to the phytoplankton stock in the surface ocean (Cavan et al. 2015; Laurenceau-Cornec et al. 2015; Maiti et al. 2013; Martin et al. 2013). Reasons for this constant export flux could be the reprocessing and fragmentation of the organic matter by zooplankton (Cavan et al. 2015; Lam and Bishop 2007; Martin et al. 2013), the remineralization by microbes (Obernosterer et al. 2008) or changes in the phytoplankton community (Laurenceau-Cornec et al. 2015). However, the involved processes which explain carbon retention in the surface ocean and the low export to deeper depths are still unclear.

Aims, objectives and research questions

Polar regions and ecosystems are drastically affected by the climate change, especially impacted by increasing temperatures and ice melt (IPCC 2021). The aim of this PhD thesis is to characterize particle fluxes and carbon export mechanisms in polar regions under changing environmental conditions. The present PhD thesis will help to understand the impact of on-going ice melt and enhanced stratification in polar regions on the efficiency and magnitude of carbon export via the biological carbon pump. This is done by looking at three different oceanic systems in the Arctic and the Antarctic, which are addressed in the following chapters:

In **Chapter I**, the carbon export via aggregates in an Arctic fjord was explored. The detailed processes of formation, transport, and transformation of the aggregates in the fjord were investigated using 16S and 18S rDNA sequencing, *in situ* camera profiles, and biogeochemical flux measurements to assess how estuarine lateral water movement affects the carbon export in the fjord.

As second study area, the particle export in the open waters of the Southern Ocean north to the North Scotia Ridge, near to the island South Georgia was investigated (**Chapter II**). The temporal development of particle export during a bloom was surveyed using *in situ* camera profiles and *in situ* sinking velocity measurements in high-temporal resolution. The measurements were used to evaluate how vertical gradients in densities and salinities influence the carbon export.

The third chapter focused on carbon export in a polar front at the marginal ice zone in the Fram Strait in the Arctic Ocean (**Chapter III**). Thereby, biogeochemical flux and primary production measurements, data of different *in situ* camera systems, sinking velocity and respiration measurements were combined with physical oceanographic measurements in the front system to investigate the impact of the complex movement and the characteristics of the water masses, as well as varying ice conditions, on the carbon export.

The overarching scientific question of this PhD thesis is, what is driving carbon export and flux attenuation in polar regions, i.e. in a Greenlandic fjord (**Chapter I)**, in Southern Ocean open waters (**Chapter II)** and at the ice-edge in Fram Strait (**Chapter III)**.

For this, several research questions are addressed in the following chapters:

- How and where are the aggregates formed in different polar systems (**Chapter I, Chapter III**)?
- What retains aggregates in the upper ocean (**Chapter I, Chapter II**)?

- How is carbon export and vertical connectivity impacted by lateral advection, physical oceanographic processes and transformation, e.g. by zooplankton activity (**Chapter I, Chapter II, Chapter III**)?
- What is influencing the spatial and temporal variability in the carbon export and which mechanism can explain the mismatch between the primary production and carbon export in the mesopelagic zone (**Chapter I, Chapter II, Chapter III**)?

The underlying hypotheses investigated were:

1. Aggregate formation takes place at the depth of the highest particle concentration at the depth of high chlorophyll. This is also the place of bacteria colonization.
2. The main share of aggregates is retained in the upper ocean due to physical properties, i.e. salinity gradients.
3. The particle retention depends on the aggregate type and size: Mainly smaller and denser aggregates, e.g. fecal pellets and ballasted phytoplankton aggregates, are able to pass increasing density gradients and be exported out of the epipelagic zone.
4. During their descend through the water column, organic aggregates undergo transformation, e.g. by zooplankton feeding, which changes the aggregate characteristics with increasing depth.
5. In polar regions, effective carbon export through aggregates is a result of ballasting by minerals, zooplankton transformation, and physical subduction processes. Carbon export is impacted by lateral advection in the water layers.

References

Alldredge, A. L., and Silver, M. W. (1988). "Characteristics, Dynamics and Significance of Marine Snow." *Progress in Oceanography*, 20(1), 41-82.

Alldredge, A. L., Passow, U., and Logan, B. E. (1993). "The abundance and significance of a class of large, transparent organic particles in the ocean." *Deep Sea Research Part I: Oceanographic Research Papers*, 40(6), 1131-1140.

Alldredge, A. L., Cowles, T. J., MacIntyre, S., Rines, J. E. B., Donaghay, P. L., Greenlaw, C. F., Holliday, D. V., Dekshenieks, M. M., Sullivan, J. M., and Zaneveld, J. R. V. (2002). "Occurrence and mechanisms of formation of a dramatic thin layer of marine snow in a shallow Pacific fjord." *Marine Ecology Progress Series*, 233, 1-12.

Alldredge, A. (2005). "The contribution of discarded appendicularian houses to the flux of particulate organic carbon from oceanic surface waters." *In G. Gorsky [ed.], Response of Marine Ecosystems to Global Change: Ecological Impact of Appendicularians. GB Science Publishers- Éditions scientifiques*, 309-326.

Arrigo, K. R., Perovich, D. K., Pickart, R. S., Brown, Z. W., van Dijken, G. L., Lowry, K. E., Mills, M. M., Palmer, M. A., Balch, W. M., Bahr, F., Bates, N. R., Benitez-Nelson, C., Bowler, B., Brownlee, E., Ehn, J. K., Frey, K. E., Garley, R., Laney, S. R., Lubelczyk, L., Mathis, J., Matsuoka, A., Mitchell, B. G., Moore, G. W. K., Ortega-Retuerta, E., Pal, S., Polashenski, C. M., Reynolds, R. A., Schieber, B., Sosik, H. M., Stephens, M., and Swift, J. H. (2012). "Massive Phytoplankton Blooms Under Arctic Sea Ice." *Science*, 336(6087), 1408-1408.

Assmy, P., Smetacek, V., Montresor, M., Klaas, C., Henjes, J., Strass, V. H., Arrieta, J. M., Bathmann, U., Berg, G. M., Breitbarth, E., Cisewski, B., Friedrichs, L., Fuchs, N., Herndl, G. J., Jansen, S., Krägefsky, S., Latasa, M., Peeken, I., Röttgers, R., Scharek, R., Schüller, S. E., Steigenberger, S., Webb, A., and Wolf-Gladrow, D. (2013). "Thick-shelled, grazer-protected diatoms decouple ocean carbon and silicon cycles in the iron-limited Antarctic Circumpolar Current." *Proceedings of the National Academy of Sciences*, 110(51), 20633-20638.

Azam, F., and Long, R. A. (2001). "Sea snow microcosms." *Nature*, 414(6863), 495-498.

Azam, F., Smith, D. C., Steward, G. F., and Hagström, Å. (1994). "Bacteria-Organic Matter Coupling and Its Significance for Oceanic Carbon Cycling." *Microbial Ecology*, 28, 167-179.

Azetsu-Scott, K., and Passow, U. (2004). "Ascending marine particles: Significance of transparent exopolymer particles (TEP) in the upper ocean." *Limnology and Oceanography*, 49(3), 741-748.

Bachmann, J., Heimbach, T., Hassenrück, C., Kopprio, G. A., Iversen, M. H., Grossart, H. P., and Gärdes, A. (2018). "Environmental Drivers of Free-Living vs. Particle-Attached Bacterial Community Composition in the Mauritania Upwelling System." *Frontiers in Microbiology*, 9, 2836.

Bathmann, U. V., Noji, T. T., and von Bodungen, B. (1991). "Sedimentation of pteropods in the Norwegian Sea in autumn." *Deep Sea Research Part A. Oceanographic Research Papers*, 38(10), 1341-1360.

Belcher, A., Iversen, M., Manno, C., Henson, S. A., Tarling, G. A., and Sanders, R. (2016). "The role of particle associated microbes in remineralization of fecal pellets in the upper mesopelagic of the Scotia Sea, Antarctica." *Limnology and Oceanography*, 61(3), 1049-1064.

Belcher, A., Tarling, G. A., Manno, C., Atkinson, A., Ward, P., Skaret, G., Fielding, S., Henson, S. A., and Sanders, R. (2017). "The potential role of Antarctic krill faecal pellets in efficient carbon export at the marginal ice zone of the South Orkney Islands in spring." *Polar Biology*, 40(10), 2001-2013.

Biermann, A., and Engel, A. (2010). "Effect of CO_2 on the properties and sinking velocity of aggregates of the coccolithophore *Emiliania huxleyi*." *Biogeosciences*, 7(3), 1017-1029.

Blain, S., Tréguer, P., Belviso, S., Bucciarelli, E., Denis, M., Desabre, S., Fiala, M., Martin Jézéquel, V., Le Fèvre, J., Mayzaud, P., Marty, J.-C., and Razouls, S. (2001). "A biogeochemical study of the island mass effect in the context of the iron hypothesis: Kerguelen Islands, Southern Ocean." *Deep Sea Research Part I: Oceanographic Research Papers*, 48(1), 163-187.

Blain, S., Sarthou, G., and Laan, P. (2008). "Distribution of dissolved iron during the natural iron-fertilization experiment KEOPS (Kerguelen Plateau, Southern Ocean)." *Deep Sea Research Part II: Topical Studies in Oceanography*, 55(5-7), 594-605.

Boetius, A., Albrecht, S., Bakker, K., Bienhold, C., Felden, J., Fernández-Méndez, M., Hendricks, S., Katlein, C., Lalande, C., Krumpen, T., Nicolaus, M., Peeken, I., Rabe, B., Rogacheva, A., Rybakova, E., Somavilla, R., and Wenzhöfer, F. (2013). "Export of Algal Biomass from the Melting Arctic Sea Ice." *Science*, 339(6126), 1430-1432.

Borrione, I., and Schlitzer, R. (2013). "Distribution and recurrence of phytoplankton blooms around South Georgia, Southern Ocean." *Biogeosciences*, 10(1), 217-231.

Boyd, P. W., Jickells, T., Law, C. S., Blain, S., Boyle, E. A., Buesseler, K. O., Coale, K. H., Cullen, J. J., de Baar, H. J. W., Follows, M., Harvey, M., Lancelot, C., Levasseur, M., Owens, N. P. J., Pollard, R., Rivkin, R. B., Sarmiento, J., Schoemann, V., Smetacek, V., Takeda, S., Tsuda, A., Turner, S., and Watson, A. J. (2007). "Mesoscale Iron Enrichment Experiments 1993-2005: Synthesis and Future Directions." *Science*, 315(5812), 612-617.

Boyd, P. W., Claustre, H., Levy, M., Siegel, D. A., and Weber, T. (2019). "Multi-faceted particle pumps drive carbon sequestration in the ocean." *Nature*, 568(7752), 327-335.

Briggs, N., Dall'Olmo, G., and Claustre, H. (2020). "Major role of particle fragmentation in regulating biological sequestration of CO_2 by the oceans." *Science*, 367(6479), 791-793.

Bruland, K. W., and Silver, M. W. (1981). "Sinking Rates of Fecal Pellets from Gelatinous Zooplankton (Salps, Pteropods, Doliolids)." *Marine Biology*, 63(3), 295-300.

Buesseler, K. O. (1998). "The decoupling of production and particulate export in the surface ocean." *Global Biogeochemical Cycles*, 12(2), 297-310.

Buesseler, K. O., Ball, L., Andrews, J., Cochran, J. K., Hirschberg, D. J., Bacon, M. P., Fleer, A., and Brzezinski, M. (2001). "Upper ocean export of particulate organic carbon and biogenic silica in the Southern Ocean along 170°W." *Deep Sea Research Part II: Topical Studies in Oceanography*, 48(19-20), 4275-4297.

Buitenhuis, E. T., Le Quéré, C., Bednaršek, N., and Schiebel, R. (2019). "Large Contribution of Pteropods to Shallow $CaCO_3$ Export." *Global Biogeochemical Cycles*, 33(3), 458-468.

Burd, A. B., and Jackson, G. A. (2009). "Particle Aggregation." *Annual Review of Marine Science*, 1(1), 65-90.

Carmack, E., and McLaughlin, F. (2011). "Towards recognition of physical and geochemical change in Subarctic and Arctic Seas." *Progress in Oceanography*, 90(1-4), 90-104.

Cavan, E., Le Moigne, F. A. C., Poulton, A. J., Tarling, G. A., Ward, P., Daniels, C. J., Fragoso, G. M., and Sanders, R. J. (2015). "Attenuation of particulate organic carbon flux in the Scotia Sea, Southern Ocean, is controlled by zooplankton fecal pellets." *Geophysical Research Letters*, 42(3), 821-830.

Cavan, E. L., Trimmer, M., Shelley, F., and Sanders, R. (2017). "Remineralization of particulate organic carbon in an ocean oxygen minimum zone." *Nature Communications*, 8(1), 4847.

Comiso, J. C., McClain, C. R., Sullivan, C. W., Ryan, J. P., and Leonard, C. L. (1993). "Coastal Zone Color Scanner Pigment Concentrations in the Southern Ocean and Relationships to Geophysical Surface Features." *Journal of Geophysical Research: Oceans*, 98(C2), 2419-2451.

Constable, A. J., Melbourne-Thomas, J., Corney, S. P., Arrigo, K. R., Barbraud, C., Barnes, D. K., Bindoff, N. L., Boyd, P. W., Brandt, A., Costa, D. P., Davidson, A. T., Ducklow, H. W., Emmerson, L., Fukuchi, M., Gutt, J., Hindell, M. A., Hofmann, E. E., Hosie, G. W., Iida, T., Jacob, S., Johnston, N. M., Kawaguchi, S., Kokubun, N., Koubbi, P., Lea, M.-A., Makhado, A., Massom, R. A., Meiners, K., Meredith, M. P., Murphy, E. J., Nicol, S., Reid, K., Richerson, M. P., Riddle, M. J., Rintoul, S. R., Smith Jr., W. O., Southwell, C., Stark, J. S., Summer, M., Swadling, K. M., Takahashi, K. T., Trathan, P. N., Welsford, D. C., Weimerskirch, H., Westwood, K. J., Wienecker, B. C., Wolf-Gladrow, D., Wright, S. W., Xavier, J. C., and Ziegler, P. (2014). "Climate change and Southern Ocean ecosystems I: how changes in physical habitats directly affect marine biota." *Global Change Biology*, 20(10), 3004-3025.

Datta, M. S., Sliwerska, E., Gore, J., Polz, M. F., and Cordero, O. X. (2016). "Microbial interactions lead to rapid micro-scale successions on model marine particles." *Nature Communications*, 7(1), 11965.

De La Rocha, C. L., and Passow, U. (2007). "Factors influencing the sinking of POC and the efficiency of the biological carbon pump." *Deep Sea Research Part II: Topical Studies in Oceanography*, 54(5-7), 639-658.

Devol, A. H., and Hartnett, H. E. (2001). "Role of the oxygen-deficient zone in transfer of organic carbon to the deep ocean." *Limnology and Oceanography*, 46(7), 1684-1690.

Dilling, L., and Alldredge, A. L. (2000). "Fragmentation of marine snow by swimming macrozooplankton: A new process impacting carbon cycling in the sea." *Deep Sea Research Part I: Oceanographic Research Papers*, 47(7), 1227-1245.

Ducklow, H. W., Steinberg, D. K., and Buesseler, K. O. (2001). "Upper Ocean Carbon Export and the Biological Pump." *Oceanography*, 14(4), 50-58.

Eilers, H., Pernthaler, J., Glöckner, F. O., and Amann, R. (2000). "Culturability and In Situ Abundance of Pelagic Bacteria from the North Sea." *Applied and Environmental Microbiology*, 66(7), 3044-3051.

Engel, A. (2000). "The role of transparent exopolymer particles (TEP) in the increase in apparent particle stickiness (α) during the decline of a diatom bloom." *Journal of Plankton Research*, 22(3), 485-497.

Eppley, R. W., and Peterson, B. J. (1979). "Particulate organic matter flux and planktonic new production in the deep ocean." *Nature*, 282(5740), 677-680.

Fadeev, E., Rogge, A., Ramondenc, S., Nöthig, E.-M., Wekerle, C., Bienhold, C., Salter, I., Waite, A. M., Hehemann, L., Boetius, A., and Iversen, M. H. (2021). "Sea ice presence is linked to higher carbon export and vertical microbial connectivity in the Eurasian Arctic Ocean." *Communications Biology*, 4(1), 1255.

Falkowski, P. G., Barber, R. T., and Smetacek, V. (1998). "Biogeochemical Controls and Feedbacks on Ocean Primary Production." *Science*, 281(5374), 200-206.

Falkowski, P., Scholes, R. J., Boyle, E., Canadell, J., Canfield, D., Elser, J., Gruber, N., Hibbard, K., Högberg, P., Linder, S., Mackenzie, F. T., Moore III, B., Pedersen, T., Rosenthal, Y., Seitzinger, S., Smetacek, V., and Steffen, W. (2000). "The Global Carbon Cycle: A Test of Our Knowledge of Earth as a System." *Science*, 290(5490), 291-296.

Fowler, S. W., and Knauer, G. A. (1986). "Role of Large Particles in the Transport of Elements and Organic Compounds Through the Oceanic Water Column." *Progress in Oceanography*, 16(3), 147-194.

Frölicher, T. L., Sarmiento, J. L., Paynter, D. J., Dunne, J. P., Krasting, J. P., and Winton, M. (2015). "Dominance of the Southern Ocean in Anthropogenic Carbon and Heat Uptake in CMIP5 Models." *Journal of Climate*, 28(2), 862-886.

Gärdes, A., Iversen, M. H., Grossart, H.-P., Passow, U., and Ullrich, M. S. (2011). "Diatom-associated bacteria are required for aggregation of *Thalassiosira weissflogii*." *The ISME Journal*, 5(3), 436-445.

Gargett, A. E., Merryfield, W. J., and Holloway, G. (2003). "Direct Numerical Simulation of Differential Scalar Diffusion in Three-Dimensional Stratified Turbulence." *Journal of Physical Oceanography*, 33(8), 1758-1782.

Geilfus, N. X., Galley, R. J., Cooper, M., Halden, N., Hare, A., Wang, F., Søgaard, D. H., and Rysgaard, S. (2013). "Gypsum crystals observed in experimental and natural sea ice." *Geophysical Research Letters*, 40(24), 6362-6367.

Giering, S. L. C., Sanders, R., Lampitt, R. S., Anderson, T. R., Tamburini, C., Boutrif, M., Zubkov, M. V., Marsay, C. M., Henson, S. A., Saw, K., Cook, K., and Mayor, D. J. (2014). "Reconciliation of the carbon budget in the ocean's twilight zone." *Nature*, 507(7493), 480-483.

Hamm, C. E. (2002). "Interactive aggregation and sedimentation of diatoms and clay-sized lithogenic material." *Limnology and Oceanography*, 47(6), 1790-1795.

Hansen, B., Fotel, F. L., Jensen, N. J., and Madsen, S. D. (1996). "Bacteria associated with a marine planktonic copepod in culture. II. Degradation of fecal pellets produced on a diatom, a nanoflagellate or a dinoflagellate diet." *Journal of Plankton Research*, 18(2), 275-288.

Heinze, C., Meyer, S., Goris, N., Anderson, L., Steinfeldt, R., Chang, N., Le Quére, C., and Bakker, D. C. E. (2015). "The ocean carbon sink – impacts, vulnerabilities and challenges." *Earth System Dynamics*, 6(1), 327-358.

Hill, V., and Cota, G. (2005). "Spatial patterns of primary production on the shelf, slope and basin of the Western Arctic in 2002." *Deep Sea Research Part II: Topical Studies in Oceanography*, 52(24-26), 3344-3354.

Howat, I. M., and Eddy, A. (2011). "Multi-decadal retreat of Greenland's marine-terminating glaciers." *Journal of Glaciology*, 57(203), 389-396.

IPCC. (2013). "Climate Change 2013: The Physical Science Basis. Contribution of Working Group I to the Fifth Assessment Report of the Intergovernmental Panel on Climate Change [Stocker, T. F., Qin, D., Plattner, G.-K., Tignor, M., Allen, S. K., Boschung, J., Nauels, A., Xia, Y., Bex, V., and Midgley, P. M. (eds.)]. Cambridge University Press, Cambridge, United Kingdom and New York, NY, USA, 1535 pp.".

IPCC. (2021). "Climate Change 2021: The Physical Science Basis. Contribution of Working Group I to the Sixth Assessment Report of the Intergovernmental Panel on Climate Change [Masson-Delmotte, V., Zhai, P., Pirani, A., Connors, S. L., Péan, C., Berger, S., Caud, N., Chen, Y., Goldfarb, L., Gomis, M. I., Huang, M., Leitzell, K., Lonnoy, E., Matthews, J. B. R., Maycock, T. K., Waterfield, T., Yelekçi, O., Yu, R., and Zhou, B. (eds.)]. Cambridge University Press, Cambridge, United Kingdom and New York, NY, USA, 2391 pp.".

Iversen, M. H., and Poulsen, L. K. (2007). "Coprorhexy, coprophagy, and coprochaly in the copepods *Calanus helgolandicus*, *Pseudocalanus elongatus*, and *Oithona similis*." *Marine Ecology Progress Series*, 350, 79-89.

Iversen, M. H., and Ploug, H. (2010). "Ballast minerals and the sinking carbon flux in the ocean: carbon-specific respiration rates and sinking velocity of marine snow aggregates." *Biogeosciences*, 7(9), 2613-2624.

Iversen, M. H., Nowald, N., Ploug, H., Jackson, G. A., and Fischer, G. (2010). "High resolution profiles of vertical particulate organic matter export off Cape Blanc, Mauritania: Degradation processes and ballasting effects." *Deep Sea Research Part I: Oceanographic Research Papers*, 57(6), 771-784.

Iversen, M. H., and Ploug, H. (2013). "Temperature effects on carbon-specific respiration rate and sinking velocity of diatom aggregates – potential implications for deep ocean export processes." *Biogeosciences*, 10(6), 4073-4085.

Iversen, M. H., and Robert, M. L. (2015). "Ballasting effects of smectite on aggregate formation and export from a natural plankton community." *Marine Chemistry*, 175, 18-27.

Iversen, M. H., and Lampitt, R. S. (2020). "Size does not matter after all: no evidence for a size-sinking relationship for marine snow." *Progress in Oceanography*, 189, 102445.

Iversen, M. H. (2023). "Carbon Export in the Ocean: A Biologist's Perspective." *Annual Review of Marine Science*, 15(1), 357-381.

Jackson, G. A., and Checkley Jr, D. M. (2011). "Particle size distributions in the upper 100 m water column and their implications for animal feeding in the plankton." *Deep Sea Research Part I: Oceanographic Research Papers*, 58(3), 283-297.

Jiao, N., Herndl, G. J., Hansell, D. A., Benner, R., Kattner, G., Wilhelm, S. W., Kirchman, D. L., Weinbauer, M. G., Luo, T., and Chen, F. (2010). "Microbial production of recalcitrant dissolved organic matter: long-term carbon storage in the global ocean." *Nature Reviews Microbiology*, 8(8), 593-599.

Jin, X., Gruber, N., Dunne, J. P., Sarmiento, J. L., and Armstrong, R. A. (2006). "Diagnosing the contribution of phytoplankton functional groups to the production and export of particulate organic carbon, $CaCO_3$, and opal from global nutrient and alkalinity distributions." *Global Biogeochemical Cycles*, 20(2).

Kanna, N., Sugiyama, S., Ohashi, Y., Sakakibara, D., Fukamachi, Y., and Nomura, D. (2018). "Upwelling of Macronutrients and Dissolved Inorganic Carbon by a Subglacial Freshwater Driven Plume in Bowdoin Fjord, Northwestern Greenland." *Journal of Geophysical Research: Biogeosciences*, 123(5), 1666-1682.

Karthäuser, C., Ahmerkamp, S., Marchant, H. K., Bristow, L. A., Hauss, H., Iversen, M. H., Kiko, R., Maerz, J., Lavik, G., and Kuypers, M. M. (2021). "Small sinking particles control anammox rates in the Peruvian oxygen minimum zone." *Nature Communications*, 12(1), 3235.

Keeling, C. D. (1968). "Carbon dioxide in surface ocean waters: 4. Global distribution." *Journal of Geophysical Research (1896-1977)*, 73(14), 4543-4553.

Keeling, C. D., Piper, S. C., Bacastow, R. B., Wahlen, M., Whorf, T. P., Heimann, M., and Meijer, H. A. (2001). "Exchanges of Atmospheric CO_2 and $^{13}CO_2$ with the Terrestrial Biosphere and Oceans from 1978 to 2000. I. Global aspects." *UC San Diego: Scripps Institution of Oceanography*, SIO Reference Series No. 01-06.

Khatiwala, S., Primeau, F., and Hall, T. (2009). "Reconstruction of the history of anthropogenic CO_2 concentrations in the ocean." *Nature*, 462(7271), 346-349.

Kindler, K., Khalili, A., and Stocker, R. (2010). "Diffusion-limited retention of porous particles at density interfaces." *Proceedings of the National Academy of Sciences*, 107(51), 22163-22168.

Kiørboe, T. (2001). "Formation and fate of marine snow: small-scale processes with large-scale implications." *Scientia Marina*, 65(S2), 57-71.

Kiørboe, T., Ploug, H., and Thygesen, U. H. (2001). "Fluid motion and solute distribution around sinking aggregates. I. Small-scale fluxes and heterogeneity of nutrients in the pelagic environment." *Marine Ecology Progress Series*, 211, 1-13.

Klaas, C., and Archer, D. E. (2002). "Association of sinking organic matter with various types of mineral ballast in the deep sea: Implications for the rain ratio." *Global Biogeochemical Cycles*, 16(4), 63-1 - 63-14.

Korb, R. E., and Whitehouse, M. (2004). "Contrasting primary production regimes around South Georgia, Southern Ocean: large blooms versus high nutrient, low chlorophyll waters." *Deep Sea Research Part I: Oceanographic Research Papers*, 51(5), 721-738.

Korb, R. E., Whitehouse, M. J., Atkinson, A., and Thorpe, S. E. (2008). "Magnitude and maintenance of the phytoplankton bloom at South Georgia: a naturally iron-replete environment." *Marine Ecology Progress Series*, 368, 75-91.

Kwon, E. Y., Primeau, F., and Sarmiento, J. L. (2009). "The impact of remineralization depth on the air–sea carbon balance." *Nature Geoscience*, 2(9), 630-635.

Lam, P. J., and Bishop, J. K. (2007). "High biomass, low export regimes in the Southern Ocean." *Deep Sea Research Part II: Topical Studies in Oceanography*, 54(5-7), 601-638.

Laurenceau-Cornec, E. C., Trull, T. W., Davies, D. M., Bray, S. G., Doran, J., Planchon, F., Carlotti, F., Jouandet, M.-P., Cavagna, A.-J., Waite, A. M., and Blain, S. (2015). "The relative importance of phytoplankton aggregates and zooplankton fecal pellets to carbon export: insights from free-drifting sediment trap deployments in naturally iron-fertilised waters near the Kerguelen Plateau." *Biogeosciences*, 12(4), 1007-1027.

Li, W. K. W., McLaughlin, F. A., Lovejoy, C., and Carmack, E. C. (2009). "Smallest Algae Thrive as the Arctic Ocean Freshens." *Science*, 326(5952), 539.

MacFarling Meure, C., Etheridge, D., Trudinger, C., Steele, P., Langenfelds, R., van Ommen, T., Smith, A., and Elkins, J. (2006). "Law Dome CO_2, CH_4 and N_2O ice core records extended to 2000 years BP." *Geophysical Research Letters*, 33(14).

MacIntyre, S., Alldredge, A. L., and Gotschalk, C. C. (1995). "Accumulation of marines now at density discontinuities in the water column." *Limnology and Oceanography*, 40(3), 449-468.

Maiti, K., Charette, M. A., Buesseler, K. O., and Kahru, M. (2013). "An inverse relationship between production and export efficiency in the Southern Ocean." *Geophysical Research Letters*, 40(8), 1557-1561.

Manno, C., Stowasser, G., Enderlein, P., Fielding, S., and Tarling, G. A. (2015). "The contribution of zooplankton faecal pellets to deep-carbon transport in the Scotia Sea (Southern Ocean)." *Biogeosciences*, 12(6), 1955-1965.

Mari, X., Passow, U., Migon, C., Burd, A. B., and Legendre, L. (2017). "Transparent exopolymer particles: Effects on carbon cycling in the ocean." *Progress in Oceanography*, 151, 13-37.

Martin, J. H., Gordon, R. M., and Fitzwater, S. E. (1990). "Iron in Antarctic waters." *Nature*, 345(6271), 156-158.

Martin, P., van der Loeff, M. R., Cassar, N., Vandromme, P., d'Ovidio, F., Stemmann, L., Rengarajan, R., Soares, M., González, H. E., Ebersbach, F., Lampitt, R. S., Sanders, R., Barnett, B. A., Smetacek, V., and Naqvi, S. W. A. (2013). "Iron fertilization enhanced net community production but not downward particle flux during the Southern Ocean iron fertilization experiment LOHAFEX." *Global Biogeochemical Cycles*, 27(3), 871-881.

Mayor, D. J., Sanders, R., Giering, S. L. C., and Anderson, T. R. (2014). "Microbial gardening in the ocean's twilight zone: Detritivorous metazoans benefit from fragmenting, rather than ingesting, sinking detritus." *Bioessays*, 36(12), 1132-1137.

McCave, I. N. (1984). "Size spectra and aggregation of suspended particles in the deep ocean." *Deep Sea Research Part A. Oceanographic Research Papers*, 31(4), 329-352.

Meire, L., Mortensen, J., Meire, P., Juul-Pedersen, T., Sejr, M. K., Rysgaard, S., Nygaard, R., Huybrechts, P., and Meysman, F. J. R. (2017). "Marine-terminating glaciers sustain high productivity in Greenland fjords." *Global Change Biology*, 23(12), 5344-5357.

Mestre, M., Ruiz-González, C., Logares, R., Duarte, C. M., Gasol, J. M., and Montserrat Sala, M. (2018). "Sinking particles promote vertical connectivity in the ocean microbiome." *Proceedings of the National Academy of Sciences*, 115(29), E6799-E6807.

Möller, K. O., St. John, M., Temming, A., Floeter, J., Sell, A. F., Herrmann, J.-P., and Möllmann, C. (2012). "Marine snow, zooplankton and thin layers: indications of a trophic link from small-scale sampling with the Video Plankton Recorder." *Marine Ecology Progress Series*, 468, 57-69.

Murray, C., Markager, S., Stedmon, C. A., Juul-Pedersen, T., Sejr, M. K., and Bruhn, A. (2015). "The influence of glacial melt water on bio-optical properties in two contrasting Greenlandic fjords." *Estuarine, Coastal and Shelf Science*, 163(Part B), 72-83.

Nöthig, E.-M., Bracher, A., Engel, A., Metfies, K., Niehoff, B., Peeken, I., Bauerfeind, E., Cherkasheva, A., Gäbler-Schwarz, S., Hardge, K., Kilias, E., Kraft, A., Mebrahtom Kidane, Y., Lalande, C., Piontek, J., Thomisch, K., and Wurst, M. (2015). "Summertime plankton ecology in Fram Strait—a compilation of long-and short-term observations." *Polar Research*, 34(1), 23349.

Nowald, N., Iversen, M. H., Fischer, G., Ratmeyer, V., and Wefer, G. (2015). "Time series of *in-situ* particle properties and sediment trap fluxes in the coastal upwelling filament off Cape Blanc, Mauritania." *Progress in Oceanography*, 137(Part A), 1-11.

Obernosterer, I., Christaki, U., Lefèvre, D., Catala, P., Van Wambeke, F., and Lebaron, P. (2008). "Rapid bacterial mineralization of organic carbon produced during a phytoplankton bloom induced by natural iron fertilization in the Southern Ocean." *Deep Sea Research Part II: Topical Studies in Oceanography*, 55(5-7), 777-789.

Passow, U. (2002). "Transparent exopolymer particles (TEP) in aquatic environments." *Progress in Oceanography*, 55(3-4), 287-333.

Passow, U., and De La Rocha, C. L. (2006). "Accumulation of mineral ballast on organic aggregates." *Global Biogeochemical Cycles*, 20(1).

Passow, U., and Carlson, C. A. (2012). "The biological pump in a high CO_2 world." *Marine Ecology Progress Series*, 470, 249-271.

Ploug, H., and Grossart, H. P. (2000). "Bacterial growth and grazing on diatom aggregates: Respiratory carbon turnover as a function of aggregate size and sinking velocity." *Limnology and Oceanography*, 45(7), 1467-1475.

Ploug, H., Iversen, M. H., and Fischer, G. (2008a). "Ballast, sinking velocity, and apparent diffusivity within marine snow and zooplankton fecal pellets: Implications for substrate turnover by attached bacteria." *Limnology and Oceanography*, 53(5), 1878-1886.

Ploug, H., Iversen, M. H., Koski, M., and Buitenhuis, E. T. (2008b). "Production, oxygen respiration rates, and sinking velocity of copepod fecal pellets: Direct measurements of ballasting by opal and calcite." *Limnology and Oceanography*, 53(2), 469-476.

Pollard, R. T., Salter, I., Sanders, R. J., Lucas, M. I., Moore, C. M., Mills, R. A., Statham, P. J., Allen, J. T., Baker, A. R., Bakker, D. C. E., Charette, M. A., Fielding, S., Fones, G. R., French, M., Hickman, A. E., Holland, R. J., Hughes, J. A., Jickells, T. D., Lampitt, R. S., Morris, P. J., Nédélec, F. H., Nielsdóttir, M., Planquette, H., Popova, E. E., Poulton, A. J., Read, J. F., Seeyave, S., Smith, T., Stinchcombe, M., Taylor, S., Thomalla, S., Venables, H. J., Williamson, R., and Zubkov, M. V. (2009). "Southern Ocean deep-water carbon export enhanced by natural iron fertilization." *Nature*, 457(7229), 577-580.

Poulsen, L. K., and Iversen, M. H. (2008). "Degradation of copepod fecal pellets: key role of protozooplankton." *Marine Ecology Progress Series*, 367, 1-13.

Prairie, J. C., Ziervogel, K., Arnosti, C., Camassa, R., Falcon, C., Khatri, S., McLaughlin, R. M., White, B. L., and Yu, S. (2013). "Delayed settling of marine snow at sharp density transitions driven by fluid entrainment and diffusion-limited retention." *Marine Ecology Progress Series*, 487, 185-200.

Quéguiner, B. (2013). "Iron fertilization and the structure of planktonic communities in high nutrient regions of the Southern Ocean." *Deep Sea Research Part II: Topical Studies in Oceanography*, 90, 43-54.

Rapp, J. Z., Fernández-Méndez, M., Bienhold, C., and Boetius, A. (2018). "Effects of Ice-Algal Aggregate Export on the Connectivity of Bacterial Communities in the Central Arctic Ocean." *Frontiers in Microbiology*, 9, 1035.

Reigstad, M., and Wassmann, P. (2007). "Does *Phaeocystis spp.* contribute significantly to vertical export of organic carbon?", in M. A. van Leeuwe, J. Stefels, S. Belviso, C. Lancelot, P. G. Verity, and W. W. C. Gieskes, (eds.), *Phaeocystis, major link in the biogeochemical cycling of climate-relevant elements*. Dordrecht: Springer Netherlands, pp. 217-234.

Rembauville, M., Blain, S., Armand, L., Quéguiner, B., and Salter, I. (2015a). "Export fluxes in a naturally iron-fertilized area of the Southern Ocean – Part 2: Importance of diatom resting spores and faecal pellets for export." *Biogeosciences*, 12(11), 3171-3195.

Rembauville, M., Salter, I., Leblond, N., Gueneugues, A., and Blain, S. (2015b). "Export fluxes in a naturally iron-fertilized area of the Southern Ocean – Part 1: Seasonal dynamics of particulate organic carbon export from a moored sediment trap." *Biogeosciences*, 12(11), 3153-3170.

Rigual-Hernández, A. S., Trull, T. W., Bray, S. G., and Armand, L. K. (2016). "The fate of diatom valves in the Subantarctic and Polar Frontal Zones of the Southern Ocean: Sediment trap versus surface sediment assemblages." *Palaeogeography, Palaeoclimatology, Palaeoecology*, 457, 129-143.

Rixen, T., Gaye, B., Emeis, K.-C., and Ramaswamy, V. (2019). "The ballast effect of lithogenic matter and its influences on the carbon fluxes in the Indian Ocean." *Biogeosciences*, 16(2), 485-503.

Rousseaux, C. S., and Gregg, W. W. (2013). "Interannual variation in phytoplankton primary production at a global scale." *Remote Sensing*, 6(1), 1-19.

Ruiz-González, C., Mestre, M., Estrada, M., Sebastián, M., Salazar, G., Agustí, S., Moreno-Ostos, E., Reche, I., Álvarez-Salgado, X. A., Morán, X. A. G., Duarte, C. M., Sala, M. M., and Gasol, J. M. (2020). "Major imprint of surface plankton on deep ocean prokaryotic structure and activity." *Molecular Ecology*, 29(10), 1820-1838.

Rysgaard, S., and Glud, R. N. (2007). "Carbon cycling and climate change: Predictions for a High Arctic marine ecosystem (Young Sound, NE Greenland)", in S. Rysgaard and R. N. Glud, (eds.), *Carbon cycling in Arctic marine ecosystems: Case study Young Sound, Meddelelser om Grønland*. Copenhagen: Bioscience Vol. 58, pp. 206-214.

Sabine, C. L., Feely, R. A., Gruber, N., Key, R. M., Lee, K., Bullister, J. L., Wanninkhof, R., Wong, C. S., Wallace, D. W. R., Tilbrook, B., Millero, F. J., Peng, T.-H., Kozyr, A., Ono, T., and Rios, A. F. (2004). "The Oceanic Sink for Anthropogenic CO_2." *Science*, 305(5682), 367-371.

Sabine, C. L., and Tanhua, T. (2010). "Estimation of Anthropogenic CO_2 Inventories in the Ocean." *Annual Review of Marine Science*, 2(1), 175-198.

Sakshaug, E. (2004). "Primary and Secondary Production in the Arctic Seas", in R. Stein and R. W. MacDonald, (eds.), *The Organic Carbon Cycle in the Arctic Ocean*. Berlin, Heidelberg: Springer Berlin Heidelberg, pp. 57-81.

Salter, I., Kemp, A. E. S., Moore, C. M., Lampitt, R. S., Wolff, G. A., and Holtvoeth, J. (2012). "Diatom resting spore ecology drives enhanced carbon export from a naturally iron-fertilized bloom in the Southern Ocean." *Global Biogeochemical Cycles*, 26(1).

Sampei, M., Sasaki, H., Forest, A., and Fortier, L. (2012). "A substantial export flux of particulate organic carbon linked to sinking dead copepods during winter 2007–2008 in the Amundsen Gulf (southeastern Beaufort Sea, Arctic Ocean)." *Limnology and Oceanography*, 57(1), 90-96.

Sarmiento, J. L., and Bender, M. (1994). "Carbon biogeochemistry and climate change." *Photosynthesis Research*, 39, 209-234.

Sarmiento, J. L., Dunne, J., Gnanadesikan, A., Key, R. M., Matsumoto, K., and Slater, R. (2002). "A new estimate of the $CaCO_3$ to organic carbon export ratio." *Global Biogeochemical Cycles*, 16(4), 54-1 - 54-12.

Schattenhofer, M., Fuchs, B. M., Amann, R., Zubkov, M. V., Tarran, G. A., and Pernthaler, J. (2009). "Latitudinal distribution of prokaryotic picoplankton populations in the Atlantic Ocean." *Environmental Microbiology*, 11(8), 2078-2093.

Schmidt, K., De La Rocha, C. L., Gallinari, M., and Cortese, G. (2014). "Not all calcite ballast is created equal: differing effects of foraminiferan and coccolith calcite on the formation and sinking of aggregates." *Biogeosciences*, 11(1), 135-145.

Schnetzer, A., and Steinberg, D. K. (2002). "Active transport of particulate organic carbon and nitrogen by vertically migrating zooplankton in the Sargasso Sea." *Marine Ecology Progress Series*, 234, 71-84.

Seifert, M., Hoppema, M., Burau, C., Elmer, C., Friedrichs, A., Geuer, J. K., John, U., Kanzow, T., Koch, B. P., Konrad, C., van der Jagt, H., Zielinski, O., and Iversen, M. H. (2019). "Influence of Glacial Meltwater on Summer Biogeochemical Cycles in Scoresby Sund, East Greenland." *Frontiers in Marine Science*, 6, 412.

Siegenthaler, U., and Sarmiento, J. L. (1993). "Atmospheric carbon dioxide and the ocean." *Nature*, 365(6442), 119-125.

Siegenthaler, U., Monnin, E., Kawamura, K., Spahni, R., Schwander, J., Stauffer, B., Stocker, T. F., Barnola, J.-M., and Fischer, H. (2005). "Supporting evidence from the EPICA Dronning Maud Land ice core for atmospheric CO_2 changes during the past millennium." *Tellus B: Chemical and Physical Meteorology*, 57(1), 51-57.

Smith, D. C., Simon, M., Alldredge, A. L., and Azam, F. (1992). "Intense hydrolytic enzyme activity on marine aggregates and implications for rapid particle dissolution." *Nature*, 359(6391), 139-142.

Smith, R. W., Bianchi, T. S., Allison, M., Savage, C., and Galy, V. (2015). "High rates of organic carbon burial in fjord sediments globally." *Nature Geoscience*, 8(6), 450-453.

Sørensen, H. L., Meire, L., Juul-Pedersen, T., de Stigter, H. C., Meysman, F. J. R., Rysgaard, S., Thamdrup, B., and Glud, R. N. (2015). "Seasonal carbon cycling in a Greenlandic fjord: an integrated pelagic and benthic study." *Marine Ecology Progress Series*, 539, 1-17.

Steinberg, D. K., Carlson, C. A., Bates, N. R., Goldthwait, S. A., Madin, L. P., and Michaels, A. F. (2000). "Zooplankton vertical migration and the active transport of dissolved organic and inorganic carbon in the Sargasso Sea." *Deep Sea Research Part I: Oceanographic Research Papers*, 47(1), 137-158.

Stemmann, L., Jackson, G. A., and Gorsky, G. (2004). "A vertical model of particle size distributions and fluxes in the midwater column that includes biological and physical processes—Part II: application to a three year survey in the NW Mediterranean Sea." *Deep Sea Research Part I: Oceanographic Research Papers*, 51(7), 885-908.

Stief, P., Elvert, M., and Glud, R. N. (2021). "Respiration by “marine snow” at high hydrostatic pressure: Insights from continuous oxygen measurements in a rotating pressure tank." *Limnology and Oceanography*, 66(7), 2797-2809.

Straneo, F., Hamilton, G. S., Sutherland, D. A., Stearns, L. A., Davidson, F., Hammill, M. O., Stenson, G. B., and Rosing-Asvid, A. (2010). "Rapid circulation of warm subtropical waters in a major glacial fjord in East Greenland." *Nature Geoscience*, 3(3), 182-186.

Tamburini, C., Boutrif, M., Garel, M., Colwell, R. R., and Deming, J. W. (2013). "Prokaryotic responses to hydrostatic pressure in the ocean – a review." *Environmental Microbiology*, 15(5), 1262-1274.

Thiele, S., Fuchs, B. M., Amann, R., and Iversen, M. H. (2015). "Colonization in the Photic Zone and Subsequent Changes during Sinking Determine Bacterial Community Composition in Marine Snow." *Applied and Environmental Microbiology*, 81(4), 1463-1471.

Tréguer, P., Nelson, D. M., Van Bennekom, A. J., DeMaster, D. J., Leynaert, A., and Quéguiner, B. (1995). "The Silica Balance in the World Ocean: A Reestimate." *Science*, 268(5209), 375-379.

Tréguer, P., Bowler, C., Moriceau, B., Dutkiewicz, S., Gehlen, M., Aumont, O., Bittner, L., Dugdale, R., Finkel, Z., Iudicone, D., Jahn, O., Guidi, L., Lasbleiz, M., Leblanc, K., Levy, M., and Pondaven, P. (2018). "Influence of diatom diversity on the ocean biological carbon pump." *Nature Geoscience*, 11(1), 27-37.

Turner, J. T. (2002). "Zooplankton fecal pellets, marine snow and sinking phytoplankton blooms." *Aquatic Microbial Ecology*, 27(1), 57-102.

Turner, J. T. (2015). "Zooplankton fecal pellets, marine snow, phytodetritus and the ocean’s biological pump." *Progress in Oceanography*, 130, 205-248.

van der Jagt, H., Friese, C., Stuut, J. B. W., Fischer, G., and Iversen, M. H. (2018). "The ballasting effect of Saharan dust deposition on aggregate dynamics and carbon export: Aggregation, settling, and scavenging potential of marine snow." *Limnology and Oceanography*, 63(3), 1386-1394.

van der Jagt, H., Wiedmann, I., Hildebrandt, N., Niehoff, B., and Iversen, M. H. (2020). "Aggregate Feeding by the Copepods *Calanus* and *Pseudocalanus* Controls Carbon Flux Attenuation in the Arctic Shelf Sea During the Productive Period." *Frontiers in Marine Science*, 7, 543124.

Volk, T., and Hoffert, M. I. (1985). "Ocean Carbon Pumps: Analysis of Relative Strengths and Efficiencies in Ocean-Driven Atmospheric CO_2 Changes." *The Carbon Cycle and Atmospheric CO_2: Natural Variations Archean to Present*, 32, 99-110.

Wassmann, P. (2011). "Arctic marine ecosystems in an era of rapid climate change." *Progress in Oceanography*, 90(1-4), 1-17.

Weber, T., and Bianchi, D. (2020). "Efficient Particle Transfer to Depth in Oxygen Minimum Zones of the Pacific and Indian Oceans." *Frontiers in Earth Science*, 8, 376.

Whitman, W. B., Coleman, D. C., and Wiebe, W. J. (1998). "Prokaryotes: The unseen majority." *Proceedings of the National Academy of Sciences*, 95(12), 6578-6583.

Wigley, T. M. L. (1983). "The pre-industrial carbon dioxide level." *Climatic change*, 5(4), 315-320.

Wollenburg, J. E., Katlein, C., Nehrke, G., Nöthig, E.-M., Matthiessen, J., Wolf- Gladrow, D. A., Nikolopoulos, A., Gázquez-Sanchez, F., Rossmann, L., Assmy, P., Babin, M., Bruyant, F., Beaulieu, M., Dybwad, C., and Peeken, I. (2018). "Ballasting by cryogenic gypsum enhances carbon export in a *Phaeocystis* under-ice bloom." *Scientific Reports*, 8(1), 7703.

Wollenburg, J. E., Iversen, M., Katlein, C., Krumpen, T., Nicolaus, M., Castellani, G., Peeken, I., and Flores, H. (2020). "New observations of the distribution, morphology and dissolution dynamics of cryogenic gypsum in the Arctic Ocean." *The Cryosphere*, 14(6), 1795-1808.

Zaikova, E., Walsh, D. A., Stilwell, C. P., Mohn, W. W., Tortell, P. D., and Hallam, S. J. (2010). "Microbial community dynamics in a seasonally anoxic fjord: Saanich Inlet, British Columbia." *Environmental Microbiology*, 12(1), 172-191.

Contributions to Manuscripts

Chapter I: Hufnagel, L., John, U., Amann, R., Fuchs, B. M., Ramondenc, S., Marchant, H., van der Jagt, H., Konrad, C., Neuhaus, S., Kühne, N., Friedrichs, A., Mera, A. and Iversen, M. H. (in prep.): "Export mechanisms of organic carbon in the Arctic fjord Scoresby Sund, East Greenland - Organic carbon export is zooplankton and silt controlled."

Author contributions: LH, MHI, HvdJ, RA and UJ designed the study. Sampling was done onboard by HvdJ, CK, RA, UJ, NK and AF. AM and NK did the sequencing of the DNA samples. SN did the bioinformatic processing of the sequencing. **LH** did the CARD-FISH counts under guidance of RA and BMF. HvdJ did the biogeochemical measurements. **LH** analyzed the data with help of SR with the statistical analysis. AF provided information about the water mass movement for the drifting sediment traps. **LH** and MHI wrote the manuscript with contributions from UJ, RA, SR and HM. All authors revised and approved the manuscript.

Chapter II: Hufnagel, L., Konrad, C. and Iversen, M. H. (in prep.): "Increasing salinities in the Southern Ocean retain and delay settling of large, porous aggregates."

Author contributions: The manuscript was written by **LH** and MHI. **LH** analyzed the data together with MHI. **LH** and CK processed the PELAGRA-CAM data. Sampling onboard was done by MHI.

Chapter III: Hufnagel, L., Ramondenc, S., Konrad, C., von Appen, W.-J., Hofmann, Z., Torres Valdés, S., Stefels, J., Moradi, N., Bracher, A., Waite, A. and Iversen, M. H. (in prep.): "Carbon export in an Arctic frontal system in Fram Strait."

Author contributions: The manuscript was written by **LH** under supervision of MHI. **LH** analyzed the data together with SR. Sampling onboard was done by **LH**, MHI, SR and CK. CK built the ROSINA camera system and processed the camera data. ZH and WJvA provided the background on the physical oceanography. **LH** prepared samples for biogeochemical analysis. STV analyzed the nutrient samples and JS analyzed the primary production samples in the home laboratory. NM modelled the oxygen consumption of the individual aggregates. AB analyzed the PAR profiles. AW provided the UVP raw data. All authors revised and approved the manuscript.

Chapter I: Export mechanisms of organic carbon in the Arctic fjord Scoresby Sund, East Greenland - Organic carbon export is zooplankton and silt controlled

Lili Hufnagel[1,2,3*], Uwe John[3,4], Rudolf Amann[5], Bernhard M. Fuchs[5], Simon Ramondenc[1,3], Hannah Marchant[1,5], Helga van der Jagt[1,3,6], Christian Konrad[1,3], Stefan Neuhaus[3], Nancy Kühne[3], Anna Friedrichs[7], Alejandra Mera[5] and Morten H. Iversen[1,2,3*]

[1] University of Bremen, MARUM, Center for Marine Environmental Sciences, Leobener Str. 8, 28359 Bremen, Germany

[2] University of Bremen, Faculty of Geosciences, Klagenfurter Str. 2-4, 28359 Bremen, Germany

[3] Alfred Wegener Institute, Helmholtz Centre for Polar and Marine Research, Am Handelshafen 12, 27570 Bremerhaven, Germany

[4] Helmholtz Institute for Functional Marine Biodiversity at the University of Oldenburg (HIFMB), Ammerländer Heersstraße 231, 26129 Oldenburg, Germany

[5] Max Planck Institute for Marine Microbiology, Celsiusstr. 1, 28359 Bremen, Germany

[6] Current affiliation: Waardenburg Ecology, Varkensmarkt 9, 4101 CK Culemborg, Netherlands

[7] Institute for Chemistry and Biology of the Marine Environment, Carl von Ossietzky University Oldenburg, Schleusenstraße 1, 26382 Wilhelmshaven, Germany

*Correspondence: lhufnagel@marum.de, morten.iversen@awi.de

Running head: Carbon export mechanism in Scoresby Sund

Keywords: carbon export, *in situ* aggregates, eukaryotes, bacteria, zooplankton mediated, fecal pellets

Abstract

High carbon export and low decomposition make Arctic fjords hotspots for carbon burial, however the driving mechanisms for carbon export and sequestration in Arctic fjords are still largely unconstrained. Here, we study the largest Arctic fjord system, the Scoresby Sund in East Greenland, focusing on the origin of sinking aggregates, their taxonomic and biogeochemical composition, colonization by bacteria and subsequent interactions between aggregates-attached and free-living eukaryotic and bacterial communities, using comparative rRNA gene sequencing and catalyzed reporter deposition fluorescence *in situ* hybridization (CARD-FISH). We found that aggregate formation primarily occurred in the inner fjord. The formed aggregates were retained at an increasing salinity gradient in the upper water column and were laterally exported eastward with the outflow water. With the exception of aggregates that were ballasted by silt near the marine-terminating Daugaard-Jensen Glacier, export of particulate organic matter throughout the fjord was driven by zooplankton feeding and fecal pellet production. The zooplankton-mediated export resulted in an enrichment of zooplankton associated bacterial groups in the sinking material. Our results indicate that if primary production under longer ice-free periods increases and large zooplankton, such as copepods, remain the dominant degraders in the ecosystem, Arctic fjords will continue to be important hotspots for carbon sequestration in the future.

Introduction

Fjords are hotspots of carbon cycling (Seifert et al. 2019; Smith et al. 2015) and are globally estimated to sequester 18 Mt organic carbon annually; equivalent to 11% of the global annual marine carbon burial (Smith et al. 2015). Arctic fjords in particular are hotspots of carbon storage (Glud et al. 1998; Smith et al. 2015; Sørensen et al. 2015), a potential that might be impacted by the ongoing climate change. The unprecedented increase in glacier melt rates is causing a significant increase in freshwater input to Arctic fjords (Bamber et al. 2012; Enderlin et al. 2014; Fettweis et al. 2013), which, together with reduction of ice-cover, is predicted to affect the estuarine circulation in the fjords (Bendtsen et al. 2014; Mortensen et al. 2011), stratification (Meire et al. 2017; Mortensen et al. 2013), nutrient supply (Hawkings et al. 2015; Kanna et al. 2018; Meire et al. 2017), primary productivity (Meire et al. 2017; Rysgaard and Glud 2007), carbon chemistry, and export (Rysgaard et al. 2012; Seifert et al. 2019). However, we still know very little about how these changes will impact carbon sequestration in Arctic fjords in the future.

With an area of 13,700 km^2, the Arctic fjord Scoresby Sund in Greenland is the largest fjord complex in the world (Dowdeswell et al. 1993). Scoresby Sund has several marine- and land-terminating glaciers that deliver on average 8.3 km^3 yr^{-1} meltwater to both the deep and narrow inner fjords and the shallower and wider outer fjord (Cofaigh et al. 2001; Dowdeswell et al. 1993; Lewis and Smith 2009). Previous studies have shown that meltwater from the Greenland Ice Sheet delivers a high supply of nutrients to Greenlandic fjords (Hawkings et al. 2015), which together with upwelled nutrients from deeper water layers with meltwater from marine terminating glaciers support high primary production (Kanna et al. 2018; Meire et al. 2017). At the same time however, surface run-off from land-terminating glaciers with silt-rich meltwater can lead to enhanced light attenuation (Holinde and Zielinski 2016; Murray et al. 2015) and together with stratification limit the primary production in Arctic fjords (Meire et al. 2017). Stratification caused by input of freshwater from melting glaciers and sea ice creates a layer of low-salinity water near the surface that can extend for several kilometers (Bendtsen et al. 2014; Seifert et al. 2019). The resulting density and salinity gradients can retard the sinking of aggregates, the primary vector of organic carbon export in marine systems (Alldredge et al. 2002; Alldredge and Crocker 1995; Kindler et al. 2010; MacIntyre et al. 1995; Prairie et al. 2013; Prairie et al. 2015), and thus could play a crucial role in regulating carbon flux.

Previously, Seifert et al (2019) found that sinking particles were indeed slowed down at the salinity gradient in Scoresby Sund, potentially decreasing carbon export. Despite a first assessment of biogeochemical cycles in Scoresby Sund by Seifert et al (2019), the underlying

mechanisms and processes that drive horizontal and vertical transport of organic matter are still unclear in this carbon burial hotspot. Understanding the complex interplay between stratification, biological processes and carbon flux is essential to predict the fate of carbon in Arctic fjords and its impact on the global carbon cycle.

Here, we studied free-living and aggregate-associated eukaryotic and prokaryotic communities throughout Scoresby Sund to identify the origin of settling aggregates, their taxonomic and biogeochemical composition, their transformation by zooplankton, as well as their vertical and horizontal transport. Our study was performed during the Arctic summer when the Scoresby Sund was largely ice-free. We used both Marine Snow Catchers (MSC) and drifting sediment traps to collect *in situ* formed aggregates, which were subsequently investigated using rRNA gene sequencing and catalyzed reporter deposition fluorescence *in situ* hybridization (CARD-FISH). Our results suggest that the aggregates formed in the inner part of Scoresby Sund were subjected to retention as well lateral transport in the upper water column where intense zooplankton grazing took place and altered the aggregate-attached bacterial communities. Fecal pellet production provided the majority of the particulate organic carbon (POC) flux in the fjord, except in the region near the marine-terminating glacier where particulate organic material was exported primarily due to high silt ballasting.

Materials and methods

Study area

Scoresby Sund in East Greenland has a total length of 350 km with an area of 13,700 km^2 (Dowdeswell et al. 1993). The fjord is divided into the shallower (200 m to 650 m deep) and wider outer fjord, the Outer Scoresby Sund (OSS), and the deep (800 m to more than 1600 m deep) and narrow inner fjords (Cofaigh et al. 2001; Dowdeswell et al. 1993). This study focuses on the Nordvestfjord, which is 140 km long and around 5 km wide, and the OSS, which are separated by an underwater sill, 350 m below the surface (Seifert et al. 2019). The mouth of the fjord at the OSS is strongly impacted by the adjacent North Atlantic while the head of the inner part of Nordvestfjord is strongly influenced by meltwater and silt release from the marine-terminating Daugaard-Jensen Glacier (Seifert et al. 2019).

The water masses in Scoresby Sund during the period of our study have been described by Seifert et al. (2019). The surface was covered by a thin layer of glacial meltwater, with salinities < 32 PSU, extending to a depth of 5 to 10 meters (Seifert et al. 2019). Below the surface meltwater, within the upper 200 m, Polar Water was located (salinity < 34 PSU, temperature < 0°C, Seifert et al. 2019). The Atlantic Water (temperature > 0°C, salinity > 34.5 PSU) was observed below the Polar Water, and filled the deeper basins of Nordvestfjord (Seifert et al. 2019). The dense Atlantic bottom water, which enters the OSS from the shelf is retained in the OSS by the sill (Seifert et al. 2019).

In the OSS the Atlantic Water is inflowing in the northern part and outflowing in the southern part of the fjord (Seifert et al. 2019). Close to the sill between the OSS and the Nordvestfjord, where the fjord is separated into two 4-km wide channels by an island, the Atlantic Water was flowing into the Nordvestfjord at depth, while the mid-water was transported into the OSS (Seifert et al. 2019). The surface showed a weak outflow from the Nordvestfjord into the OSS (Seifert et al. 2019).

Water sampling

Samples were collected in Scoresby Sund between the 10th and 19th of July 2016 with the German research vessel *RV* Maria S. Merian (Expedition MSM56) in the Outer Scoresby Sund and the inner Nordvestfjord. Thirteen stations were sampled along a transect from the Daugaard-Jensen Glacier in the Inner Nordvestfjord (station 580 to 595) to the mouth of the Outer Scoresby Sund (station 598 to 601, and 572), including 2 stations on the Greenlandic shelf adjacent to the fjord (station 574 and 575, Fig. 1).

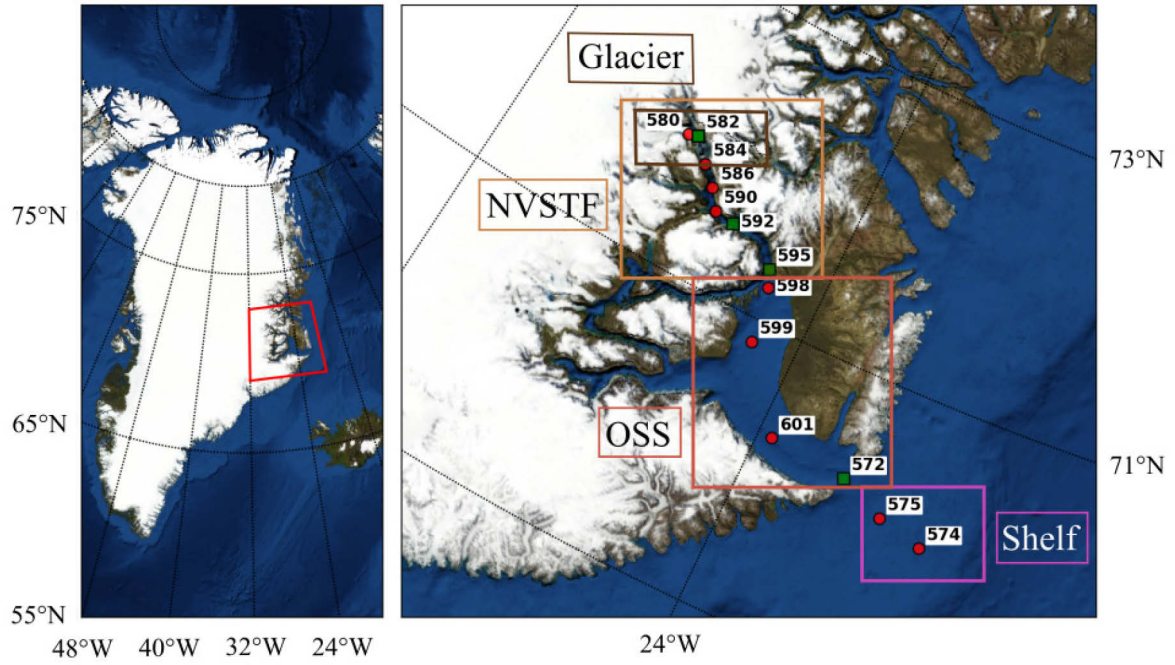

Fig. 1: Map of transect in Scoresby Sund with CTD (red) and drifting sediment trap (green) stations of the cruise MSM56 between 10 and 19 July 2016. The transect was divided in the Glacier, Nordvestfjord (NVSTF), Outer Scoresby Sund (OSS) and Shelf region.

Water sampling was carried out with 24 x 12 L Niskin bottles mounted on a CTD-Rosette (Conductivity-Temperature-Depth) that was equipped with sensors for chlorophyll a fluorescence (ECOAFL/FL, WET Labs, Sea-Bird Scientific), turbidity (ECO-NTU, WETLabs, Sea-Bird Scientific), and dissolved oxygen (SBE43, Sea-Bird Scientific) (Friedrichs et al. 2017). Water samples (~15 L) were collected in the surface melt water with low salinity (0-25 m), in the deep chlorophyll a maximum (DCM, 15-40 m), and in the deep water (1000 m). The precise sampling depth in the surface melt water layer and the DCM were determined according to the salinity, temperature, and chlorophyll a fluorescence profiles at each station.

Water samples from the surface, the DCM and from 1000 m depth were sieved by sequential gravity filtration over 150 µm and 20 µm mesh-size Nitex sieves. This was followed by sequential in-line filtrations through 3 and 0.2 µm polycarbonate membranes (145 mm diameter, Millipore, Darmstadt, Germany) with a peristaltic pump for a maximum of 30 min. These filtrations yielded two operationally defined size-fractions: nanoplankton (3 - 20 µm) and picoplankton (0.2 - 3 µm). Bacteria in the size- fraction 0.2 - 3 µm are subsequently referred to as free-living (FL), while bacteria recovered from the size fraction > 3 µm are referred to as particle-attached (PA).

Aggregate sampling

In situ formed sinking aggregates were collected using a Marine Snow Catcher (MSC) and free-drifting surface tethered sediment traps (see Seifert et al. 2019). The MSC is a 100 L PVC closing water sampler, which was deployed ~10 m below the DCM layer (i.e. 10 m below the peak in the CTD-Rosette mounted fluorescence sensor, between 30 and 35 m). After deployment the MSC was left standing on deck overnight to allow all settling aggregates to sink to the bottom part of the MSC. Hereafter, the water in the upper part of the MSC (top 95 L) was gently drained and 25 L of this water was carefully filtered over a 3 µm (145 mm diameter, Millipore, Darmstadt, Germany) and 0.2 µm filter (145 mm diameter, Millipore, Darmstadt, Germany). This generated two size fractions, one for eukaryotic and prokaryotic picoplankton communities (0.2 – 3 µm) and one for suspended or slow settling large eukaryotes and aggregates with their PA prokaryotes (> 3 µm). The bottom part of the MSC contained the remaining 5 L of water and the settling aggregates (any aggregates that sank faster than ~4 m d^{-1}). The bottom part of the MSC with the settling aggregates was brought to the laboratory where each aggregate was gently collected using a wide-bore pipette. The aggregates were sampled for aggregate-associated prokaryotic and eukaryotic community composition. The aggregates picked for DNA sequencing were centrifuged to produce an aggregate pellet for DNA extraction and frozen at -80°C until further analyses in the home laboratory. Additionally, aggregates for catalyzed reporter deposition fluorescence *in situ* hybridization (CARD-FISH) were collected (see section "CARD-FISH").

The free-drifting sediment trap array consisted of a positioning system attached to a surface buoy, 12 buoyancy spheres serving as wave-breakers, two 25 L buoyancy spheres, and three sediment traps stations, each equipped with up to four cylindrical sediment traps. The three sediment trap stations were deployed at 100 m, 200 m and 400 m depth with deployment times ranging between 2 and 10 h in Scoresby Sund. At station 572 and 582, the drifting trap array was deployed with four trap tubes at each depth. One trap tube contained a petri dish with an ethanol-based cryogel at the bottom and filtered water adjusted to three different salinities above. This allowed for fixing (1% formaldehyde, in the middle layer) and washing (no fixative in the bottom layer) of settling aggregates *in situ* before they were collected in the cryogel (Thiele et al. 2015). One trap tube was used for DNA sampling for the aggregate-associated prokaryotic and eukaryotic community analysis and one to measure the biogeochemical fluxes. At stations 592 and 595, two trap deployments were done, one short deployment (2 - 3 h) and one long deployment (10 h). The short deployment had two trap tubes for each depth, one containing the gel trap and one for DNA sampling. The time-span of the short deployment was

adjusted according to the amount of settling aggregates in the water column in order to avoid overlapping aggregates in the gel traps. The long deployment was done with two trap tubes that both sampled for biogeochemical fluxes. The collected aggregate samples for DNA sequencing were centrifuged to produce an aggregate pellet for DNA extraction and frozen at -80°C until sequencing in the home laboratory.

DNA extraction and amplicon sequencing

The DNA from the collected aggregates and from the 0.2 – 3 µm size fraction was extracted using the NucleoSpin Soil Kit (Machery-Nagel). The DNA from the 3 - 20 µm size fraction was extracted using the NucleoSpin Plant II Kit (Machery-Nagel) following the manufacturer's protocol. A bead beater (MagNA Lyser, Roche, Basel, Switzerland) was used (2 x 30 s bursts) with glass beads to break up the cells in the lysis buffer.

Identification of eukaryotes associated with the aggregates was based on the V4 region of the eukaryotic 18S rRNA gene which was amplified using the V4F_illumina and V4R_AZig_illumina primers (Xiao et al. 2017). The hyper-variable V2-V3 region from the bacterial 16S rRNA genes was amplified with barcoded 27F (Ludwig et al. 1993) and 338R (Suzuki and Giovannoni 1996) PCR primers.

PCR amplification and library construction were performed as described in the Illumina 16S metagenomic sequencing library preparation (https://support.illumina.com/downloads/16s_metagenomic_sequencing_library_preparation.html, doc.no:15044223B), with slight modifications (e.g. the use of different primers) for 18S rRNA gene amplicon preparation. Briefly, the 25 µL PCR reaction mix consisted of 2.5 µL of genomic DNA (5-10 ng), 5 µL of 1 µM forward primer, 5 µL of 1 µM reverse primer, and 12.5 µL of 2x KAPA HiFi HotStart ReadyMix (KAPABiosystems, Boston, USA). The PCR-program included an initial denaturation at 95°C for 3 min, followed by 25 cycles at 95°C for 30 seconds, annealing at 55°C for 30 seconds, extension at 72°C for 30 seconds, and a final extension at 72°C for 5 min. PCR reactions were cleaned with CleanNGS beads (CleanNA, Waddinxveen, Netherlands) and pooled in equimolar concentrations. The amplicon libraries were sequenced using the MiSeq Reagent Kit v3 (600-cycle) MS-102-3003 in a MiSeq Sequencer (Illumina, San Diego, US).

Bioinformatics

Primers and spurious sequences were trimmed with "Cutadapt" v2.10 (Martin 2011). Selected functions of the R package "DADA2" v1.14.1 (Callahan et al. 2016) were used to filter and trim the raw reads considering base quality scores, to conduct read denoising according to the "Divisive Amplicon Denoising Algorithm" (DADA), to merge denoised paired-end reads into amplicon sequence variants (ASVs), to detect and remove putative chimeric sequences and to assign taxonomy. As reference data sets for the taxonomic assignments of the 18S rRNA gene sequences the "Protist Ribosomal Reference Database" (PR2) v4.12 (Guillou et al. 2012) and of the 16S rRNA gene sequences the "SILVA ribosomal RNA gene database" v138 (Quast et al. 2012) were used. The singletons (i.e. ASVs which occurred only once in the whole data set) were excluded from further analysis.

CARD-FISH - Catalyzed reporter deposition fluorescence in situ hybridization

For bacterial cell counting, sea water samples were fixed with a final concentration of 1% formaldehyde for 1-2 h at RT (room temperature). Depending on the cell density in the water column, 10 to 100 mL of the fixed sea water were filtered onto 0.2 µm pore size polycarbonate filters (Millipore “Isopore”, diameter 47 mm), positioned on 0.45 µm pore size support filter (Sartorius, diameter 47 mm, cellulose acetate). The aggregates collected by the drifting trap were fixed *in situ* (Flintrop et al. 2018; Thiele et al. 2015), while aggregates collected by the MSC were fixed after recovery and sedimentation with 1% formaldehyde and washed in sterile filtered seawater. The aggregate samples were filtered onto 0.2 µm pore size polycarbonate filters (Millipore “Isopore”, diameter 47mm). All filters were stored at -20°C until further analysis in the home laboratory.

To quantify the FL and aggregate-attached bacterial community, the catalyzed reporter deposition fluorescence *in situ* hybridization (CARD-FISH) procedure was done according to Thiele et al. (2011) with specific oligonucleotide probes (Table 1). The oligonucleotide probes were chosen based on the presence of taxonomic groups in the 16S rRNA gene data set. When applying probe PLA46 targeting *Planctomycetes* an additional cell permeabilization step with the enzyme achromopeptidase was applied (Pizzetti et al. 2011). Relative cell abundances refer to total cell counts determined by using 4′,6-diamidino-2-phenylindole (DAPI) staining (Hicks et al. 1992). The filters were manually enumerated using a Zeiss Axiolmager.D2 microscope (Carl Zeiss AG, Oberkochen, Germany) with a metal-halide lamp LEJ HXP 120 (Carl Zeiss AG, Oberkochen, Germany) as light source.

Table 1: CARD-FISH probes used in this study with probe sequences, formamide concentration (FA), taxonomic group targeted by probe and reference

	Sequence (5' -> 3')	FA [%]	Taxonomic group	Reference
ALT1413	TTTGCATCCCACTCCCAT	40	*Alteromonas/Colwellia*	(Eilers et al. 2000)
ARC94	TGCGCCACTTAGCTGACA	20	*Arcobacter*	(Snaidr et al. 1997)
CF319a	TGGTCCGTGTCTCAGTAC	35	*Bacteroidetes/ Flavobacteriia*	(Manz et al. 1996)
EUB338I	GCTGCCTCCCGTAGGAGT	35	most bacteria	(Amann et al. 1990)
EUB338II	GCAGCCACCCGTAGGTGT	35	*Planctomycetales*	(Daims et al. 1999)
EUB338III	GCTGCCACCCGTAGGTGT	35	*Verrucomicrobiales*	(Daims et al. 1999)
NON338	ACTCCTACGGGAGGCAGC	35	Negative control	(Wallner et al. 1993)
PLA46	GACTTGCATGCCTAATCC	30	*Planctomycetes*	(Neef et al. 1998)
PSA184	CCCCTTTGGTCCGTAGAC	30	*Pseudoalteromonas/Colwellia*	(Eilers et al. 2000)
ROS537	CAACGCTAACCCCCTCC	35	*Roseobacter clade*	(Eilers et al. 2001)

Aggregate composition

Aggregates that were collected by the gel traps were photographed on board using a Basler acA1300-30gc camera (Basler, Ahrensburg, Germany) and a 16 mm Format FFL objective (Prod. 86571, Edmund Optics, York, UK). Images from each gel were analyzed as cross-sections (x – and y- directions) using the software ImageJ (Schindelin et al. 2012) to determine the size-distribution and abundance of different types of aggregates, i.e. fecal pellets and phytoplankton aggregates, including marine snow (phytoplankton aggregates larger than 500 µm). Fecal pellets were identified visually and their length and diameter were measured using the "ridge detection" tool in ImageJ (Steger 1998; Wagner et al. 2017). The total volume of aggregates was calculated from their projected area and by assuming a spherical shape, while the volume of fecal pellets was estimated as a cylindrical shape. The volumes were normalized

by the total area of the analyzed pictures and the deployment time to get the particle flux. Since the glacial melt at the inner Nordvestfjord released high amount of silt, no volume and fecal pellet flux data could be generated for the drifting sediment trap at station 582 (Glacier), as the surface of the gel traps were covered in silt completely, dragging any collected aggregate to the bottom and changing their size and structure.

Vertical profiles of aggregate size-distribution and abundance were recorded at the drifting sediment trap stations using an *in situ* camera system (ISC). The camera system consisted of an infrared camera (acA2010-25gc GigE camera, Basler) and an Edmund Optics compact fixed focal length lens 25 mm (#67-715) with aperture F#16 with backlight infrared illumination that record particle abundances and sizes through the water column. The images were processed using the image processing toolbox in Matlab R2015a (The MathWorks, Inc., Natick, MA, USA). The particles were sorted into fecal pellet and aggregates (phytoplankton aggregates and marine snow). Both the gel trap data and the ISC data were binned into size classes where bins were only considered if they contained a minimum number of 5 imaged particles. To calculate the POC flux based on only the fecal pellets, we used the numbers and sizes of fecal pellets collected by the gel trap and multiplied the pellet volumes with an average POC concentration in the fecal pellets of 0.02 mgC mm^{-3}. This is a conservative value compared to literature values where POC concentrations within fecal pellets range between 0.02 and 0.06 mgC mm^{-3} (Belcher et al. 2016; Gleiber et al. 2012; González et al. 1994; González and Smetacek 1994).

The measured particulate organic carbon (POC) fluxes from this study were previously published by Seifert et al. (2019). Here we also included sediment trap analyses for total particulate mass (TPM), particulate organic nitrogen (PON), particulate inorganic carbon (PIC), and biogenic silica (bSi). Briefly, subsamples were filtered onto pre-weighed and pre-combusted GF/F filters (25 mm, Whatman) for POC, PON, PIC, and TPM. The zooplankton swimmers were removed, the filters were dried 48 h at 40°C, and weighed for TPM. The filters for PIC were measured on a gas chromatograph (GC) elemental analyzer (EuroEA Elemental Analyser, HEKAtech) directly, while the filters for PON and POC where fumed for 24 h with 37% hydrochloric acid and dried again for 24 h before measurements. Subsamples for bSi where filtered onto cellulose acetate filters (25 mm, pore-size 0.8 µm, Sartorius). They were processed using wet-alkaline method (pretreated 12 h at 85°C in an oven), extracted for two hours at 85°C in a shaking water bath and measured spectrometrically (Bodungen et al. 1991). The measurements were normalized by the opening area of the sediment traps and the deployment time of the traps to calculate the fluxes for TPM, PON, PIC, and bSi.

In addition, the lithogenic ballast fluxes (mg m^{-2} d^{-1}) were calculated using the formula:

$$\text{lithogenic fluxes} = \text{TPM} - \text{CaCO}_3 - \text{SiO}_2 - 2\,\text{POC} = \text{TPM} - \frac{100}{12}\,\text{PIC} - \frac{60}{28}\,\text{bSi} - 2\,\text{POC} \quad (1)$$

where the calcium carbonate ($CaCO_3$) equals the PIC and silicon dioxide (SiO_2) equals bSi with their corresponding molecular weight corrections.

The ballast percent of each depth were calculated using the following formula:

$$\text{ballast percent} = 1 - (2\,\text{POC}/\text{TPM}) \quad (2)$$

Statistical analysis

The statistical analyses were done using the software R (RCoreTeam 2019). ASVs in the bacterial data set, which were identified as chloroplast origin, were removed from the data set. The abundances of 16S rRNA gene and 18S rRNA PCR-amplified gene fragments were plotted including all the genera making up at least 0.5% of the total data sets. An additional data set was generated excluding all ASVs that were identified as “Metazoa” and “Rhizaria” from the 18S rRNA gene data set. The ASVs were filtered using the package “OTUtable” (Linz 2018) by only allowing a minimum relative sequence read abundance of 0.1% in at least one sample and occurrence in at least 7% of the samples in the 16S rRNA gene data set and 4.4% in the 18S rRNA gene data set and the modified 18S rRNA gene data set (equivalent to the minimum sampling size of 3). Multivariate analyses were performed with the package “vegan” (Dixon 2003) and “ape” (Paradis and Schliep 2019). Illustration were done using the R packages “ggplot2” (Wickham 2016). Samples were clustered in dendrograms calculated on the Bray Curtis dissimilarities (method: Ward’s). For the NMDS analyses, the Bray-Curtis dissimilarity was used on the untransformed data. Environmental data (CTD and nutrients) from Seifert et al. (2019) were used for redundancy analyses (RDA) with Hellinger transformed data.

Results

Assessment of eukaryotic communities based on 18S rRNA PCR-amplified gene sequences

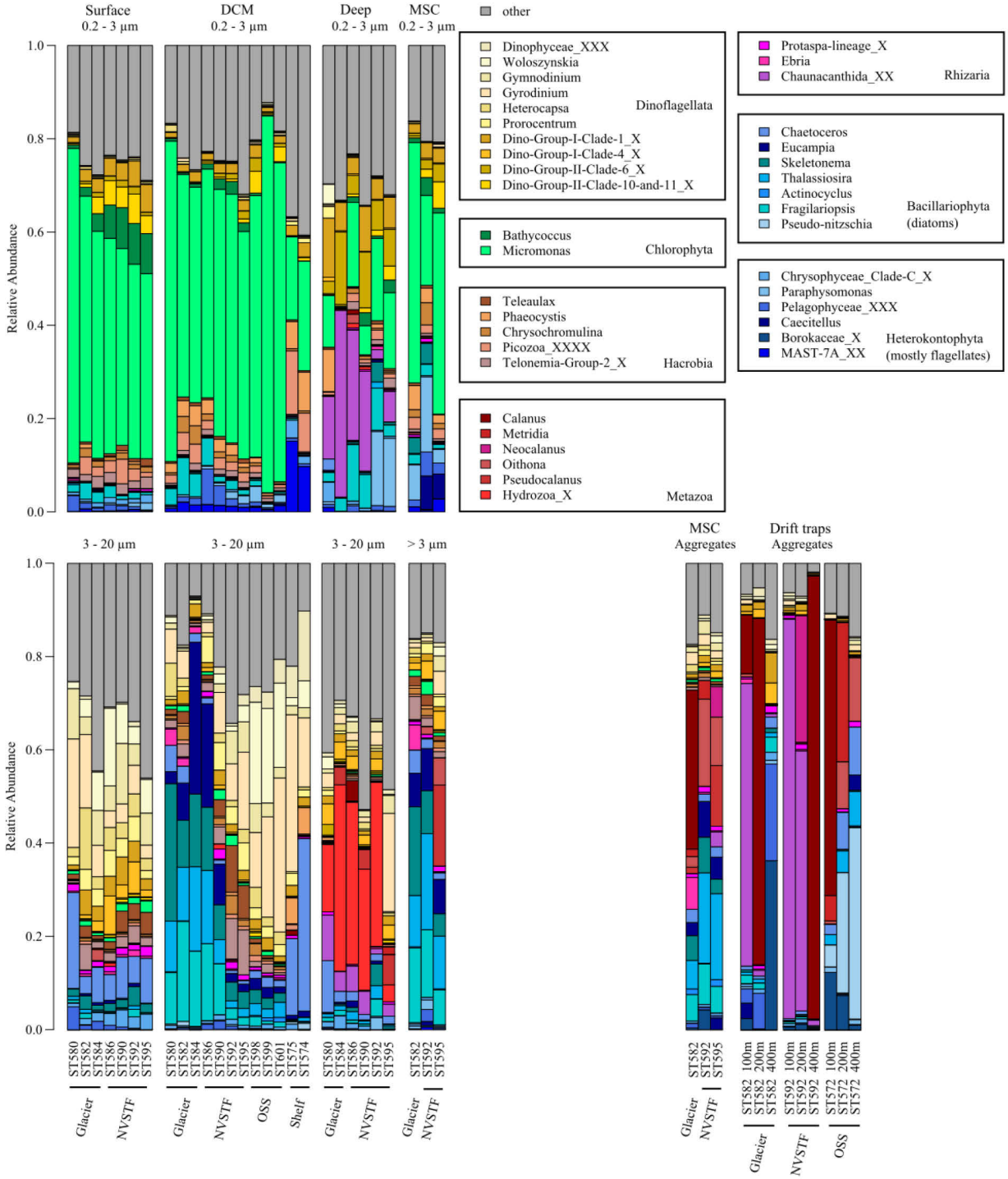

Fig. 2: Taxonomic composition of eukaryotic taxa based on read frequencies of PCR-amplified 18S rRNA gene fragments in different water depths/layers and size fractions, showing differences in the abundances of the eukaryotic communities in the surface (Surface), the deep chlorophyll a maximum (DCM) and at depth (Deep) and eukaryotic communities collected with the Marine Snow Catcher (MSC) and the drifting sediment traps (Drift traps). Types of samples were 0.2 - 3 µm filtration (Surface, DCM, Deep, MSC), 3 - 20 µm filtration (Surface, DCM, Deep), > 3 µm filtration (MSC) and aggregates (MSC, Drift traps). Sampled were the area close to the Daugaard-Jensen Glacier in the Nordvestfjord (Glacier), the Norvestfjord (NVSTF), the Outer Scoresby Sund (OSS) and the Greenland shelf (Shelf).

We assessed the eukaryotic community present within two size fractions at three depths (surface, DCM and 1000 m depth), i.e. picoplankton (0.2 - 3 µm) and nanoplankton (3 – 20 µm), and within aggregates at thirteen stations along a transect from the Daugaard-Jensen Glacier in the inner Nordvestfjord to the mouth of the Outer Scoresby Sund (Fig. 2). Based on the 18S rRNA gene amplicon read frequency data the eukaryotic communities clustered according to sample depth and size-fractions (Fig. 3), with largely different eukaryotic communities indicated for aggregates, the nanoplankton fractions and the picoplankton fractions (Fig. 2).

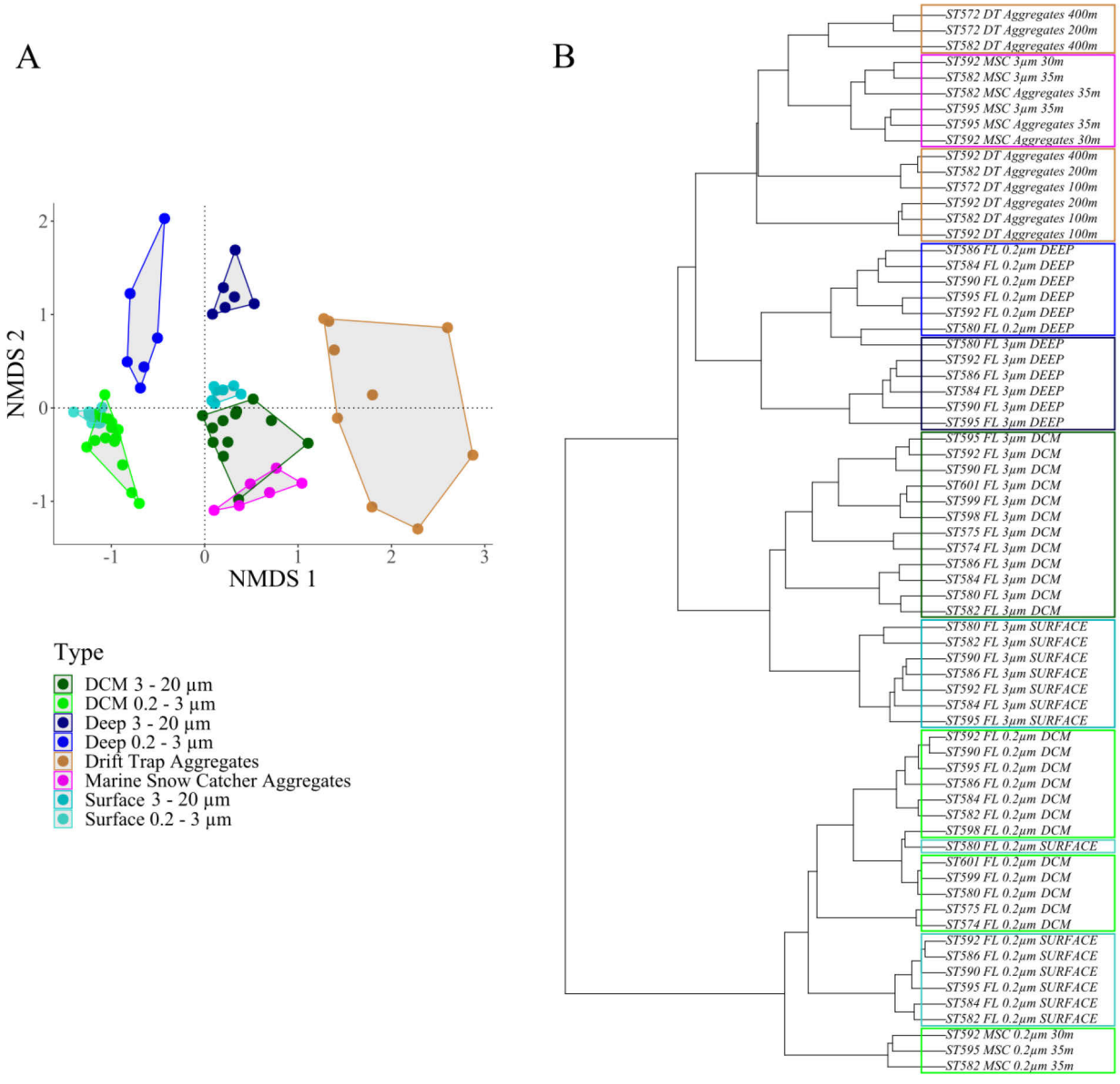

Fig. 3: (A) Non-metric Multi-dimensional Scaling (NMDS) plot on Bray-Curtis-Dissimilarity based on read frequencies of PCR-amplified 18S rRNA gene fragments and (B) dendrogram on the Bray-Curtis-Dissimilarity using the Ward.D2 clustering. Groups shown are eukaryotes in the surface (Surface, 0.2 - 3 µm and 3 - 20 µm), deep chlorophyll a maximum (DCM, 0.2 - 3 µm, including MSC 0.2 - 3 µm samples; and 3 - 20 µm) and at depth (Deep, 0.2-3 µm and 3 – 20 µm), the Marine Snow Catcher (MSC, >3µm and aggregate as one group) and of the drifting sediment trap (DT) aggregates.

Surface, DCM and deep eukaryotic communities – Surface and DCM picoeukaryotes (0.2 - 3 µm) clustered together throughout the entire fjord, suggesting that the picoeukaryotes were similar at all photic depths, and were different from the deep picoplankton community (Fig. 3). The Chlorophyta *Micromonas* was the most dominant phytoplankton group in the picoplankton (0.2 – 3 µm) fraction in the surface and DCM as indicated by relative sequence read abundances of 48.4 ± 9.5% and 51.2 ± 15.7%, respectively (Fig. 2). The small eukaryotes (0.2 – 3 µm) in the deep water samples contained the Acantharia (Rhizaria) order Chaunacanthida (17.8 ± 13.7%), the diatom *Fragilariopsis* (5.9 ± 4.2%), the microalgae *Micromonas* (11.6 ± 7.2%), and the dinoflagellates from the *Dino-Group-I-Clade-1* (7.2 ± 3.4%) and *Dino-Group-II-Clade-6* (8.1 ± 4.9%) (Fig. 2).

The surface and the DCM eukaryotic nanoplankton community (3 - 20 µm) clustered close to each other, but separately from the nanoeukaryotes at 1000 m depth (Fig. 3). While the surface nanoplankton community was primarily dominated by dinoflagellates throughout the entire fjord, e.g. *Gyrodinium* (8.9 ± 7.7%) and *Gymnodinium* (7.4 ± 3.4%) (Fig. 2), the composition of the nanoplankton at the DCM differed over the transect. It was dominated by diatoms in the Nordvestfjord and gradually changed to a dinoflagellate-dominated community in the Outer Scoresby Sund (Fig. 2). The 3 - 20 µm fraction at 1000 m had a high contribution by Hydrozoa (25.7 ± 14.1%, Fig. 2), which was not observed in the surface or DCM.

Marine Snow Catcher (MSC) aggregates – The aggregates collected by the MSC clustered closest to the drifting sediment trap aggregates but also seemed to be related to the deep eukaryotic community from 1000 m including both the nanoplankton (3 – 20 µm) and picoplankton fractions (0.2 - 3 µm; Fig. 3). The aggregates collected by the MSC below the DCM in Nordvestfjord were composed of diatoms, including *Fragilariopsis* (6.7 ± 1.7%), *Thalassiosira* (14.6 ± 7.4%), *Skeletoma* (5.3 ± 2.3%) and *Eucampia* (5.1 ± 2.5%) (Fig. 2). Additionally, the aggregates contained zooplankton DNA from copepods, mainly the genera *Oithona* (10.4 ± 8.2%) and *Calanus* (11.4 ± 19.7%). It is important to point out that we cannot determine the origin of the copepod DNA, which could originate from copepod feeding on the aggregates, fecal pellets produced by the copepods, from carcasses and moulds from the copepods, or a combination of all three. We also observed other metazoan and rhizarian groups in the aggregates (Fig. 2), which were largely absent in the eukaryotic community in the water column (collected using the CTD-Rosette). The nanoplankton (> 3 µm) sampled from the suspended/slow-settling fraction of the MSC clustered together with the MSC aggregates, and we considered them as one group for the dissimilarity analysis in the NMDS (Fig. 3). The MSC aggregates did not cluster together with any of the picoeukaryotes (0.2 – 3 µm) from the surface,

DCM or the 0.2 – 3 µm fraction collected with the MSC (Fig. 3). The MSC water samples that were collected directly below the DCM had similar picoplankton compositions to those collected in the DCM by the CTD-Rosette Sampler. Hence, we assigned the MSC picoplankton samples to the eukaryotic picoplankton from the DCM for the dissimilarity analysis (Fig. 3). The dominant eukaryotes from the size-fraction of 0.2 - 3 µm were only found at low relative abundances in the aggregates, for instance the Chlorophyta *Micromonas* (MSC aggregates: 0.6 ± 0.0%, MSC > 3µm: 1.6 ± 1.1%, Fig. 2).

To allow direct comparison between the water column plankton and the eukaryotic aggregate composition, we excluded metazoan and rhizarian groups (Fig. 4). Overall, the nanoplankton (3 - 20 µm) at the DCM near the Daugaard-Jensen Glacier (stations 580, 582, 584, and 586) clustered together with the aggregates collected below the DCM through the entire Nordvestfjord (Stations 582, 592, and 595; Fig. 4 and Fig. S1 in the supplementary information). On the other hand, the nanoeukaryotic composition at the DCM near the sill (Stations 590, 592, and 595) did not resemble any of the aggregates collected below the DCM in the same region (Stations 582, 592, and 595; Fig. 4 and Fig. S1 in the supplementary information).

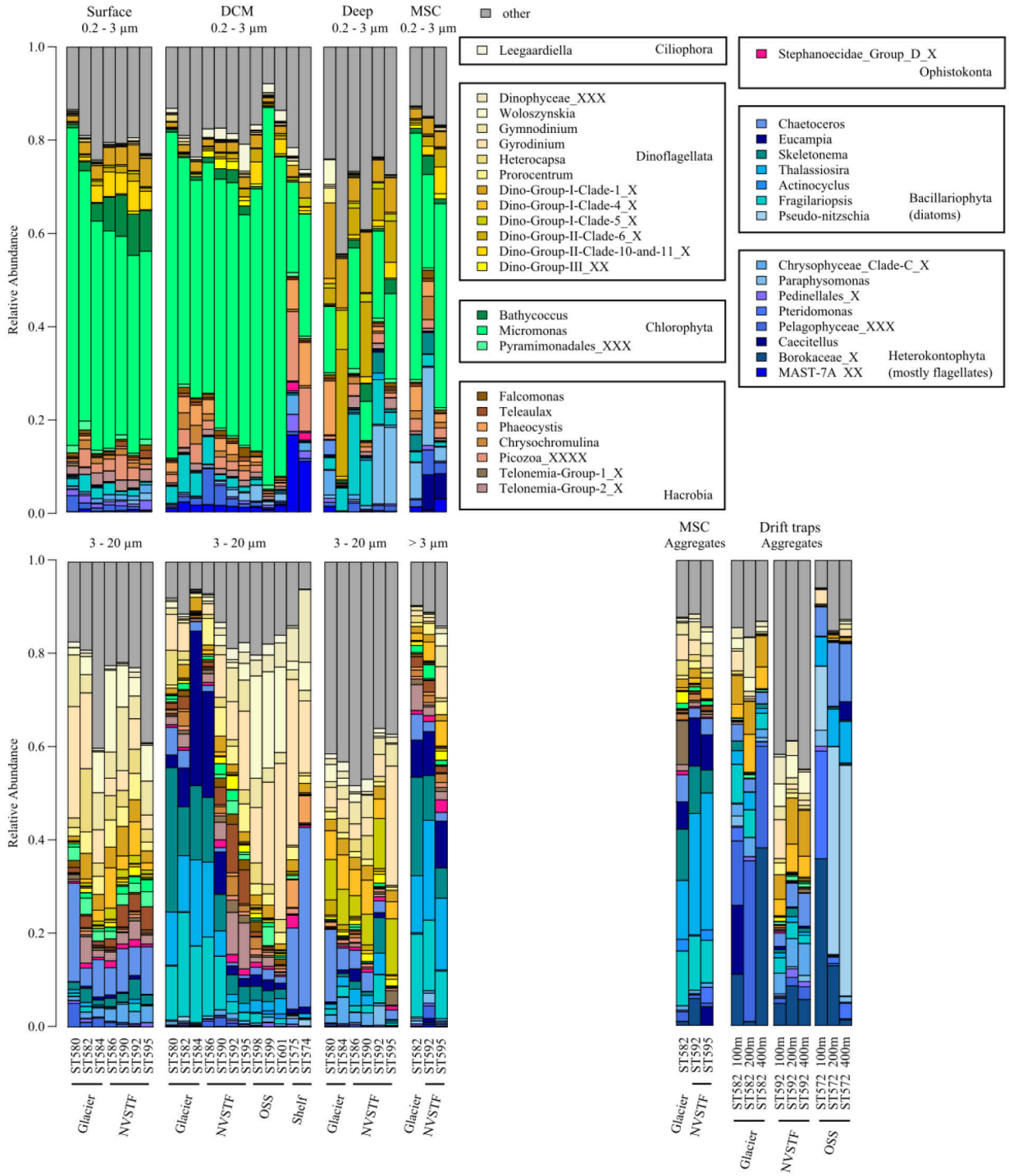

Fig. 4: Taxonomic composition of eukaryotic taxa based on read frequencies of PCR-amplified 18S rRNA gene fragments excluding the taxonomic group “Metazoa” and “Rhizaria” in different water depths/layers and size fractions, showing differences in the abundances of the eukaryotic communities without metazoan and rhizaria in the surface (Surface), the deep chlorophyll a maximum (DCM) and at depth (Deep) and eukaryotic communities without metazoan and rhizaria collected with the Marine Snow Catcher (MSC) and the drifting sediment traps (Drift traps). Types of samples were 0.2 - 3 µm filtration (Surface, DCM, Deep, MSC), 3 - 20 µm filtration (Surface, DCM, Deep), > 3 µm filtration (MSC) and aggregates (MSC, Drift traps). Sampled were the area close to the Daugaard-Jensen Glacier in the Nordvestfjord (Glacier), the Norvestfjord (NVSTF), the Outer Scoresby Sund (OSS) and the Greenland shelf (Shelf).

Sediment trap aggregates – The eukaryotic communities (including Metazoa and Rhizaria) associated with aggregates collected 10 m below the DCM (MSC) cluster closely together with those collected between 100 and 400 m using free-drifting sediment traps in the Nordvestfjord (Fig. 3). The aggregates collected by the drifting sediment traps (> 100 m) were dominated by heterotrophic groups, such as acantharians and copepods (Fig. 2). The Acantharia order Chaunacanthida was the second most abundant eukaryotic group associated with aggregates below 100 m depth with relative abundance of up to 85.6% in the Nordvestfjord. However, Chaunacanthida only contributed little to the aggregate-associated eukaryotic community in the Outer Scoresby Sund. *Calanus* (26.9 ± 38.3%) was the most abundant eukaryote associated with aggregates collected in both Nordvestfjord and Outer Scoresby Sund, while *Metridia* (up to 29.9%) and *Oithona* (up to 13.6%) were only observed to be associated with settling aggregates below 100 m in the Outer Scoresby Sund. When excluding metazoan and rhizarian groups, the aggregate composition below 100 m was highly dependent on the location in the fjord (Fig. 4). For example, the aggregates collected near the glacier in the Nordvestfjord had high relative abundances of Heterokontophyta, e.g. like family members of Borokaceae (up to 38.2%) and Pelagophyceae (up to 34.6%), and of the diatom *Fragilariopsis* (up to 8.3%), as well as of several groups of dinoflagellates, e.g. Dino-Group-I Clade-1 and Clade-4 (together up to 15.3%). When excluding metazoans and rhizarians, the dinoflagellates were contributing 24.0 – 35.4% of the total eukaryotic composition associated with the aggregates in the middle of Nordvestfjord (Fig. 4). The aggregates collected below 100 m at the mouth of the Outer Scoresby Sund showed high relative abundances of diatoms, e.g. *Pseudo-nitzschia* (13.8 - 49.6%), *Chaetoceros* (6.3 – 12.5 %) and *Thalassiosira* (6.3 – 8.9%). At 100 m, high relative abundances of the representatives of the family Borokaceae (35.8%) and *Pteridomonas* (23.1%) were observed. We only found few dinoflagellates (< 5%) within sediment trap collected aggregates in the Outer Scoresby Sund (Fig. 4).

Assessment of bacterial communities based on 16S rRNA PCR-amplified gene sequences

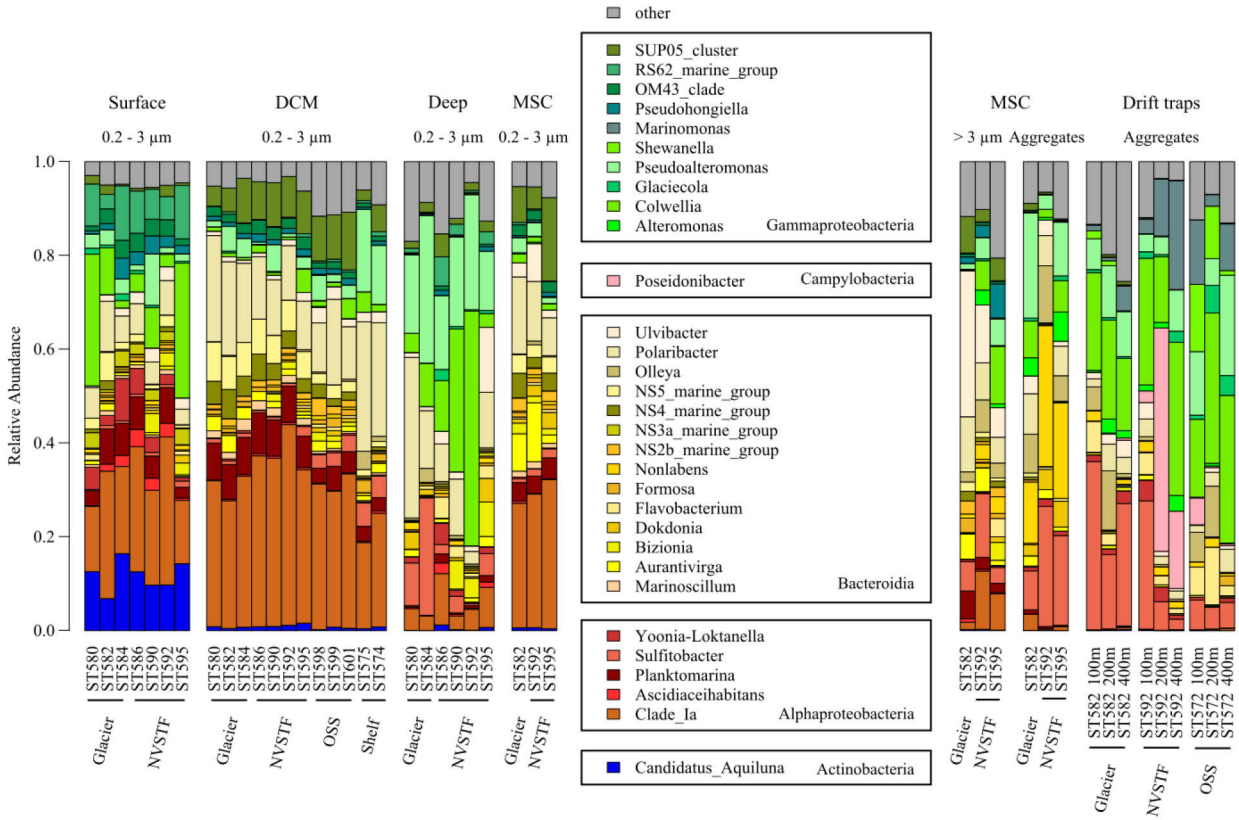

Fig. 5: Taxonomic composition of bacterial taxa based on read frequencies of PCR-amplified 16S rRNA gene fragments in different water depths/layers and size fractions, showing differences in the abundances of the free-living bacterial communities in the surface (Surface), the deep chlorophyll a maximum (DCM) and at depth (Deep), and the particle- and aggregates-attached bacterial communities collected with the Marine Snow Catcher (MSC) and the drifting sediment traps (Drift traps). Types of samples were 0.2 - 3 µm filtration (Surface, DCM, Deep, MSC), > 3 µm filtration (MSC) and aggregates (MSC, Drift traps). Sampled were the area close to the Daugaard-Jensen Glacier in the Nordvestfjord (Glacier), the Norvestfjord (NVSTF), the Outer Scoresby Sund (OSS) and the Greenland shelf.

Sequence read-based relative abundances of bacterial communities revealed a clear differentiation at the genus level between the free-living bacterial communities (FL, 0.2 – 3 µm), the particle and slow-sinking/suspended aggregate fraction (i.e. particle-attached, PA; the > 3 µm fraction from the MSC water samples) and aggregate-attached communities (aggregates collected using the MSC and drifting traps; Fig. 5). This was apparent from both, the Bray-Curtis-Dissimilarity represented in the dendrogram clustering and NMDS plot (Fig. 6).

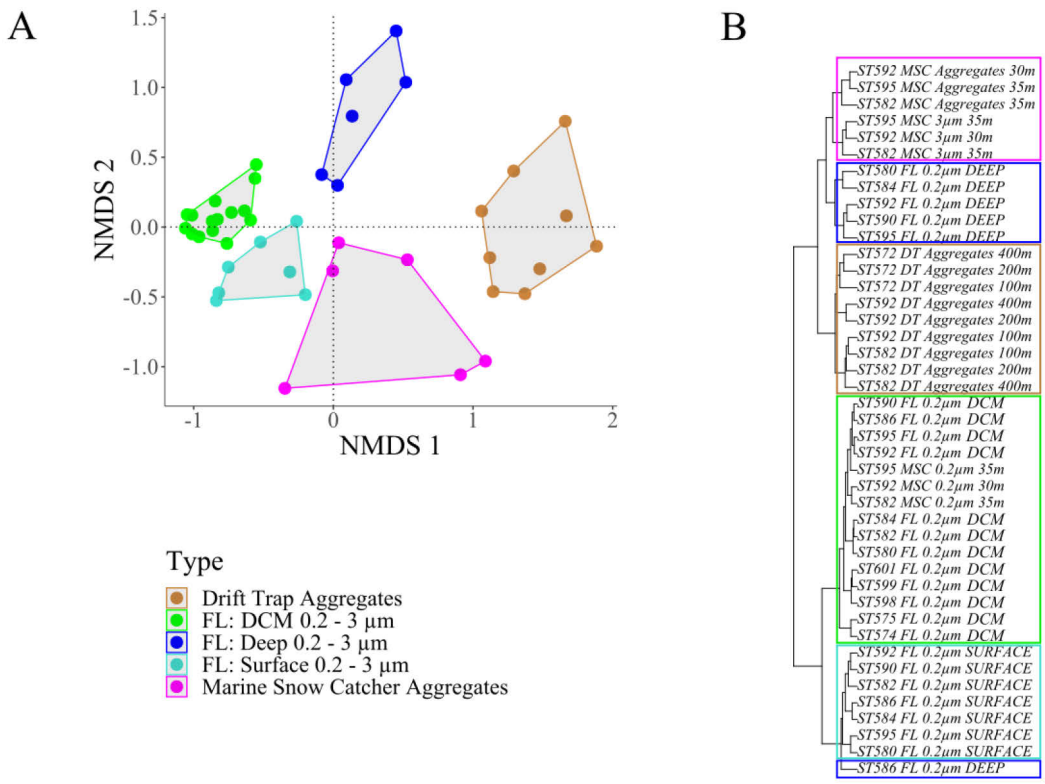

Fig. 6: (A) Non-metric Multi-dimensional Scaling (NMDS) plot on Bray-Curtis-Dissimilarity based on frequencies of PCR-amplified 16S rRNA gene fragments and (B) dendrogram on the Bray-Curtis-Dissimilarity using the Ward.D2 clustering. Groups shown are the free-living (FL) bacterial communities in the surface (Surface, 0.2 – 3 µm), deep chlorophyll a maximum (DCM, 0.2 - 3 µm, including MSC 0.2 - 3 µm samples) and at depth (Deep, 0.2 - 3 µm), the Marine Snow Catcher (MSC, >3 µm and aggregate as one group) and the drifting sediment trap (DT) aggregates.

FL bacterial communities – FL bacterial communities differed between surface and DCM (Fig. 6), and both fractions were considerably different from the FL bacterial community collected from 1000 m depth (Fig. 5). This indicated a strong vertical separation in the FL bacterial communities in the fjord. Compositional differences were mostly explained by differences in the temperature, salinity, and fluorescence (RDA, Fig. S2 in the supplementary information), which suggested that they clustered according to different water masses. Similar patterns were also found for the eukaryotes (RDA, Fig. S3 in the supplementary information). Both the surface and DCM FL bacterial communities showed highest relative abundance in the sequence read frequencies for the alphaproteobacterial SAR 11 Clade_Ia (21.7 ± 7.0% in the

surface and 31.8 ± 5.8% in the DCM, Fig. 5). The genus *Planktomarina* accounted for 5.6 ± 2.2% and 6.1 ± 2.0% in surface and DCM, respectively. Surface waters contained high relative abundances of *Candidatus* Aquiluna (11.7 ± 3.2%), a member of Actinobacteria, indicative of brackish water and therefore found at stations with meltwater at the surface. In addition to *Candidatus* Aquiluna, the gammaproteobacterial RS62_marine_group was primarily found in the surface with a relative abundance of 7.9 ± 3.2%. DCM samples, in contrast, showed a relative abundance of 15.2 ± 6.0% for the genus *Polaribacter* (phylum Bacteroidetes). The deep FL bacterial community was more heterogeneous compared to the surface and DCM communities, which was observed from a higher spread of the samples in the Shannon-Index and Inverse Simpson Index (data not shown). In the samples collected from 1000 m, high relative abundances were observed for gammaproteobacterial genera *Pseudoalteromonas* (20.0 ± 6.9%), *Colwellia* (17.9 ± 18.6%), and the bacteroidotal genus *Polaribacter* (13.5 ± 10.8%) (Fig. 5). Some stations showed high relative abundances of the alphaproteobacterial genus *Sulfitobacter* (ST580, 9.1%; ST584, 25.0%).

Marine Snow Catcher (MSC) aggregates – FL prokaryotic communities in the surface and DCM waters clustered separately from both FL prokaryotic at depth and the aggregate-attached prokaryotic communities (Fig. 6). The aggregate-attached bacterial communities from the MSC were dissimilar to the FL bacterial communities in DCM (Fig. 6). The genus *Nonlabens* was only observed in high relative abundances (21.2 ± 8.5%) from the MSC aggregates (Fig. 5). The majority of the relative abundance of Gammaproteobacteria were affiliated with genus *Pseudoalteromonas* (12.3 ± 9.7%). *Sulfitobacter* had a relative abundance of 17.7 ± 8.7% and was the most abundant group of the Alphaproteobacteria. The bacterial communities attached to single large eukaryotes and suspended/slow-sinking aggregates (PA; > 3 µm from the water samples collected with the MSC) clustered together with the aggregate-attached bacteria (aggregates collected using the MSC; Fig. 6). Hence, we combined PA and aggregate-attached bacterial communities as aggregate-attached bacterial community for the NMDS plot (Fig. 6). However, the PA and aggregate-attached bacterial communities differed by having a high relative abundance of the bacteroidetal genus *Ulvibacter* of 16.6 ± 12.9% in the PA (>3 µm) fraction, which was not observed for the aggregate-attached bacterial communities (Fig. 5). The FL bacterial communities (0.2 – 3 µm) collected by the MSC was similar to the FL bacterial community collected from the DCM using the CTD-Rosette, hence, we combined the FL bacterial communities from the DCM and MSC for the NMDS plot (Fig. 6).

Sediment trap aggregates – The aggregate-attached bacterial communities collected by the free-drifting sediment traps from 100 m, 200 m, and 400 m differed from the FL bacterial communities collected from the DCM, but were similar to the MSC aggregate-attached and the deep FL bacterial communities (Fig. 6). *Colwellia* (23.5 ± 7.5%) and *Pseudoalteromonas* (9.4 ± 5.6%) were abundant in the drifting sediment traps (Fig. 5). The *Campylobacteria Poseidonibacter* was observed attached to aggregates collected between 100 m and 400 m depth with an average relative abundance of 8.2 ± 15.7%. However, this fairly high relative abundance was driven by very high relative abundances at a few stations and depths, i.e. station 592 (Fig. 5). The Gammaproteobacterium *Marinomonas* was observed with high aggregate-attached relative abundances in the free-drifting sediment trap samples (8.0 ± 7.5%), while it was observed only at low relative abundances in the FL bacterial communities at all depths and attached to the MSC aggregates.

CARD-FISH-based assessment of bacterial communities

FL communities differed strongly in their composition over depth, with, e.g., CF319a-positive cells belonging to *Bacteroidetes* declining in relative abundance from 31.7% in the surface to 3.9% at 1000 m (Fig. 7). Within aggregates collected by drifting sediment traps, PSA184, which was used to stain *Pseudoalteromonas* as well as some representatives of *Colwelliacea*, indicated high relative abundances of 39.5 ± 14.0%. While we only observed low relative abundances in FL fractions (0.5 ± 0.3%), probe ALT1413, specific for *Alteromonas* as well as some members of the family *Colwelliaceae* showed relative aggregate-attached abundances of 10.1 ± 3.5% in sediment trap collected aggregates. Probe ROS537, which stains Alphaproteobacteria from the clade *Roseobacter*, showed higher relative abundances in the aggregates (13.1% ± 3.6%) compared to the FL communities (3.8 ± 2.4%). *Planctomycetes* (PLA46) showed low relative abundances in both aggregate-attached and FL bacterial communities (both: 0.7% ± 0.5%). While the 16S rRNA gene analyses suggested high relative aggregate-attached abundances of *Arcobacter* from the sediment trap collected aggregates, the CARD-FISH analyses (*Arcobacter*, ARC94) suggested low relative abundances in all FL (0.1 ± 0.1%) and aggregate-attached samples (0.7 ± 0.7%) (Fig. 7). The relative abundance of the *Pseudoalteromonas* as well as some *Colwelliacea* (PSA184) was positively correlated to the share of fecal pellets to the total volume detected from the *in situ* camera (ISC) profiles at the corresponding depths (Spearman's rank correlation R= 0.73, p=0.03, n=9).

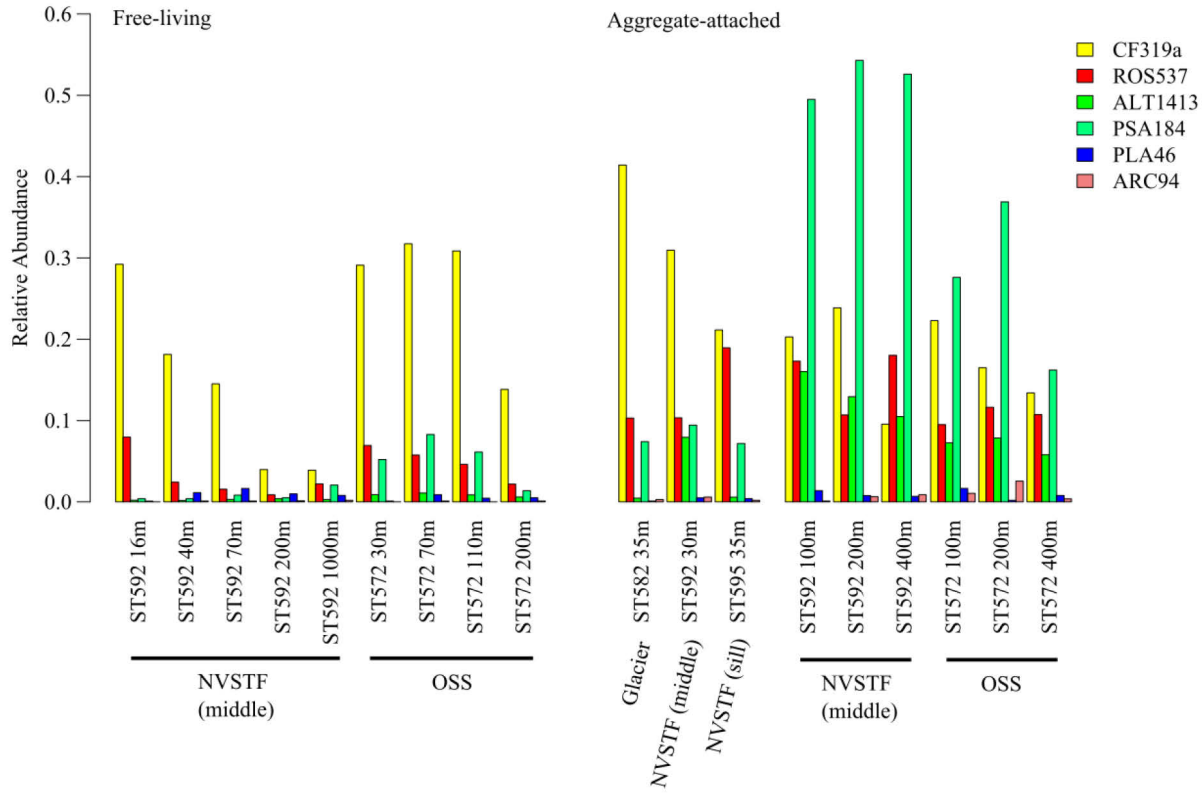

Fig. 7: Relative abundance of CARD-FISH cell counts of the free-living bacterial communities and the aggregate-attached bacterial groups (Marine Snow Catcher and drifting sediment trap) in the Outer Scoresby Sund (OSS) and in the Nordvestfjord (NVSTF). Investigated were *Bacteroidetes* (CF319a), the *Roseobacter* clade (ROS537), *Alteromonas/ Colwellia* (ALT1413), *Pseudoalteromonas/ Colwellia* (PSA184), *Planctomycetes* (PLA46) and *Arcobacter* (ARC94).

Aggregate composition

The free-drifting sediment trap at station 582 showed that the region near the Daugaard-Jensen Glacier in Nordvestfjord had the highest biogeochemical fluxes compared to all the other trap deployments in the fjord and large quantities of silt were collected. The mass flux near the glacier increased from 100 m to 400 m, which was due to a high contribution of lithogenic material presumably from the silt-release from the melting glacier (Table 2, Fig. S4 in the supplementary information). The total ballast material ($CaCO_3$, bSi, and lithogenic material) near the glacier made up between 98.4 to 99.2% of the total mass flux which was higher than at the other trap deployment locations (75 to 97.8%). The C:N ratio decreased from 12.5 at 100 m to 11.6 at 200 m and increased to 15.6 at 400 m (Table 2, Fig. S4 in the supplementary information). Based on image analyses from the ISC profiles, fecal pellets contributed between 5 to 13% to the total aggregate volume near the glacier (Fig. 8A), which was lower than observed elsewhere in the fjord (Nordvestfjord: 12 - 39%, Outer Scoresby Sund 25 - 57%).

Table 2: Biogeochemical flux measured by drifting sediment traps at 100 m, 200 m, and 400 m. The measured parameters included particulate organic carbon (POC) flux, particulate inorganic carbon (PIC) flux, particulate organic nitrogen (PON) flux, total dry mass (TDM) flux, biogenic silica (BSi) flux, carbon-to-nitrogen ratio (C:N ratio), lithogenic material flux, total ballast material, and particulate organic carbon to dry weight ratio (POC:DW).

Trap	Depth [m]	POC [mg m^{-2} d^{-1}]	PIC [mg m^{-2} d^{-1}]	PON [mg m^{-2} d^{-1}]	TDM [mg m^{-2} d^{-1}]	BSi [mg m^{-2} d^{-1}]	C:N ratio	Lithogenic material [mg m^{-2} d^{-1}]	Total Ballast Material [%]	POC:DW [%]
Glacier (Station 582)	100	362	700	34	52182	1914	12.5	41520	98.6	0.7
	200	438	1080	44	54419	2297	11.6	39624	98.4	0.8
	400	713	1501	53	187987	3091	15.6	167425	99.2	0.4
Nordvestfjord (middle) (Station 592)	100	120	114	12	10421	738	11.8	7651	97.7	1.1
	200	106	52	10	8662	624	12.2	6682	97.5	1.2
	400	188	56	9	9327	631	23.2	7134	96.0	2.0
Nordvestfjord (sill) (Station 595)	100	132	32	12	8040	488	12.7	6464	96.7	1.6
	200	114	46	8	10264	474	16.9	8639	97.8	1.1
	400	87	29	6	7060	371	17.2	5852	97.5	1.2
Outer Scoresby Sund (Station 572)	100	137	0	15	1095	143	10.9	515	75.0	12.5
	200	136	55	16	2438	343	10.2	974	88.8	5.6
	400	193	312	16	4687	477	13.8	679	91.8	4.1

Small compact brown aggregates were predominately observed in the middle of the Nordvestfjord (station 592) and at the sill (station 595). The high C:N ratios between 11.8 and 23.2 in the Nordvestfjord suggested that the collected material was highly degraded (Table 2, Fig. S4 in the supplementary information). The organic matter collected by the sediment traps in the middle of the Nordvestfjord and at the sill seemed less ballasted by lithogenic material compared to the exported material near the Daugaard-Jensen Glacier. The POC flux ranged between 87 to 188 mg m^{-2} d^{-1} with the highest flux in the middle of the Nordvestfjord at 400 m (Table 2, Fig. S4 in the supplementary information).

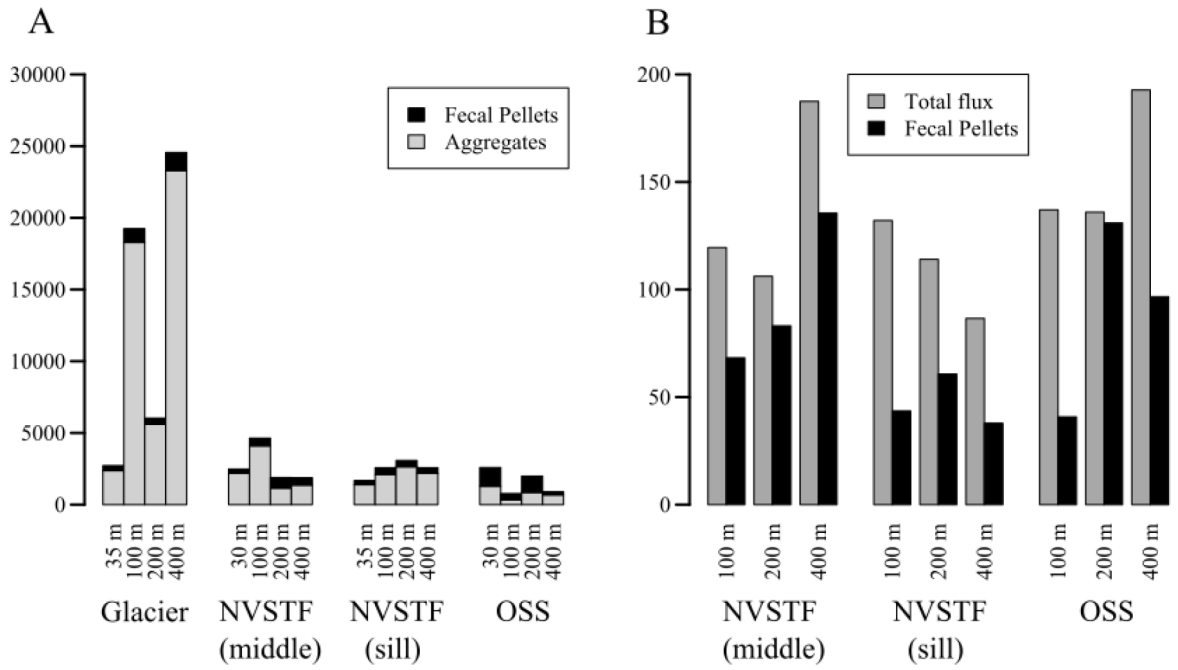

Fig. 8: (A) Total volume [mm^3 m^{-3}] of aggregates (grey) and fecal pellet (black) at 30/35 m, 100 m, 200 m and 400 m at the glacier, in the Nordvestfjord (middle and at the sill) and in the Outer Scoresby Sund (OSS), based on the *in situ* camera profiles. The fecal pellets made up 5 to 57 % of the total volume, with the highest contribution in the Outer Scoresby Sund. (B) Total POC flux (grey) and estimated fecal pellet carbon flux (black) in [mgC m^{-2} d^{-1}] at 100 m, 200 m and 400 m at the middle and at the sill in the Nordvestfjord, and in the Outer Scoresby Sund. According to the estimation the fecal pellets were making up between 30-96% of the POC flux.

To identify the contribution of aggregates and fecal pellets to the carbon export, we analyzed the particle composition (aggregates vs fecal pellets) from the ISC profiles and related that to the sediment trap depths and locations. However, it is important to keep in mind that ISC profiles provide a snapshot of the particle types, size-distribution, and abundance through the water column for a short time-period while the gel traps represent an integrated particle flux at one depth over the entire deployment time of the trap. Furthermore, it is also important to note that the deployment time of the gel trap was shorter and not done in parallel to collection of biogeochemical flux in the Nordvestfjord. The ISC suggested that 12 to 39% of the total

aggregate volume was contributed by fecal pellets in the middle of the Nordvestfjord (station 592), while only between 14 to 18% of the total aggregate volume was contributed by fecal pellets at the sill (station 595; Fig. 8A). The contribution of fecal pellets to total aggregate volume was somewhat lower when estimated from the gel trap where only 2 – 5% of the total aggregate volume was contributed by fecal pellets between 100 and 400 m during the two to three hours of gel trap deployments. However, despite the low volume contribution by fecal pellets, their contribution to total particulate organic carbon flux was estimated to range between 33 to 78% in the Nordvestfjord (Fig. 8B).

At the mouth at the Outer Scoresby Sund (station 572), the C:N ratios were 10.9 at 100 m and 10.2 at 200 m, which were lower than that observed for the traps in the Nordvestfjord (Table 2), suggesting less degraded organic matter. There was a vertical shift in types at the mouth of the Outer Scoresby Sund, with a dominance by fecal pellets at 100 m to 200 m to a dominance of small compact brown aggregates 400 m. The compact brown aggregates at 400 m at the mouth were similar in appearance to those collected in the Nordvestfjord and had a higher C:N ratio of 13.8. Even though the total mass flux was relatively low at the mouth of Scoresby Sund, the POC flux was between 137 mg m^{-2} d^{-1} and 193 mg m^{-2} d^{-1} (Table 2, Fig. S4 in the supplementary information), which was higher than the POC flux at the sill and the middle of Northvestfjord, but lower than at the glacier in the inner Nordvestfjord. The lithogenic flux and the total ballast percentage (75.0% - 91.8%) was much lower in the Outer Scoresby Sund compared to the Nordvestfjord.

We observed higher abundance of large fecal pellets in the upper 200 m of the water column at the mouth of the Outer Scoresby Sund (station 572) compared to the Nordvestfjord. This indicated active and more intense grazing by large zooplankton such as copepods and krill at the mouth of the fjord compared to the Nordvestfjord (Fig. 8A). According to our ISC analysis the fecal pellets' total volume made up between 25 - 57% of the total aggregate volume at the mouth of Scoresby Sund. Using the gel trap to estimate the total volume contribution to volume flux by fecal pellet, we observed that the pellets contributed to the total volume flux between 14 - 34%. When converted to fecal pellet carbon, we estimated the fecal pellets had a potential total contribution to the POC flux of 30 to 96% (Fig. 8B).

Discussion

In order to gain a better understanding of the mechanisms driving carbon export and sequestration in Arctic fjords, we sampled sinking aggregates in the world's largest fjord, Scoresby Sund, and compared their composition to the eukaryotic and the bacterial community composition in the free water column. We observed spatial differences throughout the fjord, from the inner deep Nordvestfjord, which is separated from the Outer Scoresby Sund (OSS) by a sill, to the mouth of the fjord, where the OSS is connected to the shelf and open ocean. The inner Nordvestfjord is highly affected by a large marine-terminating glacier, the Daugaard-Jensen Glacier, resulting in a pronounced surface meltwater layer.

Aggregate formation, retention and lateral transport in the Nordvestfjord

The eukaryotic aggregate composition at 30 – 35 m depth (MSC) of the inner Nordvestfjord was similar to the eukaryotic plankton composition (3 – 20 µm) in the deep chlorophyll maximum (DCM) at the innermost stations near the glacier, but differed from the eukaryotic composition elsewhere in the fjord (Fig. 4 and S1 in the supplementary information). This suggests that the aggregates found at 30 - 35 m depth throughout the Nordvestfjord were formed at the innermost stations, where we also observed high chlorophyll concentrations (Seifert et al. 2019), and were subsequently transported laterally eastward with the outflow of the water. They were likely retained at this depth during the lateral transport, as this was where increasing salinity and density were observed due to meltwater input to the surface in the Nordvestfjord (Seifert et al. 2019). Previous studies have shown that aggregates are retained and often accumulated at density and salinity gradients, both in laboratory studies (Kindler et al. 2010; Prairie et al. 2013; Prairie et al. 2015) and *in situ* (Alldredge et al. 2002; MacIntyre et al. 1995; Möller et al. 2012). While aggregates are able to cross density gradients caused by changes in temperature relatively fast, density gradients generated by salinity differences lead to a much longer particle retention time (MacIntyre et al. 1995; Prairie et al. 2013). Aggregate retention time by salinity is dependent on the time needed for salt diffusion into the pore-water of aggregates, retaining especially large porous aggregates (Camassa et al. 2013; Kindler et al. 2010). This indicates that especially large marine snow (aggregates >500 µm in diameter), which is very porous (Flintrop et al. 2018), was prevented from sinking out of the upper water column and therefore transported eastward from the inner Nordvestfjord to the OSS.

Our results show that the retained aggregates collected at 30 - 35 m depth had an attached bacterial community similar to the particle-attached (PA) bacteria (> 3 µm) but

different from the free-living (FL) bacteria in the surface and DCM (Fig. 5 and 6). The aggregates contained many diatom-associated bacterial groups, such as *Sulfitobacter*, bacteria from the *Roseobacter* clade and Flavobacteriia (Guannel et al. 2011; Pinhassi et al. 2004; Schäfer et al. 2002), which is consistent with the diatoms that were found in the aggregates (*Fragilariopsis*, *Thalassiosira*, *Skeletonema*, and *Eucampia,* Fig. 2). In particular representatives of Flavobacteriia, Gammaproteobacteria and Alphaproteobacteria are known to degrade diatom biomass (Teeling et al. 2012) suggesting that these bacteria were already attached to the diatoms when they aggregated.

Ballasting dominates carbon export in the innermost Nordvestfjord

Despite the retention of the aggregates and subsequent lateral transport that occurred near the glacier in the inner Nordvestfjord, the highest POC flux were observed in this region (Table 2, Fig. S4 in the supplementary information). Near the glacier, lithogenic fluxes were 1-3 orders of magnitude higher than at other stations (Table 2, Fig. S4 in the supplementary information), which taken together with observations of high turbidity (Seifert et al. 2019) and direct observations of silt in the gel traps showed that there was a high silt input from the melting glacier in this region. Silt and lithogenic ballasting of settling aggregates is known to increase their densities and sinking velocities (Iversen and Robert 2015; van der Jagt et al. 2018). Therefore, the ballasting effect of silt was likely responsible for the high POC fluxes in the inner Nordvestfjord and resulted in a 10 - to 20-fold higher aggregate abundance at depths below 100 m near the marine-terminating glacier compared to the other stations (ISC, data not shown). The enhanced export of organic carbon due to lithogenic ballasting was highest in the inner Nordvestfjord close to the marine-terminating Daugaard-Jensen Glacier, while decreasing turbidity signals (Seifert et al. 2019) with increasing distance to the glacier indicated that silt-ballasting became less important at the eastern stations in Nordvestfjord and in OSS (Table 2, Fig. S4 in the supplementary information).

Zooplankton activity dominates export in the eastern Nordvestfjord and the OSS

Aggregate export is known to not only be controlled by ballasting, but also by zooplankton, which are responsible for carbon flux attenuation (Iversen et al. 2010; Stemmann et al. 2004) but also for the transformation of the organic matter, e.g. the production of fecal pellets (Turner 2002). We observed increasing signals from meso-zooplankton and acantharians in the settling material collected below 100 m depth compared to aggregates at 30 - 35 m depth (Fig. 2). This suggests that zooplankton mediated the carbon export across the salinity gradient

in the upper water column or at least interacted with the aggregates. At sharp density gradients where aggregates accumulate, enhanced grazing on aggregates by zooplankton has previously been observed (Möller et al. 2012).

Increasing zooplankton activity and transformation of the organic material with depth was supported by increasing contributions of fecal pellet- and copepod-associated bacterial groups such as *Pseudoalteromonas*, *Colwellia* and *Alteromonas* from the MSC collected material in the surface to the sediment trap collected material at depth (Fig. 5 and Fig. 7). Gammaproteobacteria like *Alteromonas* and *Pseudoalteromonas* have been shown to be associated with copepods, possibly accumulating via food intake and being enriched during digestion (Beckman et al. 2008; Hansen and Bech 1996; Tang et al. 2009). Furthermore, the relative abundance of the *Pseudoalteromonas* and *Colwellia* was positively correlated to the total volume of fecal pellets at each depth, which is supported by direct microscopic observations of these two bacterial groups being attached to fecal pellet in high abundances (Bernhard Fuchs, unpublished data).

Both the fecal pellet abundances, which were observed below 100 m depth in the Nordvestfjord and the Outer Scoresby Sund (Fig. 8 A), and the enrichment with fecal pellet associated bacteria, suggested that fecal pellets became increasingly important in the organic carbon flux at 100 m and deeper. Fecal pellets have the potential to transport significant share of the vertical particulate organic carbon (Lalande et al. 2011; Laurenceau-Cornec et al. 2015). The high potential contribution of fecal pellet carbon to the total export POC at the middle Nordvestfjord and at the sill as well as the OSS (Fig. 8 B) indicated that zooplankton feeding and fecal pellet production were a major export mechanism of POC in Scoresby Sund in areas with less lithogenic ballasting.

Both the ballasting and fecal pellet mediated export seem to lead to a strong vertical aggregate export at depths between 100 m to 400 m, after crossing the retention zone. If the organic material was exported to 100 m depth or deeper, the material showed a strong vertical connectivity and was less subjected to horizontal advection. The aggregate composition between 100 m to 400 m seemed to be highly dependent of the location of the fjord, grazed on by dinoflagellates in the middle Nordvestfjord and mostly diatom-dominated in the Outer Scoresby Sund (Fig. 4). At depths below 100 m (mesopelagic zone), aggregates are fragmented (Briggs et al. 2020) and release their components, mainly phytoplankton and heterotrophic degraders, resulting in similarities with the eukaryotic community at 1000 m depth in the water column in the Nordvestfjord. For instance, small picoplankton is proposed to be exported by the incorporation into larger aggregates or by a zooplankton mediated export, i.e. by fecal

pellets (Richardson and Jackson 2007) and can be released at depth. A similarity of the FL bacteria at 1000 m depth to the aggregate-attached bacterial community was also observed (Fig. 5 and 6). This was likely related to the disaggregation of the settling aggregates and the release of aggregate-attached bacteria in the water column, which have been suggested to be responsible for a vertical microbial connectivity between the surface ocean and the deep sea (Fadeev et al. 2021; Mestre et al. 2018).

Conclusion - Implications for future carbon sequestration in Arctic fjords

Increasing freshwater input in Arctic fjords will lead to increasing stratification and salinity gradients, enhancing aggregate retention at the base of the mixed layer (Fig. 9). Our results indicate that ballasting by lithogenic material is a crucial factor that allows aggregates to escape the upper water column in the inner Scoresby Sund (Fig. 9). If silt-rich surface run-offs from land-terminating glaciers (Meire et al. 2017) become more abundant in the coming decades, the inner deep Arctic fjords may become increasingly important for carbon sequestration in the future. On the other hand, the retreat of marine-terminating glaciers and the potential increase of silt inputs could reduce the primary production in Arctic fjords by limiting the nutrient resupply and light availability (Kanna et al. 2018; Meire et al. 2017; Seifert et al. 2019), but this will likely be offset by increases in primary production due to the thinning of the sea-ice and longer ice-free periods of Arctic fjords (Rysgaard and Glud 2007).

We identified zooplankton feeding and fecal pellet production as the other main mechanism that allows carbon to exported in Scoresby Sund (Fig. 9). An increase in primary production (Rysgaard and Glud 2007) and a resulting increase in zooplankton feeding and fecal pellet production by copepods could significantly increase of the carbon storage capacity of Arctic fjords in the future. Nevertheless, it has been suggested that increased melt water input and longer ice-free periods could result in growing importance of small copepod species and protozooplankton degraders in the Arctic fjords due to changes in the pelagic food web (Middelbo et al. 2019; Rysgaard and Glud 2007), which could on the other hand limit the carbon export via fecal pellets.

Changes in silt inputs, the composition of plankton communities, the aggregate formation, retention and turnover will determine the significance of Arctic fjord systems for carbon sequestration in the future. Our combined results indicate that if both primary production increases and large zooplankton continue to be the main degraders in the ecosystem, it is likely that Arctic fjords will stay important hotspots for carbon sequestration, but changes in the pelagic food web could significantly impact the magnitude of carbon export.

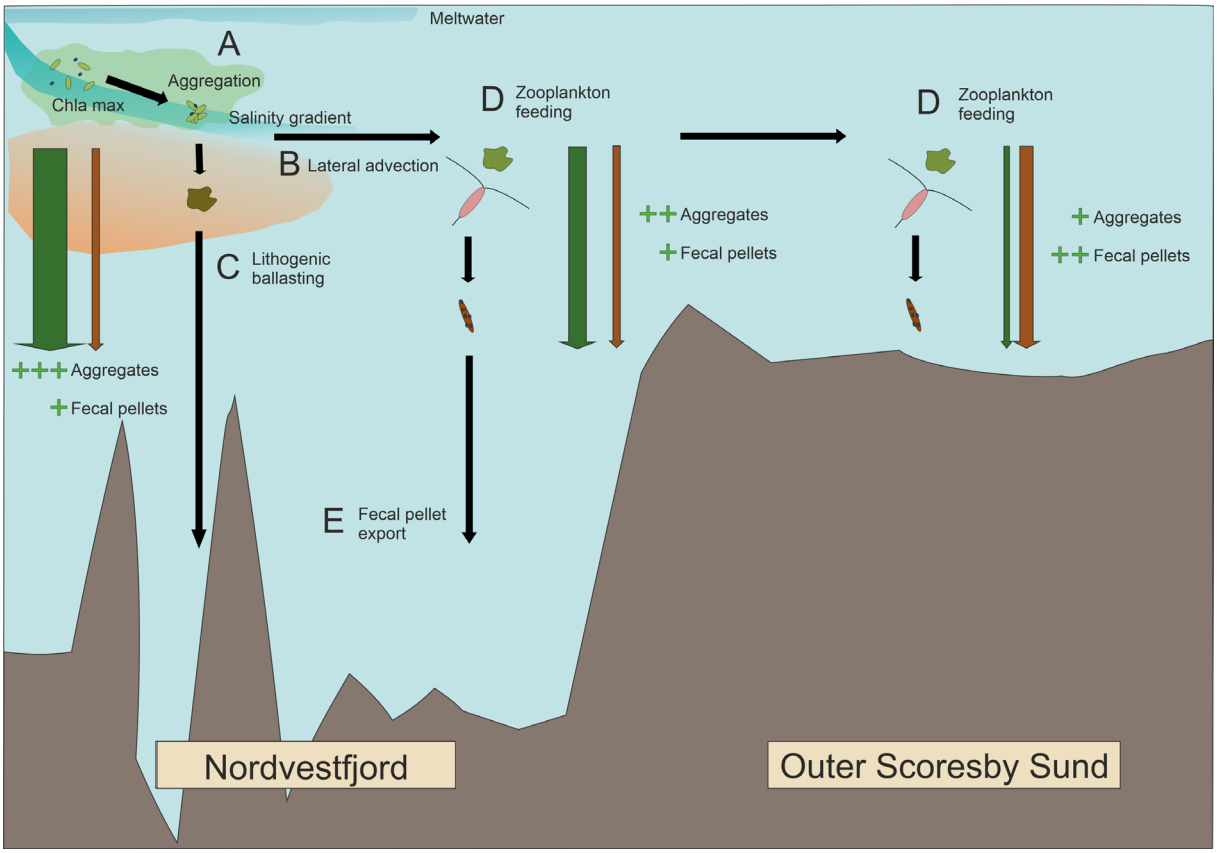

Fig. 9: Schematic overview of export processes in the Nordvestfjord and the Outer Scoresby Sund highlighted in the study. In the Nordvestfjord a melt water layer is located in the surface. The chlorophyll a maximum (Chla max) layer with growing phytoplankton is located below. Phytoplankton sized > 3 µm aggregates with their associated microbial community (A). The aggregates are transported from the inner Nordvestfjord outwards of the fjord (B) while being retained by a salinity gradient. Lithogenic material released by the melting glaciers ballasts the aggregates (C) which are efficiently exported. Aggregates which are retained in the upper water column are feed on by zooplankton like copepods (D). The copepod produces fecal pellets which are enriched with zooplankton associated bacterial groups which are efficiently exported to deeper depth (E). The local export flux is primarily vertical: in the inner Nordvestfjord the particle export is the highest with the main contribution coming from aggregates ballasted by lithogenic material (green arrow), in the Outer Scoresby Sund the particle export is the lowest but the main contributors are the fecal pellets (brown).

Author contributions

LH, MHI, HvdJ, RA and UJ designed the study. Sampling was done onboard by HvdJ, CK, RA, UJ, NK and AF. AM and NK did the sequencing of the DNA samples. SN did the bioinformatic processing of the sequencing. LH did the CARD-FISH counts under guidance of RA and BMF. HvdJ did the biogeochemical measurements. LH analyzed the data with help of SR with the statistical analysis. AF provided information about the water mass movement for the drifting sediment traps. LH and MHI wrote the manuscript with contributions from UJ, RA, SR and HM. All authors revised and approved the manuscript.

Acknowledgments

We thank the crew of F.S. Maria S. Merian for their assistance during the cruise. Jörg Wulf is acknowledged for sampling on MSM56 and teaching the CARD-FISH method to LH. We thank Christiane Hassenrück for advice in the statistical analysis and Christiane Lorenzen for the biogeochemical measurements. This study was supported by the Helmholtz Association, the Alfred Wegener Institute Helmholtz Centre for Polar and Marine Research, the Max Planck Society, and the DFG-Research Center/Cluster of Excellence "The Ocean Floor – Earth's Uncharted Interface": EXC-2077-390741603 at MARUM. This publication was supported by the HGF Young Investigator Group SeaPump "Seasonal and regional food web interactions with the biological pump": VH-NG-1000. Parts of this article have been subject of the Master thesis of LH ("Interactions between free-living and particle-associated microbial communities in an Arctic fjord (Scoresby Sund, East Greenland)", 2019).

Supplementary information

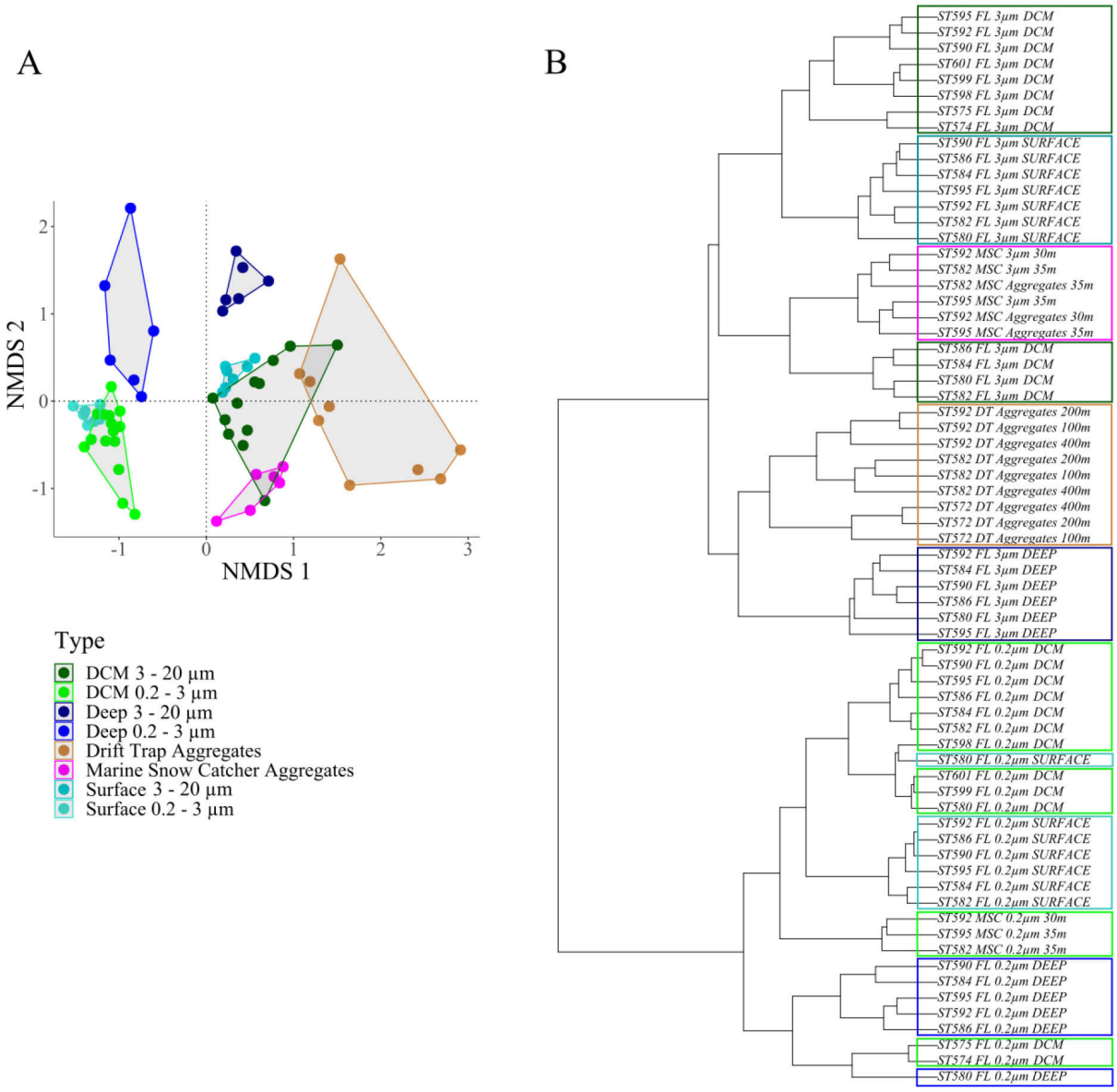

Fig. S1: (A) Non-metric Multi-dimensional Scaling (NMDS) plot on Bray-Curtis-Dissimilarity based on read frequencies of PCR-amplified 18S rRNA gene fragments excluding taxonomic group "Metazoa" and "Rhizaria" and (B) dendrogram on the Bray-Curtis-Dissimilarity using the Ward.D2 clustering. Groups shown are eukaryotes in the surface (Surface, 0.2 - 3 µm and 3 - 20 µm), deep chlorophyll a maximum (DCM, 0.2 - 3 µm, including MSC 0.2 - 3 µm samples; and 3 - 20 µm) and at depth (Deep, 0.2-3 µm and 3 – 20 µm), the Marine Snow Catcher (MSC, >3µm and aggregate as one group) and of the drifting sediment trap (DT) aggregates.

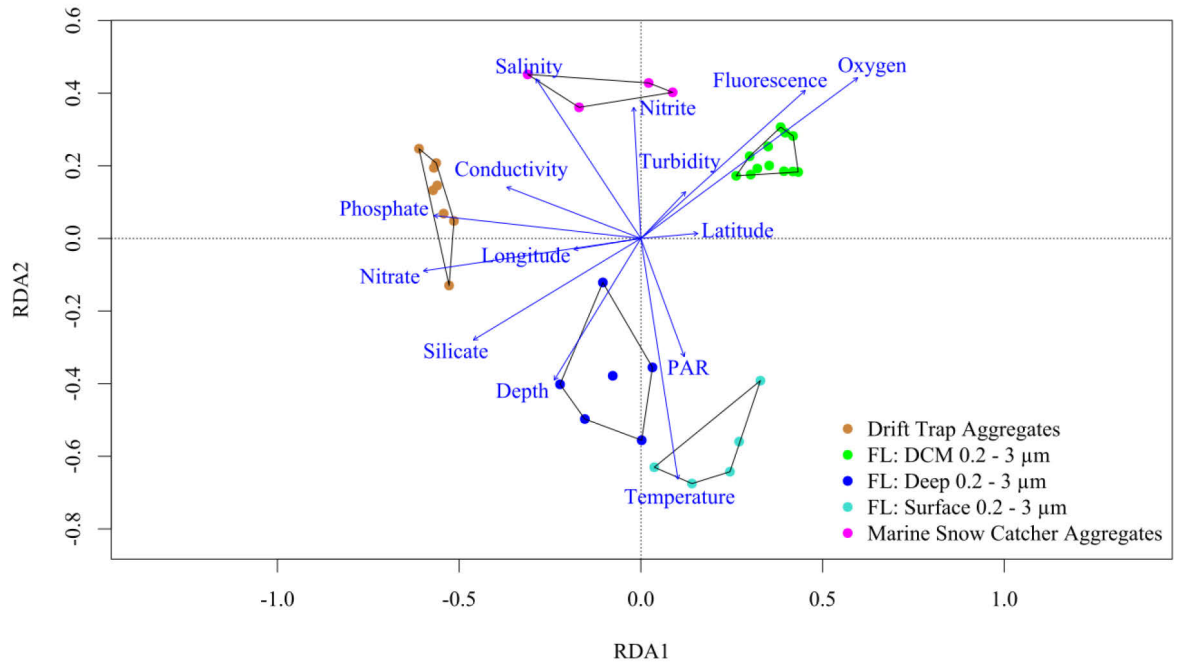

Fig. S2: Redundancy Analysis (RDA) based on read frequencies of PCR-amplified 16S rRNA gene fragments in different water depths/layers and size fractions. As environmental factors temperature, salinity, fluorescence, oxygen, photosynthetically active radiation (PAR), turbidity, conductivity, water depth, longitude, latitude and nutrients (nitrate, nitrite, phosphate and silicate) were chosen. The axis RDA 1 is explaining 15.8 % and the axis RDA 2 is explaining 5.6 % of the variances. Groups shown are drifting sediment trap aggregates, the free-living (FL) bacterial communities in the surface, DCM (including MSC 0.2 -3 µm samples) and at depth (Deep), and the Marine Snow Catcher aggregates (>3 µm and aggregate as one group).

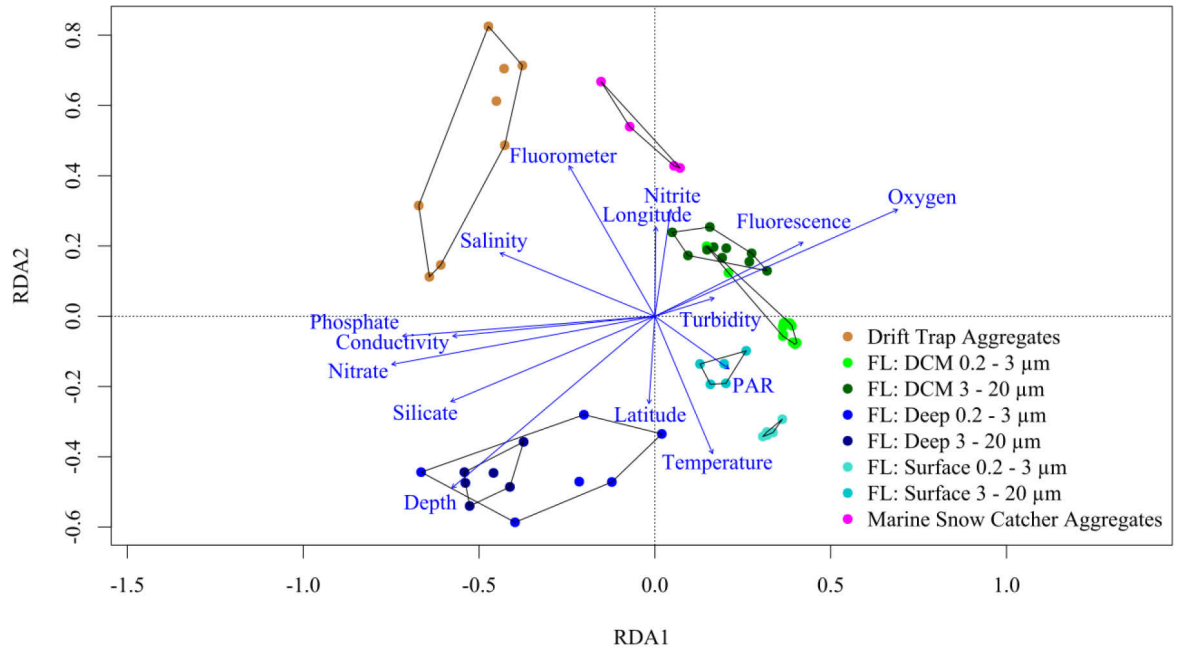

Fig. S3: Redundancy Analysis (RDA) based on read frequencies of PCR-amplified 18S rRNA gene fragments in different water depths/layers and size fractions. As environmental factors temperature, salinity, fluorescence, oxygen, photosynthetically active radiation (PAR), turbidity, conductivity, water depth, longitude, latitude and nutrients (nitrate, nitrite, phosphate and silicate) were chosen. The axis RDA 1 is explaining 9.8 % and the axis RDA 2 is explaining 5.6 % of the variances. Groups shown are drifting sediment trap aggregates, the 0.2- 3µm and 3 – 20 µm fraction communities in the surface, DCM (including MSC 0.2 -3 µm samples) and at depth (Deep), and the Marine Snow Catcher aggregates (>3 µm and aggregates as one group).

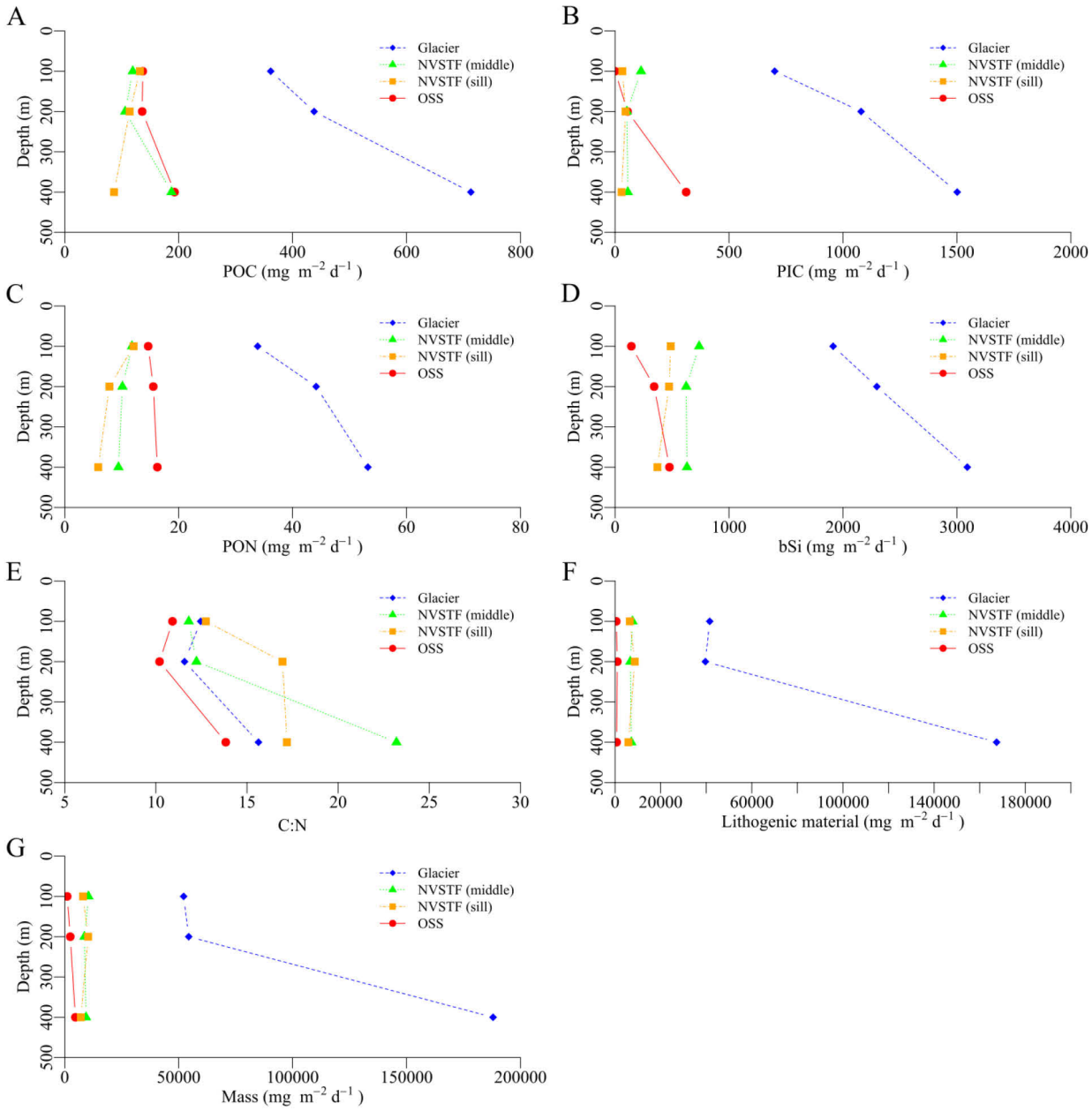

Fig. S4: Biogeochemical fluxes in the drifting sediment traps in Scoresby Sund, showing (A) the particulate organic carbon (POC) [mg m^{-2} d^{-1}], (B) the particulate inorganic carbon (PIC) [mg m^{-2} d^{-1}], (C) the particulate organic nitrogen (PON) [mg m^{-2} d^{-1}], (D) the biogenic silica (bSi) [mg m^{-2} d^{-1}], (E) the C:N ratio, (F) the lithogenic material [mg m^{-2} d^{-1}] and (G) the total dry mass [mg m^{-2} d^{-1}] in the Nordvestfjord (NVSTF) at the glacier, in the middle and at the sill as well as in the Outer Scoresby Sund (OSS).

References

Alldredge, A. L., and Crocker, K. M. (1995). "Why do sinking mucilage aggregates accumulate in the water column?" *Science of the Total Environment*, 165(1-3), 15-22.

Alldredge, A. L., Cowles, T. J., MacIntyre, S., Rines, J. E. B., Donaghay, P. L., Greenlaw, C. F., Holliday, D. V., Dekshenieks, M. M., Sullivan, J. M., and Zaneveld, J. R. V. (2002). "Occurrence and mechanisms of formation of a dramatic thin layer of marine snow in a shallow Pacific fjord." *Marine Ecology Progress Series*, 233, 1-12.

Amann, R. I., Binder, B. J., Olson, R. J., Chisholm, S. W., Devereux, R., and Stahl, D. A. (1990). "Combination of 16S rRNA-Targeted Oligonucleotide Probes with Flow Cytometry for Analyzing Mixed Microbial Populations." *Applied and environmental microbiology*, 56(6), 1919-1925.

Bamber, J., Van Den Broeke, M., Ettema, J., Lenaerts, J., and Rignot, E. (2012). "Recent large increases in freshwater fluxes from Greenland into the North Atlantic." *Geophysical Research Letters*, 39(19), L19501.

Beckman, E. M., Kawaguchi, T., Chandler, G. T., and Decho, A. W. (2008). "Development of a microplate-based fluorescence immunoassay using quantum dot streptavidin conjugates for enumeration of putative marine bacteria, *Alteromonas sp.*, associated with a benthic harpacticoid copepod." *Journal of Microbiological Methods*, 75(3), 441-444.

Belcher, A., Iversen, M., Manno, C., Henson, S. A., Tarling, G. A., and Sanders, R. (2016). "The role of particle associated microbes in remineralization of fecal pellets in the upper mesopelagic of the Scotia Sea, Antarctica." *Limnology and Oceanography*, 61(3), 1049-1064.

Bendtsen, J., Mortensen, J., and Rysgaard, S. (2014). "Seasonal surface layer dynamics and sensitivity to runoff in a high Arctic fjord (Young Sound/Tyrolerfjord, 74°N)." *Journal of Geophysical Research: Oceans*, 119(9), 6461-6478.

Bodungen, B. V., Wunsch, M., and Fürderer, H. (1991). "Sampling and analysis of suspended and sinking particles in the northern North Atlantic." *Washington DC American Geophysical Union Geophysical Monograph Series*, 63, 47-56.

Briggs, N., Dall'Olmo, G., and Claustre, H. (2020). "Major role of particle fragmentation in regulating biological sequestration of CO_2 by the oceans." *Science*, 367(6479), 791-793.

Callahan, B. J., McMurdie, P. J., Rosen, M. J., Han, A. W., Johnson, A. J. A., and Holmes, S. P. (2016). "DADA2: High resolution sample inference from Illumina amplicon data." *Nature Methods*, 13(7), 581-583.

Camassa, R., Khatri, S., McLaughlin, R. M., Prairie, J. C., White, B., and Yu, S. (2013). "Retention and entrainment effects: Experiments and theory for porous spheres settling in sharply stratified fluids." *Physics of Fluids*, 25(8), 081701.

Cofaigh, C. Ó., Dowdeswell, J. A., and Grobe, H. (2001). "Holocene glacimarine sedimentation, inner Scoresby Sund, East Greenland: the influence of fast-flowing ice-sheet outlet glaciers." *Marine Geology*, 175(1), 103-129.

Daims, H., Brühl, A., Amann, R., Schleifer, K.-H., and Wagner, M. (1999). "The Domain-specific Probe EUB338 is Insufficient for the Detection of all Bacteria: Development and Evaluation of a more Comprehensive Probe Set." *Systematic and Applied Microbiology*, 22(3), 434-444.

Dixon, P. (2003). "VEGAN, a package of R functions for community ecology." *Journal of Vegetation Science*, 14(6), 927-930.

Dowdeswell, J. A., Villinger, H., Whittington, R. J., and Marienfeld, P. (1993). "Iceberg scouring in Scoresby Sund and on the East Greenland continental shelf." *Marine Geology*, 111(1-2), 37-53.

Eilers, H., Pernthaler, J., Glöckner, F. O., and Amann, R. (2000). "Culturability and In Situ Abundance of Pelagic Bacteria from the North Sea." *Applied and Environmental Microbiology*, 66(7), 3044-3051.

Eilers, H., Pernthaler, J., Peplies, J., Glöckner, F. O., Gerdts, G., and Amann, R. (2001). "Isolation of Novel Pelagic Bacteria from the German Bight and Their Seasonal Contributions to Surface Picoplankton." *Applied and Environmental Microbiology*, 67(11), 5134-5142.

Enderlin, E. M., Howat, I. M., Jeong, S., Noh, M. J., Van Angelen, J. H., and Van Den Broeke, M. R. (2014). "An improved mass budget for the Greenland ice sheet." *Geophysical Research Letters*, 41(3), 866-872.

Fadeev, E., Rogge, A., Ramondenc, S., Nöthig, E.-M., Wekerle, C., Bienhold, C., Salter, I., Waite, A. M., Hehemann, L., Boetius, A., and Iversen, M. H. (2021). "Sea ice presence is linked to higher carbon export and vertical microbial connectivity in the Eurasian Arctic Ocean." *Communications Biology*, 4(1), 1255.

Fettweis, X., Franco, B., Tedesco, M., Van Angelen, J. H., Lenaerts, J. T. M., van den Broeke, M. R., and Gallée, H. (2013). "Estimating the Greenland ice sheet surface mass balance contribution to future sea level rise using the regional atmospheric climate model MAR." *The Cryosphere*, 7(2), 469-489.

Flintrop, C. M., Rogge, A., Miksch, S., Thiele, S., Waite, A. M., and Iversen, M. H. (2018). "Embedding and slicing of intact in situ collected marine snow." *Limnology and Oceanography: Methods*, 16(6), 339-355.

Friedrichs, A., Schwalfenberg, K., Koch, B. P., and Zielinski, O. (2017). "Physical oceanography during MARIA S. MERIAN cruise MSM56 (MECAF), https://doi.org/10.1594/PANGAEA.871015."

Gleiber, M. R., Steinberg, D. K., and Ducklow, H. W. (2012). "Time series of vertical flux of zooplankton fecal pellets on the continental shelf of the western Antarctic Peninsula." *Marine Ecology Progress Series*, 471, 23-36.

Glud, R. N., Holby, O., Hoffmann, F., and Canfield, D. E. (1998). "Benthic mineralization and exchange in Arctic sediments (Svalbard, Norway)." *Marine Ecology Progress Series*, 173, 237-251.

González, H. E., González, S. R., and Brummer, G.-J. A. (1994). "Short-term sedimentation pattern of zooplankton, faeces and microplankton at a permanent station in the Bjørnafjorden (Norway) during April–May 1992." *Marine Ecology Progress Series*, 105(1/2), 31-45.

González, H. E., and Smetacek, V. (1994). "The possible role of the cyclopoid copepod *Oithona* in retarding vertical flux of zooplankton faecal material." *Marine Ecology Progress Series*, 113(3), 233-246.

Guannel, M. L., Horner-Devine, M. C., and Rocap, G. (2011). "Bacterial community composition differs with species and toxigenicity of the diatom *Pseudo-nitzschia*." *Aquatic Microbial Ecology*, 64(2), 117-133.

Guillou, L., Bachar, D., Audic, S., Bass, D., Berney, C., Bittner, L., Boutte, C., Burgaud, G., de Vargas, C., Decelle, J., del Campo, J., Dolan, J. R., Dunthorn, M., Edvardsen, B., Holzmann, M., Kooistra, W. H. C. F., Lara, E., Le Bescot, N., Logares, R., Mahé, F., Massana, R., Montresor, M., Morard, R., Not, F., Pawlowski, J., Probert, I., Sauvadet, A.-L., Siano, R., Stoeck, T., Vaulot, D., Zimmermann, P., and Christen, R. (2012). "The Protist Ribosomal Reference database (PR2): a catalog of unicellular eukaryote Small Sub-Unit rRNA sequences with curated taxonomy." *Nucleic Acids Research*, 41(D1), D597-D604.

Hansen, B., and Bech, G. (1996). "Bacteria associated with a marine planktonic copepod in culture. I. Bacterial genera in seawater, body surface, intestines and fecal pellets and succession during fecal pellet degradation." *Journal of plankton research*, 18(2), 257-273.

Hawkings, J. R., Wadham, J. L., Tranter, M., Lawson, E., Sole, A., Cowton, T., Tedstone, A. J., Bartholomew, I., Niewnow, P., and Chandler, D. (2015). "The effect of warming climate on nutrient and solute export from the Greenland Ice Sheet." *Geochemical Perspectives Letters*, 1, 94–104.

Hicks, R. E., Amann, R. I., and Stahl, D. A. (1992). "Dual Staining of Natural Bacterioplankton with 4', 6-Diamidino-2-Phenylindole and Fluorescent Oligonucleotide Probes Targeting Kingdom-Level 16S rRNA Sequences." *Applied and Environmental Microbiology*, 58(7), 2158-2163.

Holinde, L., and Zielinski, O. (2016). "Bio-optical characterization and light availability parameterization in Uummannaq Fjord and Vaigat–Disko Bay (West Greenland)." *Ocean Science*, 12(1), 117-128.

Iversen, M. H., Nowald, N., Ploug, H., Jackson, G. A., and Fischer, G. (2010). "High resolution profiles of vertical particulate organic matter export off Cape Blanc, Mauritania: Degradation processes and ballasting effects." *Deep Sea Research Part I: Oceanographic Research Papers*, 57(6), 771-784.

Iversen, M. H., and Robert, M. L. (2015). "Ballasting effects of smectite on aggregate formation and export from a natural plankton community." *Marine Chemistry*, 175, 18-27.

Kanna, N., Sugiyama, S., Ohashi, Y., Sakakibara, D., Fukamachi, Y., and Nomura, D. (2018). "Upwelling of Macronutrients and Dissolved Inorganic Carbon by a Subglacial Freshwater Driven Plume in Bowdoin Fjord, Northwestern Greenland." *Journal of Geophysical Research: Biogeosciences*, 123(5), 1666-1682.

Kindler, K., Khalili, A., and Stocker, R. (2010). "Diffusion-limited retention of porous particles at density interfaces." *Proceedings of the National Academy of Sciences*, 107(51), 22163-22168.

Lalande, C., Bauerfeind, E., and Nöthig, E.-M. (2011). "Downward particulate organic carbon export at high temporal resolution in the eastern Fram Strait: influence of Atlantic Water on flux composition." *Marine Ecology Progress Series*, 440, 127-136.

Laurenceau-Cornec, E. C., Trull, T. W., Davies, D. M., Bray, S. G., Doran, J., Planchon, F., Carlotti, F., Jouandet, M.-P., Cavagna, A.-J., Waite, A. M., and Blain, S. (2015). "The relative importance of phytoplankton aggregates and zooplankton fecal pellets to carbon export: insights from free-drifting sediment trap deployments in naturally iron-fertilised waters near the Kerguelen Plateau." *Biogeosciences*, 12(4), 1007-1027.

Lewis, S. M., and Smith, L. C. (2009). "Hydrologic drainage of the Greenland Ice Sheet." *Hydrological Processes: An International Journal*, 23(14), 2004-2011.

Linz, A. (2018). "OTUtable: North Temperate Lakes-Microbial observatory 16S Time Series Data and Functions." *R package Version*.

Ludwig, W., Mittenhuber, G., and Friedrich, C. G. (1993). "Transfer of *Thiosphaera pantotropha* to *Paracoccus denitrificans*." *International Journal of Systematic Bacteriology*, 43(2), 363-367.

MacIntyre, S., Alldredge, A. L., and Gotschalk, C. C. (1995). "Accumulation of marines now at density discontinuities in the water column." *Limnology and Oceanography*, 40(3), 449-468.

Manz, W., Amann, R., Ludwig, W., Vancanneyt, M., and Schleifer, K.-H. (1996). "Application of a suite of 16S rRNA-specific oligonucleotide probes designed to investigate bacteria of the phylum cytophaga-flavobacter-bacteroides in the natural environment." *Microbiology*, 142(5), 1097-1106.

Martin, M. (2011). "Cutadapt removes adapter sequences from high-throughput sequencing reads." *EMBnet. journal*, 17(1), 10-12.

Meire, L., Mortensen, J., Meire, P., Juul-Pedersen, T., Sejr, M. K., Rysgaard, S., Nygaard, R., Huybrechts, P., and Meysman, F. J. R. (2017). "Marine-terminating glaciers sustain high productivity in Greenland fjords." *Global Change Biology*, 23(12), 5344-5357.

Mestre, M., Ruiz-González, C., Logares, R., Duarte, C. M., Gasol, J. M., and Montserrat Sala, M. (2018). "Sinking particles promote vertical connectivity in the ocean microbiome." *Proceedings of the National Academy of Sciences*, 115(29), E6799-E6807.

Middelbo, A. B., Møller, E. F., Engel Arendt, K., Thyrring, J., and Sejr, M. K. (2019). "Spatial, seasonal and inter-annual variation in abundance and carbon turnover of small copepods in Young Sound, Northeast Greenland." *Polar Biology*, 42, 179-193.

Möller, K. O., St. John, M., Temming, A., Floeter, J., Sell, A. F., Herrmann, J.-P., and Möllmann, C. (2012). "Marine snow, zooplankton and thin layers: indications of a trophic link from small-scale sampling with the Video Plankton Recorder." *Marine Ecology Progress Series*, 468, 57-69.

Mortensen, J., Lennert, K., Bendtsen, J., and Rysgaard, S. (2011). "Heat sources for glacial melt in a sub-Arctic fjord (Godthåbsfjord) in contact with the Greenland Ice Sheet." *Journal of Geophysical Research: Oceans*, 116(C1).

Mortensen, J., Bendtsen, J., Motyka, R. J., Lennert, K., Truffer, M., Fahnestock, M., and Rysgaard, S. (2013). "On the seasonal freshwater stratification in the proximity of fast-flowing tidewater outlet glaciers in a sub-Arctic sill fjord." *Journal of Geophysical Research: Oceans*, 118(3), 1382-1395.

Murray, C., Markager, S., Stedmon, C. A., Juul-Pedersen, T., Sejr, M. K., and Bruhn, A. (2015). "The influence of glacial melt water on bio-optical properties in two contrasting Greenlandic fjords." *Estuarine, Coastal and Shelf Science*, 163(Part B), 72-83.

Neef, A., Amann, R., Schlesner, H., and Schleifer, K.-H. (1998). "Monitoring a widespread bacterial group: in situ detection of planctomycetes with 16S rRNA-targeted probes." *Microbiology*, 144(12), 3257-3266.

Paradis, E., and Schliep, K. (2019). "ape 5.0: an environment for modern phylogenetics and evolutionary analyses in R." *Bioinformatics*, 35(3), 526-528.

Pinhassi, J., Montserrat Sala, M., Havskum, H., Peters, F., Guadayol, Ò., Malits, A., and Marrasé, C. (2004). "Changes in Bacterioplankton Composition under Different Phytoplankton Regimens." *Applied and Environmental Microbiology*, 70(11), 6753-6766.

Pizzetti, I., Fuchs, B. M., Gerdts, G., Wichels, A., Wiltshire, K. H., and Amann, R. (2011). "Temporal Variability of Coastal *Planctomycetes* clades at Kabeltonne Station, North Sea." *Applied and Environmental Microbiology*, 77(14), 5009-5017.

Prairie, J. C., Ziervogel, K., Arnosti, C., Camassa, R., Falcon, C., Khatri, S., McLaughlin, R. M., White, B. L., and Yu, S. (2013). "Delayed settling of marine snow at sharp density transitions driven by fluid entrainment and diffusion-limited retention." *Marine Ecology Progress Series*, 487, 185-200.

Prairie, J. C., Ziervogel, K., Camassa, R., McLaughlin, R. M., White, B. L., Dewald, C., and Arnosti, C. (2015). "Delayed settling of marine snow: Effects of density gradient and particle properties and implications for carbon cycling." *Marine Chemistry*, 175, 28-38.

Quast, C., Pruesse, E., Yilmaz, P., Gerken, J., Schweer, T., Yarza, P., Peplies, J., and Glöckner, F. O. (2012). "The SILVA ribosomal RNA gene database project: improved data processing and web-based tools." *Nucleic Acids Research*, 41(D1), D590-D596.

RCoreTeam. (2019). "R: A language and environment for statistical computing. R Foundation for statistical computing, Vienna, Austria. URL https://www.R-project.org/.".

Richardson, T. L., and Jackson, G. A. (2007). "Small Phytoplankton and Carbon Export from the Surface Ocean." *Science*, 315(5813), 838-840.

Rysgaard, S., and Glud, R. N. (2007). "Carbon cycling and climate change: Predictions for a High Arctic marine ecosystem (Young Sound, NE Greenland)", in S. Rysgaard and R. N. Glud, (eds.), *Carbon cycling in Arctic marine ecosystems: Case study Young Sound, Meddelelser om Grønland*. Copenhagen: Bioscience Vol. 58, pp. 206-214.

Rysgaard, S., Mortensen, J., Juul-Pedersen, T., Sørensen, L. L., Lennert, K., Søgaard, D. H., Arendt, K. E., Blicher, M. E., Sejr, M. K., and Bendtsen, J. (2012). "High air–sea CO_2 uptake rates in nearshore and shelf areas of Southern Greenland: Temporal and spatial variability." *Marine Chemistry*, 128 - 129, 26-33.

Schäfer, H., Abbas, B., Witte, H., and Muyzer, G. (2002). "Genetic diversity of 'satellite'bacteria present in cultures of marine diatoms." *FEMS Microbiology Ecology*, 42(1), 25-35.

Schindelin, J., Arganda-Carreras, I., Frise, E., Kaynig, V., Longair, M., Pietzsch, T., Preibisch, S., Rueden, C., Saalfeld, S., Schmid, B., Tinevez, J.-Y., White, D. J., Hartenstein, V., Eliceiri, K., Tomancak, P., and Cardona, A. (2012). "Fiji: an open-source platform for biological-image analysis." *Nature Methods*, 9(7), 676.

Seifert, M., Hoppema, M., Burau, C., Elmer, C., Friedrichs, A., Geuer, J. K., John, U., Kanzow, T., Koch, B. P., Konrad, C., van der Jagt, H., Zielinski, O., and Iversen, M. H. (2019). "Influence of Glacial Meltwater on Summer Biogeochemical Cycles in Scoresby Sund, East Greenland." *Frontiers in Marine Science*, 6, 412.

Smith, R. W., Bianchi, T. S., Allison, M., Savage, C., and Galy, V. (2015). "High rates of organic carbon burial in fjord sediments globally." *Nature Geoscience*, 8(6), 450-453.

Snaidr, J., Amann, R., Huber, I., Ludwig, W., and Schleifer, K.-H. (1997). "Phylogenetic Analysis and In Situ Identification of Bacteria in Activated Sludge." *Applied and Environmental Microbiology*, 63(7), 2884-2896.

Sørensen, H. L., Meire, L., Juul-Pedersen, T., de Stigter, H. C., Meysman, F. J. R., Rysgaard, S., Thamdrup, B., and Glud, R. N. (2015). "Seasonal carbon cycling in a Greenlandic fjord: an integrated pelagic and benthic study." *Marine Ecology Progress Series*, 539, 1-17.

Steger, C. (1998). "An unbiased detector of curvilinear structures." *IEEE Transactions on Pattern Analysis and Machine Intelligence*, 20(2), 113-125.

Stemmann, L., Jackson, G. A., and Gorsky, G. (2004). "A vertical model of particle size distributions and fluxes in the midwater column that includes biological and physical processes—Part II: application to a three year survey in the NW Mediterranean Sea." *Deep Sea Research Part I: Oceanographic Research Papers*, 51(7), 885-908.

Suzuki, M. T., and Giovannoni, S. J. (1996). "Bias Caused by Template Annealing in the Amplification of Mixtures of 16S rRNA Genes by PCR." *Applied and environmental microbiology*, 62(2), 625-630.

Tang, K., Dziallas, C., Hutalle-Schmelzer, K., and Grossart, H.-P. (2009). "Effects of food on bacterial community composition associated with the copepod *Acartia tonsa* Dana." *Biology Letters*, 5(4), 549-553.

Teeling, H., Fuchs, B. M., Becher, D., Klockow, C., Gardebrecht, A., Bennke, C. M., Kassabgy, M., Huang, S., Mann, A. J., Waldmann, J., Weber, M., Klindworth, A., Otto, A., Lange, J., Bernhardt, J., Reinsch, C., Hecker, M., Peplies, J., Bockelmann, F. D., Callies, U., Gerdts, G., Wichels, A., Wiltshire, K. H., Glöckner, F. O., Schweder, T., and Amann, R. (2012). "Substrate-Controlled Succession of Marine Bacterioplankton Populations Induced by a Phytoplankton Bloom." *Science*, 336(6081), 608-611.

Thiele, S., Fuchs, B. M., Amann, R., and Iversen, M. H. (2015). "Colonization in the Photic Zone and Subsequent Changes during Sinking Determine Bacterial Community Composition in Marine Snow." *Applied and Environmental Microbiology*, 81(4), 1463-1471.

Turner, J. T. (2002). "Zooplankton fecal pellets, marine snow and sinking phytoplankton blooms." *Aquatic Microbial Ecology*, 27(1), 57-102.

Thiele, S., Fuchs, B. M., and Amann, R. I. (2011). "Identification of Microorganisms Using the Ribosomal RNA Approach and Fluorescence in Situ Hybridization", in P. Wilderer, (ed.), *Treatise on Water Science*. Oxford: Academic Press.

van der Jagt, H., Friese, C., Stuut, J. B. W., Fischer, G., and Iversen, M. H. (2018). "The ballasting effect of Saharan dust deposition on aggregate dynamics and carbon export: Aggregation, settling, and scavenging potential of marine snow." *Limnology and Oceanography*, 63(3), 1386-1394.

Wagner, T., Hiner, M., and Xraynaud. (2017). "thorstenwagner/ij-ridgedetection: Ridge Detection 1.4.0 (Version v1.4.0)." *Zenodo*.

Wallner, G., Amann, R., and Beisker, W. (1993). "Optimizing Fluorescent In Situ Hybridization With rRNA-Targeted Oligonucleotide Probes for Flow Cytometric Identification of Microorganisms." *Cytometry: The Journal of the International Society for Analytical Cytology*, 14(2), 136-143.

Wickham, H. (2016). "ggplot2: elegant graphics for data analysis."

Xiao, C., Wu, X., Liu, T., Xu, G., and Chi, R. (2017). "Microbial Community Structure of Activated Sludge for Biosolubilization of Two Different Rock Phosphates." *Applied Biochemistry and Biotechnology*, 182, 742-754.

Chapter II: Increasing salinities in the Southern Ocean retain and delay settling of large, porous aggregates

Lili Hufnagel[1,2,3], Christian Konrad[1,3] and Morten H. Iversen[1,2,3]

[1] University of Bremen, MARUM, Center for Marine Environmental Sciences, 28359 Bremen, Germany

[2] University of Bremen, Faculty of Geosciences, 28359 Bremen, Germany

[3] Alfred Wegener Institute, Helmholtz Centre for Polar and Marine Research, 27570 Bremerhaven, Germany

Keywords: carbon export, particle retention, *in situ* camera profiles, salinity gradient

Abstract

In the Southern Ocean the vast majority of the organic material is attenuated below the photic zone. The mechanisms responsible for this rapid loss of particulate organic matter in the upper 100 m are still unclear. In November and December of 2017, the development and decline of a diatom bloom was observed close to South Georgia in the Southern Ocean. The carbon export and attenuation in the epipelagic and mesopelagic zone was investigated using PELAGRA traps and *in situ* cameras to measure the particulate organic carbon flux, the particle distribution and the aggregate sinking velocities. We generally observed higher variability in POC flux in the upper 100 m compared to depths below 100 m. Large, porous aggregates were retained or had their settling delayed by increasing salinity gradients in the lower epipelagic and the upper mesopelagic zone. This resulted in the majority of the export occurring via small and dense particles, such as zooplankton fecal pellets with low porosities. This suggests that large, porous aggregates will be exported less efficiently in the future Southern Ocean as warming increases ice melt and freshwater inputs to the region. Furthermore, it provides a mechanism to explain the often-observed time-lag between production and export in the Southern Ocean.

Introduction

Globally, biological activity in the surface ocean is responsible for 50 Gt carbon uptake from the atmosphere annually (Field et al. 1998). However, only 5 - 25% of the carbon that is fixed into biological biomass in the surface ocean sinks to deeper depths (De La Rocha and Passow 2007; Henson et al. 2012), thereby becoming part of the biological carbon pump (Volk and Hoffert 1985), which stores carbon on climate-relevant timescales. The timescales of carbon sequestration depend on the remineralization depth of particulate organic carbon (Kwon et al. 2009), meaning that the deeper organic matter sinks in the ocean before remineralization, the longer it is stored away from exchange with the atmosphere. Typically, timescales of sequestration range from 10 to 100 years in the mesopelagic zone, 1000 years in the bathypelagic zone, and millennia if the settling organic matter reaches, and is stored in the seafloor (see Iversen 2023 and references therein). Model estimates of carbon export out of the surface ocean show large variability and range around 4 and >11 Gt carbon (DeVries and Weber 2017; Henson et al. 2011; Laws et al. 2000; Nowicki et al. 2022; Schlitzer 2002; Siegel et al. 2014), and in order to constrain this estimate we need to better understand the processes that impact carbon export and flux attenuation.

The prevailing mechanisms for carbon attenuation differ with regions and structure of the ecosystem (Henson et al. 2019; Wassmann 1997). Microbial degradation is typically the main carbon attenuation mechanism in the deep ocean, whereas zooplankton feeding is the main mechanism for carbon attenuation in the upper water column, at the base of the euphotic zone and in the upper mesopelagic zone (Iversen et al. 2010; Stemmann et al. 2004). Zooplankton can remove settling organic matter by direct ingestion but also convert settling to suspended matter by sloppy feeding, excretion, and fragmentation (Briggs et al. 2020; Dilling and Alldredge 2000; Steinberg et al. 2000), produce settling fecal pellets from suspended single cells which contribute to the carbon export (Ducklow et al. 2001; Turner 2002; Turner 2015, and references therein), and can actively transport of organic matter from the surface to depth via diel vertical migration (Schnetzer and Steinberg 2002; Steinberg et al. 2000).

On top of the complex biological processes producing and removing settling organic aggregates, the pathways by which the organic carbon is transported downwards in the water column are also poorly constrained and quantified (see Boyd et al. 2019 and references therein). These pathways are the gravitational pump, the mixing pump and the migrant pump (see Boyd et al. 2019, Nowicki et al. 2022, Iversen 2023, and references therein). Nowicki et al. 2022 estimated that 70% of the carbon is transported by the gravitational carbon pump, 20% by physical mixing and 10% by zooplankton migration. This suggests that the gravitational pump,

i.e. settling aggregates and fecal pellets, contribute the most to carbon export and potentially sequestration (Nowicki et al. 2022). However, there are still uncertainties regarding the importance of fecal pellets versus marine snow (e.g. Lalande et al. 2011; Laurenceau-Cornec et al. 2015; Nowicki et al. 2022), small versus large aggregates (e.g. Clements et al. 2023), slow-sinking and fast-sinking aggregates (e.g. Baker et al. 2017; Boyd et al. 2019) and aggregates versus single phytoplankton cells and resting spores (e.g. Rembauville et al. 2015a; Rembauville et al. 2016), as well as how these contributions differ regionally and seasonally.

From a more practical point of view, the temporal and spatial displacement between origin of organic matter production and the depth of organic carbon flux collection further complicates our biological and biogeochemical understanding of the BCP, which is especially true for the Southern Ocean where extreme seasons and massive spring blooms are not directly reflected in carbon fluxes to the deep ocean (Rembauville et al. 2015b). In fact, there seems to be a half - to two-month time-lag between production in the surface ocean and export (Henson et al. 2015; Rembauville et al. 2015b; Rigual-Hernández et al. 2015). Additionally, only a small fraction of the produced organic matter is exported out of the upper mixed layer (Rembauville et al. 2015b), e.g. at the Kerguelen Plateau, where a seasonal net community productivity of 6.6 mol carbon m^{-2} has been observed (Jouandet et al. 2008) but only 100 mmol carbon m^{-2} yr^{-1} are exported to depths of 300 m (Rembauville et al. 2015b). The deep carbon flux at depths of > 2000 m is rather low and homogenous in the Southern Ocean, as in regions around South Georgia and Crozet Islands (Manno et al. 2015; Salter et al. 2012). Together with the high and variable surface production, this can lead to an inverse relationship between primary production and export efficiency in the Southern Ocean (Maiti et al. 2013). It is believed that high microbial remineralization (Christaki et al. 2014; Obernosterer et al. 2008) and high zooplankton grazing and aggregate fragmentation (Briggs et al. 2020) are the cause of the negative relationship. However, recent studies have shown that microbial degradation of settling aggregates cannot explain the high attenuation (Belcher et al. 2016; Iversen et al. 2010; Iversen and Ploug 2013) and zooplankton grazing would result in events of fecal pellet export, especially during period with high abundance of krill (Belcher et al. 2017; Pauli et al. 2021). Hence, we do not understand the mechanisms driving the effective retention and attenuation of organic matter at the base of the mixed layer in the Southern Ocean.

Some repeated seasonal peaks in carbon export have been observed in sediment trap time-series of carbon export in the productive region north of South Georgia (Manno et al. 2015; Manno et al. 2022; Rembauville et al. 2016). Here, it was observed that export of zooplankton fecal pellets caused a large carbon export peak in spring followed by a smaller

export peak during the late austral summer / early autumn (Manno et al. 2015; Manno et al. 2022). This suggests that there is a link between production and export but that the coarse sampling resolution of weeks to a month for the sediment traps does not allow identification of the processes that determine the magnitude and timing of export (Manno et al. 2015; Manno et al. 2022; Rembauville et al. 2015b). To combine long-term observations with short-term mechanistic processes, we conducted the COMICS cruise (Controls over Ocean Mesopelagic Interior Carbon Storage; Sanders et al. 2016), which coincided with four months of glider observations within the GOCART project (Gauging Ocean organic Carbon Attenuation using Robotic Technologies; Henson et al. et al. 2023) and five days sampling resolution time-series of a moored sediment trap in the study region P3 (52°43.40' S and 40°08.83' W) in the downstream area of South Georgia in the northern Scotia Sea (Manno et al. 2022). This allowed detailed studies of the processes responsible to retention and attenuation of carbon flux in a hotspot region for biological productivity in the Southern Ocean.

The GOCART glider program followed the seasonal bloom during a period of four months from 19 October 2017 to 13 February 2018 and revealed large temporal variability in the magnitude and efficiency of carbon flux (Henson et al. 2023). These different production and export periods can be divided into four phases, i) early bloom, ii) bloom ramp-up, iii) bloom-peak, and iv) post-bloom. **i)** End-October to mid-November showed an early bloom phase with increase in primary production and a fairly high, but constant, export of carbon out of the upper mixed layer, which caused a decline in export efficiency (Henson et al. 2023). Hence, there was an accumulation of particulate organic matter in the upper productive layer of the water column, which suggested that there was low heterotrophic respiration and phytoplankton growth outpaced grazing during this period (Henson et al. 2023). **ii)** During the bloom ramp-up, the export was primarily made up by direct settling of heavily silicified live diatoms (Manno et al. 2022). **iii)** During the bloom peak, the export was composed of partially grazed phytodetritus, including full diatoms (Manno et al. 2022), suggesting that the maximum capacity of zooplankton grazing was exceeded by flux and the system 'leaked' organic carbon to deeper depths (Henson et al. 2023). **iv)** During the post-bloom, primary production and export flux varied in synchrony and export efficiency had low variability, suggesting that there was a match between phytoplankton growth and zooplankton grazing (Henson et al. 2023). The flux at depth was dominated by fecal pellets (Manno et al. 2022). Giering et al. (2023) observed that there was a transient accumulation of organic matter in the upper mesopelagic zone, the developing bloom showed strong accumulation until the bloom peak, while the period after the bloom-peak showed a decrease in accumulated organic matter in the upper mesopelagic zone.

Giering et al. (2023) concluded that particulate organic carbon concentrations followed the pattern observed for primary production in the surface ocean, but with a time-lag of two to three weeks and with a vertical separation between the upper and lower mesopelagic zone, i.e. 100 - 200 m and 200 - 1000 m, respectively.

While all different flux determinations during COMICS showed large variability in productivity and carbon export during the relatively short study period (Giering et al. 2023; Henson et al. 2023; Manno et al. 2022), it was so far not possible to identify the processes that caused this variability. By linking our existing knowledge of export, retention, and attenuation during the COMICS cruise with direct observations of the vertical abundance and size-distribution of particles and aggregates from *in situ* optics and sediment trap collections, we here attempt to get a step closer to understand the production and export dynamics. We focus on the processes that determined carbon export from epi- to mesopelagic zone to investigate if we can explain the flux attenuation and retention of organic matter by biological and physical processes. We do this by linking previous COMICS studies on export processes (Giering et al. 2023; Henson et al. 2023; Manno et al. 2022) and microbial and zooplankton turnover of organic (Cook et al. 2023; Hemsley et al. 2023) to detailed observations of the composition, settling, and attenuation of the carbon flux over time.

Material and methods

Study site

We investigated the biological and physical processes that control biogeochemical fluxes during the RSS Discovery cruise DY086 near South Georgia (Southern Ocean) in 2017, which was part of the COMICS project (Controls over Ocean Mesopelagic Interior Carbon Storage, Sanders et al. 2016). The research area was north of the North Scotia Ridge where the British Antarctic Survey are maintaining a long-term mooring at station P3 (Fig. 1). Our study followed the export processes to 500 m depth during a bloom dynamic between 15 Nov. and 14 Dec. 2017. The investigations were divided into 3 time-periods where we returned to the study region: P3A: 15 Nov. – 22 Nov. 2017, P3B: 29 Nov. – 5 Dec. 2017 (P3B-1: 29 Nov. – 3 Dec. 2017, P3B-2: 3 Dec. – 5 Dec. 2017) and P3C: 9 Dec. – 14 Dec. 2017. The study region at station P3 is situated northwest South Georgia, where regularly large phytoplankton blooms with chlorophyll a concentration reaching above 10 mg m^{-3} develop (Korb et al. 2004). It is believed that these large blooms are sustained by iron run-off from South Georgia and the island's shelf (Borrione and Schlitzer 2013; Korb and Whitehouse 2004; Korb et al. 2008).

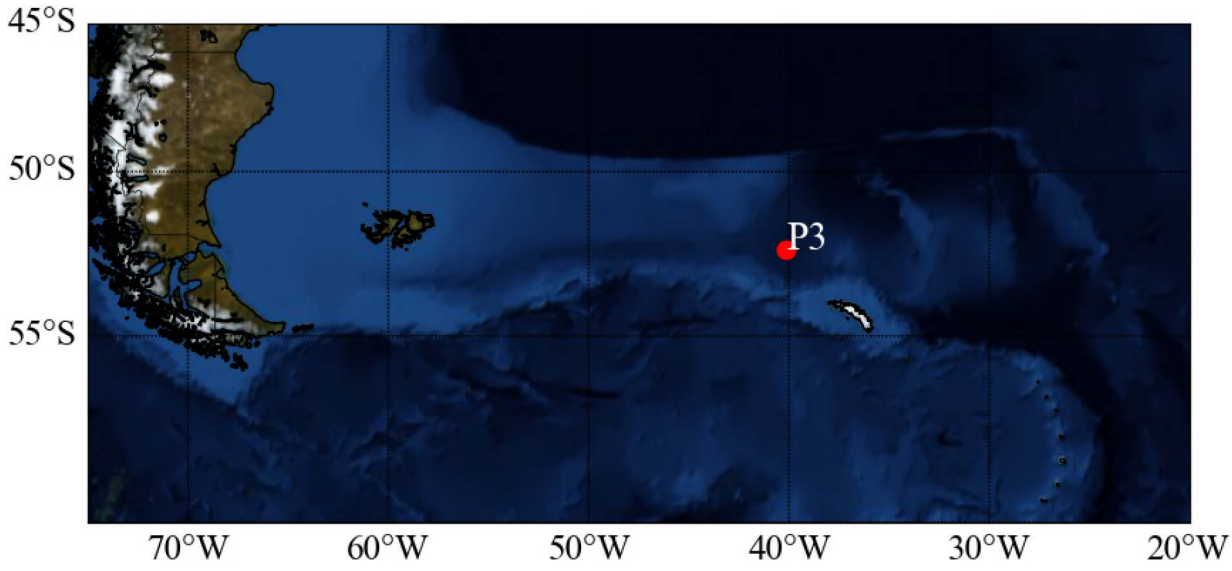

Fig. 1: Map of sampling area with station P3 (red) next to the island South Georgia.

Particulate organic carbon collected in drifting traps

To measure the particulate organic carbon (POC) flux, *in situ* sinking velocities and to collect individual *in situ* aggregates, PELAGRA traps (**P**article **E**xport measurement using a **LAGRA**ngian trap) were deployed (Iversen and Lampitt 2020; Lampitt et al. 2008; Salter et al. 2007; Saw et al. 2004). PELAGRA traps are neutrally buoyant sediment trap platforms based on an APEX float (Webb Research Corporation, USA) which actively controls the buoyancy to maintain a constant depth while remaining in the same water mass during a deployment (based on pressure and density control), i.e. "locked" into a water mass and drifting with the ocean current. Two PELAGRA types were used (1) standard PELAGRA traps that were equipped with 4 collecting funnels and four programmable opening and closing collection cups and (2) modified PELAGRA traps that were equipped with a particle camera designed to measure *in situ* size-specific settling velocities of sinking particles (Iversen and Lampitt 2020). Additionally, the modified PELAGRA traps had two collecting funnels with programmable collection cups and two gel cups that preserved the size and structure of the collected aggregates. The collection cups were filled with filtered seawater (> 500 m), which had increased density through an addition of 5 g NaCl L^{-1} and were fixed with a 10% formalin (final concentration) prior to the deployment. The gel cups contained an ethanol based viscous cryo-gel (Tissue-Tek, O.C.T.^{TM} COMPOUND, Sakura) which allowed the aggregate to sink into gel where they remained intact during recovery of the PELAGRA traps (Thiele et al. 2015). The PELAGRA traps were deployed at depths ranging from the base of the mixed layer (~90 m) and down to 500 m depth. After recovery, the gel traps were imaged using an x-y-stage on board and the material collected for biogeochemical fluxes were stored cold and dark until analyses in the home laboratory. The processing and measurement were described by Giering et al., 2023. Briefly, POC was analyzed from 16^{th} or 64^{th} subsamples from the collected material, from which zooplankton swimmers were picked before the material was filtered onto combusted (500°C, overnight) GF/F filters (0.7 µm nominal pore-size, 25 mm, Whatman filters). The filters were fumed with 35% HCl for overnight, whereafter they were dried at 50°C overnight and were packed into tin discs (30 mm, Elementar). The POC content was measured on an Elementar Vario Isotope Select Elemental Analyser.

Sinking velocities

In situ sinking velocities of sinking aggregates were measured at 100 m and 500 m using the PELAGRAs that were equipped with camera systems (PELAGRA-CAM, see Iversen and Lampitt 2020). This was done by capturing sinking particles during 18 seconds of time-lapse images every hour. Each image was captured with an interval of 2 seconds between the images, which allowed us to follow the vertical trajectory and calculate the settling velocity from the distance each aggregate sank over time (up to 18 seconds). The PELAGRA-CAM consisted of a Canon EOS 6D digital SLR camera equipped with a 50 mm macro lens and a Canon Speedlite 600EX RT flash gun, which was placed perpendicular to the camera for optimal light conditions. The camera settings were adjusted to a lens focus of 1.5 feet, an aperture of f/32, a shutter speed of 1/160 s and an ISO of 2500 with a flash output of 1/8 and a straight flash direction. Images were captured every 2 seconds using a Hahnel Giga T Pro II remote timer. The total water volume per image was 2.15 L. The field of view was 157 mm wide, 101 mm high and 135 mm deep. The PELAGRAs were equipped with a CTD (RBRconcerto, RBR) that measured temperature, salinity and pressure. Image sequences were excluded if the filmed particles were not sinking vertically but instead moved side - or upwards. The image sequences were analyzed and processed for particle sinking velocities with an image tracking software for *in situ* cameras based on C++ with Qt using OpenCV libraries for image processing (Iversen and Lampitt 2020). Particles with a minimum area of 5 pixels were included in the analysis, with 1 pixel equaling 40.8 μm^2. Since the particle concentration was relatively high, especially in the upper trap, the particles were separated into three size classes (5 – 100 pixels: 204 – 4,080 μm^2, 101 - 250 pixels: 4,121 – 10.200 μm^2, >250 pixels: > 10.200 μm^2) and all size classes were analyzed for particle trajectories independently. Here, we allowed the small size-class vary 2-fold in size, since small differences in illumination of small particles can have a huge impact on the estimated equivalent spherical diameters. The intermediate size-class were allowed a 15% variability in detected sizes for an individual particle, while the large particles only were allowed 10% variability. Additionally, the size-classes allowed us to change the search area for the same particle between images. Small and slow-settling particles and aggregates had a smaller search area than large and fast-settling aggregates: 2 mm x 16 mm (width x height) for small, 4 mm x 16 mm for intermediate particles and 8 mm x 24 mm for large particles. The trajectories were manually checked to eliminate any wrong trajectory assignments.

Vertical particle distributions and particulate organic carbon flux calculations based on in situ camera observations

An underwater *in situ* particle camera system (Red Camera Frame, RCF) was used to capture vertical profiles of aggregate size-distribution and abundance through the water column (Table S1 in the supplementary information). The RCF was based on the set-up used for the PELAGRA-CAM. The RCF was deployed down to 500 m with a descent speed of 0.2 m s^{-1} and ascent with 0.2 to 1 m s^{-1}. Only the downcast images were used for the particle profiles. The RCF was equipped with a CTD (RBRconcerto, RBR), which measured temperature, salinity, pressure, fluorescence and backscatter. The captured particles and aggregates were analyzed for size and abundance using image analyzing software within the Image Processing Toolbox in Matlab (The Mathworks, Inc.) (Markussen et al. 2020).

We used the area that was detected from each particle and aggregate when thresholding white particles against a black background (Iversen and Lampitt 2020; Markussen et al. 2020) to calculate the equivalent spherical diameter (ESD). We excluded all particles which we could identify as zooplankton with visual inspection. Hereafter, we assigned the aggregates and particles into logarithmically spaced bins (size ranges). ESDs smaller than the minimum bin size (10 µm) were excluded due to optical resolution limitation of the PELAGRA-CAM. We calculated the particle size-spectra (*N*) based on the size-specific particle concentrations and the bin-width of each size-bin (Jackson and Burd 1998):

$$N = \frac{\Delta C}{\Delta d} \quad (1)$$

where ΔC is the concentration of the particles per imaged volume with a given size range Δd (Iversen et al. 2010). The volume size spectra, i.e. the total particle volume of each size bin, was calculated based on the ESD and abundances of particle size spectra assuming spherical shape of the particles.

The particulate organic carbon flux (POC flux) was calculated by combining vertical particle profiles with the measured flux from the PELAGRA traps using the method described in details in Guidi et al., 2008. This means that we assumed that the total mass flux (*F*) is resulting from the integration of the mass flux spectrum over all particle sizes:

$$F = \int_0^\infty n(d)m(d)w(d)dd \quad (2)$$

where *n(d)* is the size-spectra, *m(d)* is the mass, *w(d)* is the sinking velocity and *dd* is the diameter of a particle *d*.

We used the *in situ* measured size-specific settling velocities (w) and assumed that the mass m as a function of aggregate size followed a power function (Guidi et al. 2008):

$$m = A * d^b \quad (3)$$

The A and b values were calculated using the Matlab function fminsearch (The Mathworks,Inc.), by minimizing the differences between the log-transformed PELAGRA trap and particle size-spectra estimated fluxes (Guidi et al. 2008; Iversen et al. 2010). This was done by averaging the integrated particle size-spectra in the corresponding depth and time and calculating their flux (equation 2), then assigning those to the POC value of the PELAGRA trap. Using the estimated A and b values, we calculated a time series of vertical POC export profiles through the water column over the sampling periods based on the particle size-spectra.

The loss of particulate organic carbon (POC_{loss}, mgC m^{-3} d^{-1}) was calculated according to the equation 5 in Iversen (2023) as negative quotient of the difference in POC flux (F, mgC m^{-2} d^{-1}) and in depth (z, m) of 50 m to 100 m, 100 m to 150 m and 150 m to 250 m:

$$POC_{loss} = -1 \frac{\Delta F}{\Delta z} \quad (4)$$

The carbon loss of 50 m to 100 m, 100 m to 150 m and 150 m to 250 m was averaged for P3A, P3B, P3C, respectively, and multiplied by the total depth of each depth-layer (z, m) to calculated the carbon loss in mgC m^{-2} d^{-1}.

In order to compare the total carbon-loss with the zooplankton ingestion, the zooplankton ingestion was estimated for each depth-layer based on the values for total community ingestion provided in Figure 5 by Cook et al. (2023). For this, the daily ingestion rates for each depth strata and net type in mgC m^{-2} d^{-1} were calculated and then their proportional contributions to the depth layer of 50 m to 100 m, 100 m to 150 m and 150 m to 250 m were summed. This was done for the two last visits, P3B and P3C, as not all net data was available for P3A (Cook et al. 2023).

Data analysis

The plots and statistical analyses were done using R (RCoreTeam 2019) and Python. To compare the sinking velocities between the different depth and timepoints, the data was log-transformed and linear regressions were calculated. The linear regressions were compared as linear model in their homogeneity of slope and intercept.

Results

Environmental conditions

The highest fluorescence signal was observed in the beginning of the bloom with 18.7 mg m^{-3} and with fluorescence peaks in the upper 100 m of the water column (P3A). The fluorescence signal decreased over time during the bloom period (Fig. S1 in the supplementary information). The salinity was lowest in the surface ocean with a minimum of 33.75 PSU, remained stable until around 50 to 80 m depth, whereafter salinity continuously increased down to 450 m depth. The salinity gradient between 100 m and 200 m became greater in magnitude during the study period (P3A - P3C, Fig. S1 in the supplementary information). The temperature was the highest in surface ocean with temperature maxima of 3.7°C and decreased to below 1° C at depths between 100 – 200 m. The surface temperature increased during the study period (P3A-P3C, Fig. S1 in the supplementary information). This resulted in an increased magnitude of the temperature gradient from the surface to 100 m throughout the study.

Particle and aggregate abundance, sizes and composition

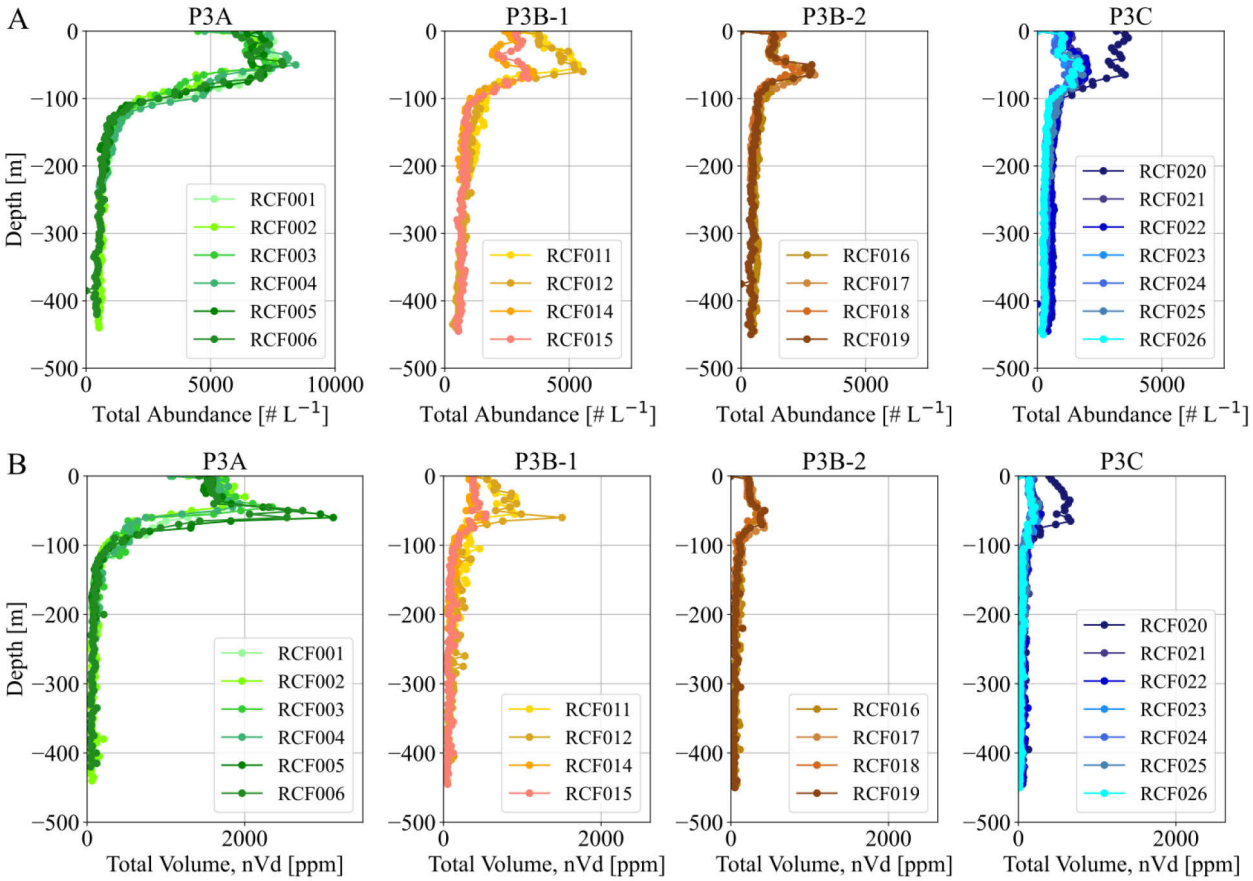

Fig. 2: (A) Total Aggregate Abundance [# L^{-1}] and (B) Total Particle Volume, nVd [ppm] according to depth [m] for all stations (P3A, P3B-1, P3B-2, P3C) with the respective profiles from the Red Camera Frame (RCF).

We observed the highest abundance and largest average particle sizes (equivalent spherical diameter - ESD) in the upper water column, while low average ESDs and particle abundances prevailed for the particles and aggregates detected below 100 m (Fig. 2, and S2 in the supplementary information). Taking a closer look at the upper 100 m, we observed a higher average ESD in the upper 65 m together with low density, low salinity and, to a lesser extent, the high temperature at these depths (Fig. 3). There was a sharp decrease in aggregate size with increasing seawater density, salinity, and decreasing temperature, most pronounced for salinity (Fig. 3).

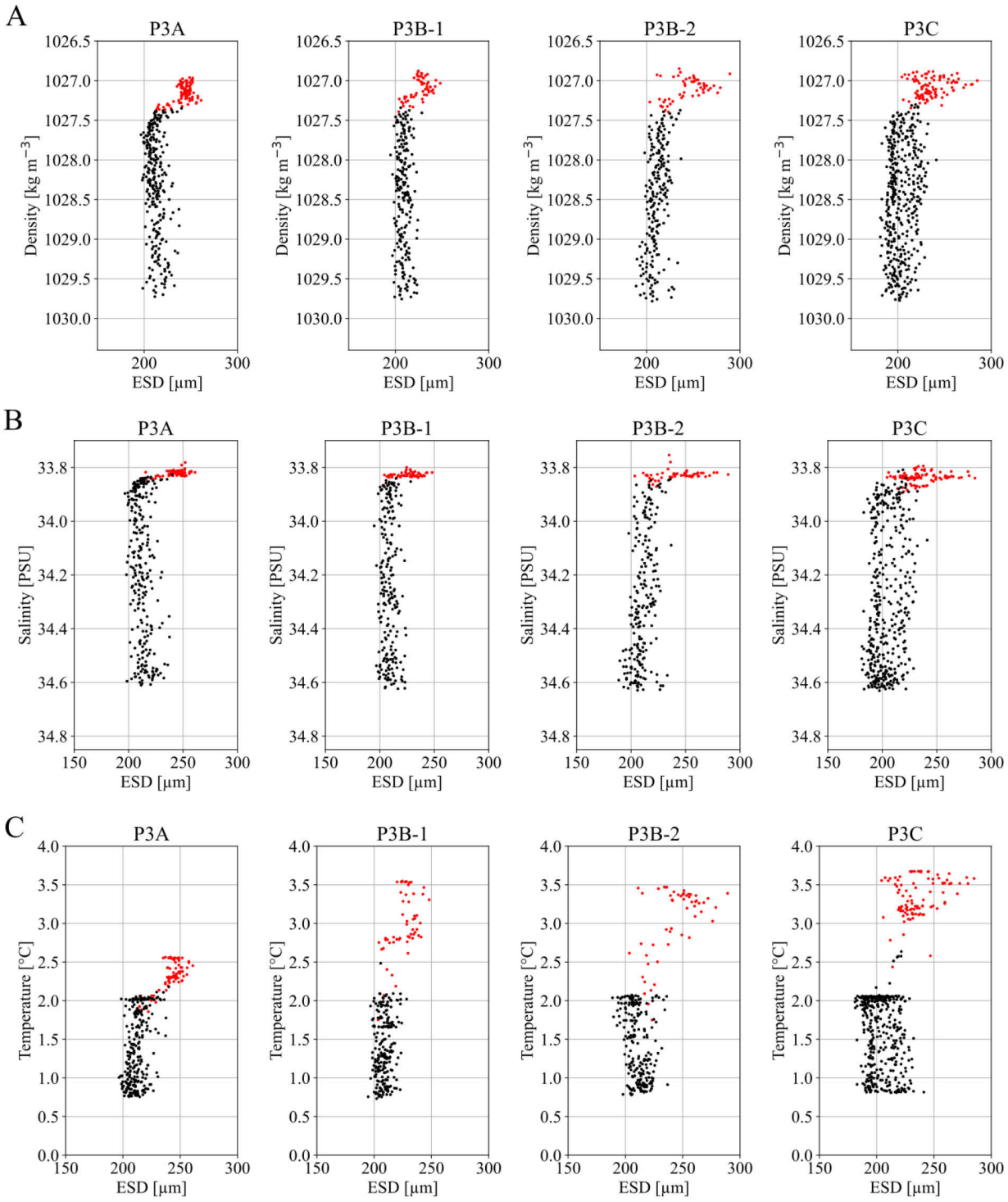

Fig. 3: Average equivalent spherical diameter (ESD) in µm according to (A) density [kg m^{-3}], (B) salinity [PSU] and (C) temperature [°C] for all stations (P3A, P3B-1, P3B-2, P3C). In red all measurements from < 65 m depth, in black all measurements from > 65 m depth.

There were a higher abundance and size-distribution of particles at P3A at 50 m compared to the subsequent visits where the abundance of the intermediate size-classes had decreased (Fig. 2, 4 and 5). This seemed due to a reduction in the abundance of colony-forming diatom which occurred in high numbers during P3A, while they were rare during P3B and absent at P3C (Fig. 5). Zooplankton fecal pellets were increasing in abundance throughout the three visits suggesting that zooplankton grazing was becoming increasingly important (Fig. 5). At 100 m depth, we observed that it was primarily the larger fecal pellets and small dense particles that sank out, while marine snow was less frequent here compared to 50 m (Fig. 5). At 150 m depth, we mainly observed small and compact particles and very few marine snow and fecal pellets during all three visits (Fig. 5).

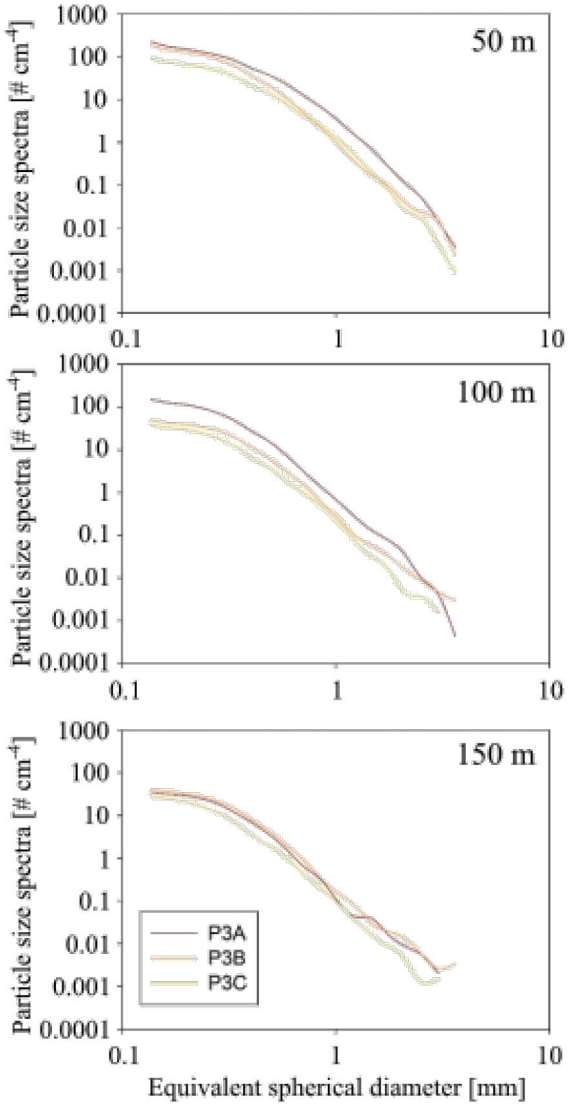

Fig. 4: Particle size-spectra [# cm^{-4}] according to equivalent spherical diameter [mm] for 50, 100, and 150 m depths for P3A (RCF01, red), P3B (RCF11, orange), and P3C (RCF20, yellow).

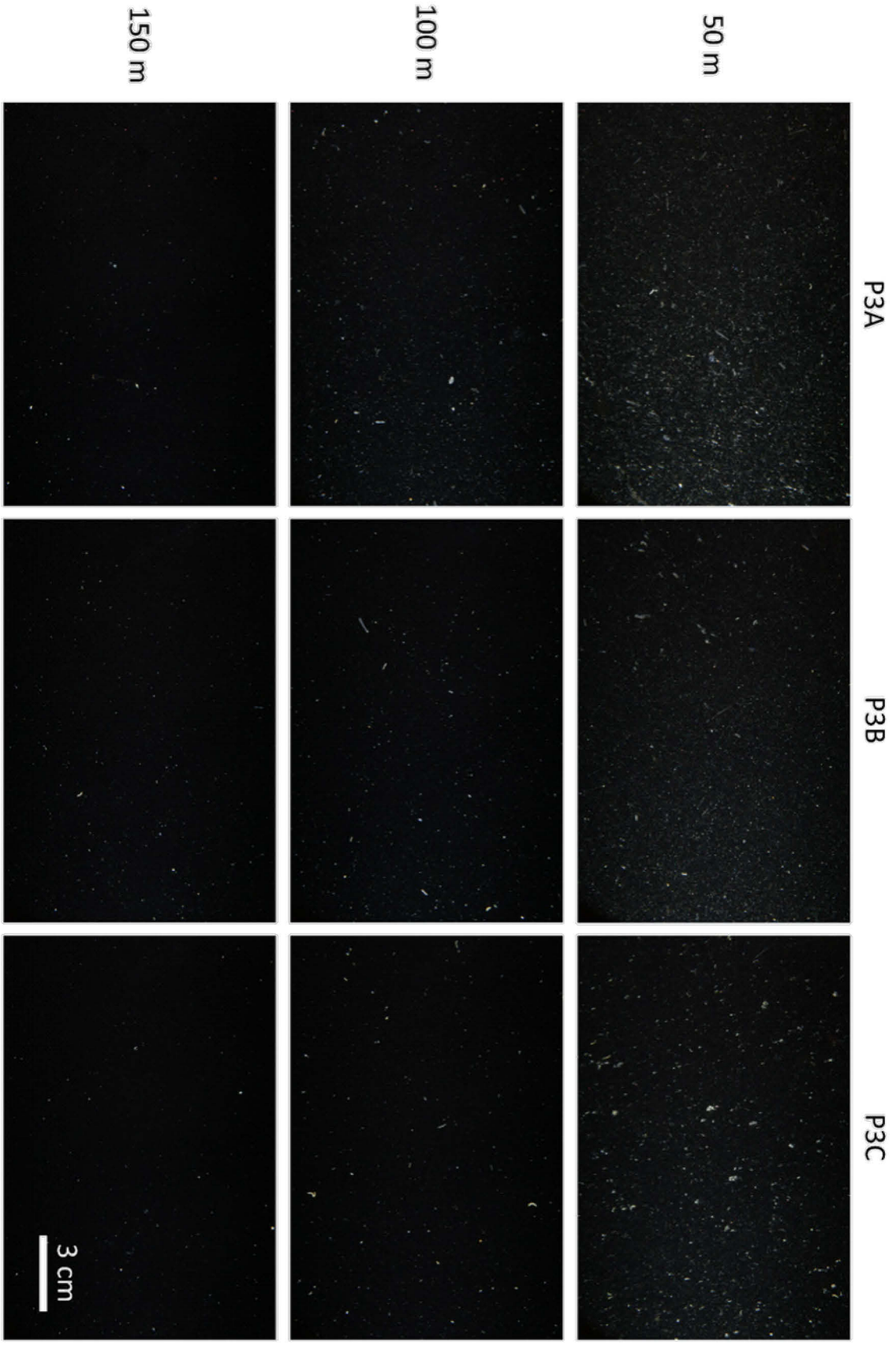

Fig. 5: Examples of *in situ* images captured by the Red Camera Frame (RCF) from 50 m, 100 m, and 150 m depths from the three visits; P3A (RCF01), P3B (RCF11), and P3C (RCF20).

During the first visit to the study area (P3A), the material collected by the PELAGRA traps (both conventional and gel traps) was dominated by single diatoms and some fragmentated, but non-degraded fecal pellets (Fig. 6). Though phytoplankton aggregates were observed from the RCF, they were very fragile and broke apart in the PELAGRA traps (both the biogeochemical and the gel traps) and did not remain intact during collection with Marine Snow Catchers, which resulted in organic material collected as a fluffy layer of single diatoms. During the second visit (P3B-1), the organic material consisted of pennate diatoms, including *Fragilariopsis kerguelensis* and *Thalassionema spp.* (Fig. 6). There was heavy zooplankton grazing, which was evident as an increase in exported intact and seeming freshly produced krill fecal pellets, freshly produced as well as degraded copepod fecal pellets, and some, but not dominant, numbers of appendicularian fecal pellets (Fig. 6). During P3B-2, we only collected low numbers of krill fecal pellets and some appendicularian fecal pellets. The copepod fecal pellets during P3B-2 mostly consisted of degraded and fragmented pellets (Fig. 6). Additionally, the collected fecal pellets were colonized by flagellates. Apart from intact diatoms, P3B-2 showed export of empty diatom frustules (Fig. 6). During the final visit at the end of the spring bloom (P3C), the exported organic matter appeared reworked and recycled, meaning empty and broken diatoms frustules (Fig. 6), i.e. diatoms that had been fed upon by zooplankton. The krill fecal pellets were no longer smooth, but with broken membranes and loosely packed, which indicated that they were in the process of being degraded. Additionally, large chains of the diatom *Fragilariopsis kerguelensis* were collected (Fig. 6).

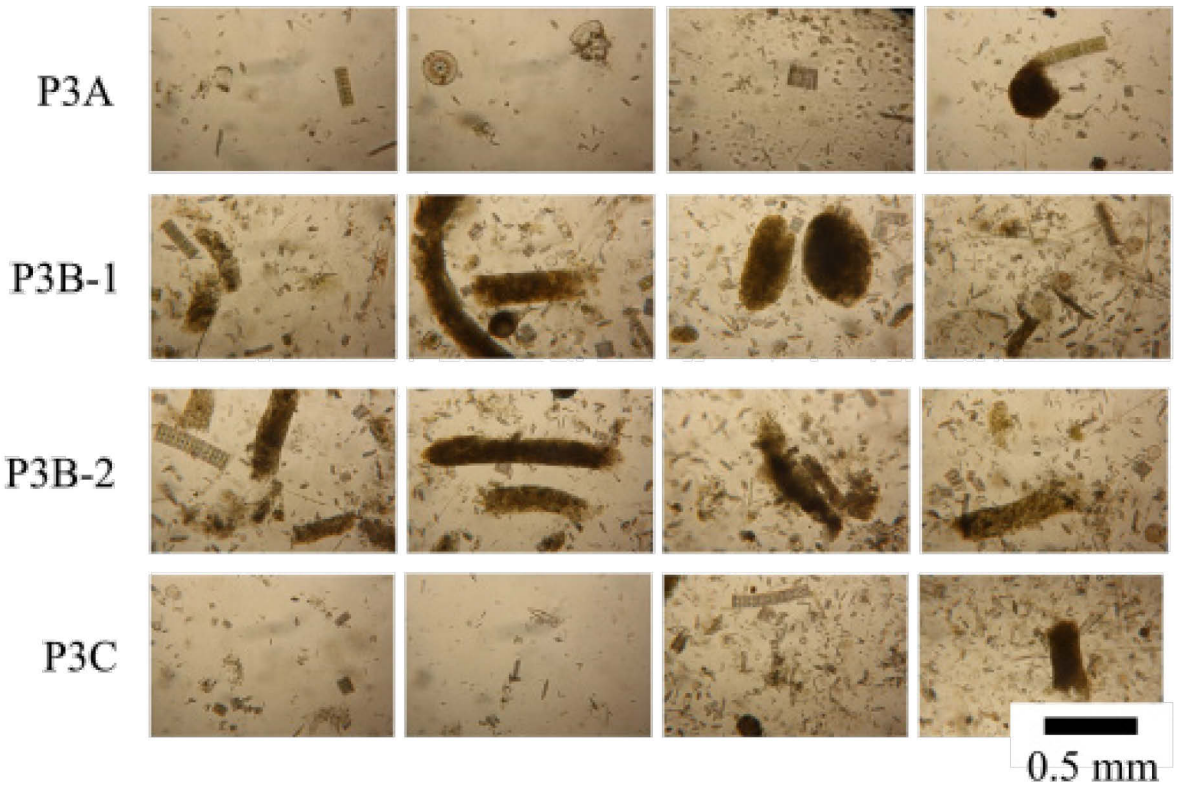

Fig. 6: Composition from settling material collected by the PELAGRA traps. P3A: many single diatoms and some fragmentated, but non-degraded fecal pellets. P3B-1: pennate diatoms, including *Fragilariopsis kerguelensis* and *Thalassionema spp.*, freshly produced krill fecal pellets, freshly produced and degraded copepod fecal pellets, and some appendicularian fecal pellets. P3B-2: few krill fecal pellets and appendicularian fecal pellets, degraded copepod fecal pellets, intact and empty diatoms. P3C: empty and broken diatoms frustules, degraded krill fecal pellets, large chains of the diatom *Fragilariopsis kerguelensis*.

Sinking velocities

The log-transformed sinking velocities were plotted against the log-transformed ESD and a linear regression was calculated for each trap deployment (R^2 = 0.11 - 0.48, Fig 7). This showed that there was a stronger size dependency of the sinking velocities (steeper slope of > 0.7 between sinking velocities and ESD) during the first visit (P3A, Fig. 7), than during the second (P3B) and third visit (P3C, slope < 0.45). The homogeneity of slope and intercept was tested as linear models. There were no significant differences between the slope or intercept of the sinking velocities at 100 m and 500 m during the second (P3B) and third visit (P3C, p-values > 0.05). Contrary to this, the sinking velocities at 100 m during P3A differed in slope from the sinking velocities at 500 m during P3B and P3C (p-values < 0.05), while the sinking velocities at 500 m during P3A differed in slope from both 100 m and 500 m during P3B as well as in both slope and intercept during P3C (p-values < 0.05).

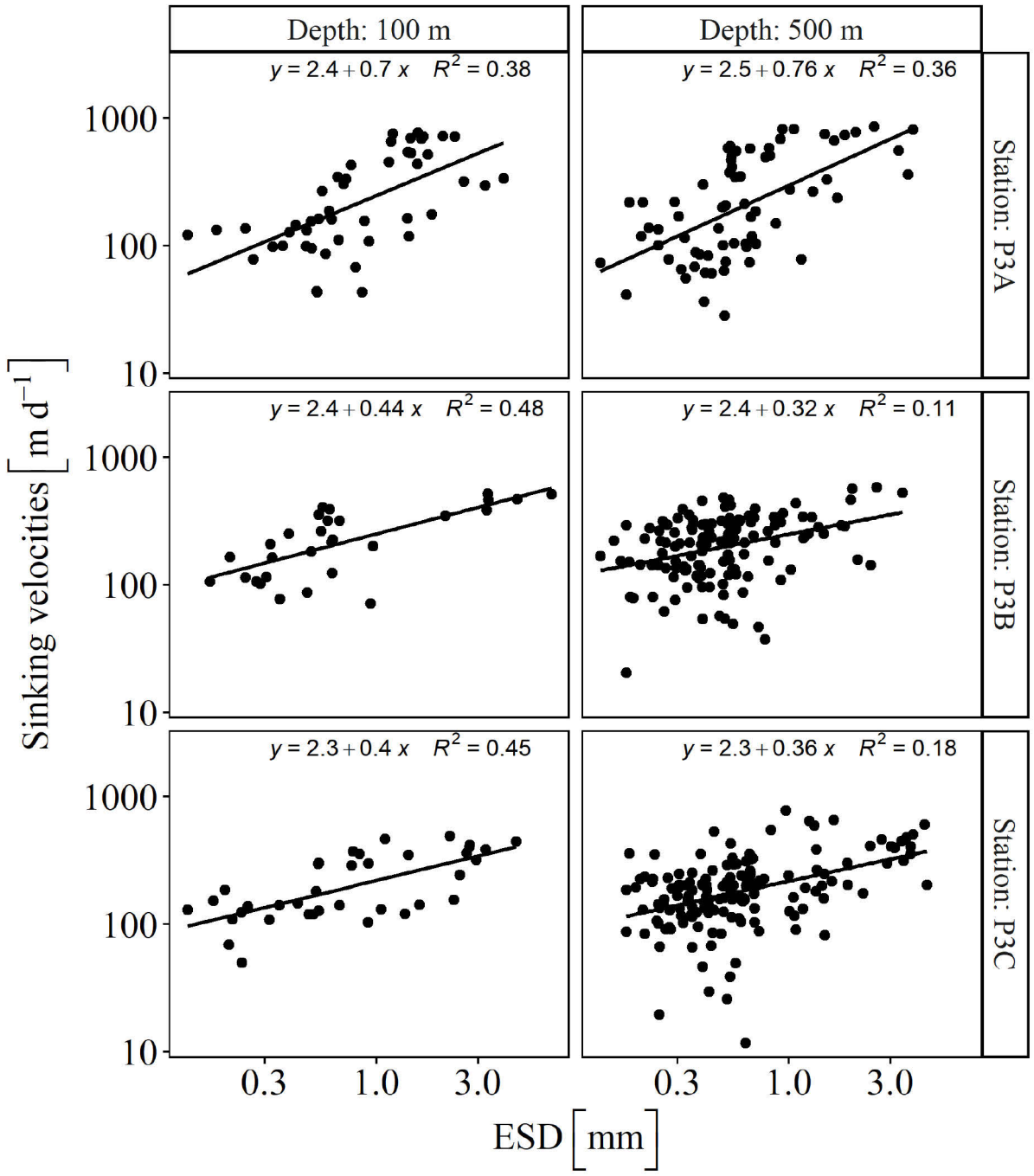

Fig. 7: Logarithmically scaled sinking velocities in m d^{-1} according to logarithmically scaled equivalent spherical diameter (ESD) in mm for all stations (P3A, P3B, P3C) at shallow depth (100 m) and deep depth (500 m) with linear regression (Equation & R^2)

Particle and particulate organic carbon export

Total particle abundances and total particle volumes in the upper 100 m of the water column were highest during P3A, whereafter they decreased as the phytoplankton bloom progressed, resulting in the lowest observed total abundances and total volumes during our last visit to the region (PC3, Fig. 2). Despite the decrease in total abundance and volume in the upper 100 m, we did not observe any increase in abundance or volume of particles between 300 – 400 m, where the abundance averaged to 499.6 ± 149.0 # L^{-1} and the average total volumes was 58.1 ± 29.0 ppm throughout the entire study period (Fig. 2). The depths between 50 and 150 m showed a sharp decrease in total abundance and total volume of particles and aggregates during the study (Fig. 2).

Similarly, there was a higher variability of POC flux in the upper ocean (< 100 m) compared to the depths below 100 m during the study (Fig. 8 and 9). The highest POC flux was observed between 40 and 80 m during the first visit (P3A, Fig. 8), with maximum POC values > 1 gC m^{-2} d^{-1}. During the second visit (P3B), the POC flux peak in the upper 100 m was less in magnitude, while only a small peak in POC flux was detected in the upper 100 m during our last visit (P3C). The POC flux between 300 and 400 m depth was relative stable with values between 0.1 and 0.2 gC m^{-2} d^{-1} throughout the entire study, suggesting that there was no direct link between the POC flux within the upper 100 m with high variation and the constant POC flux below 100 m (Fig. 8 and 9).

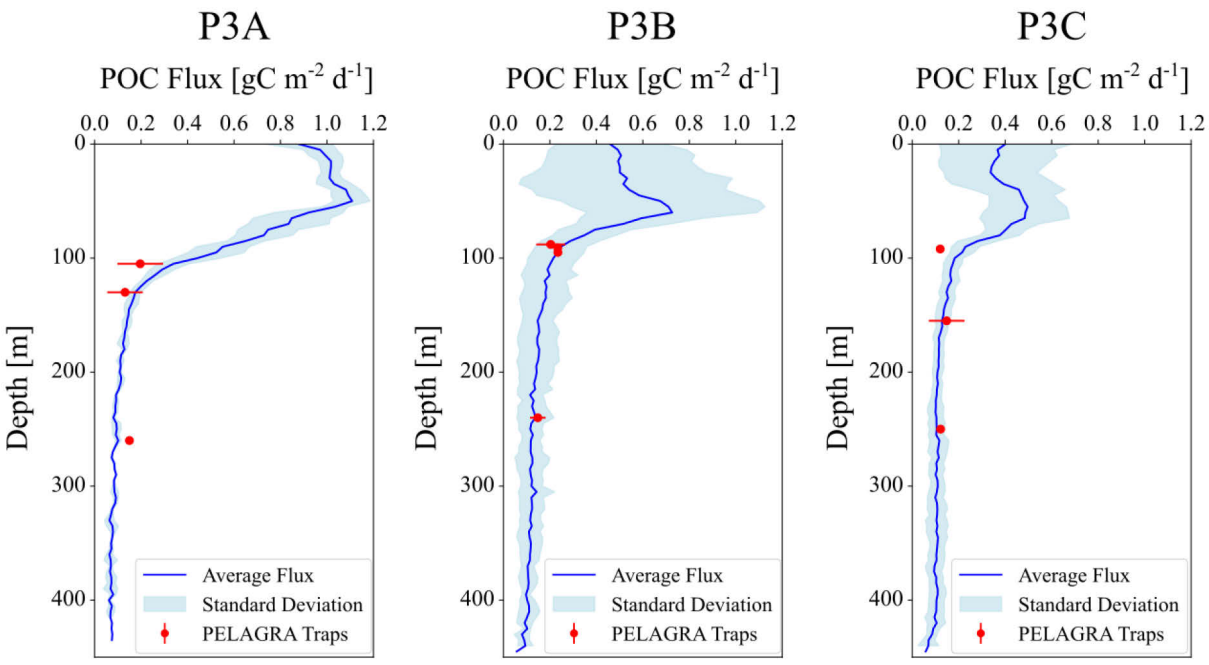

Fig 8: Average particulate organic carbon (POC) flux [gC m^{-2} d^{-1}] calculated from the Red Camera Frame profiles made during each of the three visits to the study region. The shaded area is standard deviation for the calculated POC flux and the red dots and lines are the average carbon flux and the standard deviation for flux measured with the PELAGRA traps.

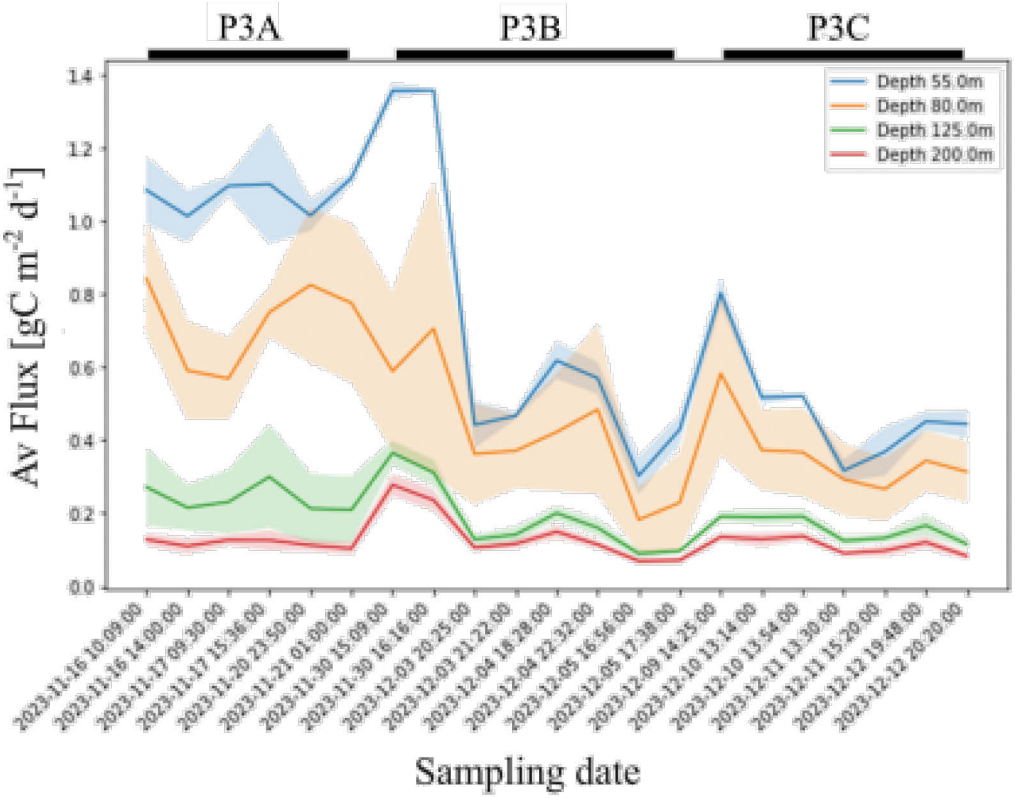

Fig 9: The average particulate organic carbon (POC) flux [gC m^{-2} d^{-1}] plotted for specific depths (55 m = blue, 80 m = orange, 125 m = green, and 200 m = red) over time throughout the entire study. The shaded areas represent standard deviation.

The flux-estimated carbon loss at 50 - 100 m was highest and 3 (P3C) to 6 (P3B) times as large as the estimated zooplankton ingestion in the depth-layer (Fig. 10). The flux-estimated carbon loss in 100 - 150 m and 150 - 250 m at P3B and P3C was low and close in number to the zooplankton ingestion at these depths (Fig. 10).

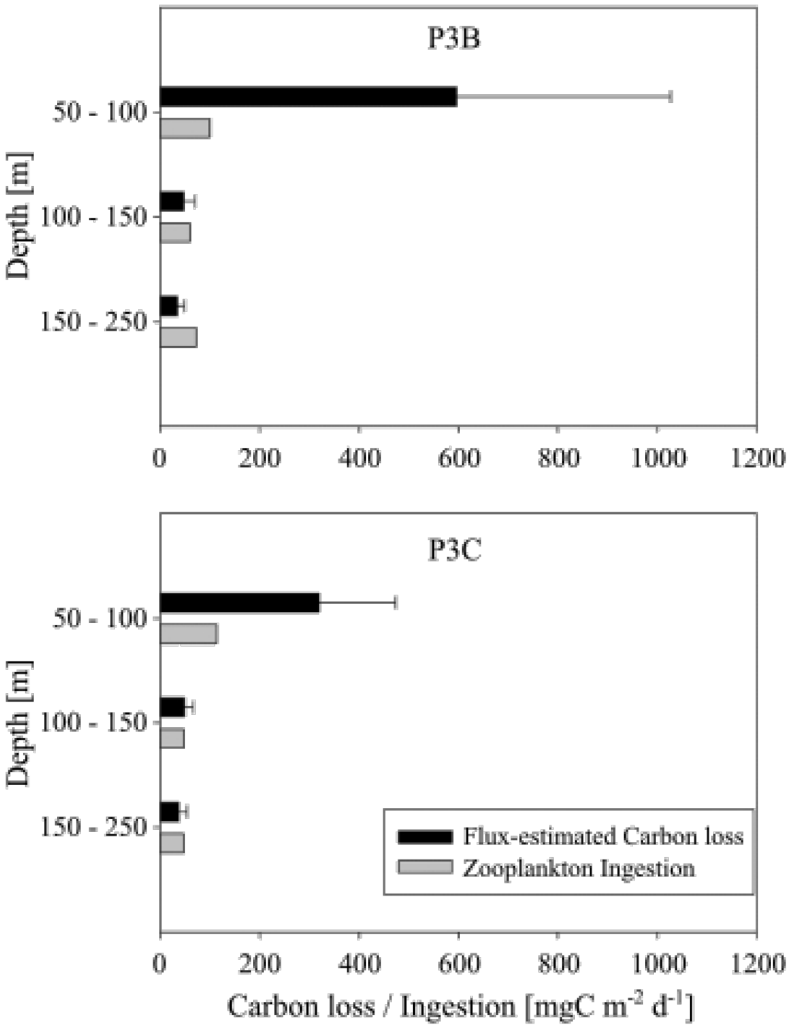

Fig. 10: Estimated carbon loss and zooplankton ingestion [mgC m^{-2} d^{-1}] for three depth-layers (50 - 100 m, 100 - 150 m, and 150 - 250 m) for P3B and P3C. The carbon-loss is calculated according to equation 5 in Iversen (2023), which provides carbon-loss in mgC m^{-3} d^{-1}. To get the total carbon loss within the depth-layer per day, the carbon-loss from equation 5 (Iversen 2023) was multiplied by the total depth of the depth-layer. The total zooplankton ingestion was calculated for each depth-layer based on the values provided in Figure 5 by Cook et al. (2023).

Discussion

Throughout the COMICS cruise we followed the development and the export processes of a spring bloom northwest of the island South Georgia in the Southern Ocean. This is a region that receives iron run-off from South Georgia, which sustains large and long-lasting phytoplankton blooms with chlorophyll *a* concentrations > 10 mg m^{-3} (Korb et al. 2008; Korb et al. 2004). In the study region, low current velocities were observed, indicating that lateral advection only has a minor impact on the vertical export processes in the region (Henson et al. 2023; Manno et al. 2022). Henson et al. (2023) measured surface current velocities of ~ 3.5 km d^{-1}, suggesting that the horizontal displacement is < 70 km for aggregates sinking with 100 m d^{-1} from the surface ocean to 2000 m depth. In this study, we focus on the connection between the surface ocean and the upper mesopelagic zone (to 450 m depth), suggesting that we have a strong vertical connectivity and that the horizontal advection was < 10 - 20 km if the aggregates maintained a constant settling velocity of 100 m d^{-1}. Despite a potentially strong vertical connectivity, we observed large temporal and spatial differences in particle size-distribution and abundance with more particles at 50 and 100 m during P3A compared to the two later visits, while there were no large differences in particle size-spectra between the three visits at > 150 m (Fig. 2, 4 and 5). The vast majority of particles captured by the *in situ* images revealed that less dense and more porous particles and aggregates were observed mainly in the upper 100 m of the water column while primarily dense particles sank to depths below 100 m. Furthermore, it seemed that zooplankton fecal pellets and heavily silicified diatoms were effective vectors for export to deeper depths, which is supported by deep ocean peak fluxes of fecal pellets and single cell diatoms (Manno et al. 2022).

The change of particle types during the bloom development and decline was represented in the size to settling velocity relationship of the aggregates (Fig. 7). The efficiency of the carbon export is directly depending on the settling velocities of the aggregates and their remineralization rate, as it is decisive for the depth of remineralization (Kwon et al. 2009). Generally, fast-sinking particles have higher chances of reaching greater depth due to the shorter time available for degradation within a specific depth-layer, while slow sinking particles are available for a longer time for remineralization at shallow depths (Iversen et al. 2010). Especially, fecal pellets with their high sinking velocities are effective vectors for carbon export in the Southern Ocean (Belcher et al. 2017; Manno et al. 2015; Manno et al. 2022; Pauli et al. 2021). The size to settling velocity relationship was stronger during the first visit (P3A, Fig. 7) where settling aggregates were more uniform in their characteristics and mainly made of phytoplankton detritus. As the aggregate types became more diverse, the relationship of the

plotted settling velocity as a function of aggregate size became weaker (P3B and P3C, Fig. 7). The increasing grazing activity and increasing dominance of fecal pellets at greater depths (this study; Manno et al. 2022) combined with small dense particles such as silicified diatoms resulted in a heterogenous pool of settling particles that weakened the size to settling velocity relationship. Hence, varying density and porosity of the aggregate types due to ongoing transformation processes by zooplankton and microbes impacted the settling more than their size (Iversen and Ploug 2010; Ploug et al. 2008).

When combining the directly measured particulate organic carbon (POC) flux from the PELAGRA traps with the RCF *in situ* images to calculate high resolution POC flux, we observed large variability in the upper 100 m, while the POC flux at depths below 100 m only showed marginal changes throughout the entire study (Fig. 8 and 9). While this study only investigated POC flux down to 450 m, simultaneous studies using gliders and Marine Snow Catchers have shown that POC flux was remarkably constant down to 1000 m during the entire study period (Giering et al. 2023). Hence, there seemed to be a retention mechanism which prevented the majority of the organic matter from sinking to depths below 100 m. This is in line with previous observations from the Southern Ocean where Henson et al. (2012) found that only 15-25% of the carbon fixed via primary production sank out of the surface ocean. Furthermore, there are frequent observations of a deep chlorophyll maximum in the Southern Ocean (Carranza et al. 2018; Parslow et al. 2001; Tripathy et al. 2015), which persists for extended periods from spring and until late-autumn. In the fall large export events take place, associated with fall and winter mixing and the breakdown of the stratified surface water layer (Kemp et al. 2000). Often these late export events are dominated by diatom resting spores (Rembauville et al. 2015a; Salter et al. 2012), which was also the case for the end of the COMICS bloom in January (Manno et al. 2022). There generally seem to be a time-lag between production and export in the Southern Ocean, which has been reported to be up to 2 months (Henson et al. 2015; Rembauville et al. 2015b; Rigual-Hernández et al. 2015). During COMICS, a 15-day time-lag caused a decoupling between primary production and export flux to 1000 m (Henson et al. 2023). However, only a fraction of the produced organic matter sank to 1000 m and there was a significant vertical imbalance between the production in the upper water column and the export to the lower mesopelagic zone (Giering et al. 2023).

When assuming that the organic matter was continuously sinking from the surface ocean to the lower mesopelagic zone, we can estimate the flux attenuation from the decreasing POC flux at specific depth-layers (Iversen 2023). Here we use equation 5 in Iversen (2023) to calculate the total carbon loss for three depth-layers (50-100 m, 100-150 m, and 150-250 m) for

the two last visits, P3B and P3C (Fig. 10) in order to compare the total carbon loss with the estimated zooplankton ingestion rates at specific water depths during COMICS (Cook et al. 2023). We only performed this exercise for the two last visits since data for one of the zooplankton net samplings was not available for P3A (Cook et al. 2023). This shows that the majority of flux decrease occurs in the depth-layer between 50 and 100 m, while there is only a minor flux attenuation taking place in the two deeper depth-layers between 100 and 150 m and between 150 and 250 m (Fig. 10). Furthermore, it is clear that zooplankton are not able to explain the flux attenuation between 50 and 100 m (Fig. 10; Cook et al. 2023) and since the bacterial degradation of settling aggregates is only 3% (Hemsley et al. 2023) this process can also not explain the large flux attenuation. The flux attenuation in the two deeper depth-layers can, however, be explained by zooplankton ingestion (Fig. 10). Hence, our assumption that the particles and aggregates are continuingly settling from the surface to the upper and lower mesopelagic zone seems to be wrong and instead, the majority of the aggregates seem to be retained in the epipelagic zone.

Considering the aggregate sizes within each of the depth-layers, we observed that larger aggregates were retained in the upper water column and only the small aggregates escaped to depths below 100 m (Fig. S2 in the supplementary information). It is possible that the large aggregates were either slow-sinking or suspended, which could be the case if the large aggregates contained high amount of mucous or transparent exopolymer particles (TEP), as TEP-rich aggregates have been shown to have low excess densities and low settling velocities (Azetsu-Scott and Passow 2004; Engel and Schartau 1999; Mari et al. 2017). In the mesopelagic zone, we did occasionally observe clusters or groups of very large aggregates (~ 3 mm equivalent spherical diameter, Fig. S3 and S4 in the supplementary information), with sinking velocities of 430 ± 120 m d^{-1} (Fig. 7). However, the aggregates making up the clusters of these giant aggregates in the mesopelagic zone were different in appearance in comparison to the large aggregates in the surface ocean. While the giant aggregates at depth were very compact, aggregates in above 100 m depth were fluffy and more porous in appearance. Large fast-sinking aggregates at depth could possibly originate from zooplankton transformation of the material, e.g. salp fecal pellets show similar sizes and settling velocities (Iversen et al. 2017) as the giant aggregates observed at depth. On the other hand, it is unlikely that the large aggregates in the surface ocean were fast-sinking, as due to their porous structures their settling should be retarded by physical process (Kindler et al. 2010; Prairie et al. 2013).

Laboratory studies have shown that increasing salinity gradients can retain settling aggregates as a function of the time it takes for salt to diffuse into the aggregate pore-water,

decreasing the excess density of the aggregates as they enter saltier and denser water depth (Kindler et al. 2010; Prairie et al. 2013; Prairie et al. 2015). This mechanism has been observed as layers of particle and aggregate accumulations at density discontinuities (Alldredge et al. 2002; Dekshenieks et al. 2001; MacIntyre et al. 1995). Supporting that there was a retention of large aggregates in the epipelagic zone at increasing salinity gradients, we observed a sharp decrease in aggregate size when we plotted the average sizes against seawater density, salinity, and temperature (Fig. 3). Here we observed the steepest decrease in aggregate size with increasing salinity (Fig. 3), as diffusion of salt is a slow process in comparison to heat diffusion explaining why temperature had little impact aggregate size (Gargett et al. 2003; MacIntyre et al. 1995; Prairie et al. 2013). Thus, it seems that especially large and porous aggregates were retained by increasing salinity gradients. This also explains why fecal pellets were efficiently exported (Manno et al. 2022), since zooplankton fecal pellets are more dense than marine snow (Ploug et al. 2008).

Still, a simple calculation of diffusion into a spherical aggregate with a radius, *r*, of 1.5 and 2.5 mm suggests that it should only take 9.2 and 25.7 min for salt to enter the center of the aggregates, respectively; assuming a diffusion coefficient, *D*, for salt in seawater on the order of 2.03×10^{-9} m^2 s^{-1} (diffusion time [s] = r^2 / 2 * D). This seems a fairly short time for the diffusion, however, considering that the salinity is continuously increasing from ~ 50 m depth, it means, that in each new depth with increasing sea water density due to salinity, the aggregate will experience a delay of several minutes. It therefore seems likely that large, porous aggregates are physically retained or delayed by increasing salinity gradients and that this mechanism may explain time-lags between production and export in the Southern Ocean. This is a mechanism that might become of increasing importance at high latitudes as sea ice melt will increase due to warming and generate stronger salinity gradients in the surface ocean.

Conclusion

The carbon flux attenuation in high latitude systems does not only originate from zooplankton feeding and microbial remineralization but also results from salinity gradient based particle retention. Particle retention by salinity gradients contributes to lower particle concentrations at depth which should be kept in mind for the calculation of carbon attenuation. Nevertheless, the accumulation and retention of particles with increasing salinity will also promote intense zooplankton feeding and longer retention time will promote microbial degradation. The aggregate transformation and fecal pellet production by zooplankton play a crucial role to export carbon from the surface ocean in the Southern Ocean. This prolongation of particle retention should apply for all high latitude systems with surface melt water that lowers the salinity in the upper ocean. In the future the impact of this salinity-based retention will become of higher importance as the input of freshwater by melting ice is increasing, resulting in increasing salinity gradients. However, in a scenario where glaciers and sea-ice have fully retreated and freshwater supply is reduced, salinity-based retention might become neglectable.

Author contributions

The manuscript was written by LH and MHI. LH analyzed the data together with MHI. LH and CK processed the PELAGRA-CAM data. Sampling onboard was done by MHI.

Acknowledgments

Richard Lampitt and Sarah L. C. Giering are acknowledged for the work on board on the PELAGRA traps and the Red Camera Frame and providing the POC measurements of the PELAGRA trap. We thank the crew and captain of RSS Discovery for their assistance during the cruises. This study was supported by the Helmholtz Association, the Alfred Wegener Institute Helmholtz Centre for Polar and Marine Research and the DFG-Research Center/Cluster of Excellence “The Ocean Floor – Earth’s Uncharted Interface”: EXC-2077-390741603 at MARUM.

Supplementary information

Table S1: List of camera profiles with station, date, time, latitude and longitude.

Camera profile	Station	Date	Time (GMT)	Latitude (S)	Longitude (W)
RCF001	P3A	16. Nov	10:09	52 41.40	40 07.50
RCF002	P3A	16. Nov	14:00	52 41.40	40 07.50
RCF003	P3A	17. Nov	09:30	52 41.4	40 07.6
RCF004	P3A	17. Nov	15:36	52 41.5	40 08.0
RCF005	P3A	20. Nov	23:50	52 46.52	40 20.96
RCF006	P3A	21. Nov	00:44	52 46.52	40 20.96
RCF011	P3B-1	30. Nov	15:09	52 42.27	40 06.14
RCF012	P3B-1	30. Nov	16:16	52 42.27	40 06.14
RCF014	P3B-1	03. Dez	20:25	52 31.0	40 0.21
RCF015	P3B-1	03. Dez	21:22	52 31.0	40 0.21
RCF016	P3B-2	04. Dez	18:28	52 41.3	40 20.7
RCF017	P3B-2	04. Dez	22:32	52 43.24	40 19.57
RCF018	P3B-2	05. Dez	16:56	52 43.3	40 19.6
RCF019	P3B-2	05. Dez	17:38	52 43.3	40 19.6
RCF020	P3C	09. Dez	14:25	52 43.2	40 19.7
RCF021	P3C	10. Dez	13:14	52 41.7	40 19.4
RCF022	P3C	10. Dez	13:54	52 41.7	40 19.0
RCF023	P3C	11. Dez	13:30	52 43.0	40 14.3
RCF024	P3C	11. Dez	15:20	52 42.99	40 14.32
RCF025	P3C	12. Dez	19:48	52 38.8	40 12.6
RCF026	P3C	12. Dez	20:20	52 38.8	40 12.6

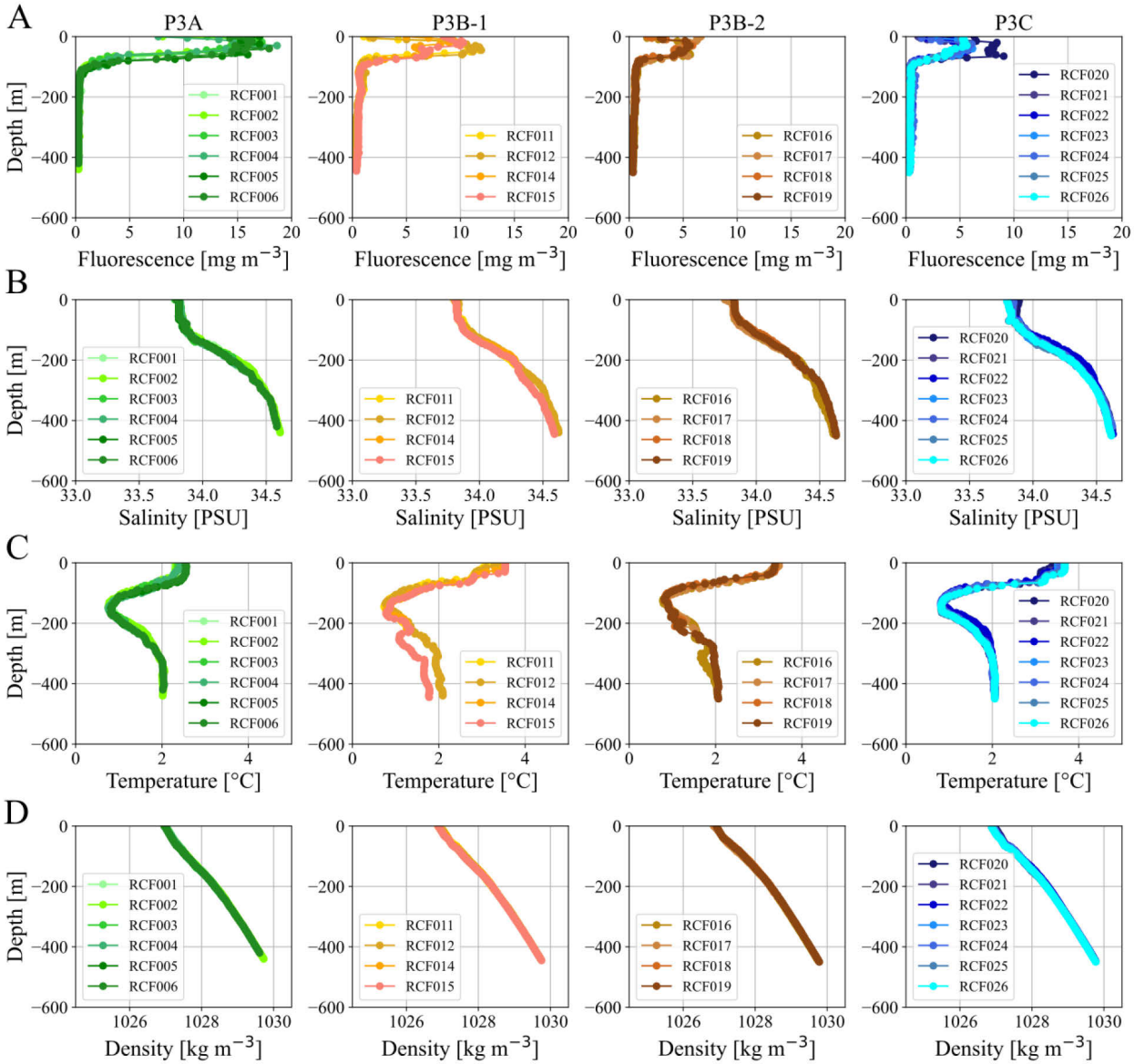

Fig. S1: Environmental conditions, including (A) fluorescence [mg m^{-3}], (B) salinity [PSU], (C) temperature [°C] and (D) density [kg m^{-3}] according to depth for all stations (P3A, P3B-1, P3B-2, P3C) with the respective profiles from the Red Camera Frame (RCF).

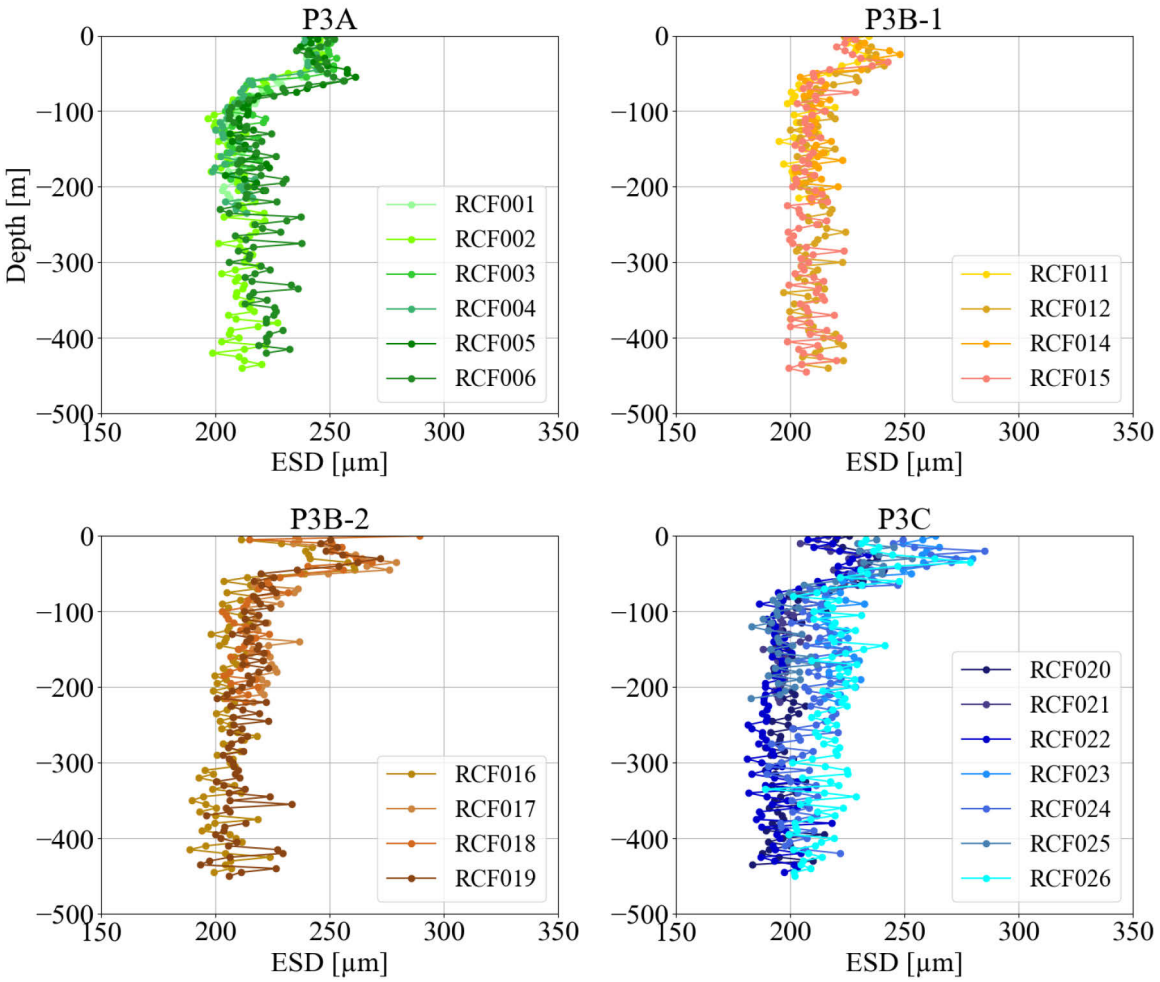

Fig. S2: Average equivalent spherical diameter (ESD) according to depth for all stations (P3A, P3B-1, P3B-2, P3C) with the respective profiles from the Red Camera Frame (RCF).

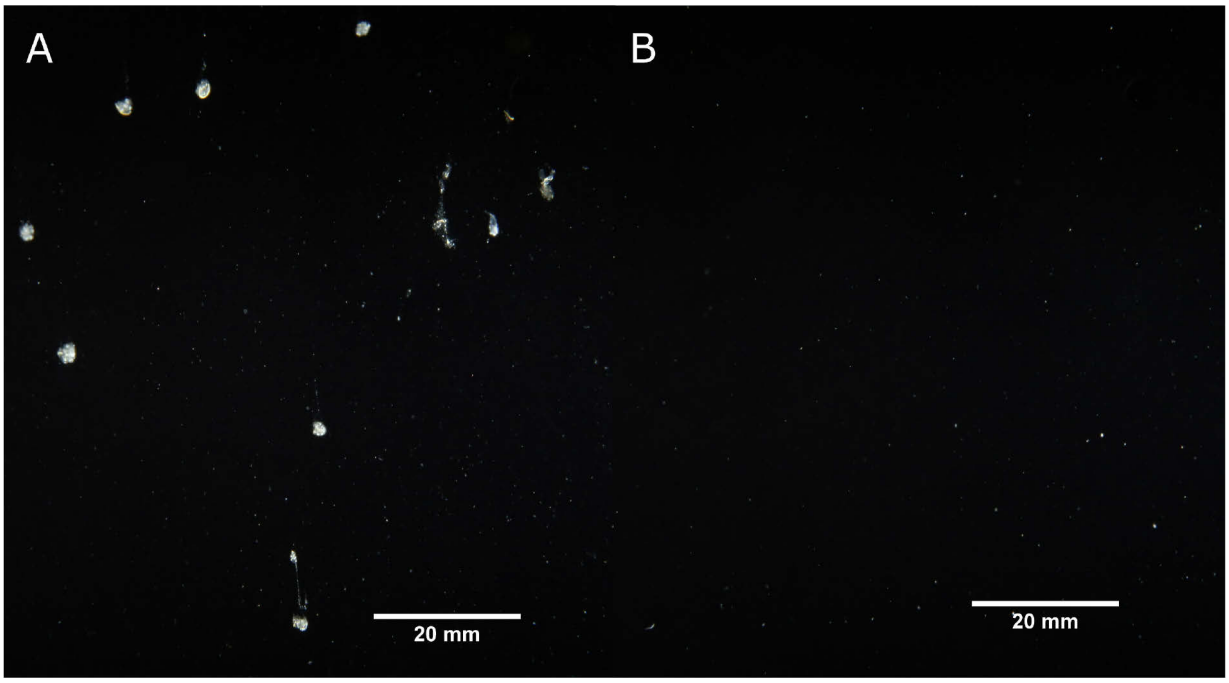

Fig. S3: Example picture of (A) a cluster of giant aggregates and (B) normal aggregates recorded by the Red Camera Frame (RCF). Aggregates sized > 2750 µm sank with sinking velocities of 430 ± 120 m d^{-1}.

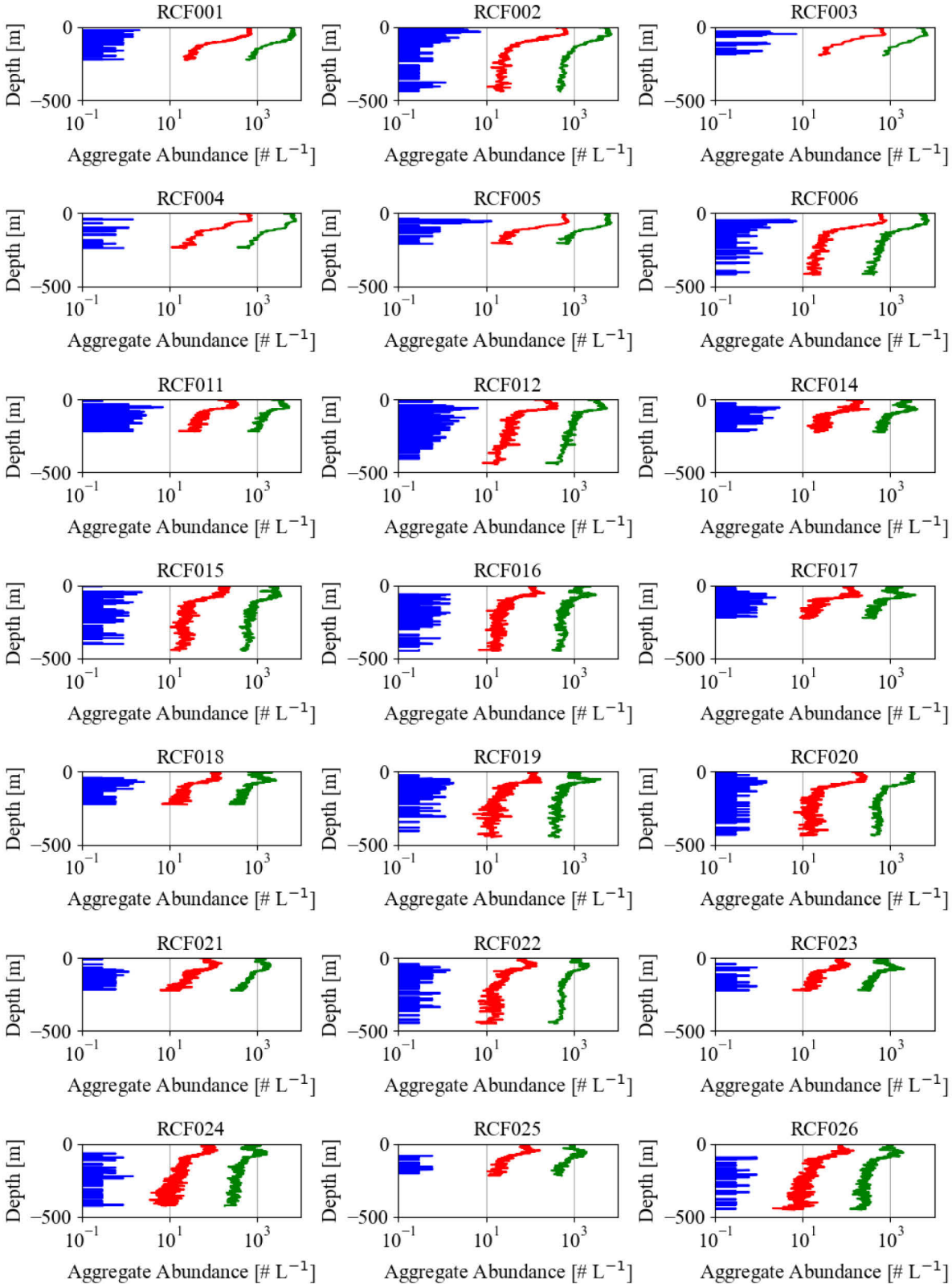

Fig. S4: Logarithmic scaled aggregate abundance [# L^{-1}] according to depth profiles from the Red Camera Frame (RCF) in 3 size groups according to binned equivalent spherical diameter: blue >2750 µm, red 530 - 2750 µm and green < 530 µm.

References

Alldredge, A. L., Cowles, T. J., MacIntyre, S., Rines, J. E. B., Donaghay, P. L., Greenlaw, C. F., Holliday, D. V., Dekshenieks, M. M., Sullivan, J. M., and Zaneveld, J. R. V. (2002). "Occurrence and mechanisms of formation of a dramatic thin layer of marine snow in a shallow Pacific fjord." *Marine Ecology Progress Series*, 233, 1-12.

Azetsu-Scott, K., and Passow, U. (2004). "Ascending marine particles: Significance of transparent exopolymer particles (TEP) in the upper ocean." *Limnology and Oceanography*, 49(3), 741-748.

Baker, C. A., Henson, S. A., Cavan, E. L., Giering, S. L. C., Yool, A., Gehlen, M., Belcher, A., Riley, J. S., Smith, H. E. K., and Sanders, R. (2017). "Slow-sinking particulate organic carbon in the Atlantic Ocean: Magnitude, flux, and potential controls." *Global Biogeochemical Cycles*, 31(7), 1051-1065.

Belcher, A., Iversen, M., Manno, C., Henson, S. A., Tarling, G. A., and Sanders, R. (2016). "The role of particle associated microbes in remineralization of fecal pellets in the upper mesopelagic of the Scotia Sea, Antarctica." *Limnology and Oceanography*, 61(3), 1049-1064.

Belcher, A., Tarling, G. A., Manno, C., Atkinson, A., Ward, P., Skaret, G., Fielding, S., Henson, S. A., and Sanders, R. (2017). "The potential role of Antarctic krill faecal pellets in efficient carbon export at the marginal ice zone of the South Orkney Islands in spring." *Polar Biology*, 40(10), 2001-2013.

Borrione, I., and Schlitzer, R. (2013). "Distribution and recurrence of phytoplankton blooms around South Georgia, Southern Ocean." *Biogeosciences*, 10(1), 217-231.

Boyd, P. W., Claustre, H., Levy, M., Siegel, D. A., and Weber, T. (2019). "Multi-faceted particle pumps drive carbon sequestration in the ocean." *Nature*, 568(7752), 327-335.

Briggs, N., Dall'Olmo, G., and Claustre, H. (2020). "Major role of particle fragmentation in regulating biological sequestration of CO_2 by the oceans." *Science*, 367(6479), 791-793.

Carranza, M. M., Gille, S. T., Franks, P. J. S., Johnson, K. S., Pinkel, R., and Girton, J. B. (2018). "When Mixed Layers Are Not Mixed. Storm-Driven Mixing and Bio-optical Vertical Gradients in Mixed Layers of the Southern Ocean." *Journal of Geophysical Research: Oceans*, 123(10), 7264-7289.

Christaki, U., Lefèvre, D., Georges, C., Colombet, J., Catala, P., Courties, C., Sime-Ngando, T., Blain, S., and Obernosterer, I. (2014). "Microbial food web dynamics during spring phytoplankton blooms in the naturally iron-fertilized Kerguelen area (Southern Ocean)." *Biogeosciences*, 11(23), 6739-6753.

Clements, D. J., Yang, S., Weber, T., McDonnell, A. M. P., Kiko, R., Stemmann, L., and Bianchi, D. (2023). "New Estimate of Organic Carbon Export From Optical Measurements Reveals the Role of Particle Size Distribution and Export Horizon." *Global Biogeochemical Cycles*, 37(3), e2022GB007633.

Cook, K. B., Belcher, A., Bondyale Juez, D., Stowasser, G., Fielding, S., Saunders, R. A., Elsafi, M. A., Wolff, G. A., Blackbird, S. J., Tarling, G. A., and Mayor, D. J. (2023). "Carbon budgets of Scotia Sea mesopelagic zooplankton and micronekton communities during austral spring." *Deep Sea Research Part II: Topical Studies in Oceanography*, 210, 105296.

De La Rocha, C. L., and Passow, U. (2007). "Factors influencing the sinking of POC and the efficiency of the biological carbon pump." *Deep Sea Research Part II: Topical Studies in Oceanography*, 54(5-7), 639-658.

Dekshenieks, M. M., Donaghay, P. L., Sullivan, J. M., Rines, J. E., Osborn, T. R., and Twardowski, M. S. (2001). "Temporal and spatial occurrence of thin phytoplankton layers in relation to physical processes." *Marine Ecology Progress Series*, 223, 61-71.

DeVries, T., and Weber, T. (2017). "The export and fate of organic matter in the ocean: New constraints from combining satellite and oceanographic tracer observations." *Global Biogeochemical Cycles*, 31(3), 535-555.

Dilling, L., and Alldredge, A. L. (2000). "Fragmentation of marine snow by swimming macrozooplankton: A new process impacting carbon cycling in the sea." *Deep Sea Research Part I: Oceanographic Research Papers*, 47(7), 1227-1245.

Ducklow, H. W., Steinberg, D. K., and Buesseler, K. O. (2001). "Upper Ocean Carbon Export and the Biological Pump." *Oceanography*, 14(4), 50-58.

Engel, A., and Schartau, M. (1999). "Influence of transparent exopolymer particles (TEP) on sinking velocity of Nitzschia closterium aggregates." *Marine Ecology Progress Series*, 182, 69-76.

Field, C. B., Behrenfeld, M. J., Randerson, J. T., and Falkowski, P. (1998). "Primary Production of the Biosphere: Integrating Terrestrial and Oceanic Components." *Science*, 281(5374), 237-240.

Gargett, A. E., Merryfield, W. J., and Holloway, G. (2003). "Direct Numerical Simulation of Differential Scalar Diffusion in Three-Dimensional Stratified Turbulence." *Journal of Physical Oceanography*, 33(8), 1758-1782.

Giering, S. L. C., Sanders, R., Blackbird, S., Briggs, N., Carvalho, F., East, H., Espinola, B., Henson, S. A., Kiriakoulakis, K., Iversen, M. H., Lampitt, R. S., Pabortsava, K., Pebody, C., Peel, K., Preece, C., Saw, K., Villa-Alfageme, M., and Wolff, G. A. (2023). "Vertical imbalance in organic carbon budgets is indicative of a missing vertical transfer during a phytoplankton bloom near South Georgia (COMICS)." *Deep Sea Research Part II: Topical Studies in Oceanography*, 209, 105277.

Guidi, L., Jackson, G. A., Stemmann, L., Miquel, J. C., Picheral, M., and Gorsky, G. (2008). "Relationship between particle size distribution and flux in the mesopelagic zone." *Deep Sea Research Part I: Oceanographic Research Papers*, 55(10), 1364-1374.

Hemsley, V., Füssel, J., Duret, M. T., Rayne, R. R., Iversen, M. H., Henson, S. A., Sanders, R., Lam, P., and Trimmer, M. (2023). "Suspended particles are hotspots of microbial remineralization in the ocean's twilight zone." *Deep Sea Research Part II: Topical Studies in Oceanography*, 212, 105339.

Henson, S. A., Sanders, R., Madsen, E., Morris, P. J., Le Moigne, F., and Quartly, G. D. (2011). "A reduced estimate of the strength of the ocean's biological carbon pump." *Geophysical Research Letters*, 38(4).

Henson, S. A., Sanders, R., and Madsen, E. (2012). "Global patterns in efficiency of particulate organic carbon export and transfer to the deep ocean." *Global Biogeochemical Cycles*, 26(1).

Henson, S. A., Yool, A., and Sanders, R. (2015). "Variability in efficiency of particulate organic carbon export: A model study." *Global Biogeochemical Cycles*, 29(1), 33-45.

Henson, S. A., Le Moigne, F., and Giering, S. (2019). "Drivers of Carbon Export Efficiency in the Global Ocean." *Global biogeochemical cycles*, 33(7), 891-903.

Henson, S. A., Briggs, N., Carvalho, F., Manno, C., Mignot, A., and Thomalla, S. (2023). "A seasonal transition in biological carbon pump efficiency in the northern Scotia Sea, Southern Ocean." *Deep Sea Research Part II: Topical Studies in Oceanography*, 208, 105274.

Iversen, M. H., and Ploug, H. (2010). "Ballast minerals and the sinking carbon flux in the ocean: carbon-specific respiration rates and sinking velocity of marine snow aggregates." *Biogeosciences*, 7(9), 2613-2624.

Iversen, M. H., Nowald, N., Ploug, H., Jackson, G. A., and Fischer, G. (2010). "High resolution profiles of vertical particulate organic matter export off Cape Blanc, Mauritania: Degradation processes and ballasting effects." *Deep Sea Research Part I: Oceanographic Research Papers*, 57(6), 771-784.

Iversen, M. H., and Ploug, H. (2013). "Temperature effects on carbon-specific respiration rate and sinking velocity of diatom aggregates – potential implications for deep ocean export processes." *Biogeosciences*, 10(6), 4073-4085.

Iversen, M. H., Pakhomov, E. A., Hunt, B. P., Van der Jagt, H., Wolf-Gladrow, D., and Klaas, C. (2017). "Sinkers or floaters? Contribution from salp pellets to the export flux during a large bloom event in the Southern Ocean." *Deep Sea Research Part II: Topical Studies in Oceanography*, 138, 116-125.

Iversen, M. H., and Lampitt, R. S. (2020). "Size does not matter after all: no evidence for a size-sinking relationship for marine snow." *Progress in Oceanography*, 189, 102445.

Iversen, M. H. (2023). "Carbon Export in the Ocean: A Biologist's Perspective." *Annual Review of Marine Science*, 15(1), 357-381.

Jackson, G. A., and Burd, A. B. (1998). "Aggregation in the Marine Environment." *Environmental Science & Technology*, 32(19), 2805-2814.

Jouandet, M. P., Blain, S., Metzl, N., Brunet, C., Trull, T. W., and Obernosterer, I. (2008). "A seasonal carbon budget for a naturally iron-fertilized bloom over the Kerguelen Plateau in the Southern Ocean." *Deep Sea Research Part II: Topical Studies in Oceanography*, 55(5), 856-867.

Kemp, A. E. S., Pike, J., Pearce, R. B., and Lange, C. B. (2000). "The “Fall dump” — a new perspective on the role of a “shade flora” in the annual cycle of diatom production and export flux." *Deep Sea Research Part II: Topical Studies in Oceanography*, 47(9), 2129-2154.

Kindler, K., Khalili, A., and Stocker, R. (2010). "Diffusion-limited retention of porous particles at density interfaces." *Proceedings of the National Academy of Sciences*, 107(51), 22163-22168.

Korb, R. E., and Whitehouse, M. (2004). "Contrasting primary production regimes around South Georgia, Southern Ocean: large blooms versus high nutrient, low chlorophyll waters." *Deep Sea Research Part I: Oceanographic Research Papers*, 51(5), 721-738.

Korb, R. E., Whitehouse, M. J., and Ward, P. (2004). "SeaWiFS in the southern ocean: spatial and temporal variability in phytoplankton biomass around South Georgia." *Deep Sea Research Part II: Topical Studies in Oceanography*, 51(1-3), 99-116.

Korb, R. E., Whitehouse, M. J., Atkinson, A., and Thorpe, S. E. (2008). "Magnitude and maintenance of the phytoplankton bloom at South Georgia: a naturally iron-replete environment." *Marine Ecology Progress Series*, 368, 75-91.

Kwon, E. Y., Primeau, F., and Sarmiento, J. L. (2009). "The impact of remineralization depth on the air–sea carbon balance." *Nature Geoscience*, 2(9), 630-635.

Lalande, C., Bauerfeind, E., and Nöthig, E.-M. (2011). "Downward particulate organic carbon export at high temporal resolution in the eastern Fram Strait: influence of Atlantic Water on flux composition." *Marine Ecology Progress Series*, 440, 127-136.

Lampitt, R. S., Boorman, B., Brown, L., Lucas, M., Salter, I., Sanders, R., Saw, K., Seeyave, S., Thomalla, S. J., and Turnewitsch, R. (2008). "Particle export from the euphotic zone: Estimates using a novel drifting sediment trap, ^{234}Th and new production." *Deep Sea Research Part I: Oceanographic Research Papers*, 55(11), 1484-1502.

Laurenceau-Cornec, E. C., Trull, T. W., Davies, D. M., Bray, S. G., Doran, J., Planchon, F., Carlotti, F., Jouandet, M.-P., Cavagna, A.-J., Waite, A. M., and Blain, S. (2015). "The relative importance of phytoplankton aggregates and zooplankton fecal pellets to carbon export: insights from free-drifting sediment trap deployments in naturally iron-fertilised waters near the Kerguelen Plateau." *Biogeosciences*, 12(4), 1007-1027.

Laws, E. A., Falkowski, P. G., Smith Jr., W. O., Ducklow, H., and McCarthy, J. J. (2000). "Temperature effects on export production in the open ocean." *Global Biogeochemical Cycles*, 14(4), 1231-1246.

MacIntyre, S., Alldredge, A. L., and Gotschalk, C. C. (1995). "Accumulation of marines now at density discontinuities in the water column." *Limnology and Oceanography*, 40(3), 449-468.

Maiti, K., Charette, M. A., Buesseler, K. O., and Kahru, M. (2013). "An inverse relationship between production and export efficiency in the Southern Ocean." *Geophysical Research Letters*, 40(8), 1557-1561.

Manno, C., Stowasser, G., Enderlein, P., Fielding, S., and Tarling, G. A. (2015). "The contribution of zooplankton faecal pellets to deep-carbon transport in the Scotia Sea (Southern Ocean)." *Biogeosciences*, 12(6), 1955-1965.

Manno, C., Stowasser, G., Fielding, S., Apeland, B., and Tarling, G. A. (2022). "Deep carbon export peaks are driven by different biological pathways during the extended Scotia Sea (Southern Ocean) bloom." *Deep Sea Research Part II: Topical Studies in Oceanography*, 205, 105183.

Mari, X., Passow, U., Migon, C., Burd, A. B., and Legendre, L. (2017). "Transparent exopolymer particles: Effects on carbon cycling in the ocean." *Progress in Oceanography*, 151, 13-37.

Markussen, T. N., Konrad, C., Waldmann, C., Becker, M., Fischer, G., and Iversen, M. H. (2020). "Tracks in the Snow – Advantage of Combining Optical Methods to Characterize Marine Particles and Aggregates." *Frontiers in Marine Science*, 7, 476.

Nowicki, M., DeVries, T., and Siegel, D. A. (2022). "Quantifying the Carbon Export and Sequestration Pathways of the Ocean's Biological Carbon Pump." *Global Biogeochemical Cycles*, 36(3), e2021GB007083.

Obernosterer, I., Christaki, U., Lefèvre, D., Catala, P., Van Wambeke, F., and Lebaron, P. (2008). "Rapid bacterial mineralization of organic carbon produced during a phytoplankton bloom induced by natural iron fertilization in the Southern Ocean." *Deep Sea Research Part II: Topical Studies in Oceanography*, 55(5-7), 777-789.

Parslow, J. S., Boyd, P. W., Rintoul, S. R., and Griffiths, F. B. (2001). "A persistent subsurface chlorophyll maximum in the Interpolar Frontal Zone south of Australia: Seasonal progression and implications for phytoplankton-light-nutrient interactions." *Journal of Geophysical Research: Oceans*, 106(C12), 31543-31557.

Pauli, N.-C., Flintrop, C. M., Konrad, C., Pakhomov, E. A., Swoboda, S., Koch, F., Wang, X.-L., Zhang, J.-C., Brierley, A. S., Bernasconi, M., Meyer, B., and Iversen, M. H. (2021). "Krill and salp faecal pellets contribute equally to the carbon flux at the Antarctic Peninsula." *Nature Communications*, 12(1), 7168.

Ploug, H., Iversen, M. H., and Fischer, G. (2008). "Ballast, sinking velocity, and apparent diffusivity within marine snow and zooplankton fecal pellets: Implications for substrate turnover by attached bacteria." *Limnology and Oceanography*, 53(5), 1878-1886.

Prairie, J. C., Ziervogel, K., Arnosti, C., Camassa, R., Falcon, C., Khatri, S., McLaughlin, R. M., White, B. L., and Yu, S. (2013). "Delayed settling of marine snow at sharp density transitions driven by fluid entrainment and diffusion-limited retention." *Marine Ecology Progress Series*, 487, 185-200.

Prairie, J. C., Ziervogel, K., Camassa, R., McLaughlin, R. M., White, B. L., Dewald, C., and Arnosti, C. (2015). "Delayed settling of marine snow: Effects of density gradient and particle properties and implications for carbon cycling." *Marine Chemistry*, 175, 28-38.

RCoreTeam. (2019). "R: A language and environment for statistical computing. R Foundation for statistical computing, Vienna, Austria. URL https://www.R-project.org/.".

Rembauville, M., Blain, S., Armand, L., Quéguiner, B., and Salter, I. (2015a). "Export fluxes in a naturally iron-fertilized area of the Southern Ocean – Part 2: Importance of diatom resting spores and faecal pellets for export." *Biogeosciences*, 12(11), 3171-3195.

Rembauville, M., Salter, I., Leblond, N., Gueneugues, A., and Blain, S. (2015b). "Export fluxes in a naturally iron-fertilized area of the Southern Ocean – Part 1: Seasonal dynamics of particulate organic carbon export from a moored sediment trap." *Biogeosciences*, 12(11), 3153-3170.

Rembauville, M., Manno, C., Tarling, G. A., Blain, S., and Salter, I. (2016). "Strong contribution of diatom resting spores to deep-sea carbon transfer in naturally iron-fertilized waters downstream of South Georgia." *Deep Sea Research Part I: Oceanographic Research Papers*, 115, 22-35.

Rigual-Hernández, A. S., Trull, T. W., Bray, S. G., Closset, I., and Armand, L. K. (2015). "Seasonal dynamics in diatom and particulate export fluxes to the deep sea in the Australian sector of the southern Antarctic Zone." *Journal of Marine Systems*, 142, 62-74.

Salter, I., Lampitt, R. S., Sanders, R., Poulton, A., Kemp, A. E. S., Boorman, B., Saw, K., and Pearce, R. (2007). "Estimating carbon, silica and diatom export from a naturally fertilised phytoplankton bloom in the Southern Ocean using PELAGRA: A novel drifting sediment trap." *Deep Sea Research Part II: Topical Studies in Oceanography*, 54(18-20), 2233-2259.

Salter, I., Kemp, A. E. S., Moore, C. M., Lampitt, R. S., Wolff, G. A., and Holtvoeth, J. (2012). "Diatom resting spore ecology drives enhanced carbon export from a naturally iron-fertilized bloom in the Southern Ocean." *Global Biogeochemical Cycles*, 26(1).

Sanders, R. J., Henson, S. A., Martin, A. P., Anderson, T. R., Bernardello, R., Enderlein, P., Fielding, S., Giering, S. L. C., Hartmann, M., Iversen, M., Khatiwala, S., Lam, P., Lampitt, R., Mayor, D. J., Moore, M. C., Murphy, E., Painter, S. C., Poulton, A. J., Saw, K., Stowasser, G., Tarling, G. A., Torres-Valdes, S., Trimmer, M., Wolff, G. A., Yool, A., and Zubkov, M. (2016). "Controls over Ocean Mesopelagic Interior Carbon Storage (COMICS): Fieldwork, Synthesis, and Modeling Efforts." *Frontiers in Marine Science*, 3.

Saw, K., Boorman, B., Lampitt, R., and Sanders, R. (2004). "PELAGRA: early development of an autonomous, neutrally buoyant sediment trap." *Institute of Marine Engineering, Science and Technology*.

Schlitzer, R. (2002). "Carbon export fluxes in the Southern Ocean: results from inverse modeling and comparison with satellite-based estimates." *Deep Sea Research Part II: Topical Studies in Oceanography*, 49(9), 1623-1644.

Schnetzer, A., and Steinberg, D. K. (2002). "Active transport of particulate organic carbon and nitrogen by vertically migrating zooplankton in the Sargasso Sea." *Marine Ecology Progress Series*, 234, 71-84.

Siegel, D. A., Buesseler, K. O., Doney, S. C., Sailley, S. F., Behrenfeld, M. J., and Boyd, P. W. (2014). "Global assessment of ocean carbon export by combining satellite observations and food-web models." *Global Biogeochemical Cycles*, 28(3), 181-196.

Steinberg, D. K., Carlson, C. A., Bates, N. R., Goldthwait, S. A., Madin, L. P., and Michaels, A. F. (2000). "Zooplankton vertical migration and the active transport of dissolved organic and inorganic carbon in the Sargasso Sea." *Deep Sea Research Part I: Oceanographic Research Papers*, 47(1), 137-158.

Stemmann, L., Jackson, G. A., and Gorsky, G. (2004). "A vertical model of particle size distributions and fluxes in the midwater column that includes biological and physical processes—Part II: application to a three year survey in the NW Mediterranean Sea." *Deep Sea Research Part I: Oceanographic Research Papers*, 51(7), 885-908.

Thiele, S., Fuchs, B. M., Amann, R., and Iversen, M. H. (2015). "Colonization in the Photic Zone and Subsequent Changes during Sinking Determine Bacterial Community Composition in Marine Snow." *Applied and Environmental Microbiology*, 81(4), 1463-1471.

Tripathy, S. C., Pavithran, S., Sabu, P., Pillai, H. U. K., Dessai, D. R. G., and Anilkumar, N. (2015). "Deep chlorophyll maximum and primary productivity in Indian Ocean sector of the Southern Ocean: Case study in the Subtropical and Polar Front during austral summer 2011." *Deep Sea Research Part II: Topical Studies in Oceanography*, 118, 240-249.

Turner, J. T. (2002). "Zooplankton fecal pellets, marine snow and sinking phytoplankton blooms." *Aquatic Microbial Ecology*, 27(1), 57-102.

Turner, J. T. (2015). "Zooplankton fecal pellets, marine snow, phytodetritus and the ocean's biological pump." *Progress in Oceanography*, 130, 205-248.

Volk, T., and Hoffert, M. I. (1985). "Ocean Carbon Pumps: Analysis of Relative Strengths and Efficiencies in Ocean-Driven Atmospheric CO_2 Changes." *The Carbon Cycle and Atmospheric CO_2: Natural Variations Archean to Present*, 32, 99-110.

Wassmann, P. (1997). "Retention versus export food chains: processes controlling sinking loss from marine pelagic systems." *Hydrobiologia*, 363(1-3), 29-57.

Chapter III: Carbon export in an Arctic frontal system in Fram Strait

Lili Hufnagel[1,2], Simon Ramondenc[2], Christian Konrad[2], Wilken-Jon von Appen[2], Zerlina Hofmann[2], Sinhué Torres Valdés[2], Jacqueline Stefels[3], Nasrollah Moradi[2], Astrid Bracher[2,4], Anya Waite[5] and Morten H. Iversen[1, 2]

[1] University of Bremen, MARUM - Center for Marine Environmental Sciences and Faculty of Geosciences, Bremen, Germany

[2] Alfred Wegener Institute for Polar and Marine Research, Bremerhaven, Germany

[3] Groningen Institute for Evolutionary Life Sciences, University of Groningen, Groningen, Netherlands

[4] Institute of Environmental Physics, Department of Physics and Electrical Engineering, University of Bremen, Bremen, Germany

[5] Department of Oceanography, Ocean Frontier Institute, Dalhousie University, Halifax, Canada

Keywords: marginal ice zone, submesoscale front, subduction, carbon export, minerals

Abstract

Recent studies show high carbon export efficiencies in Arctic regions with seasonal sea ice compared to ice-free regions. However, the mechanisms that are responsible for this enhanced export are still unclear. In the marginal ice zone (MIZ), the area between pack ice and open ocean, eddies and filaments frequently develop. To gain insight into the prevailing carbon export mechanisms associated with such fronts, we combined direct *in situ* observations of export processes and physical oceanographic conditions, using free-drifting sediment traps, Marine Snow Catchers and *in situ* optics during an expedition to Fram Strait in July 2020. Dense Atlantic Water (AW) met lighter surface meltwater and Polar Water (PW) at the MIZ and was subducted. The interaction of the water masses structured the biogeochemical and biological processes in the front system, determining the magnitude of chlorophyll and primary production, the zooplankton abundances, the microbial respiration, and the size-distribution, abundance and characteristics of aggregates. We observed enhanced aggregate formation and occasionally high particle abundances at depths below 65 m, likely caused by the subduction of chlorophyll-rich AW. The majority of the aggregates were formed from diatoms and ballasted by the silica-rich diatom frustules. However, aggregates formed in ice-associated PW also could be ballasted by cryo-minerals, which resulted in significantly higher sinking velocities compared to diatom aggregates. High carbon flux occurred in the AW and at the front, implying that increasing Atlantification and broadening of the MIZ may lead to enhanced carbon export in subduction zones near melting sea ice edges. The observed processes are expected to become increasingly important for larger areas of the Arctic, as sea ice retreats due to climate change.

Introduction

The Arctic is strongly subjected to anthropogenic climate change, which impacts the Arctic ecosystems, biogeochemistry, carbon export, and sequestration. Sea ice extent is declining under climate change (Parkinson and DiGirolamo 2021), which is affecting all connected biological processes. It has been shown that there is an increasing carbon flux with decreasing distance to sea ice, suggesting that in Arctic regions with seasonal sea ice cover carbon export is higher compared to ice-free regions (Fadeev et al. 2021a). The export efficiency in ice-covered regions is very high, especially during export events such as release and sedimentation of ice algae (Arrigo et al. 2012; Boetius et al. 2013). Thinning of sea ice and increased light penetration has been suggested to enhance primary production and ice-algae carbon export (Arrigo et al. 2012; Boetius et al. 2013), at least in the short term until sea ice has retreated in the Arctic. Nevertheless, enhanced stratification by sea ice melt is slowing the carbon export via the biological carbon pump (von Appen et al. 2021).

On the other hand, increasing warming and intrusion of Atlantic Water (AW) in the Arctic may lead to a shift in seasonal zooplankton distribution and a community change towards Atlantic species (Neukermans et al. 2018; Ramondenc et al. 2023), as it is already observed with increasing occurrence of the haptophyte *Phaeocystis* (Nöthig et al. 2015). Less carbon is exported in *Phaeocystis*-dominated regions, with smaller aggregates than in ice-covered diatom-dominated regions (Fadeev et al. 2021a). Slower sinking velocities of the non-ballasted *Phaeocystis* aggregates allow more time for microbial degradation and remineralization at shallow depths compared to faster settling diatom-dominated aggregates, weakening pelagic-benthic coupling and export efficiency (Fadeev et al. 2021a; Reigstad and Wassmann 2007). Thus, it is crucial to understand how future sea ice conditions will impact the Arctic ecosystem and carbon sequestration.

The marginal ice zone (MIZ), i.e. the region where sea ice meets the open ocean and the surface ocean is impacted by meltwater, is narrowing during the cold season, while it is widening in the warm season (Strong and Rigor 2013). In the past decades, the MIZ experienced a 39% widening in summer (Strong and Rigor 2013). In the MIZ in Fram Strait, especially in areas with ice concentration below 20%, submesoscale or mesoscale eddies occur frequently (Kozlov and Atadzhanova 2021). In this region, denser and warmer AW is subducted below the lighter and fresher Polar Water (PW), which is possibly connected to eddy processes (Hattermann et al. 2016). These subduction processes can transport organic material, including slow-sinking and suspended particles to depth and enhance the carbon export and export efficiency (Boyd et al. 2019; Omand et al. 2015). Additionally, the vertical mixing in Fram

Strait can also resupply nutrients and enhance primary production (Mahadevan 2016; Tippenhauer et al. 2021).

Submesoscale or mesoscale eddies can result in the formation of frontal filaments. One of such submesoscale Arctic frontal filaments was first investigated in summer 2017 (Fadeev et al. 2021b; von Appen et al. 2018). The filament was characterized by density anomalies down to 400 m depth, pointing towards possible deep effects of the front on biological processes (von Appen et al. 2018). The submesoscale mixing process resulted in high primary productivity and carbon export (Fadeev et al. 2021b). Within just a few kilometers distance, the microbial community and the observed biogeochemistry varied in the different water masses (Fadeev et al. 2021b). Due to limited time spent at the frontal filament, the processes responsible for the carbon export were not fully determined in the study and the effect of meltwater and ice coverage was not quantified.

To address these largely uninvestigated processes, we targeted a frontal system in the MIZ in Fram Strait. The aim was to assess the carbon export, export mechanisms, and export efficiency in the front and their relation to the physical oceanographic processes (e.g. advection and subduction). Water masses showed differences in biological characteristics, e.g. phytoplankton concentration, zooplankton abundances, microbial respiration, carbon export, the abundance of aggregates and aggregate characteristics. Using free-drifting sediment traps, Marine Snow Catchers (MSCs), *in situ* optics, and water mass properties, we identified the dominating export mechanism in the frontal zone.

Materials and methods

Sampling region and physical oceanographic conditions

In Fram Strait, warm and salty Atlantic Water (AW) in the West Spitsbergen Current (WSC) is flowing northward (Aagaard et al. 1987; Beszczynska-Möller et al. 2012), while cold and fresher Polar Water (PW) in the East Greenland Current (EGC) is flowing southward (Håvik et al. 2017). The two water masses meet in central Fram Strait, mostly due to recirculating AW (Hofmann et al. 2021). This results in the development of density fronts between PW and AW in the marginal ice zone (MIZ). During the cruise MSM93 of RV *Maria S. Merian* in July 2020, a front system at the ice edge in the MIZ in Fram Strait was targeted (Fig. 1 A). The surface meltwater was characterized by temperatures between 0.5 and 2°C and salinities of < 33.3 PSU (Hofmann et al. 2024). The PW had temperatures between -2 and 0°C and salinities between 33.7 and 34.4 PSU, the AW had temperatures between 3 and 5°C and salinities of > 34.5 PSU (Hofmann et al. 2024).

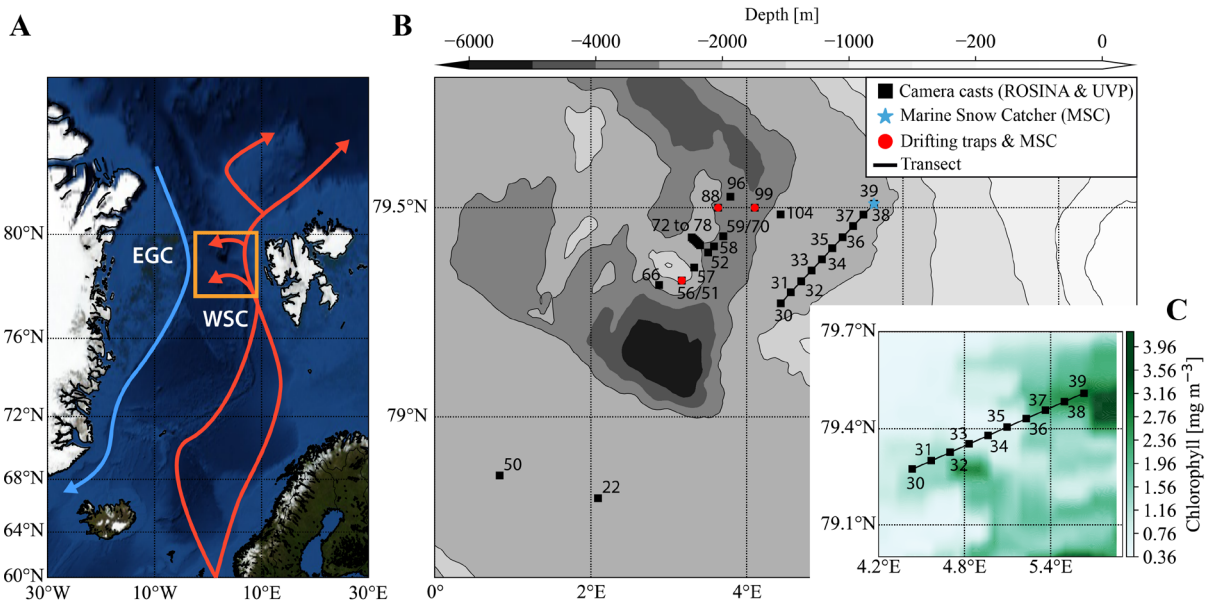

Fig. 1: (A) Map with study region (orange square) showing the West Spitsbergen Current (WSC, red) and the East Greenland Current (EGC, blue), (B) map of sampling stations of camera, Marine Snow Catcher and drifting traps, with shading showing bathymetry, and (C) surface daily mean chlorophyll a (Chla) distribution [mg m^{-3}] based on Aqua MODIS in the environs of the camera transect (Station 30 - 39).

Particle cameras together with a CTD were deployed at 29 stations (Fig. 1 B), including a camera transect (Station 30 – 39, 7th of July 2020) of 36 km (Fig. 1 C), to investigate particle dynamics in the frontal system in relation to the water mass velocity fields (vessel-mounted

Acoustic Doppler Current Profiler (ADCP) data), satellite data, and the physical oceanographic conditions described in Hofmann et al., 2024. Data processing for the vessel-mounted ADCP (75 kHz Teledyne RDI) is described by Hofmann et al., 2024. To get an overview of the distribution of the chlorophyll-rich water masses in the camera transect, chlorophyll a (Chla) concentrations were extracted from the daily mean Chla data set (Hu et al. 2012) based on the Aqua MODIS (Moderate Resolution Imaging Spectroradiometer sensor, available at https://oceandata.sci.gsfc.nasa.gov) satellite data. The data had a 4 km spatial resolution and was recorded on the 6th of July 2020, one day prior to sampling, as no data was available on the 7th due to cloud coverage.

Vertical particle distributions and morphological particle classification

Vertical profiles of particle size-distribution and abundance (i.e. aggregate profiles) were recorded with *in situ* camera systems. These consisted of an underwater vision profiler UVP5 (Picheral et al. 2010) and a "remotely observing *in situ* camera for aggregates" system (ROSINA), which were mounted together on one frame and were lowered with a speed of 0.3 m s^{-1}. The UVP was used to determine zooplankton abundances in the camera transect. The ROSINA system was used for the determination of particle abundances and properties in the water column. The ROSINA camera system includes a 29 MPixel camera (SVS-Vistek) and a Canon EF 60mm f/2.8 Macro USM lens with an image acquisition rate of 2 pictures per second. The light source was a custom-made background light source with a reflective light source (Falcon Illumination, Kronemeyer LED Driver). A CTD (Idronaut OceanSeven 310) with optical oxygen sensor, Seapoint Turbidity Meter, and a Seapoint Chlorophyll Fluorometer was attached to the camera system. At some stations, the implemented CTD had a system failure and we used the pressure sensor of the UVP for depth calibration and data from rosette CTD for the environmental conditions, when available.

The field of view was 64.116 x 42.744 mm (Length x Width, 6576 x 4384 pixels) with a depth of field of 30 mm resulting in a sampling volume of 82.2 mL. The pixel size in the acquired images of the ROSINA camera system was 9.75 µm pixel^{-1}. The images were processed with an OpenCV image processing software. A reference image was calculated by averaging all images in a downcast and used to subtract image artefacts. A threshold binary with subsequent erosion and dilation was used on the images. The program searched for particle contours (minimum particle size = 5 pixel) and determined the particle parameters. The image parameters were calculated according to Trudnowska et al. 2021, including e.g. area, equivalent spherical diameter (ESD), volume, circularity, elongation, mean grey value (Table S1 in the supplementary information). Zooplankton images of the UVP were sorted using the EcoTaxa

web application (Picheral et al. 2017) in larger taxonomic groups such as copepoda, ostracoda, chaetognatha, amphipoda, mullusca, annelida, cnidaria, detritus, and fibers.

Biogeochemistry

To collect settling aggregates, an array of free-drifting surface-tethered sediment traps was deployed three times, targeting the AW, the PW, and the front. The free-drifting sediment traps were deployed for a duration of between 12 to 21 h and were equipped with a surface buoy, 18 buoyancy spheres serving as wave-breakers, two 25 L buoyancy spheres and a positioning system. Three sediment trap stations were vertically deployed at 100 m, 200 m and 400 m depth, respectively, with four collection tubes at each collection depth. Filtered seawater was added in the collection tubes prior to the deployment with additional NaCl to increase the salinity by about 3 PSU. One trap tube per depth contained a gel trap with an ethanol-based viscous cryo-gel (Tissue-Tek, O.C.T.^{TM} COMPOUND, Sakura) that preserved the structure, shape, and size of the fragile settling particles and aggregates for microscopic analysis. The remaining three of the trap tubes collected the sinking material that was used for subsequent biogeochemical analyses. One of these trap tubes was fixed with $HgCl_2$ and used for bulk biogeochemical analyses. The remaining two trap tubes were frozen at -20 °C and stored for future analyses.

The collection tubes contained high densities of suspended *Phaeocystis* colonies, which were likely artefacts entering the collection tube during the deployment or recovery, as neither camera or pigment data (Astrid Bracher, pers. comm.) indicated an occurrence of *Phaeocystis* at 100 m depth or deeper. The *Phaeocystis* colonies were collected and excluded from biogeochemical flux calculations. The fast-settling material was collected at the bottom of the trap tube and was analyzed for total particulate mass (TPM), particulate organic carbon (POC), particulate organic nitrogen (PON), particulate inorganic carbon (PIC), and biogenic silica (bSi). For POC, PON and PIC measurements, material was filtered onto GF/F filters (Whatman, 25 mm), dried at 50°C for 24 h and weighed. For POC measurements, the filters were fumed with 37% HCl for 24 h and dried again at 50°C for 24 h. The filters were analyzed with a GC elemental analyser (EuroEA Elemental Analyser, HEKAtech). The PIC content was calculated by subtracting the carbon measured on the fumed filter (i.e. the GF/F filter prepared for POC) from the non-fumed filter. For bSi, the material from the collection tubes was filtered onto cellulose acetate 0.8 μm filters (Sartorius, 25 mm), dried, processed by wet-alkaline digestion and spectrometrically determined (Bodungen et al. 1991). All biogeochemical measurements were normalized by the area and deployment time.

Lithogenic fluxes where calculated with the following equation:

$$\text{lithogenic fluxes } [\text{mg m}^{-2}\ \text{d}^{-1}] = \text{TPM} - \text{CaCO}_3 - \text{SiO}_2 - 2\ \text{POC}$$
$$= \text{TPM} - \frac{60}{28}\ \text{bSi} - \frac{100}{12}\ \text{PIC} - 2\ \text{POC}$$

Water sampling for nutrients, microscopic plankton community assessments and primary production

A CTD (SBE11plus, Sea-Bird Scientific) was deployed to measure temperature, salinity, chlorophyll a fluorescence, turbidity and dissolved oxygen. On the CTD rosette, 24 Niskin bottles each with a volume of 10 L were mounted to collect water samples for nutrient analysis at six to eight different water depths. Ammonium concentrations were measured on board with the standard fluorometric method (Holmes et al. 1999). 50 mL water samples were frozen at -20 °C for nutrient analysis and measured at the home laboratory. The nutrients (nitrate, nitrite, phosphate, silicate) were analyzed using a QuAAtro Seal Analytical Continuous Segmented Flow Autoanalysers following colorimetric techniques (Aminot and Kérouel 2007; Aminot et al. 2009; Grasshoff et al. 2009; Kirkwood 1996) and GO-SHIP best practices (Becker et al. 2020; Hydes et al. 2010).

Additionally, a microscopic assessment of phytoplankton and microzooplankton was done onboard. For this, 50 mL water samples were taken from the Chla maximum depth and the settled material was analyzed under a light microscope semi-quantitatively.

Primary production was measured at each free-drifting sediment trap deployment. With the Niskin bottle rosette sampler, water from 10 m, 25 m, 50 m and 75 m was collected and 1 - 1.2 L were filled airtight into PE bottles. One light and one dark bottle were labeled with stable carbon-13 isotopes ($NaH^{13}CO_3$) for each depth, attached to the drifting traps at the corresponding depths and were incubated during the deployment of the free-drifting trap array. Dissolved inorganic carbon (DIC) samples were taken from each of the bottles prepared for primary production and fixed with $HgCl_2$ and stored in Exetainer® vials (Labco, 12 mL) to measure the labeling concentration, before deployment and after recovery. The DIC samples were analyzed on a Picarro G2101-i equipped with a custom-built purge system for total DIC measurements in the home laboratory. After recovery, the remaining bottle content was filtered onto GF/F filters (Whatman, 47 mm) for POC analysis. The filters were dried at 50°C for 24 h, fumed with 37% HCl for 24 h and dried again at 50°C for 24 h. A quarter of each fumigated and dried filter was measured with a combustion module attached to a cavity ring-down spectroscopy analyser (CM-CRDS, with a Picarro G2101-i Analyzer).

The gross specific primary production rate (μ_{POC}, d^{-1}) was derived from the Mass-Ratio Progress model for DMSP production (Stefels et al. 2009):

$$\mu_{POC} = \frac{\ln(\frac{\%^{13}C\ DIC - \%^{13}C\ POC_{start}}{\%^{13}C\ DIC - \%^{13}C\ POC_{end}})}{t}$$

using the label ratio of ^{13}C in the dissolved inorganic carbon in the incubation *($\%^{13}C\ DIC$)*, the ratio of ^{13}C in the POC at the start of the incubation *($\%^{13}C\ POC_{start}$)*, the ratio of ^{13}C in the POC at the end of the incubation *($\%^{13}C\ POC_{end}$)* and time (*t*, d). Then, the primary production (*PP*, mgC m^{-3} d^{-1}) in the incubations was calculated by multiplying the POC concentration (POC_{conc}, mgC m^{-3}) in the water by the gross specific growth rate (μPOC, d^{-1}).

To calculate the total primary production in the euphotic zone, we used depth profiles of photosynthetically active radiation (PAR), since there was no clear mixed layer in the frontal system. The PAR profiles have been obtained from the integral over depth resolved hyperspectral downwelling irradiance spectra measured by a radiometers (RAMSES ACC-2-VIS, TriOS GmbH, Germany) covering a wavelength range of 320 nm to 950 nm with an optical resolution of 3.3 nm and a spectral accuracy of 0.3 nm installed on a light profiler and lowered until 100 m at CTD stations (Bracher et al. 2020). We fitted a logarithmic function through the measured primary production rate (mgC m^{-3} d^{-1}) as a function of the percentage of PAR at the corresponding depth [%] and used this function to calculated the primary production stepwise in 5 m steps between 5 – 70 m. We summed the calculated step-wise primary production to get the total primary production of the photic zone (mgC m^{-2} d^{-1}).

Sinking velocities and respiration

To collect newly formed aggregates from the Chla maximum layer, a Marine Snow Catcher (MSC) were deployed at approximately 10 m below this maximum, targeting the AW, the PW and the front. After recovery, the MSC was left standing on deck for a few hours so that the aggregates could settle to the bottom. The aggregates were recovered with a wide bore pipette from the bottom part after the water was drained from the MSC. The aggregates were transferred to a modified vertical flow chamber (Ploug and Jørgensen 1999) where the size, the sinking velocities and, for a selection of aggregates, also the microbial respiration rate were measured. The microbial respiration rate was measured with an O_2 microsensor (Unisense, Denmark) at a standard of 3.5 °C and calculated according to Moradi et al. 2021 using the correction terms for spheres (Moradi et al. 2018). A few exemplary aggregates were photographed to document the composition. According to size and type (fecal pellets, mucous

aggregates and aggregates containing minerals), the aggregates were pooled and filtered on GF/F filter (Whatman, 25 mm) to determine dry weight, POC and PON (see *Biogeochemistry* section for methods).

To estimate the potential carbon specific degradation rate according to the loss of POC in the water column, first the POC start concentration (POC_{conc}, mgC m^{-3}) was calculated at 15 m, 100 m and 200 m depth for the AW, the PW and the front:

$$POC_{conc} = \frac{F}{w_{av}}$$

where F represents the POC flux (F, mgC m^{-2} d^{-1}) and w_{av} the average sinking velocities of sinking aggregates (w_{av}, m d^{-1}).

The POC loss (POC_{loss}, mgC m^{-3} d^{-1}) was calculated as the negative quotient of the difference in POC flux and in depth (z, m) of 15 m to 100 m, 100 m to 200 m and 200 m to 400 m, assuming vertical sinking of the organic material (Iversen 2023):

$$POC_{loss} = -1 \frac{\Delta F}{\Delta z}$$

The potential carbon specific degradation (C_{spec}, d^{-1}) was then calculated as the ratio between POC_{loss} and the POC_{conc} (Iversen 2023):

$$C_{spec} = \frac{POC_{loss}}{POC_{conc}}$$

Statistical analyses

All statistical analyses and visualizations were done with the software R (RCoreTeam 2019) and Python. To test the differences in sinking velocities between different aggregates types, the non-parametric Wilcoxon rank sum test was used. To compare the carbon specific respiration rates according to the water masses (PW, AW, front), a Kruskal-Wallis rank sum test was used with a pairwise comparisons based on a Wilcoxon rank sum test as post-hoc test. To compare the aggregate size of the aggregates analyzed for carbon specific respiration rates, an analysis of variance (ANOVA) was done with a Tukey's multiple comparison test as post-hoc test. We used a Principal Component Analysis (PCA) on the particle data observed with the camera system in the transect to identify the characteristics of the particles explaining the main variation.

Results

Water masses and particle distribution in the transect

During the cruise, we observed several fronts on submesoscale (100 m – 1 km, hours to days) scales in the marginal ice zone (MIZ) (Hofmann et al. 2024). The resolution of our observation did not allow to distinguish between individual (submesoscale) features of the larger-scale gradient, as the submesoscale water mass distributions were highly complex (Hofmann et al. 2024). We categorized the features according to surface meltwater, Polar Water (PW), Atlantic Water (AW), and the front - between colder, fresher water (meltwater or PW) and warmer, saltier water (AW).

Along the camera transect, the (north-)westward moving warm and saline AW (3 - 5°C, > 34.5 PSU) was observed between 0 – 5 km distance and from 20 km onwards in the upper 100 m (Fig 2 A, B, C and D). Very saline (> 34.8 PSU) and not colder than 1.5°C AW was distributed below depths of around 100 m throughout the transect. Colder and fresher PW (-2 – 0°C, 33.7 – 34.4 PSU) intruded from the north at 20 - 40 m depth between 5 – 12 km distance (Fig 2 A, B, C and D). Between 0 – 10 km distance of the transect, meltwater with low salinities was located at the surface (0.5 – 2°C, < 33.3 PSU) between 0 – 15 m depth (Fig 2 C and D). The Chla was distributed according to the water masses as detected from satellite data and vertical fluorescence profiles in the transect (Fig. 1 C and 2 E): The surface meltwater was low in Chla with < 2 mg m^{-3}. High concentrations of Chla of > 10 mg m^{-3} were observed in the AW in the camera transect, with high values from the surface down to 40 m depth (Fig. 2 E).

Particle distributions were also consistent with water masses, showing patches of particles over several meter depth with particle abundance peaks at around 35 to 65 m depth (Fig. 2 F). High particle concentrations were observed in particular below the high Chla concentration in the AW between 0 – 5 km distance and from 25 - 32 km, with the highest particle concentrations and particle volumes located below the AW overlaid by meltwater at 0 - 5 km distance (Fig. 2 F and G). This occurred together with a ca. 1 m thin layer of elevated Chla concentrations (> 12 mg m^{-3}) which was observed at the upper boundary of the AW below the meltwater.

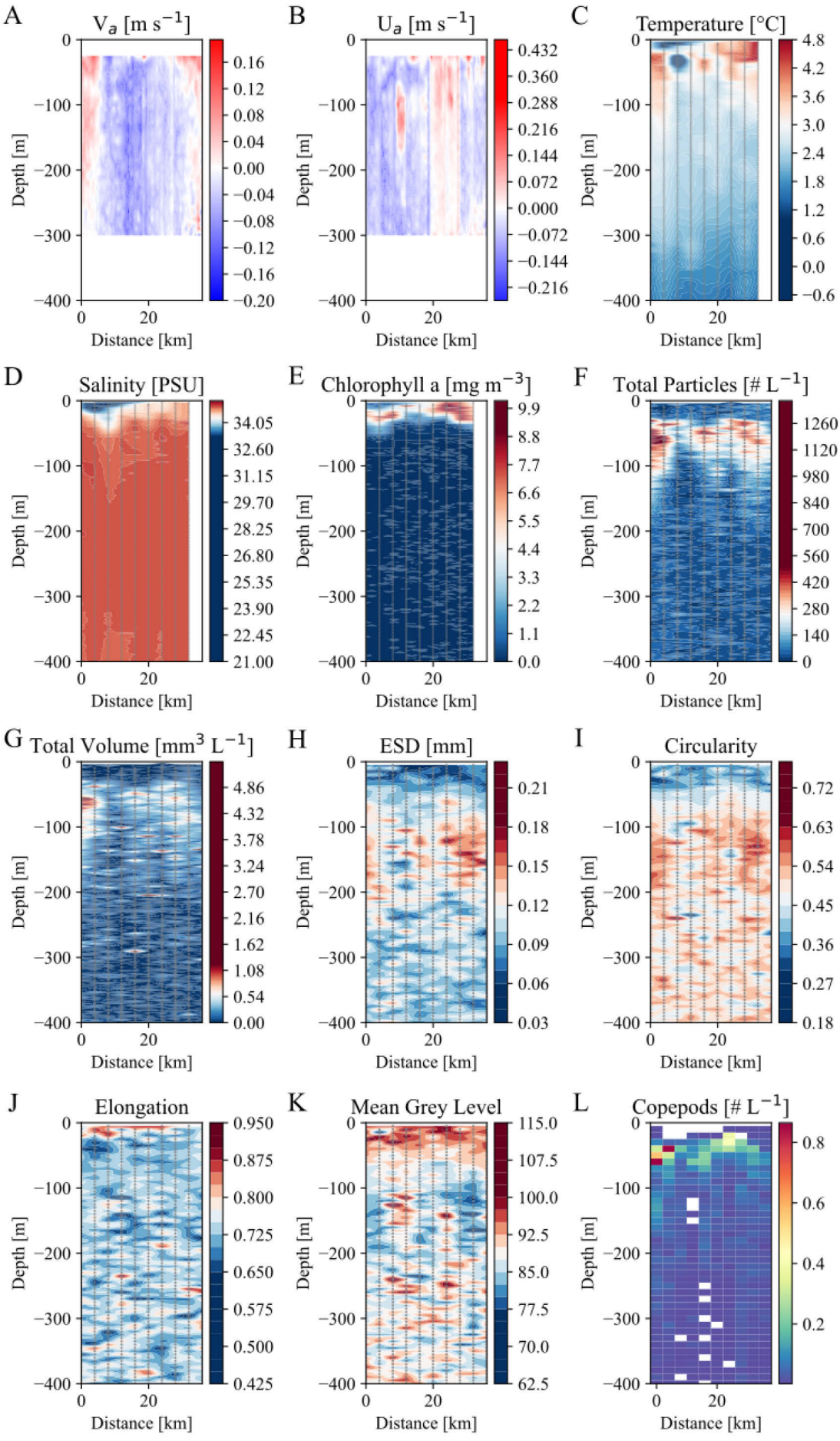
A
V_a [m s^{-1}]
B
U_a [m s^{-1}]
C
Temperature [°C]
D
Salinity [PSU]
E
Chlorophyll a [mg m^{-3}]
F
Total Particles [# L^{-1}]
G
Total Volume [mm^3 L^{-1}]
H
ESD [mm]
I
Circularity
J
Elongation
K
Mean Grey Level
L
Copepods [# L^{-1}]
Depth [m]
Distance [km]

Fig. 2: (A) Across-transect flow velocities V_a and (B) along-transect flow velocities U_a, (C) temperature [°C], (D) salinity [PSU], (E) Chlorophyll a from fluorescence sensor [mg m^{-3}], (F) total particle abundance [# L^{-1}], (G) total particle volume [mm^3 L^{-1}], (H) equivalent spherical diameter (ESD) [mm], (I) circularity, (J) elongation, (K) mean grey level, and (L) number of copepods [# L^{-1}] in a camera transect (station 30 to 39) down to 400 m depth.

The main drivers for the morphological differences in the particles were the size (equivalent spherical diameter, area, volume), the compactness (grey scale), and the circularity (PCA, Fig. S1 in the supplementary information). The equivalent spherical diameter of the particles was high below the chlorophyll-rich AW from 100 m to 200 m depth between 0 – 5 km distance and from 25 km onwards (Fig. 2 H). The circularity of the aggregates increased with increasing depth and was high below 100 m depth, while elongation was low (Fig. 2 I and J). Increased elongation was observed in the surface meltwater only (Fig. 2 J). The mean grey level was lower below the chlorophyll-rich AW, suggesting an increased compactness of the particles (Fig. 2 K).

The distribution of copepods followed the depth of high chlorophyll, showing high and low concentrations in the AW and in the PW, respectively (Fig. 2 L). Other zooplankton, such as chaetognaths or ostracods, only occurred sporadically, showing no clear pattern in relation to water masses and depths (data not shown).

Nutrient and particle distribution for individual stations

The lowest nutrient concentrations were observed in the surface meltwater (silicate: 2.2 – 3.3 µM, phosphate 0.1 – 0.4 µM, nitrate: 0.1 – 3.2 µM). In the PW, silicate concentrations were between 2.8 – 4.7 µM, phosphate concentrations between 0.4 – 0.6 µM, and nitrate concentrations between 4.2 – 10.3 µM. The AW had nutrient concentrations of 3.1 – 4.6 µM of silicate, 0.2 – 0.7 µM of phosphate and 0.8 – 12.9 µM of nitrate. High ammonium concentrations were located between 20 m to 80 m with maximum concentrations of 0.4 - 1.5 µM. From 100 m to 400 m, high silicate (4.6 – 5.6 µM), phosphate (0.6 – 0.8 µM) and nitrate (11.6 – 14.5 µM) concentrations were observed.

The particle abundances at stations outside the transect (sampled 1 - 8 days after, 16 - 90 kilometers away from the transect) showed either a single aggregate patch distributed over several meter depth, similar to the transect, or two separate shallower patches with peaks in depths of 25 - 50 m and 65 - 100 m (examples in Fig. 3). If two particle peaks were observed in the water column, higher Chla concentrations, i.e. from fluorescence data, were detected directly above the second particle peak (Fig. 3).

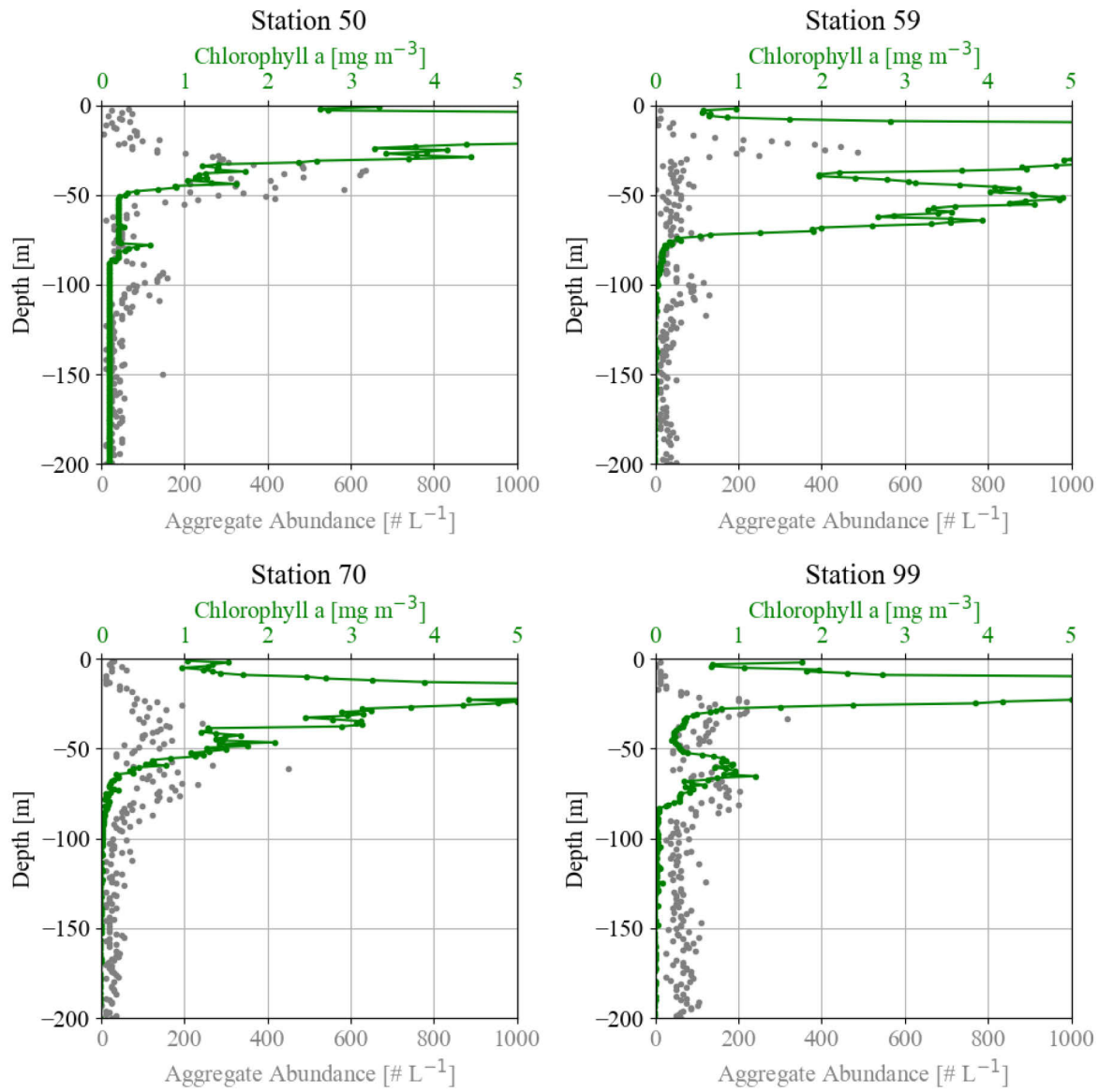

Fig. 3: Vertical profiles of aggregate abundance [# L^{-1}] in grey and chlorophyll a (Chla) concentration [mg m^{-3}] in green according to depth [m] for station 50, 59, 70 and 99 showing peaks in aggregate concentration at depth with higher chlorophyll concentration located above.

Carbon export

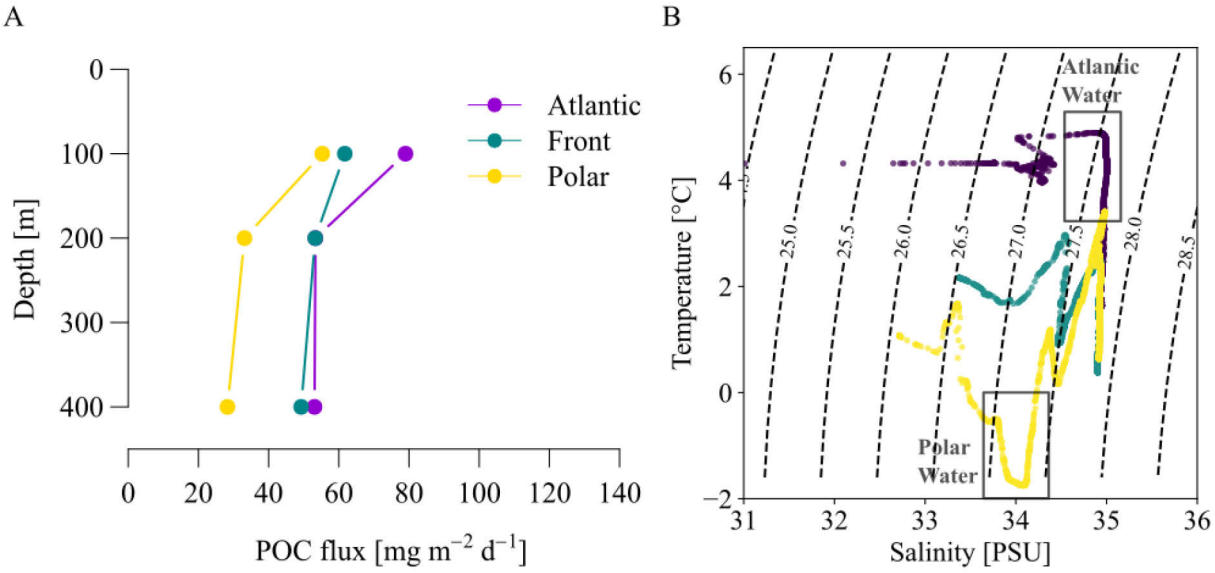

Fig. 4: (A) Particulate organic carbon (POC) flux [mg m^{-2} d^{-1}] measured in the drifting sediment traps, and (B) the temperature-salinity diagram showing the Atlantic Water (purple, station 56), the front (turquoise, station 88) and the Polar Water (yellow, station 99). The dashed black lines show isopycnals.

We categorized the different drift traps as AW (≈3 - 5°C), PW (≈−2 - 0°C) and a mixture at the front as shown in a temperature-salinity diagram, to compare biogeochemical fluxes (Fig. 4). The total mass flux was lowest in the PW (219 – 438 mg m^{-2} d^{-1}) and higher in the AW (453 – 586 mg m^{-2} d^{-1}) and the front (482 – 558 mg m^{-2} d^{-1}, see biogeochemical fluxes in the supplementary information, Fig. S2). The overall contribution of the particulate organic carbon (POC) to the total mass flux was 9 – 17%. The highest POC fluxes were measured in the AW (53 – 79 mg m^{-2} d^{-1}) and at the front (49 – 62 mg m^{-2} d^{-1}, Fig. 4 A). The POC flux in the PW only amounted to 28 – 55 mg m^{-2} d^{-1}. The export efficiency of POC from the primary production in the surface to 100 m depth was between 13 – 22 %, the transfer efficiency from 100 – 200 m depth between 60 – 86 % and from 200 m to 400 m between 85 – 99.5 %, with the lowest efficiencies in the PW (Table 1). In the AW high biogenic silica (bSi) fluxes of 36 – 40 mg m^{-2} d^{-1} were observed (Fig. S2 in the supplementary information), but the average bSi concentration in all traps was below 10% of the total mass flux. The C:N ratio of the sinking material was between 11 – 15, with higher C:N ratio at depth in the PW and the front (Fig. S2 in the supplementary information).

Table 1: Primary production [mgC m^{-2} d^{-1}], export efficiency to 100 m [%], transfer efficiency 100 m to 200 m [%] and 200 m to 400 m [%] in the Atlantic Water, the front and the Polar Water.

	Primary production PP [mgC m^{-2} d^{-1}]	**Export efficiency PP to 100 m [%]**	**Transfer efficiency 100 m to 200 m [%]**	**Transfer efficiency 200 m to 400 m [%]**
Atlantic Water	456	17	68	99.5
Front	278	22	86	92
Polar Water	421	13	60	85

Sinking velocities and respiration

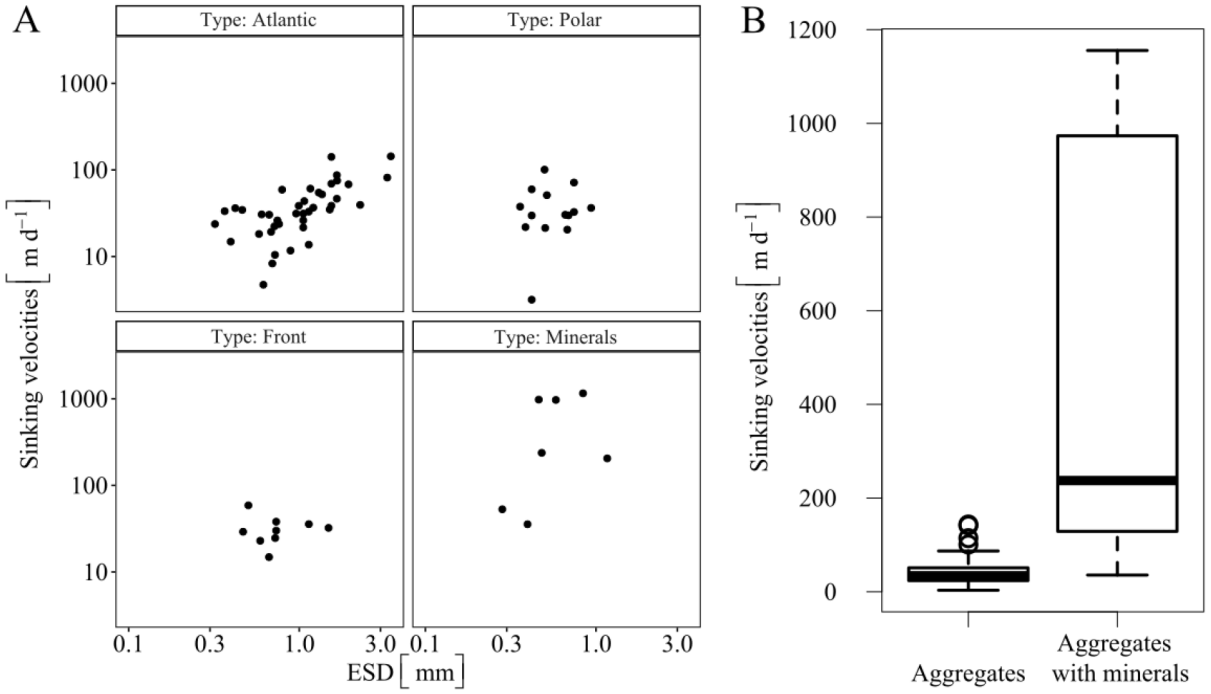

Fig. 5: (A) Logarithmically scaled sinking velocities in m d^{-1} according to logarithmically scaled equivalent spherical diameter (ESD) in mm of aggregates in the Atlantic Water, in the Polar Water, and in the front, and aggregates containing minerals. (B) Sinking velocities [m d^{-1}] of aggregates without minerals and aggregates containing minerals. The horizontal line depicts the median, the box shows the 25th percentile and the 75th percentile, the whiskers represent a 1.5* interquartile range from the box and the points potential outliers.

In the PW, high abundances of small crystalline minerals were collected with the drifting sediment trap and the MSC. The PW contained aggregates, which had crystalline minerals incorporated and were fast sinking (36 – 1156 m d^{-1}). The sinking velocities of aggregates without crystalline minerals in the PW, AW and in the front were significantly lower with 3 – 144 m d^{-1} (Wilcoxon rank sum test, p-value < 0.05, Fig. 5). The carbon content of the aggregates containing minerals was below the limit of detection of the CN analyzer, indicating very low carbon content in the mineral-rich aggregates.

The carbon-specific respiration rate of the aggregates in the AW (0.083 ± 0.007 d^{-1}) was significantly higher (pairwise Wilcoxon rank sum test, p-value < 0.05) than in the PW (0.017 ± 0.013 d^{-1}) or the front (0.010 ± 0.004 d^{-1}). The aggregates measured for respiration were bigger in size (Tukey's multiple comparison test, p-value < 0.05) in the AW than in the PW and in the front, and higher in carbon content (Table 2).

Table 2: Sample size, aggregate equivalent spherical diameter ESD [mm] with standard deviation, carbon specific respiration rate [d^{-1}] with standard deviation measured at 3.5°C, settling velocity [m s^{-1}] with standard deviation and summed particulate organic carbon to dry weight ratio POC:DW [%] for aggregates analyzed for respiration originating from the Atlantic Water, the front and the Polar Water.

	No. in sample	Aggregate ESD [mm]	Carbon specific respiration rate [d^{-1}]	Settling velocity [m s^{-1}]	Summed POC:DW [%]
Atlantic Water	4	1.8 ± 0.3	0.083 ± 0.007	52 ± 21	47
Front	4	0.8 ± 0.2	0.010 ± 0.004	32 ± 5	12
Polar Water	4	0.7 ± 0.2	0.017 ± 0.013	60 ± 28	3

Based on the POC loss measured using the primary production incubations and the drifting sediment traps, the calculated carbon-specific degradation rate between 15 m to 100 m was 5 to 28 times the magnitude of the measured carbon specific respiration rate and up to 9 times between 100 m to 200 m (Fig. 6).

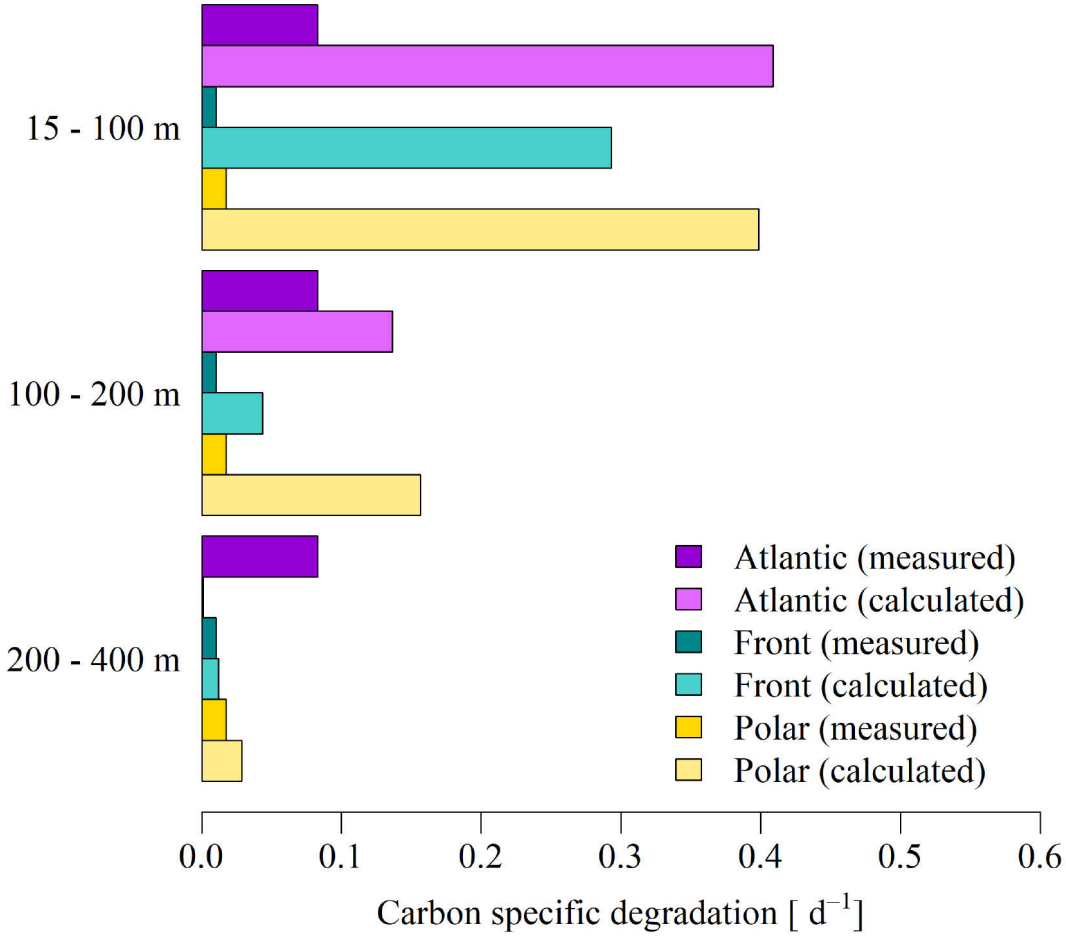

Fig. 6: Measured microbial respiration and calculated carbon specific degradation [d^{-1}] in the Atlantic Water (purple, station 56), in the front (turquoise, station 88) and in the Polar Water (yellow, station 99) at 15 - 100 m, at 100 - 200 m and at 200 - 400 m. The measured microbial carbon-specific respiration rate is based on direct measurements of aggregates collected by the Marine Snow Catcher, the calculated potential carbon degradation is based on the loss of particulate organic carbon through the water column measured by the drift trap and primary production incubation, assuming vertical sinking of the organic matter.

Microscopic assessments

The plankton community consisted primarily of colonies of the haptophyte *Phaeocystis* and diatoms, including *Skeletonema*, *Chaetoceros*, *Fragilariopsis* and *Pseudo-nitzschia*. Heterotrophic or mixotrophic degraders were associated with phytoplankton and aggregates, such as ciliates, nanoflagellates and dinoflagellates, like *Protoperidinium* and *Gyrodinium*. The dominant group of the marine snow aggregates were mostly diatom aggregates mixed with *Phaeocystis* with high mucous content. In the MSC and the drifting sediment traps, fecal pellets were only observed at low abundance, except for the traps that were deployed in the AW (Fig. S3 in the supplementary information). The majority of the aggregates were shaped more circular, looking dense, with dark brownish coloring.

Discussion

Water masses structure biology

In the front system, three different water masses interacted: Atlantic Water (AW) originating from the West Spitsbergen Current, Polar Water (PW) originating from the East Greenland Current and meltwater from sea ice in the marginal ice zone (MIZ). We observed that the structure and interaction of the water masses determined the biogeochemical and biological processes in the front system in the MIZ. In the period prior to our investigation, the study area was covered by low sea ice concentrations, but the ice had retreated by the time the investigation started (data not shown). Ice melt produced meltwater that was characterized by temperatures between 0 – 2°C, low salinity, low nutrients, and low Chla, which intruded the study region at the surface from the northwest. At the surface, the meltwater encountered the warmer and more saline AW (Fig. 1 C). The denser AW with a high Chla concentration was subducted below the meltwater to a depth of 20 m and resulted in a Chla peak in AW directly below the meltwater. In consequence, the particle abundance in the AW below meltwater increased in comparison to non-subducted AW, resulting in a higher particle volume (Fig. 2 F and G). As the chlorophyll is concentrated in the upper boundary of the chlorophyll patch in the subducted AW directly below the meltwater, this could have led to an increased particle encounter rate of small particles, such as phytoplankton cells, and hence to enhanced aggregate formation (Jackson and Kiørboe 2008). In general, the productive AW with high Chla concentration resulted in higher particle abundances in the AW below and the aggregates seemed to be of greater size and more compact.

The high Chla and the resulting higher particle abundance in the AW below directly impacted the zooplankton distribution in the front system. The distribution of copepods followed Chla concentrations and particle abundances (Fig. 2 L), probably feeding below the chlorophyll maximum at the particle maximum (Jackson and Checkley Jr 2011). This was also supported by the high ammonium concentrations found below the Chla maximum.

The zooplankton feeding activity seemed to directly impact the characteristics of the sinking aggregates, likely via aggregate fragmentation (Dilling and Alldredge 2000). Aggregate fragmentation has been shown to be responsible for half of the loss of large aggregates in the water column (Briggs et al. 2020). While aggregates were smaller in the surface, where copepods were more abundant (Fig. 2 L), the aggregate size increased below the peak in aggregate abundance below 100 m depth (Fig. 2 H). Possibly, aggregates at these depths escaped copepod feeding and fragmentation due to high sinking velocities and low zooplankton abundances in the water column (Fig. 2 L). Since aggregates simultaneously also increased in

circularity and did not show an increase in elongation (Fig. 2 I and J), the contribution by copepod fecal pellets to the total aggregate pool seemed to be low. Furthermore, the gel traps that were deployed in the front system also only showed fecal pellets at low abundances.

Instead, dense phytoplankton aggregates, which were circularly shaped with brownish coloring, were dominating the downward flux. Some stations in the front system showed high abundances of heterotrophic degraders, like dinoflagellates, nanoflagellates and ciliates, which have previously been observed to have high feeding rates on copepod fecal pellets (Hansen et al. 1996; Poulsen and Iversen 2008; Poulsen et al. 2011). Hence, low fecal pellets observations could also be due to intense grazing on the pellets by protozooplankton. Moreover, fragmentation of the fecal pellets by copepods themselves could decrease fecal pellet occurrence in the water column (Iversen and Poulsen 2007).

Carbon export

Even though the flux of particulate organic carbon (POC) was lower in the less productive PW than in the AW or at the front (Fig. 4), the carbon export in all water masses in the front system was highly efficient: 13 – 22% of the primary production was exported from the upper ocean to 100 m, 60 – 86% was transferred from 100 m to 200 m and 85 – 99.5 % of the POC was transferred from 200 m to 400 m. The fact that the carbon export was more efficient and higher in magnitude at front and in the AW, suggest that export in the Fram Strait might be enhanced with the inflow of more Atlantic Water, i.e. increasing Atlantification (Polyakov et al. 2017; Randelhoff et al. 2018; Tesi et al. 2021; Wang et al. 2020). Due to the strong boundary currents, horizontal advection and dislocation of organic material is typical in Fram Strait (Wekerle et al. 2018). Here, the material at depth often originates from places further away, resulting in a higher flux at depth than supported by the direct surface primary production. With the complex water movements in the front system, dislocation of sinking material is likely and one has to consider that there is a strong spatial decoupling between production and export when accessing the efficiency of the biological carbon pump.

According to the export and transfer efficiencies (Table 1), the depth of highest biological activity and attenuation was located in the upper 200 m. Our measured potential microbial respiration cannot explain the observed degradation rate within this layer (Fig. 6). Due to higher copepod abundances in the upper 200 m (Fig. 2 L), it is likely that zooplankton feeding was responsible for the main share of attenuation there (Iversen et al. 2010; Jackson and Checkley Jr 2011; Stemmann et al. 2004). Copepods are important grazers in the Arctic, as only few key species can be responsible for more than 60% of the carbon attenuation (van der Jagt et al. 2020). Below 200 m, microbial respiration can explain most of the observed

degradation rate and zooplankton degradation seemed to play only a minor role (Iversen et al. 2010; Stemmann et al. 2004).

Carbon-specific respiration

The carbon specific respiration was much higher in aggregates collected in the AW than in the PW or in the front (Table 2), even when measured at the same temperature (3.5°C) due to limitations in the minimum temperature for the experimental set-up. Aggregates from the PW (-1.7°C) and the front (1.2°C) were therefore measured at temperatures that were higher than the *in situ* temperatures at which they were collected. The increase in temperature should lead to an increase in the carbon specific respiration (Iversen and Ploug 2013), so the *in situ* carbon specific respiration rate in the PW and in the front might be even lower than observed. On the other hand, the aggregate-attached microbes might have had insufficient readjustment time (only minutes) to the warmer temperature in our set-up, which could result in an underestimation of the carbon-specific respiration rate due to temperature shock. Iversen and Ploug (2013), for example, incubated the aggregates over several days at constant temperatures before measuring microbial respiration. Also, we cannot exclude the possibility that differences in carbon or nutrient sources could have changed the composition of the aggregate associated microbes, impacting microbial degradation (Datta et al. 2016).

Since the carbon respiration rate in the AW was higher (Table 2), one could assume a lower associated export efficiency. Additionally, taking into account the temperature dependency of the carbon specific respiration, i.e. higher respiration rates with increasing temperature (Iversen and Ploug 2013), aggregates would lose more carbon sinking in the warmer AW than in the colder PW, when sinking at the same velocities. This does not seem to be the case, as the lowest export and transfer efficiency were observed in the PW (Table 1). Our measured *in situ* carbon-specific respiration rates might overestimate the microbial respiration below 100 m depth, as respiration of surface ocean microbes attached to aggregates tend to decrease with increasing hydrostatic pressure (Stief et al. 2021; Tamburini et al. 2013). Overall, the underlying carbon export mechanism seems to affect the carbon export noticeably more than carbon respiration by microbes.

Export mechanisms

At the surface in the frontal system, the subduction of Chla-rich water determines the depth of aggregate formation. Aside from enhanced aggregate formation below the meltwater, deeper aggregate formation due to subducted Chla-rich water could also enhance the carbon export. A second peak in aggregate abundance was observed at 65 - 100 m depth at some

stations in correspondence with increased Chla concentration at depth (Fig. 3). Living phytoplankton cells can be transported into deeper water layers by eddy driven subduction (Omand et al. 2015), subduction at fronts (Hofmann et al. 2024), or possibly by the alternating generation of deep and shallow mixed layers (Dall'Olmo and Mork 2014), making aggregation at depth possible. As salinity and temperature gradients retain aggregates in the surface ocean (Alldredge et al. 2002; MacIntyre et al. 1995; Möller et al. 2012), surface stratification by meltwater limits the carbon export in the Arctic (von Appen et al. 2021). If the formation of aggregate takes place at deeper depth, the sinking aggregates are to a lesser extent subjected to surface stratification and retention by salinity and temperature gradients. Thus, aggregate formation at depth due to the subduction of Chla-rich water could enhance the carbon export in the front system.

The most frequent ballasting mechanism in the frontal system was the aggregate export via diatom ballasting. The majority of the aggregates consisted of a mixture of diatoms and colonies of the haptophyte *Phaeocystis.* In Fram Strait, increasing abundances of *Phaeocystis* have been observed, possibly because of the increasing inflow and warming by AW (Nöthig et al. 2015). We also observed high concentration of *Phaeocystis* colonies in the upper water layer of the frontal system. Due to the stickiness of the polysaccharide-rich mucous colony matrix of *Phaeocystis*, they form aggregates together with diatoms (Alderkamp et al. 2007; Passow and Wassmann 1994). This led to the export of light and almost neutrally buoyant *Phaeocystis* colonies (Peperzak et al. 2003) in the aggregates due to the ballasting with heavy biogenic silica of diatoms (Tréguer et al. 2018). As *Phaeocystis* colonies have high C/N ratios and are rich in carbon (Alderkamp et al. 2007), the integration of *Phaeocystis* colonies into aggregates could have added additional particulate carbon to the export flux and might explain the fairly high C/N ratios observed for the exported material (Fig. 2S in the supplementary information).

An export mechanism associated with PW was the aggregate export via mineral ballasting. We observed a spontaneous export event of aggregates in PW, which had crystalline structures incorporated, and were characterized by high sinking velocities of up to 1156 m d^{-1} (Fig. 5). These minerals could possibly be cryogenic gypsum (Geilfus et al. 2013). In the Arctic, large amounts of gypsum particles have been found under the ice (Wollenburg et al. 2020; Wollenburg et al. 2018). Cryogenic gypsum forms by precipitation in brine channels or pockets in sea ice during freezing (Geilfus et al. 2013; Wollenburg et al. 2020). These gypsums crystal reach sinking velocities between 200 – 7000 m d^{-1} (Wollenburg et al. 2020)**.** If the minerals are scavenged by aggregates, these fast-sinking particles could transport slow-sinking aggregates or suspended material downwards, since they would increase their sinking velocity by several

orders of magnitude as shown for Saharan dust ballasting (van der Jagt et al. 2018). Thus, aggregates made of slow-sinking *Phaeocystis* with their sticky polysaccharide matrix can be efficiently exported to the seafloor when ballasted by cryogenic gypsum (Alderkamp et al. 2007; Passow and Wassmann 1994; Wollenburg et al. 2018). Nevertheless, the fast-sinking aggregates were low in carbon content, which suggests low carbon export. This would explain why the PW displayed a lower export and transfer efficiency (Table 1), even though we found high abundances of crystalline particles in the drifting sediment traps.

Conclusion - Implication of frontal systems on export in the Arctic

Since eddies often develop near the ice edge and in areas with ice concentration of less than 20% (Kozlov and Atadzhanova 2021), and the extent of sea ice cover in the Arctic is decreasing (Parkinson and DiGirolamo 2021), frontal systems are likely to develop more frequently in the future. In areas with enhanced vertical and horizontal mixing, this could lead to enhanced carbon export or nutrient upwelling (Klein and Lapeyre 2009; von Appen et al. 2018). Our results indicate that surface meltwater led to the subduction of high chlorophyll concentrations which resulted in increased particle formation. Especially the AW seemed to be responsible for a high rate of carbon export in the front system, even though it was subjected to zooplankton feeding. This is in contrast to the findings of Fadeev et al (2021a), who suggested higher carbon export associated with sea ice cover and predicted decreasing export efficiencies with increasing sea ice loss. Nevertheless, this could also be due to different ecosystem states at the point of sampling, since our investigated front system only had remnants of ice and was dominated by meltwater at the surface. Hence, large export events of ice algae (Boetius et al. 2013) could have already taken place prior to our sampling.

We identified three major mechanism supporting the export in the front system: **i)** Due to subduction of Chla-rich water, deep aggregate formation took place, potentially enhancing the carbon export, as the aggregates were less subjected surface stratification and were able to escape the surface ocean faster. **ii)** The majority of the exported aggregates was ballasted by diatoms, which formed aggregates together with slow-sinking *Phaeocystis* colonies. **iii)** We observed aggregates that were ballasted by cryogenic minerals, which increased their size-specific settling velocities 10-fold compared to aggregates that were ballasted by diatom-silica. In consequence, our results suggest that the broadening of the MIZ, increasing Atlantification under climate change, and the frequent development of fronts could enhance the carbon export in the Arctic in the future.

Author contributions

The manuscript was written by LH under supervision of MHI. LH analyzed the data together with SR. Sampling onboard was done by LH, MHI, SR and CK. CK built the ROSINA camera system and processed the camera data. ZH and WJvA provided the background on the physical oceanography. LH prepared samples for biogeochemical analysis. STV analyzed the nutrient samples and JS analyzed the primary production samples in the home laboratory. NM modelled the oxygen consumption of the individual aggregates. AB analyzed the PAR profiles. AW provided the UVP raw data. All authors revised and approved the manuscript.

Acknowledgments

We thank the crew and captain of F.S. Maria S. Merian for their assistance during the cruises. For the phytooptics PAR and pigment data, we thank Julia Oelker for the work on board and Christian Hohe for analyzing phytoplankton pigments with the HPLC and taking care of logistic. Special thanks to Sandra Murawski for the biogeochemical measurements. Nutrient analyses were done at the AWI Nutrient Facility. This study was supported by the Helmholtz Association, the Alfred Wegener Institute Helmholtz Centre for Polar and Marine Research and the DFG-Research Center/Cluster of Excellence "The Ocean Floor – Earth's Uncharted Interface": EXC-2077-390741603 at MARUM. The authors gratefully acknowledge the funding by the Deutsche Forschungsgemeinschaft (DFG, German Research Foundation) -- Projektnummer 268020496 -- TRR 172, within the Transregional Collaborative Research Center "ArctiC Amplification: Climate Relevant Atmospheric and SurfaCe Processes, and Feedback Mechanisms $(AC)^3$." Ship time for this study was provided under Grant No. GPF 18-1_33.

Supplementary information

Table S1: List of parameters with unit and description for particles observed from the ROSINA camera system after Trudnowska et al. 2021

Parameter	Unit	Description
Area	mm^2	Area of particle
EquiDia	mm	Equivalent spherical diameter of particle
Volume	mm^3	Volume of particle
Feret	mm	Maximum feret diameter of particle
Perimeter	mm	Length of outside boundary of particle
Circularity	[a.u.]	Circularity of particle $(4*\pi*Area)/Perim^2$
Elongation	[a.u.]	Ratio between major/minor axes of particle
Major	mm	Primary axis of best fitting ellipse for particle
PartSymV	[a.u.]	Bilateral vertical symmetry of particle
PartSymH	[a.u.]	Bilateral horizontal symmetry of particle
Mean	[a.u.]	Mean grey value of pixels of particle
StdDev	[a.u.]	Standard deviation of mean grey value of pixels of particle
Median	[a.u.]	Median grey value of pixels of particle
Modal	[a.u.]	Modal grey value of pixels of particle
Intden	[a.u.]	Integrated density, i.e. sum of grey values of pixels of particle
Range	[a.u.]	Maximum − minimum of grey values of pixels of particle
MeanPos	[a.u.]	(maximum − mean)/range of grey values of pixels of particle
Cv	[a.u.]	100∗(StdDev /mean) of grey values of pixels of particle
Sr	[a.u.]	100∗(StdDev/(maximum − minimum)) of grey values of pixel of particle

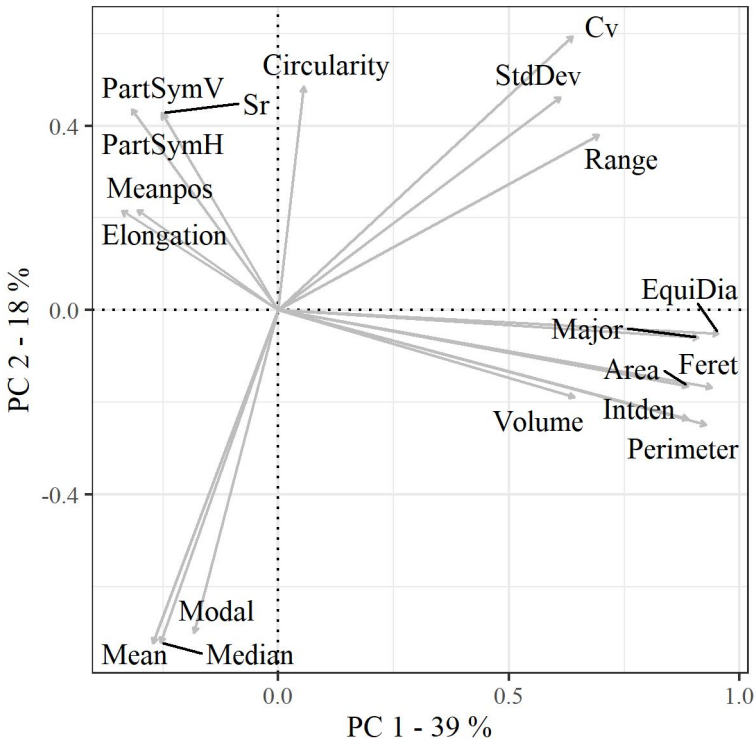

Fig. S1: Principal Component Analysis for particle parameters which were observed with the ROSINA camera system. The particle parameters are explained in Table S1. The axis PC 1 is explaining 39% and axis PC 2 is explaining 18% of the variance.

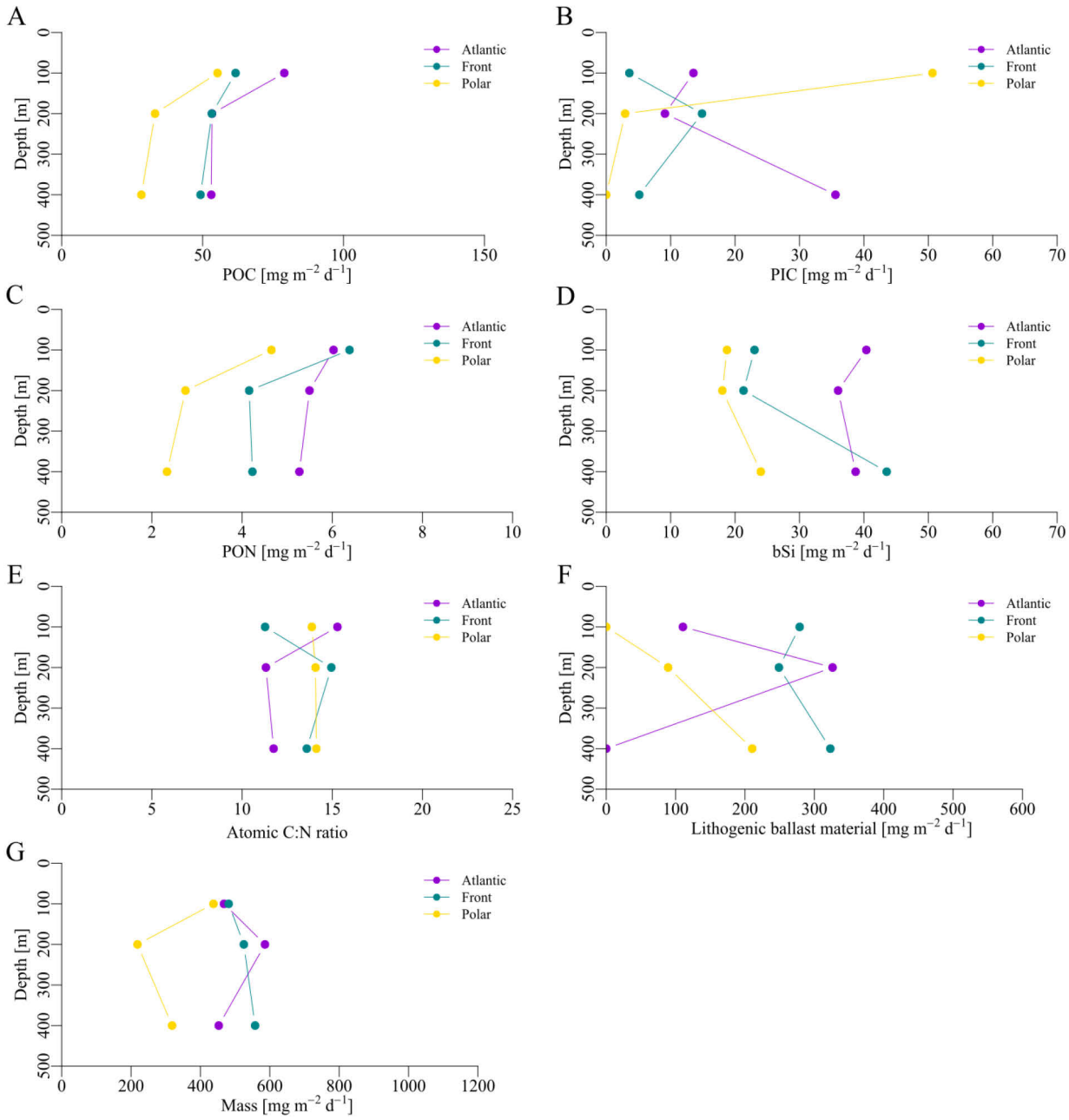

Fig. S2: Biogeochemical fluxes in the drifting sediment traps in the frontal system, showing (A) the particulate organic carbon (POC) flux [mg m^{-2} d^{-1}], (B) the particulate inorganic carbon (PIC) flux [mg m^{-2} d^{-1}], (C) the particulate organic nitrogen (PON) flux [mg m^{-2} d^{-1}], (D) the biogenic silica (bSi) flux [mg m^{-2} d^{-1}], (E) the atomic C:N ratio, (F) the lithogenic ballast material flux [mg m^{-2} d^{-1}] and (G) the mass flux [mg m^{-2} d^{-1}] in the Atlantic Water (purple), in the front (turquoise) and in the Polar Water (yellow).

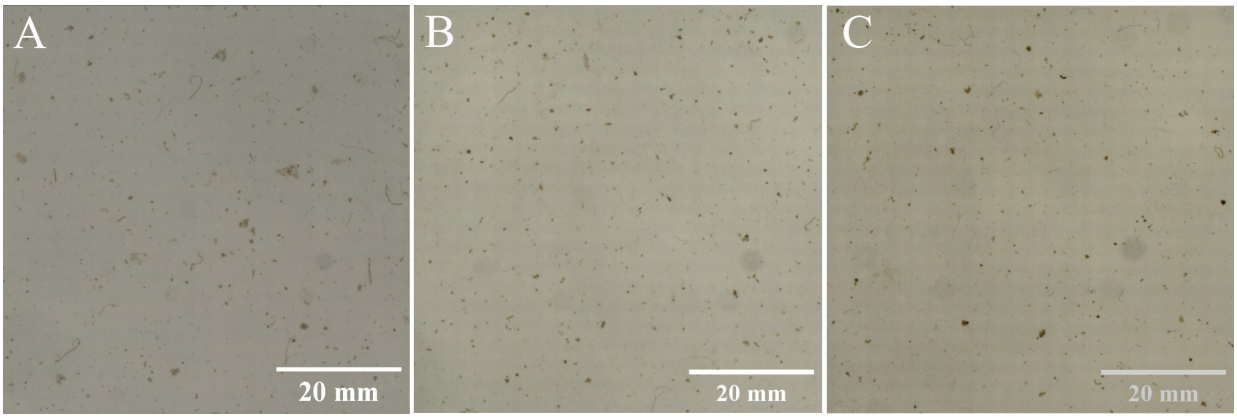

Fig. S3: Collected aggregates in the drifting sediment trap at 100 m in the (A) Atlantic Water, (B) the front and the (C) Polar Water

References

Aagaard, K., Foldvik, A., and Hillman, S. (1987). "The West Spitsbergen Current: Disposition and Water Mass Transformation." *Journal of Geophysical Research: Oceans*, 92(C4), 3778-3784.

Alderkamp, A.-C., Buma, A. G., and van Rijssel, M. (2007). "The carbohydrates of *Phaeocystis* and their degradation in the microbial food web." *Biogeochemistry*, 83, 99-118.

Alldredge, A. L., Cowles, T. J., MacIntyre, S., Rines, J. E. B., Donaghay, P. L., Greenlaw, C. F., Holliday, D. V., Dekshenieks, M. M., Sullivan, J. M., and Zaneveld, J. R. V. (2002). "Occurrence and mechanisms of formation of a dramatic thin layer of marine snow in a shallow Pacific fjord." *Marine Ecology Progress Series*, 233, 1-12.

Aminot, A., and Kérouel, R. (2007). *Dosage automatique des nutriments dans les eaux marines: méthodes en flux continu*: Editions Quae.

Aminot, A., Kérouel, R., and Coverly, S. C. (2009). "Nutrients in seawater using segmented flow analysis." *Practical guidelines for the analysis of seawater*, 143-178.

Arrigo, K. R., Perovich, D. K., Pickart, R. S., Brown, Z. W., van Dijken, G. L., Lowry, K. E., Mills, M. M., Palmer, M. A., Balch, W. M., Bahr, F., Bates, N. R., Benitez-Nelson, C., Bowler, B., Brownlee, E., Ehn, J. K., Frey, K. E., Garley, R., Laney, S. R., Lubelczyk, L., Mathis, J., Matsuoka, A., Mitchell, B. G., Moore, G. W. K., Ortega-Retuerta, E., Pal, S., Polashenski, C. M., Reynolds, R. A., Schieber, B., Sosik, H. M., Stephens, M., and Swift, J. H. (2012). "Massive Phytoplankton Blooms Under Arctic Sea Ice." *Science*, 336(6087), 1408-1408.

Becker, S., Aoyama, M., Woodward, E. M. S., Bakker, K., Coverly, S., Mahaffey, C., and Tanhua, T. (2020). "GO-SHIP repeat hydrography nutrient manual: the precise and accurate determination of dissolved inorganic nutrients in seawater, using continuous flow analysis methods." *Frontiers in Marine Science*, 7, 581790.

Beszczynska-Möller, A., Fahrbach, E., Schauer, U., and Hansen, E. (2012). "Variability in Atlantic water temperature and transport at the entrance to the Arctic Ocean, 1997–2010." *ICES Journal of Marine Science*, 69(5), 852-863.

Bodungen, B. V., Wunsch, M., and Fürderer, H. (1991). "Sampling and analysis of suspended and sinking particles in the northern North Atlantic." *Washington DC American Geophysical Union Geophysical Monograph Series*, 63, 47-56.

Boetius, A., Albrecht, S., Bakker, K., Bienhold, C., Felden, J., Fernández-Méndez, M., Hendricks, S., Katlein, C., Lalande, C., Krumpen, T., Nicolaus, M., Peeken, I., Rabe, B., Rogacheva, A., Rybakova, E., Somavilla, R., and Wenzhöfer, F. (2013). "Export of Algal Biomass from the Melting Arctic Sea Ice." *Science*, 339(6126), 1430-1432.

Boyd, P. W., Claustre, H., Levy, M., Siegel, D. A., and Weber, T. (2019). "Multi-faceted particle pumps drive carbon sequestration in the ocean." *Nature*, 568(7752), 327-335.

Bracher, A., Xi, H., Dinter, T., Mangin, A., Strass, V., Von Appen, W.-J., and Wiegmann, S. (2020). "High Resolution Water Column Phytoplankton Composition Across the Atlantic Ocean From Ship-Towed Vertical Undulating Radiometry." *Frontiers in Marine Science*, 7, 235.

Briggs, N., Dall'Olmo, G., and Claustre, H. (2020). "Major role of particle fragmentation in regulating biological sequestration of CO_2 by the oceans." *Science*, 367(6479), 791-793.

Dall'Olmo, G., and Mork, K. A. (2014). "Carbon export by small particles in the Norwegian Sea." *Geophysical Research Letters*, 41, 2921–2927.

Datta, M. S., Sliwerska, E., Gore, J., Polz, M. F., and Cordero, O. X. (2016). "Microbial interactions lead to rapid micro-scale successions on model marine particles." *Nature Communications*, 7(1), 11965.

Dilling, L., and Alldredge, A. L. (2000). "Fragmentation of marine snow by swimming macrozooplankton: A new process impacting carbon cycling in the sea." *Deep Sea Research Part I: Oceanographic Research Papers*, 47(7), 1227-1245.

Fadeev, E., Rogge, A., Ramondenc, S., Nöthig, E.-M., Wekerle, C., Bienhold, C., Salter, I., Waite, A. M., Hehemann, L., Boetius, A., and Iversen, M. H. (2021a). "Sea ice presence is linked to higher carbon export and vertical microbial connectivity in the Eurasian Arctic Ocean." *Communications Biology*, 4(1), 1255.

Fadeev, E., Wietz, M., von Appen, W. J., Iversen, M. H., Nöthig, E. M., Engel, A., Grosse, J., Graeve, M., and Boetius, A. (2021b). "Submesoscale physicochemical dynamics directly shape bacterioplankton community structure in space and time." *Limnology and Oceanography*, 66(7), 2901-2913.

Geilfus, N. X., Galley, R. J., Cooper, M., Halden, N., Hare, A., Wang, F., Søgaard, D. H., and Rysgaard, S. (2013). "Gypsum crystals observed in experimental and natural sea ice." *Geophysical Research Letters*, 40(24), 6362-6367.

Grasshoff, K., Kremling, K., and Ehrhardt, M. (2009). *Methods of seawater analysis*: John Wiley & Sons.

Hansen, B., Fotel, F. L., Jensen, N. J., and Madsen, S. D. (1996). "Bacteria associated with a marine planktonic copepod in culture. II. Degradation of fecal pellets produced on a diatom, a nanoflagellate or a dinoflagellate diet." *Journal of Plankton Research*, 18(2), 275-288.

Hattermann, T., Isachsen, P. E., von Appen, W. J., Albretsen, J., and Sundfjord, A. (2016). "Eddy-driven recirculation of Atlantic water in Fram Strait." *Geophysical Research Letters*, 43(7), 3406-3414.

Håvik, L., Pickart, R., Våge, K., Torres, D., Thurnherr, A., Beszczynska-Möller, A., Walczowski, W., and von Appen, W. J. (2017). "Evolution of the East Greenland Current from Fram Strait to Denmark Strait: Synoptic measurements from summer 2012." *Journal of Geophysical Research: Oceans*, 122(3), 1974-1994.

Hofmann, Z., von Appen, W.-J., and Wekerle, C. (2021). "Seasonal and Mesoscale Variability of the Two Atlantic Water Recirculation Pathways in Fram Strait." *Journal of Geophysical Research: Oceans*, 126(7), e2020JC017057.

Hofmann, Z., von Appen, W.-J, Kanzow, T., Becker, H., Hagemann, J., Hufnagel, L., and Iversen, M.H. (2024): "Stepwise Subduction Observed at a Front in the Marginal Ice Zone in Fram Strait." *Journal of Geophysical Research: Oceans*, 129(5), e2023JC020641.

Holmes, R. M., Aminot, A., Kérouel, R., Hooker, B. A., and Peterson, B. J. (1999). "A simple and precise method for measuring ammonium in marine and freshwater ecosystems." *Canadian Journal of Fisheries and Aquatic Sciences*, 56(10), 1801-1808.

Hu, C., Lee, Z., and Franz, B. (2012). "Chlorophyll *a* algorithms for oligotrophic oceans: A novel approach based on three-band reflectance difference." *Journal of Geophysical Research: Oceans*, 117(C1), C01011.

Hydes, D., Aoyama, M., Aminot, A., Bakker, K., Becker, S., Coverly, S., Daniel, A., Dickson, A., Grosso, O., and Kerouel, R. (2010). "Recommendations for the determination of nutrients in seawater to high levels of precision and inter-comparability using continuous flow analysers". GO-SHIP (Unesco/IOC).

Iversen, M. H., and Poulsen, L. K. (2007). "Coprorhexy, coprophagy, and coprochaly in the copepods *Calanus helgolandicus*, *Pseudocalanus elongatus*, and *Oithona similis*." *Marine Ecology Progress Series*, 350, 79-89.

Iversen, M. H., Nowald, N., Ploug, H., Jackson, G. A., and Fischer, G. (2010). "High resolution profiles of vertical particulate organic matter export off Cape Blanc, Mauritania: Degradation processes and ballasting effects." *Deep Sea Research Part I:*

Oceanographic Research Papers, 57(6), 771-784.

Iversen, M. H., and Ploug, H. (2013). "Temperature effects on carbon-specific respiration rate and sinking velocity of diatom aggregates – potential implications for deep ocean export processes." *Biogeosciences*, 10(6), 4073-4085.

Iversen, M. H. (2023). "Carbon Export in the Ocean: A Biologist's Perspective." *Annual Review of Marine Science*, 15(1), 357-381.

Jackson, G. A., and Kiørboe, T. (2008). "Maximum phytoplankton concentrations in the sea." *Limnology and Oceanography*, 53(1), 395-399.

Jackson, G. A., and Checkley Jr, D. M. (2011). "Particle size distributions in the upper 100 m water column and their implications for animal feeding in the plankton." *Deep Sea Research Part I: Oceanographic Research Papers*, 58(3), 283-297.

Kirkwood, D. (1996). "Nutrients: Practical notes on their determination in sea water."

Klein, P., and Lapeyre, G. (2009). "The Oceanic Vertical Pump Induced by Mesoscale and Submesoscale Turbulence." *Annual Review of Marine Science*, 1(1), 351-375.

Kozlov, I. E., and Atadzhanova, O. A. (2021). "Eddies in the Marginal Ice Zone of Fram Strait and Svalbard from Spaceborne SAR Observations in Winter." *Remote Sensing*, 14(1), 134.

MacIntyre, S., Alldredge, A. L., and Gotschalk, C. C. (1995). "Accumulation of marines now at density discontinuities in the water column." *Limnology and Oceanography*, 40(3), 449-468.

Mahadevan, A. (2016). "The Impact of Submesoscale Physics on Primary Productivity of Plankton." *Annual Review of Marine Science*, 8(1), 161-184.

Möller, K. O., St. John, M., Temming, A., Floeter, J., Sell, A. F., Herrmann, J.-P., and Möllmann, C. (2012). "Marine snow, zooplankton and thin layers: indications of a trophic link from small-scale sampling with the Video Plankton Recorder." *Marine Ecology Progress Series*, 468, 57-69.

Moradi, N., Liu, B., Iversen, M., Kuypers, M. M., Ploug, H., and Khalili, A. (2018). "A new mathematical model to explore microbial processes and their constraints in phytoplankton colonies and sinking marine aggregates." *Science Advances*, 4(10), eaat1991.

Moradi, N., Klawonn, I., Iversen, M. H., Wenzhöfer, F., Grossart, H.-P., Ploug, H., Fischer, G., and Khalili, A. (2021). "A Novel Measurement-Based Model for Calculating Diffusive Fluxes Across Substrate-Water Interfaces of Marine Aggregates, Sediments and Biofilms." *Frontiers in Marine Science*, 8, 689977.

Neukermans, G., Oziel, L., and Babin, M. (2018). "Increased intrusion of warming Atlantic water leads to rapid expansion of temperate phytoplankton in the Arctic." *Global Change Biology*, 24(6), 2545-2553.

Nöthig, E.-M., Bracher, A., Engel, A., Metfies, K., Niehoff, B., Peeken, I., Bauerfeind, E., Cherkasheva, A., Gäbler-Schwarz, S., Hardge, K., Kilias, E., Kraft, A., Mebrahtom Kidane, Y., Lalande, C., Piontek, J., Thomisch, K., and Wurst, M. (2015). "Summertime plankton ecology in Fram Strait—a compilation of long-and short-term observations." *Polar Research*, 34(1), 23349.

Omand, M. M., D'Asaro, E. A., Lee, C. M., Perry, M. J., Briggs, N., Cetinić, I., and Mahadevan, A. (2015). "Eddy-driven subduction exports particulate organic carbon from the spring bloom." *Science*, 348(6231), 222-225.

Parkinson, C. L., and DiGirolamo, N. E. (2021). "Sea ice extents continue to set new records: Arctic, Antarctic, and global results." *Remote Sensing of Environment*, 267, 112753.

Passow, U., and Wassmann, P. (1994). "On the trophic fate of *Phaeocystis pouchetii* (Hariot): IV. The formation of marine snow by *P. pouchetii*." *Marine Ecology Progress Series*, 104(1/2), 153-161.

Peperzak, L., Colijn, F., Koeman, R., Gieskes, W. W. C., and Joordens, J. C. A. (2003). "Phytoplankton sinking rates in the Rhine region of freshwater influence." *Journal of Plankton Research*, 25(4), 365-383.

Picheral, M., Guidi, L., Stemmann, L., Karl, D. M., Iddaoud, G., and Gorsky, G. (2010). "The Underwater Vision Profiler 5: An advanced instrument for high spatial resolution studies of particle size spectra and zooplankton." *Limnology and Oceanography: Methods*, 8(9), 462-473.

Picheral, M., Colin, S., and Irisson, J.-O. (2017). "EcoTaxa, a tool for the taxonomic classification of images."

Ploug, H., and Jørgensen, B. B. (1999). "A net-jet flow system for mass transfer and microsensor studies of sinking aggregates." *Marine Ecology Progress Series*, 176, 279-290.

Polyakov, I. V., Pnyushkov, A. V., Alkire, M. B., Ashik, I. M., Baumann, T. M., Carmack, E. C., Goszczko, I., Guthrie, J., Ivanov, V. V., Kanzow, T., Krishfield, R., Kwok, R., Sundfjord, A., Morison, J., Rember, R., and Yulin, A. (2017). "Greater role for Atlantic inflows on sea-ice loss in the Eurasian Basin of the Arctic Ocean." *Science*, 356(6335), 285-291.

Poulsen, L. K., and Iversen, M. H. (2008). "Degradation of copepod fecal pellets: key role of protozooplankton." *Marine Ecology Progress Series*, 367, 1-13.

Poulsen, L. K., Moldrup, M., Berge, T., and Hansen, P. J. (2011). "Feeding on copepod fecal pellets: a new trophic role of dinoflagellates as detritivores." *Marine Ecology Progress Series*, 441, 65-78.

Ramondenc, S., Nöthig, E. M., Hufnagel, L., Bauerfeind, E., Busch, K., Knüppel, N., Kraft, A., Schröter, F., Seifert, M., and Iversen, M. H. (2023). "Effects of Atlantification and changing sea-ice dynamics on zooplankton community structure and carbon flux between 2000 and 2016 in the eastern Fram Strait." *Limnology and Oceanography*, 68(S1), S39-S53.

Randelhoff, A., Reigstad, M., Chierici, M., Sundfjord, A., Ivanov, V., Cape, M., Vernet, M., Tremblay, J.-É., Bratbak, G., and Kristiansen, S. (2018). "Seasonality of the Physical and Biogeochemical Hydrography in the Inflow to the Arctic Ocean Through Fram Strait." *Frontiers in Marine Science*, 5, 224.

RCoreTeam. (2019). "R: A language and environment for statistical computing. R Foundation for statistical computing, Vienna, Austria. URL https://www.R-project.org/.".

Reigstad, M., and Wassmann, P. (2007). "Does *Phaeocystis spp.* contribute significantly to vertical export of organic carbon?", in M. A. van Leeuwe, J. Stefels, S. Belviso, C. Lancelot, P. G. Verity, and W. W. C. Gieskes, (eds.), *Phaeocystis, major link in the biogeochemical cycling of climate-relevant elements*. Dordrecht: Springer Netherlands, pp. 217-234.

Stefels, J., Dacey, J. W. H., and Elzenga, J. T. M. (2009). "In vivo DMSP-biosynthesis measurements using stable-isotope incorporation and proton-transfer-reaction mass spectrometry (PTR-MS)." *Limnology and Oceanography: Methods*, 7(8), 595-611.

Stemmann, L., Jackson, G. A., and Gorsky, G. (2004). "A vertical model of particle size distributions and fluxes in the midwater column that includes biological and physical processes—Part II: application to a three year survey in the NW Mediterranean Sea." *Deep Sea Research Part I: Oceanographic Research Papers*, 51(7), 885-908.

Stief, P., Elvert, M., and Glud, R. N. (2021). "Respiration by “marine snow” at high hydrostatic pressure: Insights from continuous oxygen measurements in a rotating pressure tank." *Limnology and Oceanography*, 66(7), 2797-2809.

Strong, C., and Rigor, I. G. (2013). "Arctic marginal ice zone trending wider in summer and narrower in winter." *Geophysical Research Letters*, 40(18), 4864-4868.

Tamburini, C., Boutrif, M., Garel, M., Colwell, R. R., and Deming, J. W. (2013). "Prokaryotic responses to hydrostatic pressure in the ocean – a review." *Environmental Microbiology*, 15(5), 1262-1274.

Tesi, T., Muschitiello, F., Mollenhauer, G., Miserocchi, S., Langone, L., Ceccarelli, C., Panieri, G., Chiggiato, J., Nogarotto, A., Hefter, J., Ingrosso, G., Giglio, F., Giordano, P., and Capotondi, L. (2021). "Rapid Atlantification along the Fram Strait at the beginning of the 20th century." *Science Advances*, 7(48), eabj2946.

Tippenhauer, S., Janout, M., Chouksey, M., Torres-Valdes, S., Fong, A., and Wulff, T. (2021). "Substantial Sub-Surface Chlorophyll Patch Sustained by Vertical Nutrient Fluxes in Fram Strait Observed With an Autonomous Underwater Vehicle." *Frontiers in Marine Science*, 8, 605225.

Tréguer, P., Bowler, C., Moriceau, B., Dutkiewicz, S., Gehlen, M., Aumont, O., Bittner, L., Dugdale, R., Finkel, Z., Iudicone, D., Jahn, O., Guidi, L., Lasbleiz, M., Leblanc, K., Levy, M., and Pondaven, P. (2018). "Influence of diatom diversity on the ocean biological carbon pump." *Nature Geoscience*, 11(1), 27-37.

Trudnowska, E., Lacour, L., Ardyna, M., Rogge, A., Irisson, J. O., Waite, A. M., Babin, M., and Stemmann, L. (2021). "Marine snow morphology illuminates the evolution of phytoplankton blooms and determines their subsequent vertical export." *Nature Communications*, 12(1), 2816.

van der Jagt, H., Friese, C., Stuut, J. B. W., Fischer, G., and Iversen, M. H. (2018). "The ballasting effect of Saharan dust deposition on aggregate dynamics and carbon export: Aggregation, settling, and scavenging potential of marine snow." *Limnology and Oceanography*, 63(3), 1386-1394.

van der Jagt, H., Wiedmann, I., Hildebrandt, N., Niehoff, B., and Iversen, M. H. (2020). "Aggregate Feeding by the Copepods *Calanus* and *Pseudocalanus* Controls Carbon Flux Attenuation in the Arctic Shelf Sea During the Productive Period." *Frontiers in Marine Science*, 7, 543124.

von Appen, W. J., Wekerle, C., Hehemann, L., Schourup-Kristensen, V., Konrad, C., and Iversen, M. H. (2018). "Observations of a Submesoscale Cyclonic Filament in the Marginal Ice Zone." *Geophysical Research Letters*, 45(12), 6141-6149.

von Appen, W.-J., Waite, A. M., Bergmann, M., Bienhold, C., Boebel, O., Bracher, A., Cisewski, B., Hagemann, J., Hoppema, M., Iversen, M. H., Konrad, C., Krumpen, T., Lochthofen, N., Metfies, K., Niehoff, B., Nöthig, E.-M., Purser, A., Salter, I., Schaber, M., Scholz, D., Soltwedel, T., Torres-Valdes, S., Wekerle, C., Wenzhöfer, F., Wietz, M., and Boetius, A. (2021). "Sea-ice derived meltwater stratification slows the biological carbon pump: results from continuous observations." *Nature Communications*, 12(1), 7309.

Wang, Q., Wekerle, C., Wang, X., Danilov, S., Koldunov, N., Sein, D., Sidorenko, D., von Appen, W. J., and Jung, T. (2020). "Intensification of the Atlantic Water Supply to the Arctic Ocean Through Fram Strait Induced by Arctic Sea Ice Decline." *Geophysical Research Letters*, 47(3), e2019GL086682.

Wekerle, C., Krumpen, T., Dinter, T., von Appen, W.-J., Iversen, M. H., and Salter, I. (2018). "Properties of Sediment Trap Catchment Areas in Fram Strait: Results From Lagrangian Modeling and Remote Sensing." *Frontiers in Marine Science*, 5, 407.

Wollenburg, J. E., Katlein, C., Nehrke, G., Nöthig, E.-M., Matthiessen, J., Wolf- Gladrow, D. A., Nikolopoulos, A., Gázquez-Sanchez, F., Rossmann, L., Assmy, P., Babin, M., Bruyant, F., Beaulieu, M., Dybwad, C., and Peeken, I. (2018). "Ballasting by cryogenic gypsum enhances carbon export in a *Phaeocystis* under-ice bloom." *Scientific Reports*, 8(1), 7703.

Wollenburg, J. E., Iversen, M., Katlein, C., Krumpen, T., Nicolaus, M., Castellani, G., Peeken, I., and Flores, H. (2020). "New observations of the distribution, morphology and dissolution dynamics of cryogenic gypsum in the Arctic Ocean." *The Cryosphere*, 14(6), 1795-1808.

General Discussion

Changing environmental conditions in the polar regions endanger polar ecosystems. Especially warming of the oceans and ongoing ice melt (IPCC 2021) impact fundamental processes in the ecosystems and influence the potential for carbon export. To infer how carbon export will be affected in the future, it is crucial to understand the processes involved in the formation, transformation, and transportation of carbon-rich aggregates. In this thesis underlying carbon export processes were investigated in three different oceanic systems in the Arctic and the Antarctic. This included carbon export processes in a Greenlandic fjord (**Chapter I**), in open waters of the Southern Ocean (**Chapter II**) and in a polar front system at the marginal ice zone in the Fram Strait in the Arctic Ocean (**Chapter III**).

How/where are aggregates formed?

Formation and export of settling aggregates contribute 50 - 70% to the total particulate organic carbon (POC) export in regard to carbon export via the biological carbon pump, while physical mixing and active migratory carbon export via zooplankton (‘particle injection pumps’) contribute the rest (Boyd et al. 2019; Nowicki et al. 2022). As many details of processes involved in the formation and export of aggregates are still not fully understood, further research on the formation and export of aggregates is needed to facilitate more precise estimates of the scope of carbon export in the ocean.

Aggregates form when a critical maximum concentration of particles, e.g. phytoplankton cells, is reached, which increases the probability of encounters and aggregate formation (Jackson and Kiørboe 2008; Kiørboe 2001). As a result, aggregate formation is most likely to occur within or immediately below the depth of chlorophyll maximum (**Chapter I**), resulting in highest aggregate abundances below the chlorophyll peak (**Chapter II, III**). In polar front systems, meltwater with a low density and low nutrient concentrations forms a stratified layer in the surface ocean **(Chapter III)**. This causes high phytoplankton concentrations directly below the meltwater layer where both light and nutrient concentrations are high, and thus enhance the aggregation processes at these depths **(Chapter III)**. The subduction of chlorophyll-rich waters in polar front systems results in deep aggregate formation and peaks in aggregate abundance at depth of up to 100 m **(Chapter III)**.

The particulate organic carbon flux was primarily formed from plankton cells that are larger than 3 µm, while smaller picoplankton (<3 µm) were rarely observed within exported material (**Chapter I**), suggesting a plankton size dependency within the collected aggregated material. Due to their small sizes and slow sinking velocity, fast recycling is assumed for

picoplankton in the surface waters, but nevertheless picoplankton can contribute to carbon export when integrated into larger aggregates or fecal pellets (Richardson and Jackson 2007). This seems not to be the case in the Greenlandic fjord Scoresby Sund, likely since larger-celled plankton are dominating the polar ecosystems and picoplankton only occur in comparatively low concentrations (Hirata et al. 2011). In addition, size selective feeding of copepods and other zooplankton could explain low export of picoplankton in fecal pellets, as zooplankton capture larger cells more efficiently (Nival and Nival 1976; Riisgård and Larsen 2010, and references therein). The preferable particle size range for feeding depends on the species and stage of development (Nival and Nival 1976; Riisgård and Larsen 2010, and references therein), and larger zooplankton species in the investigated region likely select for larger plankton cells.

During the aggregate formation the phytoplankton attached bacterial community is integrated into the aggregates as the phytoplankton coagulate (**Chapter I**). For instance, diatoms have been shown to possess associated bacteria which are crucial for the aggregation of the phytoplankton (Den et al. 2023; Gärdes et al. 2011), and probably remain attached during aggregation. This explains why the aggregate-associated bacterial community in the surface ocean is similar with the free-living bacterial community around chlorophyll maximum depth (Bachmann et al. 2018; Thiele et al. 2015). The bacterial community attached to the aggregates is exported together with the aggregates to deeper water layers, resulting in a vertical community connectivity of the prokaryotic community between the aggregates in the surface ocean and the deep ocean (**Chapter I**, Fadeev et al. 2021a; Mestre et al. 2018; Thiele et al. 2015).

What is retaining the particles in the surface ocean in polar regions?

Typically, when discussing the carbon attenuation of the POC flux, it is assumed that biological processes (e.g. grazing, respiration, remineralization) are responsible for the majority of the carbon attenuation (Giering et al. 2014; Iversen et al. 2010; Stemmann et al. 2004). However, particle distribution in the water column can only be explained when physical processes, such as retention of aggregates by density stratification in the surface ocean, are also considered. This seems to be important especially in polar ecosystems (**Chapter I, Chapter II, Chapter III**).

Density gradients are able to retain the aggregates and keep them from sinking, resulting in thin layers of high particle abundances in the surface ocean (Alldredge et al. 2002; MacIntyre et al. 1995; Möller et al. 2012). Density increase with depth reduces the sinking velocities of the aggregates with lower excess density (Kindler et al. 2010). In the Polar region with meltwater, the changes in salinity play a crucial role for the stratification (von Appen

et al. 2021). Salinity-driven density changes and the resulting stratification tend to be more stable than temperature-driven stratification (Shroyer et al. 2020). While aggregates can relatively fast cross temperature-dependent density changes, salinity-based density changes will result in a longer retention time of aggregates (Kindler et al. 2010; MacIntyre et al. 1995; Prairie et al. 2013), as diffusion of salt is a slow process, which is around 100 times slower compared to heat diffusion (Gargett et al. 2003). Hence, primarily large aggregates are retained in the surface ocean (**Chapter II**), since the duration of salt diffusion into the aggregate pore space is dependent on aggregate size and pore water volume, and less efficient over long distances (Kindler et al. 2010). Therefore, it is mainly aggregates which are ballasted by lithogenic or biogenic minerals (**Chapter I, Chapter III**) or particles which are compacted into dense aggregates, such as zooplankton fecal pellets (**Chapter I**), that are able to cross sharp density gradients.

To illustrate the impact of density gradients on aggregate export in polar systems, a rough estimate is presented here, how size-specific sinking velocities are decreasing when crossing water depths with increasing salinity gradients. It was estimated for *in situ* salinity-driven density gradients using measured sinking velocities of *in situ* collected aggregates. First, the potential density of different aggregate sizes was derived from their sinking velocities as described in Prairie et al. 2013.

For this, the Reynolds numbers (*Re*) were estimated as:

$$Re = \frac{dU}{v} \quad (1)$$

where d [cm] is the equivalent spherical diameter, U [cm s^{-1}] is the sinking velocity, and v [cm^2 s^{-1}] is the kinematic viscosity of the surrounding water.

Then, the drag coefficients (C_D) were calculated as (White 1974):

$$C_D = \frac{24}{Re} + \frac{6}{1+ Re^{0.5}} + 0.4 \quad (2)$$

The density of the aggregates ρ_a [kg m^{-3}] was derived using the equation (Ploug et al. 2008a; Prairie et al. 2013):

$$U = \sqrt{\frac{4g(\rho_a - \rho_f)d}{3\rho_f C_D}} \quad (3)$$

where g is the gravitational acceleration of 980.665 cm s^{-2}, and ρf [kg m^{-3}] is the density of the surrounding water. After the densities of the aggregates were derived, they were used to

calculate the decreased size-specific sinking velocities with changing depth and densities according to equation (3).

Figure 1 shows the drastic decrease in calculated size-specific settling velocities that aggregates of different sizes would experience as they sink into waters with higher salinity. In the example the potential sinking behavior in a meltwater impacted front system in the marginal ice zone was calculated, but similar trends likely apply for all meltwater-impacted polar regions. The calculated simulation shows that especially large aggregates have a large decrease in their settling velocities due to higher aggregate porosities and lower densities, when encountering density gradients. This example is a simple approach to gain insights in general size-specific trends, but neglects ongoing diffusion into the aggregates as they sink through a gradient, which presumably causes higher settling velocities than showed here.

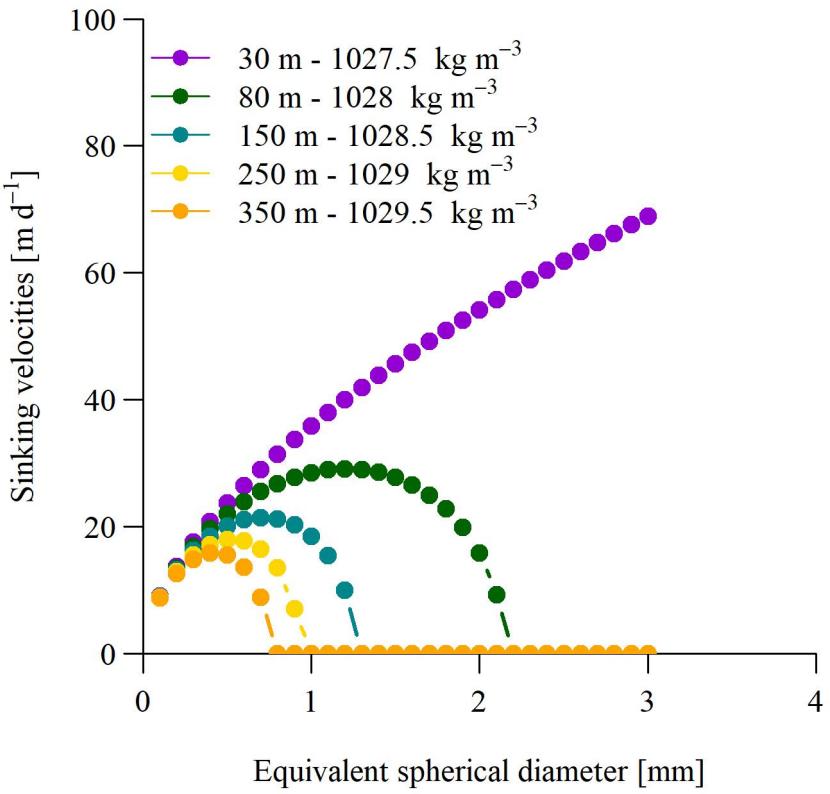

Fig. 1: (A) Sinking velocities in m d^{-1} according to equivalent spherical diameter (ESD) in mm at different depth and densities in a polar front system: at 30 m corresponding to a density of 1027.5 kg m^{-3}, 80 m corresponding to a density of 1028 kg m^{-3}, 150 m corresponding to a density of 1028.5 kg m^{-3}, 250 m corresponding to a density of 1029 kg m^{-3} and 350 m corresponding to a density of 1029.5 kg m^{-3}. The sinking velocities were calculated based on the *in situ* measurements of Marine Snow Catcher collected aggregates during the Maria S. Merian cruise MSM93 in 2020.

How does particle export change during a phytoplankton bloom development?

The changes in the export of the particulate organic matter from the epipelagic to the mesopelagic zone were investigated during an Antarctic phytoplankton bloom (**Chapter II**). During the bloom, the carbon concentrations observed in the mixed layer varied by several orders of magnitude, while at the same time the carbon flux in the lower mesopelagic zone remained constant and showed only low variability (**Chapter II**, Giering et al. 2023; Henson et al. 2023). There appears to be a decoupling between production and export of particulate organic carbon in the Southern Ocean (**Chapter II**, Giering et al. 2023; Henson et al. 2023; Maiti et al. 2013; Martin et al. 2013). It is likely that this decoupling in the Southern Ocean is caused by salinity-based particle retention (**Chapter II**) and takes also place in regions with high freshwater inflow in the Arctic Ocean resulting in a strong stratification (von Appen et al. 2021, **Chapter I, III**). Carbon export modelling based on satellite primary production observation (Siegel et al. 2014), is neglecting processes like particle retention in the surface ocean. However, the relevant constraining variable for modelling of carbon export should be the carbon flux below the retention zone, especially in polar regions. The results of the present thesis demonstrate the need to adapt current carbon export models of polar regions to consider the effect of the particle retention zones.

How does lateral advection affect particle retention?

In polar regions, aggregates are retained in the surface ocean during their export, and are subjected to lateral advection (**Chapter I**). This is making it difficult to link the area of export to the area of production and aggregate formation, which might lead to over- or underestimations of export efficiency regionally. Several studies have attempted to model the origin of aggregates that are collected at depth (Fadeev et al. 2021a; Siegel and Deuser 1997; Siegel et al. 1990; Waniek et al. 2000; Waniek et al. 2005; Wekerle et al. 2018). Depending on the speed of lateral water movement in the surface, and the density and sinking velocity of the aggregates, it has been observed that aggregates can be laterally transported, e.g. by more than 50 kilometers while being retained in the epipelagic zone in the Fram Strait (Wekerle et al. 2018). In particular in polar fjords, this lateral movement seems to be important (**Chapter I**), due to the strong estuarine movement as a result of meltwater run-offs (Bendtsen et al. 2014; Mortensen et al. 2011). However, when the particles have crossed the particle retention zone, i.e. the depths with increasing salinity gradients, they tend to be less subjected to lateral advection and show a strong vertical export (**Chapter I**). The majority of the sinking particles at depth are heavily ballasted phytoplankton aggregates or fecal pellets (**Chapter I**),

demonstrating that aggregates need to be dense and compact with relatively high size-specific settling velocities in order to be exported out of the upper ocean. These fast-settling aggregates are more likely to leave the surface ocean fast with less horizontal displacement and therefore result in less decoupling between production and export. Ultimately, it should be considered when modeling particle trajectories and carbon export, that sinking velocities of aggregates are not constant throughout the water column, which is a common assumption for models (Fadeev et al. 2021a; Siegel and Deuser 1997; Siegel et al. 1990; Waniek et al. 2000; Waniek et al. 2005; Wekerle et al. 2018). Lateral advection is impacting aggregates much stronger in the retention zone where the settling of aggregates is slowed down, which needs to be taken in account to improve particle export modelling in polar systems.

What influences the sinking velocities in polar systems aside from salinity-based particle retention?

Sinking velocities of aggregates play a crucial role for the magnitude of the carbon export (Iversen 2023). A strong size to settling velocity relationship of the aggregates is observed for aggregates of the same type e.g. in laboratory set-ups (Iversen and Ploug 2010; Iversen and Ploug 2013), but not for sinking velocities of diverse *in situ* measured aggregates in the polar ecosystem (**Chapter II, Chapter III**) or in other oceanic regions (Diercks and Asper 1997; Iversen and Lampitt 2020; Karakaş et al. 2009; Nowald et al. 2009). At the beginning of a phytoplankton bloom, the aggregates are of similar composition and the settling velocities show a stronger size dependency (**Chapter II**). This relationship becomes less size-dependent with ongoing transformation and recycling (**Chapter II**), when the aggregate composition becomes more diverse. Therefore, the status of the ecosystem, the occurring primary producers and degraders should be considered for a site-specific, realistic modelling of carbon export.

During the phytoplankton bloom in the Southern Ocean phytoplankton bloom (**Chapter II)**, aggregates became more homogenous in size, in circularity, and in solidity with depth (Giering et al. 2020; Giering et al. 2023). Increasing homogeneity of the aggregates with depth could indicate a stronger size dependency of the settling velocity again in the deep sea, but no changes in the settling behavior between 100 m and 500 m depth were observed (**Chapter II**). Those findings implied that once aggregates have crossed the retention zone in the surface ocean, they continue to sink (**Chapter II**).

Furthermore, ice-melt in polar regions and the concurrent release of lithogenic material (**Chapter I)** and cryogenic minerals (**Chapter III**) enhance the sinking velocities of aggregates. Gypsum crystals from sea ice sink with sinking velocities between 200 – 7000 m d^{-1}

(Wollenburg et al. 2020). If aggregates are ballasted by these cryogenic minerals, this results in measured sinking velocities of 40 – 1200 m d^{-1} of the aggregates (**Chapter III**). The occasional fast export events by lithogenic and cryogenic minerals make the sinking velocities for aggregates in the polar regions even more variable.

What is the impact of zooplankton feeding and transformation on the aggregates?

Zooplankton play an important role in transforming the organic matter by fragmentation (Briggs et al. 2020; Dilling and Alldredge 2000; Iversen and Poulsen 2007) and by repacking of the sinking aggregates, e.g. in fecal pellets (see Turner 2002 and references therein). Correspondingly, the organic matter below the mixed layer shows high abundances in meso-zooplankton and acantharian 18S rDNA signals (**Chapter I**), indicating a great amount of zooplankton interaction with the aggregates. Zooplankton feeding and transformation of aggregates can facilitate a strong carbon export e.g. via the production of fecal pellets (**Chapter I**) and can be regionally and temporarily the dominating carbon export mechanism. Thus, peaks in the deep-sea carbon flux occur, which are dominated by sinking fecal pellets (Lalande et al. 2011; Manno et al. 2022).

Zooplankton repacking of aggregates increases the carbon content per volume in the aggregates, especially if the carbon is exported as freshly produced fecal pellet. Hence, zooplankton repacking of aggregates should be accounted for as well when calculating carbon export according to particle size and distribution. Additional experiments on the carbon content and sinking velocities of freshly produced phytoplankton aggregates and fecal pellets were performed during the polar front study by incubating fresh phytoplankton from the marginal ice zone with copepods in roller tanks. Copepods produced fresh fecal pellets with a carbon content of 330 µg mm^{-3}, while at the same time the carbon content of fresh phytoplankton aggregates was between 0.4 – 4 µg mm^{-3}, and thereby notably less compared to the fecal pellets of the copepods (Fig. 2). Nevertheless, it is important to keep in mind that the carbon content of fecal pellets is dependent on diet of the copepods (Ploug et al. 2008b). Fecal pellets of copepods reached similar sinking velocities as phytoplankton aggregates despite having smaller equivalent spherical diameters (ESD), when sinking velocities of the experimental particles were measured (Fig. 2). The small, fast-sinking and carbon-rich fecal pellets are very efficient in carbon export in comparison to phytoplankton aggregates.

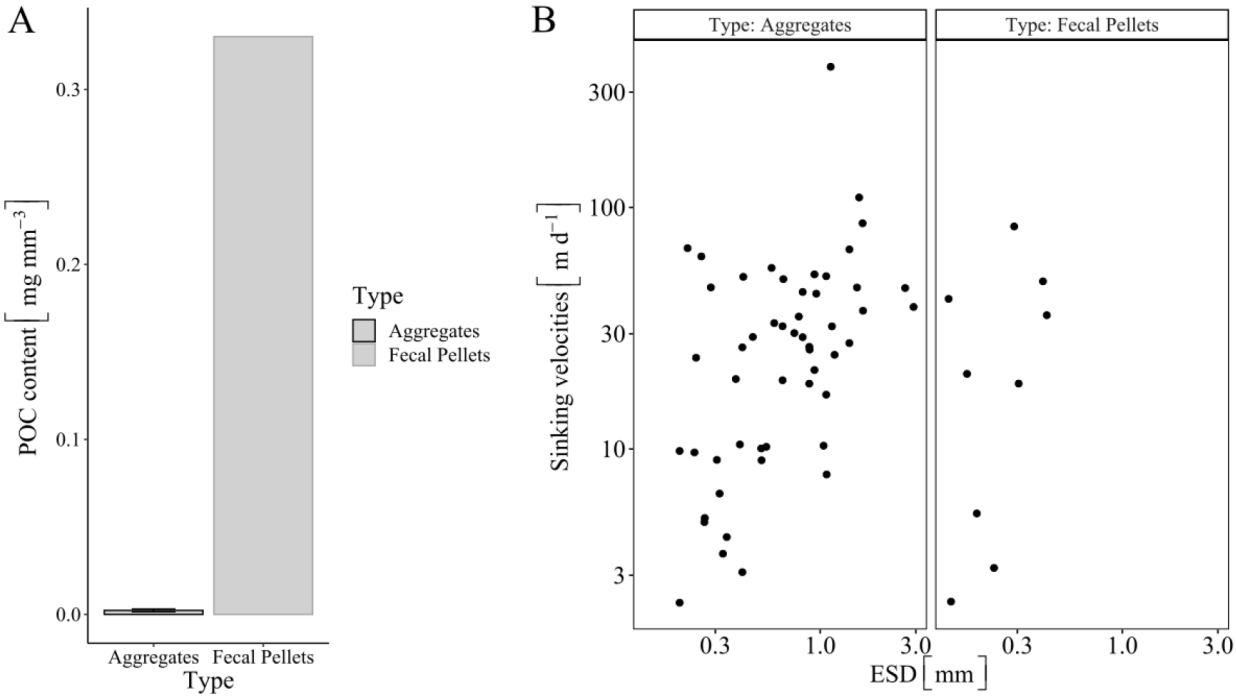

Fig. 2: (A) Particulate organic carbon (POC) content in mg mm^{-3} for phytoplankton aggregates and fecal pellets and (B) logarithmically scaled sinking velocities in m d^{-1} according to logarithmically scaled equivalent spherical diameter (ESD) in mm of aggregates and fecal pellets.

The zooplankton-aggregate interactions do not only impact the carbon export and the aggregate composition and structure, but also the associated microbial community. With the transformation of organic matter into fecal pellets by zooplankton, bacteria associated to zooplankton are enriched in the aggregate and subsequently also in the particulate organic matter flux (**Chapter I**). This can serve as another explanation why the aggregate-attached microbial communities at depth differ from the free-living bacteria in the surrounding water column (Fadeev et al. 2021a; Thiele et al. 2015).

How does the aggregate export impact the availability of non-aggregated eukaryotes or bacteria at depth?

The availability of small eukaryotes and bacteria in the water column at mesopelagic depth and deeper is mainly determined by the aggregates crossing the retention zone and ongoing zooplankton-aggregate interactions at depth (**Chapter I**). During the process of disaggregation, the aggregates release their components, including eukaryotes and bacteria, to the surrounding water column (**Chapter I**). The vertical connectivity between aggregate-attached and free-living organisms is widely observed and described for bacteria (Fadeev et al. 2021a; Mestre et al. 2018; Thiele et al. 2015), but likely also applies to the eukaryotic components of the aggregates to a certain extent. Nevertheless, as only DNA samples were

analyzed at depth (**Chapter I**), this cannot tell anything about the conditions of the eukaryotes released into the water column during disaggregation. Phototrophic eukaryotic primary producers from the surface ocean are likely not active in the dark ocean anymore, and were probably non-viable and released as detritus. Heterotrophic eukaryotic degraders, on the other hand, might still be viable and active. Hence, the type of aggregates that are able to cross the retention zone can impact the eukaryotic and prokaryotic community composition which is found at depth. If sinking particulate organic matter does not disintegrate before reaching the sea floor, it can contribute to the benthic-pelagic coupling by introducing organic material to the benthic zone. Thereby, sinking aggregates directly impact the benthic community in quality and quantity of the available organic material, e.g. large deposition by ice algae (Boetius et al. 2013), and the species composition of the benthic community (Fadeev et al. 2021a; Rapp et al. 2018).

What is the influence of meltwater on the carbon export in polar regions in the future?

Carbon export in polar regions is highly dependent on the salinity-induced stratification (von Appen et al. 2021). There is strong particle retention in the Southern Ocean (**Chapter II**) and in the Arctic (**Chapter I, III)**. This particle retention is the reason why areas, which are influenced by meltwater, show lower carbon export compared to areas with a formed mixed layer (von Appen et al. 2021). The longer the aggregates are retained in the upper water column, the more is the organic matter subjected to reprocessing and recycling by microorganisms as well as zooplankton (von Appen et al. 2021). On the other hand, the carbon export can be enhanced by melting ice that releases ice algae (Boetius et al. 2013) as well as cryogenic minerals, e.g. gypsum, (Wollenburg et al. 2020; Wollenburg et al. 2018) together with meltwater. In addition, more particulate organic carbon is exported in regions covered by sea ice with diatom-rich aggregates, as in region without sea ice cover and *Phaeocystis*-rich aggregates (Fadeev et al. 2021a). Overall, the export of carbon in meltwater-influenced areas results from a complex interplay of biological and physical processes, and small changes in this complex interacting system can have serious consequences for magnitude of carbon export.

In the near future, the increasing temperature in the polar regions will lead to enhanced ice melt in polar areas and a widening of the marginal ice zone in summer time (Strong and Rigor 2013). The salinity gradients will increase in their magnitude due to the intensified release of fresh meltwater, which reinforce stratification and ultimately strengthen the particle retention in surface waters. Limited nutrient resupply into surface waters by stratification can result in decreasing primary production (von Appen et al. 2021). The carbon export will most likely be reduced with more intense stratification, leading to a reinforced decoupling between the

primary production in the euphotic zone and the export of particulate organic matter into the mesopelagic zone (**Chapter II**). In coastal areas or fjord systems with high lithogenic input, the carbon export might on the other hand increase (**Chapter I**) in limited areas. Also, short intense carbon export events due to ice algae release at the beginning of the ice melt (Boetius et al. 2013) or cryomineral release (**Chapter III**) might take place, but will be less important with ongoing ice melt and with low concentration of sea-ice in the future. Predicted shifts in the phytoplankton community towards higher abundances of the haptophyte *Phaeocystis* (Nöthig et al. 2015), which lead to more slow-sinking aggregates (Fadeev et al. 2021a), will further decrease the carbon export in polar system in the future.

The efficiency of the carbon export will, besides physical parameters influencing melting of sea ice and stratification, directly depend on the reaction of zooplankton communities on the changing environmental conditions. Zooplankton, such as copepods, contribute a major share to the carbon export by the production of dense and fast-sinking fecal pellets (**Chapter I**). Zooplankton can, together with other heterotrophic organisms, possibly prolong primary productivity by releasing nutrients in the surface ocean (Iversen 2023). If the increased stratification and retention of particulate organic carbon in the surface ocean is followed by an increased zooplankton feeding and fecal pellet production, carbon could still be efficiently exported. On the other hand, shifts in the dominating grazers can decrease the carbon flux in the respective regions, e.g. shifts from krill to salps in the Southern Ocean, as salp fecal pellets are more prone to fragmentation and recycling than krill fecal pellets, and are more likely retained in the surface ocean (Pauli et al. 2021).

An additional parameter influencing the carbon export in the future is earlier ice-break up, which can lead to an earlier phytoplankton bloom in the year that could result in a mismatch in timing between primary production and zooplankton growth (Sakshaug 2004). This could prevent the production of carbon-rich fecal pellets and reduce the carbon export. Furthermore, a shift to phytoplankton-aggregate dominated carbon export may intensify the loss of nutrients for the surface planktonic community, as phytoplankton contain much higher nutrient ratios than fecal pellets (Daly et al. 1999).

Altogether, multiple processes and parameters influence the carbon export in polar regions and will impact future changes. While the interactions are complex and make it complicate to infer on direct changes in the carbon export, key players involved in carbon fluxes in polar regions, which can have major impacts on the magnitude of export, are the salinity-driven density stratification, the present zooplankton community and temporal and spatial co-occurrence of phytoplankton

Implication for carbon export in non-polar ecosystems

Retention of aggregates in salinity gradients, as it occurs in polar systems impacted by meltwater from glaciers or sea-ice, plays also a role in coastal or brackish ecosystems with a lot of freshwater input by the run-off from rivers, e.g. in the Pacific (Alldredge et al. 2002; MacIntyre et al. 1995) or the Baltic Sea (Möller et al. 2012). In low latitude systems, the surface ocean is subjected to high evaporation, which leads in contrast to high salinities in the surface waters, e.g. in the North and South Atlantic gyre (Melzer and Subrahmanyam 2017). Aggregates that are formed in these saline surface waters contain those high-saline waters in their pore spaces, which likely increase their sinking velocities when they reach less saline water zones below the aggregate-formation areas. Nevertheless, these regions are dominated by small-celled phytoplankton (Acevedo-Trejos et al. 2015; Hirata et al. 2011), which results in smaller aggregates with low sinking velocities and more intense microbial recycling (Guidi et al. 2009). Overall, the effect of high salinity in the pore water is presumably neglectable for the sinking velocities of those small aggregates, as their porosity and thus pore water volume is considerably smaller compared to large aggregates (Logan and Wilkinson 1990). Salinity-driven density gradients will, therefore, likely not impact carbon export in non-polar systems as much as in polar systems. Those regional differences in mechanisms driving the carbon export must be reflected in global carbon export modelling.

Future scientific sampling and research

The results in the present thesis highlight the complex interactions of multiple factors and processes involved in carbon export in polar regions and suggest that more *in situ* observations of the detailed processes related to carbon export are needed. While laboratory set-ups allow experiments under controlled conditions varying only in one or two variables, they are not able to simulate the complex interaction of physical environmental conditions and biological processes occurring in nature. However, sampling in the natural environment also comes with several challenges. Lateral advection, e.g. in polar fjords (**Chapter I)**, or subduction of water masses, e.g. in the marginal ice zone (**Chapter III,** Hofmann et al. 2024) are displacing the organic matter from its area of formation horizontally or in depth. Strong water movement can lead to changing environmental conditions in just a few meters or kilometers distance both horizontally and vertically in the water column, e.g. in submesoscale filaments (Fadeev et al. 2021b), front systems (**Chapter III**), or fjords (**Chapter I**). Therefore, it is a great challenge to ensure, that samples and measurements of different scientific gear deployed after each other from research vessels target the same water mass and sample e.g. the same aggregate type.

Furthermore, there is the risk of missing locally restricted spontaneous export events such as cryogenic mineral ballasting or export of ice algae.

Scientific devices which are able to measure multiple parameters simultaneously are of interest for studying these complex and fast-changing systems. A first step was done by combining several camera systems to simultaneously sample for aggregate abundance, aggregate characteristics, and zooplankton abundance in a polar front system (**Chapter III).** Additionally, *in situ* measurements of settling, respiration, as well as the structure and biogeochemical composition of aggregates are necessary to identify changes in these parameters in changing environmental condition with varying water masses. For *in situ* respiration measurements in the water column, the RESPIRE trap (Boyd et al. 2015) has been developed but the trap does not acquire information on the settling velocities or the 3-D structures of the aggregates. For the long-term observatory HAUSGARTEN in the Fram Strait, first trail runs for joint sampling of *in situ* measurements of settling, respiration, and the structure and biogeochemical the composition of aggregates are planned using moored BioOptical Platforms with integrated oxygen sensor, which is being developed by the SeaPump Group (bridging group between the Alfred Wegener Institute for Polar and Marine Research, University of Bremen, and MARUM - Center for Marine Environmental Sciences). Smaller samplings systems for short-term deployment could, besides long-term monitoring systems, fill current knowledge gaps and provide new insight on the behavior of settling, respiration, and the composition of aggregates under *in situ* environmental conditions.

As carbon export is driven by biological, physical, as well as chemical processes, more interdisciplinary approaches combining data, such as long-term mooring observation, data from automatic samplers and autonomous vehicles, shipboard data, and satellite data, are needed in the future. This will also help to get a better understanding of carbon cycling during the winter time with difficult ice conditions, as sampling in the polar regions is at the moment still limited mainly to summer time.

New possibilities for data analysis are opening with the use of machine learning or the use of artificial intelligence, which can be used to optimize current carbon export models. Using morphological information of aggregates from the Underwater Vision Profiler (UVP), Trudnowska et al. (2021) classified different types of aggregates. In the present thesis, a first attempt was done to classify different morphotypes of aggregates recorded with a “remotely observing *in situ* camera for aggregates” system (ROSINA) system and differentiate between different aggregate types in the mixing water masses in an Arctic front system in the Fram Strait. During the front study, it was not possible to differentiate between different morphotypes

of aggregates occurring in different water masses. This could either be because of optical limits of ROSINA by technical parameters, e.g. low visibility of transparent *Phaeocystis* colonies, but also because of low biological variability in the majority of aggregates observed in the front system, an explanation that was also supported by microscopic assessments. Nevertheless, scientific camera gear and algorithms for data analysis will be improved in the future and will likely be able to differentiate aggregates by their morphology in different types already underwater during sampling.

Carbon content, sinking velocities and export efficiency vary for different aggregates types and compositions (e.g. Fadeev et al. 2021a; Iversen and Ploug 2010; Pauli et al. 2021). For accurate prediction on future developments in the oceanic carbon export, it is crucial to improve global models such as PISCES (Aumont et al. 2015) or PlankTOM12 (Denvil-Sommer et al. 2023). We need to understand, how different plankton communities of primary producers and degraders and environmental factors, such as sea ice or lithogenic ballasting, influence the aggregate types in the ecosystem and their retention in the surface water. By understanding how much carbon is typically exported by different aggregate morphotypes using changing *in situ* carbon content, sinking velocities and respiration rate with depth, model prediction will get closer to reality.

Conclusion

Several research questions were addressed in the present PhD thesis focusing on the formation, transportation and transformation of the organic matter from the surface ocean to the deep sea. To address the hypothesis postulated in the beginning of this thesis, the following main conclusions can be drawn:

1. **Aggregate formation takes place at the depth of the highest particle concentration at the depth of high chlorophyll. This is also the place of bacteria colonization.**

This hypothesis was supported by the results of the present thesis, as aggregates were formed within or directly below the depth of high chlorophyll (**Chapter I, II, III**), resulting in deep aggregate formation if chlorophyll-rich water was subducted (**Chapter III**). Furthermore, the majority of bacteria seemed to be attached to phytoplankton or small particles prior to aggregation and were incorporated into the aggregates during aggregate formation (**Chapter I**).

2. **The main share of aggregates is retained in the upper ocean due to physical properties, i.e. salinity gradients.**

The majority of the aggregates and particulate organic carbon was retained in the epipelagic ocean due to stratification by meltwater which formed an increasing salinity gradient in the upper water column (**Chapter I, II**), supporting the postulated hypothesis. The particle retention can lead to a spatial and temporal decoupling of primary production in the photic zone and carbon flux to the deep ocean (**Chapter I, II**). This phenomenon should apply for all areas in high latitudes with continuing surface meltwater input.

3. **The particle retention depends on the aggregate type and size: Mainly smaller and denser aggregates, e.g. fecal pellets and ballasted phytoplankton aggregates, are able to pass increasing density gradients and be exported out of the epipelagic zone.**

The results underpin the hypothesis, since primarily large porous aggregates with low excess densities were retained by increasing salinities with deeper depth (**Chapter II**). Dense aggregates, such as fecal pellets or aggregates ballasted by lithogenic ballast material, on the other hand, were efficiently exported from the epipelagic zone (**Chapter I**).

4. **During their descend through the water column, organic aggregates undergo transformation, e.g. by zooplankton feeding, which changes the aggregate characteristics with increasing depth.**

Zooplankton feeding and the resulting production of fecal pellet led to denser aggregates with higher carbon content and faster sinking velocities and to an enrichment of zooplankton-associated bacterial groups in the sinking organic matter (**Chapter I**), supporting the initial hypothesis.

5. **In polar regions, effective carbon export through aggregates is a result of ballasting by minerals, zooplankton transformation, and physical subduction processes. Carbon export is impacted by lateral advection in the water layers.**

Results in the present thesis demonstrate that different processes contributed to carbon export in the polar ecosystems: i) carbon export by deeper aggregate formation due to subduction of chlorophyll-rich water (**Chapter III**, Fig. 3 A), ii) by the production and export of zooplankton fecal pellets (**Chapter I**, Fig. 3 B), and iii) by enhanced sinking velocities of aggregates as a result of the incorporation of lithogenic ballast material (**Chapter I**, Fig. 3 C) or cryogenic minerals from ice (**Chapter III**, Fig. 3 A). In polar fjords (**Chapter I**) and fronts (**Chapter III**), aggregates are subjected to strong lateral advection during sinking, resulting in a displacement of the organic matter before export from the epipelagic zone. Effects of different carbon export mechanisms and horizontal transport need to be considered to accurately assess the carbon export to the deep ocean by sinking organic material.

In summary, carbon content, sinking velocities, and export efficiency vary for different aggregate types and within the different ocean areas but are crucial parameters for accurate prediction on future developments of the carbon export in the ocean. Carbon export models can only be improved when processes such as the decoupling of primary production and carbon export in polar regions, density gradients leading to particle retention, lateral advection and subduction of particulate organic matter, and local shifts due to melting sea ice, lithogenic ballasting, and changes in zooplankton communities are appropriately reflected in the models. By further understanding how much carbon is typically exported by which key processes in the different regions with their local characteristics, model prediction will get closer to reality. Ultimately, those models will facilitate a more precise insight in the ocean's role as carbon sink.

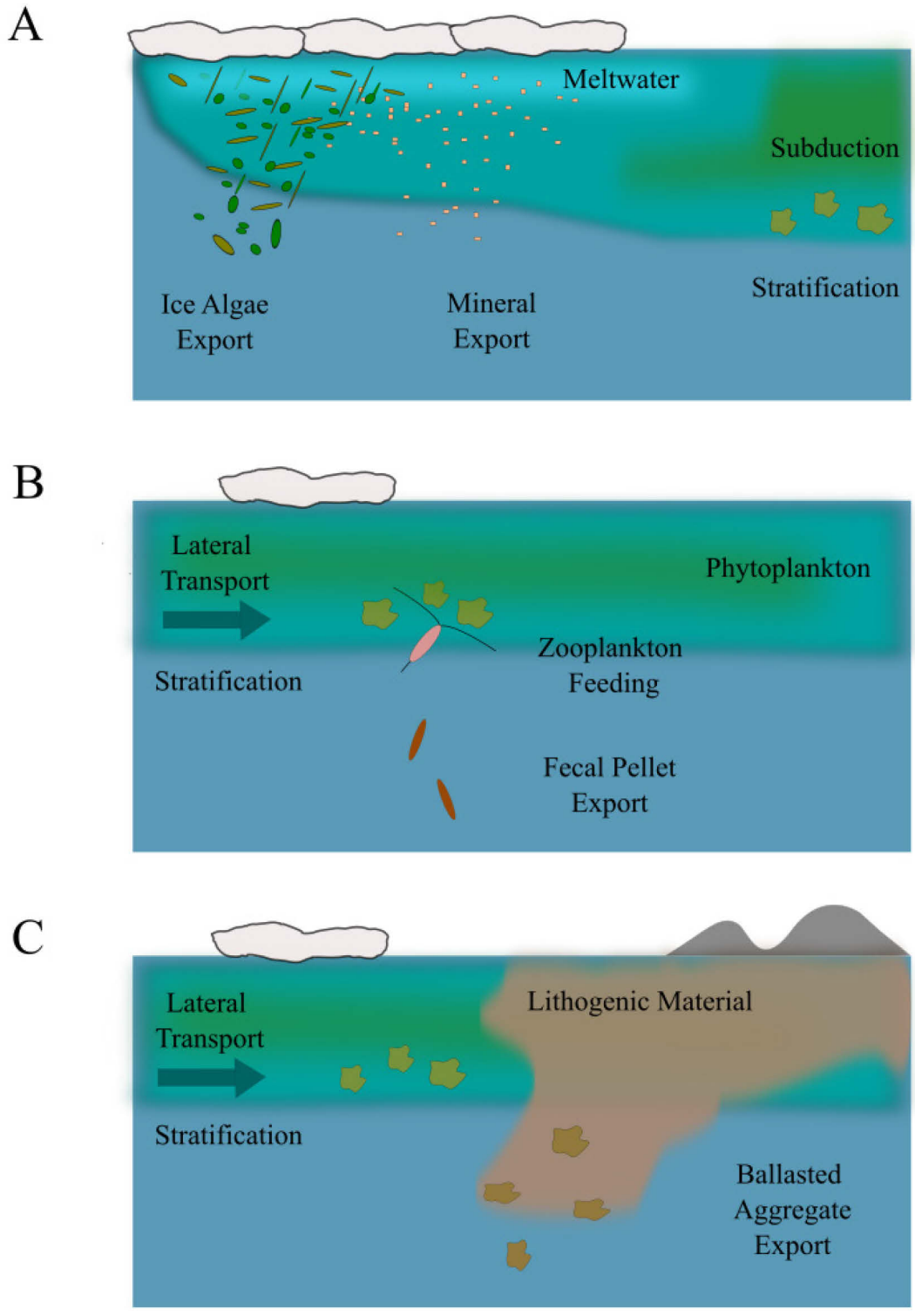

Fig. 3: Export mechanisms in polar ecosystem: (A) Melting of sea ice results into the export of organic matter by the ice algae and cryogenic minerals, chlorophyll-rich water is subducted below meltwater resulting into efficient aggregate formation. (B) Aggregates are laterally transported while being retained in the stratified surface ocean. Particulate organic carbon (POC) is exported by zooplankton feeding and the subsequent generation of fecal pellets or (C) by aggregates ballasted by lithogenic material.

References

Acevedo-Trejos, E., Brandt, G., Bruggeman, J., and Merico, A. (2015). "Mechanisms shaping size structure and functional diversity of phytoplankton communities in the ocean." *Scientific Reports*, 5(1), 8918.

Alldredge, A. L., Cowles, T. J., MacIntyre, S., Rines, J. E. B., Donaghay, P. L., Greenlaw, C. F., Holliday, D. V., Dekshenieks, M. M., Sullivan, J. M., and Zaneveld, J. R. V. (2002). "Occurrence and mechanisms of formation of a dramatic thin layer of marine snow in a shallow Pacific fjord." *Marine Ecology Progress Series*, 233, 1-12.

Aumont, O., Éthé, C., Tagliabue, A., Bopp, L., and Gehlen, M. (2015). "PISCES-v2: an ocean biogeochemical model for carbon and ecosystem studies." *Geoscientific Model Development*, 8(8), 2465-2513.

Bachmann, J., Heimbach, T., Hassenrück, C., Kopprio, G. A., Iversen, M. H., Grossart, H. P., and Gärdes, A. (2018). "Environmental Drivers of Free-Living vs. Particle-Attached Bacterial Community Composition in the Mauritania Upwelling System." *Frontiers in Microbiology*, 9, 2836.

Bendtsen, J., Mortensen, J., and Rysgaard, S. (2014). "Seasonal surface layer dynamics and sensitivity to runoff in a high Arctic fjord (Young Sound/Tyrolerfjord, 74°N)." *Journal of Geophysical Research: Oceans*, 119(9), 6461-6478.

Boetius, A., Albrecht, S., Bakker, K., Bienhold, C., Felden, J., Fernández-Méndez, M., Hendricks, S., Katlein, C., Lalande, C., Krumpen, T., Nicolaus, M., Peeken, I., Rabe, B., Rogacheva, A., Rybakova, E., Somavilla, R., and Wenzhöfer, F. (2013). "Export of Algal Biomass from the Melting Arctic Sea Ice." *Science*, 339(6126), 1430-1432.

Boyd, P. W., McDonnell, A., Valdez, J., LeFevre, D., and Gall, M. P. (2015). "RESPIRE: An in situ particle interceptor to conduct particle remineralization and microbial dynamics studies in the oceans' Twilight Zone." *Limnology and Oceanography: Methods*, 13(9), 494-508.

Boyd, P. W., Claustre, H., Levy, M., Siegel, D. A., and Weber, T. (2019). "Multi-faceted particle pumps drive carbon sequestration in the ocean." *Nature*, 568(7752), 327-335.

Briggs, N., Dall'Olmo, G., and Claustre, H. (2020). "Major role of particle fragmentation in regulating biological sequestration of CO_2 by the oceans." *Science*, 367(6479), 791-793.

Daly, K. L., Wallace, D. W. R., Smith Jr., W. O., Skoog, A., Lara, R., Gosselin, M., Falck, E., and Yager, P. L. (1999). "Non-Redfield carbon and nitrogen cycling in the Arctic: Effects of ecosystem structure and dynamics." *Journal of Geophysical Research: Oceans*, 104(C2), 3185-3199.

Den, T. Q., Neu, T. R., Sultana, S., Giebel, H.-A., Simon, M., and Billerbeck, S. (2023). "Distinct glycoconjugate cell surface structures make the pelagic diatom *Thalassiosira rotula* an attractive habitat for bacteria." *Journal of Phycology*, 59(2), 309-322.

Denvil-Sommer, A., Buitenhuis, E. T., Kiko, R., Lombard, F., Guidi, L., and Le Quéré, C. (2023). "Testing the reconstruction of modelled particulate organic carbon from surface ecosystem components using PlankTOM12 and machine learning." *Geoscientific Model Development*, 16(10), 2995-3012.

Diercks, A.-R., and Asper, V. L. (1997). "*In situ* settling speeds of marine snow aggregates below the mixed layer: Black Sea and Gulf of Mexico." *Deep Sea Research Part I: Oceanographic Research Papers*, 44(3), 385-398.

Dilling, L., and Alldredge, A. L. (2000). "Fragmentation of marine snow by swimming macrozooplankton: A new process impacting carbon cycling in the sea." *Deep Sea Research Part I: Oceanographic Research Papers*, 47(7), 1227-1245.

Fadeev, E., Rogge, A., Ramondenc, S., Nöthig, E.-M., Wekerle, C., Bienhold, C., Salter, I., Waite, A. M., Hehemann, L., Boetius, A., and Iversen, M. H. (2021a). "Sea ice presence is linked to higher carbon export and vertical microbial connectivity in the Eurasian Arctic Ocean." *Communications Biology*, 4(1), 1255.

Fadeev, E., Wietz, M., von Appen, W. J., Iversen, M. H., Nöthig, E. M., Engel, A., Grosse, J., Graeve, M., and Boetius, A. (2021b). "Submesoscale physicochemical dynamics directly shape bacterioplankton community structure in space and time." *Limnology and Oceanography*, 66(7), 2901-2913.

Gärdes, A., Iversen, M. H., Grossart, H.-P., Passow, U., and Ullrich, M. S. (2011). "Diatom-associated bacteria are required for aggregation of *Thalassiosira weissflogii*." *The ISME Journal*, 5(3), 436-445.

Gargett, A. E., Merryfield, W. J., and Holloway, G. (2003). "Direct Numerical Simulation of Differential Scalar Diffusion in Three-Dimensional Stratified Turbulence." *Journal of Physical Oceanography*, 33(8), 1758-1782.

Giering, S. L. C., Sanders, R., Lampitt, R. S., Anderson, T. R., Tamburini, C., Boutrif, M., Zubkov, M. V., Marsay, C. M., Henson, S. A., Saw, K., Cook, K., and Mayor, D. J. (2014). "Reconciliation of the carbon budget in the ocean's twilight zone." *Nature*, 507(7493), 480-483.

Giering, S. L. C., Hosking, B., Briggs, N., and Iversen, M. H. (2020). "The Interpretation of Particle Size, Shape, and Carbon Flux of Marine Particle Images Is Strongly Affected by the Choice of Particle Detection Algorithm." *Frontiers in Marine Science*, 7, 564.

Giering, S. L. C., Sanders, R., Blackbird, S., Briggs, N., Carvalho, F., East, H., Espinola, B., Henson, S. A., Kiriakoulakis, K., Iversen, M. H., Lampitt, R. S., Pabortsava, K., Pebody, C., Peel, K., Preece, C., Saw, K., Villa-Alfageme, M., and Wolff, G. A. (2023). "Vertical imbalance in organic carbon budgets is indicative of a missing vertical transfer during a phytoplankton bloom near South Georgia (COMICS)." *Deep Sea Research Part II: Topical Studies in Oceanography*, 209, 105277.

Guidi, L., Stemmann, L., Jackson, G. A., Ibanez, F., Claustre, H., Legendre, L., Picheral, M., and Gorskya, G. (2009). "Effects of phytoplankton community on production, size, and export of large aggregates: A world-ocean analysis." *Limnology and Oceanography*, 54(6), 1951-1963.

Henson, S. A., Briggs, N., Carvalho, F., Manno, C., Mignot, A., and Thomalla, S. (2023). "A seasonal transition in biological carbon pump efficiency in the northern Scotia Sea, Southern Ocean." *Deep Sea Research Part II: Topical Studies in Oceanography*, 208, 105274.

Hirata, T., Hardman-Mountford, N. J., Brewin, R. J. W., Aiken, J., Barlow, R., Suzuki, K., Isada, T., Howell, E., Hashioka, T., and Noguchi-Aita, M. (2011). "Synoptic relationships between surface Chlorophyll-*a* and diagnostic pigments specific to phytoplankton functional types." *Biogeosciences*, 8(2), 311-327.

Hofmann, Z., von Appen, W.-J, Kanzow, T., Becker, H., Hagemann, J., Hufnagel, L., and Iversen, M.H. (2024): "Stepwise Subduction Observed at a Front in the Marginal Ice Zone in Fram Strait." *Journal of Geophysical Research: Oceans*, 129(5), e2023JC020641.

IPCC. (2021). "Climate Change 2021: The Physical Science Basis. Contribution of Working Group I to the Sixth Assessment Report of the Intergovernmental Panel on Climate Change [Masson-Delmotte, V., Zhai, P., Pirani, A., Connors, S. L., Péan, C., Berger, S., Caud, N., Chen, Y., Goldfarb, L., Gomis, M. I., Huang, M., Leitzell, K., Lonnoy, E., Matthews, J. B. R., Maycock, T. K., Waterfield, T., Yelekçi, O., Yu, R., and Zhou, B. (eds.)]. Cambridge University Press, Cambridge, United Kingdom and New York, NY, USA, 2391 pp.".

Iversen, M. H., and Poulsen, L. K. (2007). "Coprorhexy, coprophagy, and coprochaly in the copepods *Calanus helgolandicus*, *Pseudocalanus elongatus*, and *Oithona similis*." *Marine Ecology Progress Series*, 350, 79-89.

Iversen, M. H., and Ploug, H. (2010). "Ballast minerals and the sinking carbon flux in the ocean: carbon-specific respiration rates and sinking velocity of marine snow aggregates."

Biogeosciences, 7(9), 2613-2624.

Iversen, M. H., Nowald, N., Ploug, H., Jackson, G. A., and Fischer, G. (2010). "High resolution profiles of vertical particulate organic matter export off Cape Blanc, Mauritania: Degradation processes and ballasting effects." *Deep Sea Research Part I: Oceanographic Research Papers*, 57(6), 771-784.

Iversen, M. H., and Ploug, H. (2013). "Temperature effects on carbon-specific respiration rate and sinking velocity of diatom aggregates – potential implications for deep ocean export processes." *Biogeosciences*, 10(6), 4073-4085.

Iversen, M. H., and Lampitt, R. S. (2020). "Size does not matter after all: no evidence for a size-sinking relationship for marine snow." *Progress in Oceanography*, 189, 102445.

Iversen, M. H. (2023). "Carbon Export in the Ocean: A Biologist's Perspective." *Annual Review of Marine Science*, 15(1), 357-381.

Jackson, G. A., and Kiørboe, T. (2008). "Maximum phytoplankton concentrations in the sea." *Limnology and Oceanography*, 53(1), 395-399.

Karakaş, G., Nowald, N., Schäfer-Neth, C., Iversen, M., Barkmann, W., Fischer, G., Marchesiello, P., and Schlitzer, R. (2009). "Impact of particle aggregation on vertical fluxes of organic matter." *Progress in Oceanography*, 83(1-4), 331-341.

Kindler, K., Khalili, A., and Stocker, R. (2010). "Diffusion-limited retention of porous particles at density interfaces." *Proceedings of the National Academy of Sciences*, 107(51), 22163-22168.

Kiørboe, T. (2001). "Formation and fate of marine snow: small-scale processes with large-scale implications." *Scientia Marina*, 65(S2), 57-71.

Lalande, C., Bauerfeind, E., and Nöthig, E.-M. (2011). "Downward particulate organic carbon export at high temporal resolution in the eastern Fram Strait: influence of Atlantic Water on flux composition." *Marine Ecology Progress Series*, 440, 127-136.

Logan, B. E., and Wilkinson, D. B. (1990). "Fractal geometry of marine snow and other biological aggregates." *Limnology and Oceanography*, 35(1), 130-136.

MacIntyre, S., Alldredge, A. L., and Gotschalk, C. C. (1995). "Accumulation of marines now at density discontinuities in the water column." *Limnology and Oceanography*, 40(3), 449-468.

Maiti, K., Charette, M. A., Buesseler, K. O., and Kahru, M. (2013). "An inverse relationship between production and export efficiency in the Southern Ocean." *Geophysical Research Letters*, 40(8), 1557-1561.

Manno, C., Stowasser, G., Fielding, S., Apeland, B., and Tarling, G. A. (2022). "Deep carbon export peaks are driven by different biological pathways during the extended Scotia Sea (Southern Ocean) bloom." *Deep Sea Research Part II: Topical Studies in Oceanography*, 205, 105183.

Martin, P., van der Loeff, M. R., Cassar, N., Vandromme, P., d'Ovidio, F., Stemmann, L., Rengarajan, R., Soares, M., González, H. E., Ebersbach, F., Lampitt, R. S., Sanders, R., Barnett, B. A., Smetacek, V., and Naqvi, S. W. A. (2013). "Iron fertilization enhanced net community production but not downward particle flux during the Southern Ocean iron fertilization experiment LOHAFEX." *Global Biogeochemical Cycles*, 27(3), 871-881.

Melzer, B. A., and Subrahmanyam, B. (2017). "Decadal changes in salinity in the oceanic subtropical gyres." *Journal of Geophysical Research: Oceans*, 122(1), 336-354.

Mestre, M., Ruiz-González, C., Logares, R., Duarte, C. M., Gasol, J. M., and Montserrat Sala, M. (2018). "Sinking particles promote vertical connectivity in the ocean microbiome." *Proceedings of the National Academy of Sciences*, 115(29), E6799-E6807.

Möller, K. O., St. John, M., Temming, A., Floeter, J., Sell, A. F., Herrmann, J.-P., and Möllmann, C. (2012). "Marine snow, zooplankton and thin layers: indications of a trophic link from small-scale sampling with the Video Plankton Recorder." *Marine Ecology Progress Series*, 468, 57-69.

Mortensen, J., Lennert, K., Bendtsen, J., and Rysgaard, S. (2011). "Heat sources for glacial melt in a sub-Arctic fjord (Godthåbsfjord) in contact with the Greenland Ice Sheet." *Journal of Geophysical Research: Oceans*, 116(C1).

Nival, P., and Nival, S. (1976). "Particle retention efficiencies of an herbivorous copepod, *Acartia clausi* (adult and copepodite stages): Effects on grazing 1." *Limnology and Oceanography*, 21(1), 24-38.

Nöthig, E.-M., Bracher, A., Engel, A., Metfies, K., Niehoff, B., Peeken, I., Bauerfeind, E., Cherkasheva, A., Gäbler-Schwarz, S., Hardge, K., Kilias, E., Kraft, A., Mebrahtom Kidane, Y., Lalande, C., Piontek, J., Thomisch, K., and Wurst, M. (2015). "Summertime plankton ecology in Fram Strait—a compilation of long-and short-term observations." *Polar Research*, 34(1), 23349.

Nowald, N., Fischer, G., Ratmeyer, V., Iversen, M., Reuter, C., and Wefer, G. (2009). "In-situ sinking speed measurements of marine snow aggregates acquired with a settling chamber mounted to the Cherokee ROV"*Oceans 2009-Europe*. City: Bremen,

Germany, pp. 1-6.

Nowicki, M., DeVries, T., and Siegel, D. A. (2022). "Quantifying the Carbon Export and Sequestration Pathways of the Ocean's Biological Carbon Pump." *Global Biogeochemical Cycles*, 36(3), e2021GB007083.

Pauli, N.-C., Flintrop, C. M., Konrad, C., Pakhomov, E. A., Swoboda, S., Koch, F., Wang, X.-L., Zhang, J.-C., Brierley, A. S., Bernasconi, M., Meyer, B., and Iversen, M. H. (2021). "Krill and salp faecal pellets contribute equally to the carbon flux at the Antarctic Peninsula." *Nature Communications*, 12(1), 7168.

Ploug, H., Iversen, M. H., and Fischer, G. (2008a). "Ballast, sinking velocity, and apparent diffusivity within marine snow and zooplankton fecal pellets: Implications for substrate turnover by attached bacteria." *Limnology and Oceanography*, 53(5), 1878-1886.

Ploug, H., Iversen, M. H., Koski, M., and Buitenhuis, E. T. (2008b). "Production, oxygen respiration rates, and sinking velocity of copepod fecal pellets: Direct measurements of ballasting by opal and calcite." *Limnology and Oceanography*, 53(2), 469-476.

Prairie, J. C., Ziervogel, K., Arnosti, C., Camassa, R., Falcon, C., Khatri, S., McLaughlin, R. M., White, B. L., and Yu, S. (2013). "Delayed settling of marine snow at sharp density transitions driven by fluid entrainment and diffusion-limited retention." *Marine Ecology Progress Series*, 487, 185-200.

Rapp, J. Z., Fernández-Méndez, M., Bienhold, C., and Boetius, A. (2018). "Effects of Ice-Algal Aggregate Export on the Connectivity of Bacterial Communities in the Central Arctic Ocean." *Frontiers in Microbiology*, 9, 1035.

Richardson, T. L., and Jackson, G. A. (2007). "Small Phytoplankton and Carbon Export from the Surface Ocean." *Science*, 315(5813), 838-840.

Riisgård, H. U., and Larsen, P. S. (2010). "Particle capture mechanisms in suspension-feeding invertebrates." *Marine Ecology Progress Series*, 418, 255-293.

Sakshaug, E. (2004). "Primary and Secondary Production in the Arctic Seas", in R. Stein and R. W. MacDonald, (eds.), *The Organic Carbon Cycle in the Arctic Ocean*. Berlin, Heidelberg: Springer Berlin Heidelberg, pp. 57-81.

Shroyer, E. L., Gordon, A. L., Jaeger, G. S., Freilich, M., Waterhouse, A. F., Farrar, J. T., Sarma, V. V. S. S., Venkatesan, R., Weller, R. A., Moum, J. N., and Mahadevan, A. (2020). "Upper layer thermohaline structure of the Bay of Bengal during the 2013 northeast monsoon." *Deep Sea Research Part II: Topical Studies in Oceanography*, 172, 104630.

Siegel, D. A., Granata, T. C., Michaels, A. F., and Dickey, T. D. (1990). "Mesoscale eddy diffusion, particle sinking, and the interpretation of sediment trap data." *Journal of Geophysical Research: Oceans*, 95(C4), 5305-5311.

Siegel, D. A., and Deuser, W. G. (1997). "Trajectories of sinking particles in the Sargasso Sea: modeling of statistical funnels above deep-ocean sediment traps." *Deep Sea Research Part I: Oceanographic Research Papers*, 44(9-10), 1519-1541.

Siegel, D. A., Buesseler, K. O., Doney, S. C., Sailley, S. F., Behrenfeld, M. J., and Boyd, P. W. (2014). "Global assessment of ocean carbon export by combining satellite observations and food-web models." *Global Biogeochemical Cycles*, 28(3), 181-196.

Stemmann, L., Jackson, G. A., and Gorsky, G. (2004). "A vertical model of particle size distributions and fluxes in the midwater column that includes biological and physical processes—Part II: application to a three year survey in the NW Mediterranean Sea." *Deep Sea Research Part I: Oceanographic Research Papers*, 51(7), 885-908.

Strong, C., and Rigor, I. G. (2013). "Arctic marginal ice zone trending wider in summer and narrower in winter." *Geophysical Research Letters*, 40(18), 4864-4868.

Thiele, S., Fuchs, B. M., Amann, R., and Iversen, M. H. (2015). "Colonization in the Photic Zone and Subsequent Changes during Sinking Determine Bacterial Community Composition in Marine Snow." *Applied and Environmental Microbiology*, 81(4), 1463-1471.

Trudnowska, E., Lacour, L., Ardyna, M., Rogge, A., Irisson, J. O., Waite, A. M., Babin, M., and Stemmann, L. (2021). "Marine snow morphology illuminates the evolution of phytoplankton blooms and determines their subsequent vertical export." *Nature Communications*, 12(1), 2816.

Turner, J. T. (2002). "Zooplankton fecal pellets, marine snow and sinking phytoplankton blooms." *Aquatic Microbial Ecology*, 27(1), 57-102.

von Appen, W.-J., Waite, A. M., Bergmann, M., Bienhold, C., Boebel, O., Bracher, A., Cisewski, B., Hagemann, J., Hoppema, M., Iversen, M. H., Konrad, C., Krumpen, T., Lochthofen, N., Metfies, K., Niehoff, B., Nöthig, E.-M., Purser, A., Salter, I., Schaber, M., Scholz, D., Soltwedel, T., Torres-Valdes, S., Wekerle, C., Wenzhöfer, F., Wietz, M., and Boetius, A. (2021). "Sea-ice derived meltwater stratification slows the biological carbon pump: results from continuous observations." *Nature Communications*, 12(1), 7309.

Waniek, J., Koeve, W., and Prien, R. D. (2000). "Trajectories of sinking particles and the catchment areas above sediment traps in the northeast Atlantic." *Journal of Marine Research*, 58(6), 983-1006.

Waniek, J. J., Schulz-Bull, D. E., Blanz, T., Prien, R. D., Oschlies, A., and Müller, T. J. (2005). "Interannual variability of deep water particle flux in relation to production and lateral sources in the northeast Atlantic." *Deep Sea Research Part I: Oceanographic Research Papers*, 52(1), 33-50.

Wekerle, C., Krumpen, T., Dinter, T., von Appen, W.-J., Iversen, M. H., and Salter, I. (2018). "Properties of Sediment Trap Catchment Areas in Fram Strait: Results From Lagrangian Modeling and Remote Sensing." *Frontiers in Marine Science*, 5, 407.

White, F. M. (1974). *Viscous Fluid Flow*, New York, NY: McGraw-Hill.

Wollenburg, J. E., Katlein, C., Nehrke, G., Nöthig, E.-M., Matthiessen, J., Wolf- Gladrow, D. A., Nikolopoulos, A., Gázquez-Sanchez, F., Rossmann, L., Assmy, P., Babin, M., Bruyant, F., Beaulieu, M., Dybwad, C., and Peeken, I. (2018). "Ballasting by cryogenic gypsum enhances carbon export in a *Phaeocystis* under-ice bloom." *Scientific Reports*, 8(1), 7703.

Wollenburg, J. E., Iversen, M., Katlein, C., Krumpen, T., Nicolaus, M., Castellani, G., Peeken, I., and Flores, H. (2020). "New observations of the distribution, morphology and dissolution dynamics of cryogenic gypsum in the Arctic Ocean." *The Cryosphere*, 14(6), 1795-1808.

Appendix – Additional Publications

Ramondenc, S., Nöthig, E. M., **Hufnagel, L.**, Bauerfeind, E., Busch, K., Knüppel, N., Kraft, A., Schröter, F., Seifert, M., and Iversen, M. H. (2023). "Effects of Atlantification and changing sea-ice dynamics on zooplankton community structure and carbon flux between 2000 and 2016 in the eastern Fram Strait." *Limnology and Oceanography*, 68(S1), S39-S53.

Hofmann, Z., von Appen, W.-J, Kanzow, T., Becker, H., Hagemann, J., **Hufnagel, L**., and Iversen, M.H. (2024): "Stepwise Subduction Observed at a Front in the Marginal Ice Zone in Fram Strait." *Journal of Geophysical Research: Oceans*, 129(5), e2023JC020641.

Moradi, N., **Hufnagel, L**., Ramondenc, S., Flintrop, C., Kiko, R., Fischer, T., Körtzinger, A., Fischer, G., and Iversen, M. H. (in prep.): "Insights into Particulate Organic Carbon and Nitrogen Export in Cyclonic Eddies: A Case Study Integrating In-Situ and Remote Observations Off Cape Verde Islands."

Acknowledgements

Eidesstattliche Erklärung

Versicherung an Eides Statt / *Affirmation in lieu of an oath*

gem. § 5 Abs. 5 der Promotionsordnung vom 28.04.2021 /
according to § 5 (5) of the Doctoral Degree Rules and Regulations of 28 April, 2021

Ich / I, _____
(Vorname / First *Name*, Name / *Name*, Anschrift / *Address*, ggf. Matr.-Nr. / *student ID no., if applicable)*

versichere an Eides Statt durch meine Unterschrift, dass ich die vorliegende Dissertation selbständig und ohne fremde Hilfe angefertigt und alle Stellen, die ich wörtlich dem Sinne nach aus Veröffentlichungen entnommen habe, als solche kenntlich gemacht habe, mich auch keiner anderen als der angegebenen Literatur oder sonstiger Hilfsmittel bedient habe und die zu Prüfungszwecken beigelegte elektronische Version (PDF) der Dissertation mit der abgegebenen gedruckten Version identisch ist. / *With my signature I affirm in lieu of an oath that I prepared the submitted dissertation independently and without illicit assistance from third parties, that I appropriately referenced any text or content from other sources, that I used only literature and resources listed in the dissertation, and that the electronic (PDF) and printed versions of the dissertation are identical.*

Ich versichere an Eides Statt, dass ich die vorgenannten Angaben nach bestem Wissen und Gewissen gemacht habe und dass die Angaben der Wahrheit entsprechen und ich nichts verschwiegen habe. / *I affirm in lieu of an oath that the information provided herein to the best of my knowledge is true and complete.*

Die Strafbarkeit einer falschen eidesstattlichen Versicherung ist mir bekannt, namentlich die Strafandrohung gemäß § 156 StGB bis zu drei Jahren Freiheitsstrafe oder Geldstrafe bei vorsätzlicher Begehung der Tat bzw. gemäß § 161 Abs. 1 StGB bis zu einem Jahr Freiheitsstrafe oder Geldstrafe bei fahrlässiger Begehung. / *I am aware that a false affidavit is a criminal offence which is punishable by law in accordance with § 156 of the German Criminal Code (StGB) with up to three years imprisonment or a fine in case of intention, or in accordance with § 161 (1) of the German Criminal Code with up to one year imprisonment or a fine in case of negligence.*

_____ _____
Ort / *Place*, Datum / *Date* Unterschrift / *Signature*